UNIVERSIDADE ESTADUAL DE CAMPINAS
FACULDADE DE ENGENHARIA DE ALIMENTOS

GABRIELLI NUNES CLIMACO

GÉIS MISTOS COMO VEÍCULO DE COMPOSTOS BIOATIVOS DA FOLHA DO *HIBISCUS SABDARIFFA* L. EXTRAÍDOS POR TECNOLOGIAS SUSTENTÁVEIS

BIGELS AS A VEHICLE OF BIOACTIVE COMPOUNDS FROM *HIBISCUS SABDARIFFA* L. LEAF EXTRACTED BY SUSTAINABLE TECHNOLOGIES

Campinas
2023

GABRIELLI NUNES CLIMACO

GÉIS MISTOS COMO VEÍCULO DE COMPOSTOS BIOATIVOS DA FOLHA DO *HIBISCUS SABDARIFFA* L. EXTRAÍDOS POR TECNOLOGIAS SUSTENTÁVEIS

BIGELS AS A VEHICLE OF BIOACTIVE COMPOUNDS FROM *HIBISCUS SABDARIFFA* L. LEAF EXTRACTED BY SUSTAINABLE TECHNOLOGIES

Tese apresentada à Faculdade de Engenharia de Alimentos da Universidade Estadual de Campinas como requisito exigido para obtenção do título de Doutora em Engenharia de Alimentos.

Thesis presented to the Faculty of Food Engineering of the University of Campinas as a requirement to obtain the title of Doctor in Food Engineering.

Orientador: Prof. Dr. Luiz Henrique Fasolin

ESTE TRABALHO CORRESPONDE À VERSÃO FINAL DA TESE DEFENDIDA PELA ALUNA GABRIELLI NUNES CLIMACO, E ORIENTADA PELO PROF. DR. LUIZ HENRIQUE FASOLIN

Campinas

2023

Ficha catalográfica
Universidade Estadual de Campinas
Biblioteca da Faculdade de Engenharia de Alimentos
Claudia Aparecida Romano - CRB 8/5816

C613g

Climaco, Gabrielli Nunes, 1993-
Géis mistos como veículo de compostos bioativos da folha do *Hibicus Sabdariffa* L. extraídos por tecnologias sustentáveis / Gabrielli Nunes Climaco. – Campinas, SP : [s.n.], 2023.

Orientador: Luiz Henrique Fasolin.
Tese (doutorado) – Universidade Estadual de Campinas, Faculdade de Engenharia de Alimentos.

1. Compostos bioativos. 2. Fluídos supercrítico. 3. Hibisco. 4. Digestibilidade. 5. Bigels. I. Fasolin, Luiz Henrique. II. Universidade Estadual de Campinas. Faculdade de Engenharia de Alimentos. III. Título.

Informações Complementares

Título em outro idioma: Bigels as a vehicle of bioactive compounds from *Hibiscus Sabdariffa* L. leaf extracted by sustainable technologies
Palavras-chave em inglês:
Bioactive compounds
Supercritical fluids
Hibiscus
Digestibility
Bigels
Área de concentração: Engenharia de Alimentos
Titulação: Doutora em Engenharia de Alimentos
Banca examinadora:
Luiz Henrique Fasolin [Orientador]
Samantha Cristina de Pinho
Miriam Dupas Hubinger
Ana Carla Kawazoe Sato
Rejane de Castro Santana
Data de defesa: 03-10-2023
Programa de Pós-Graduação: Engenharia de Alimentos

Identificação e informações acadêmicas do(a) aluno(a)
- ORCID do autor: 0000-0002-6113-1616
- Currículo Lattes do autor: http://lattes.cnpq.br/8787435220285629

LOCAL E DATA DA DEFESA: Campinas, 03 de outubro de 2023

COMISSÃO AVALIADORA

_____

Prof. Luiz Henrique Fasolin (Orientador)

_____

Profa. Samantha Cristina de Pinho

_____

Profa. Miriam Dupas Hubinger

_____

Profa. Ana Carla Kawazoe Sato

_____

Profa. Rejane de Castro Santana

Programa de Pós-Graduação em Engenharia de Alimentos da Faculdade de Engenharia de Alimentos da Universidade Estadual de Campinas.

A Ata da defesa com as respectivas assinaturas dos membros encontra-se no SIGA/Sistema de Fluxo de Dissertação/Tese e na Secretaria do Programa da Unidade.

AGRADECIMENTOS

Primeiramente a Deus por se fazer presente em minha vida, transformando os momentos mais difíceis em experiências que me fizeram crescer, amadurecer e que consequentemente me ajudaram a chegar até aqui.

Aos meus pais e meu irmão, por serem meu "porto seguro", por todo amor, apoio e incentivo, pois foram esses fatores que me deram a oportunidade de chegar até este momento, de superar as dificuldades e seguir firme.

Ao meu parceiro de vida, que sempre esteve do meu lado, me incentivando em cada etapa, além de aguentar os "tormentos" de alguém em fase final de doutorado.

Agradeço também os meus amigos de Campinas, que são minha família aqui, pois me acolheram e estiveram ao meu lado em todos os momentos, me dando forças pra continuar. Aos amigos de Imperatriz, que mesmo distantes, se fazem tão presente, me incentivando cada vez mais a seguir meus sonhos.

Agradeço ao professor Luiz Fasolin, por ter me aceito como orientanda e pela dedicação durante esses quatro anos, à UNICAMP e ao LASEFI, por ter sido "casa" para os meus experimentos.

Agradeço a todo o pessoal do LIP e ao professor Vicente, por terem me acolhido de forma única, durante os 6 meses de intercâmbio, deixando claro que não poderia ter escolhido melhor lugar para esta experiência.

Agradeço também à Coordenação de Aperfeiçoamento de Pessoal de Nível Superior – Brasil (CAPES) pelo apoio financeiro através da bolsa de doutorado e da bolsa de doutorado sanduíche (PRINT/CAPES) e a Fundação de Amparo à Pesquisa de São Paulo (FAPESP) (Brasil, bolsas 2019/27354–3 e 2021/07639–3).

Por fim, agradeço aos membros da banca pela disponibilidade e empenho em todas as revisões propostas para a melhoria desta tese.

Muito obrigada!

RESUMO

A *Hibiscus Sabdariffa* L. é conhecida por seu cálice e flores, que apresentam uma diversidade de compostos benéficos à saúde. Suas folhas também são ricas em diferentes compostos, contudo, são geralmente desperdiçadas durante o processamento. Tecnologias de extração alternativas às convencionais, bem como formas de veiculação dos extratos que promovam a proteção dos efeitos biológicos e potencializam sua biodisponibilidade têm sido estudados. Diante disso, o objetivo deste trabalho foi desenvolver um bigel com óleo de girassol, monoestearato de glicerol e isolado protéico de soro do leite como veículo para compostos bioativos da folha do *Hibiscus Sabdariffa* L. obtidos por alta pressão. Primeiramente, foram obtidos os extratos por meio de extração com fluido supercrítico (SFE) e líquido pressurizado (PLE). Comparando os métodos em condições otimizadas de extração, notou-se que o SFE permitiu um melhor resultado em relação ao teor de compostos, pois resultou em extratos mais concentrados. Contudo, em termos de rendimento de compostos bioativos o PLE foi superior, pois recuperou uma maior quantidade dos compostos exigindo menos tempo e solvente. Na segunda etapa foram desenvolvidos os bigéis através da gelificação a frio e à quente das proteínas. Os resultados mostraram que o processo de gelificação exerceu influência na estrutura final dos bigéis e consequentemente nas propriedades mecânicas. A razão hidrogel:oleogel também foi um parâmetro importante, onde os arranjos físicos (O/A, A/O ou bicontínuo) também foram dependentes do processo de gelificação da proteína. De forma geral, os bigéis produzidos à quente resultaram em géis de ruptura com maior módulo de elasticidade, enquanto os produzidos à frio foram mais elásticos e não apresentaram ruptura. Em seguida, os géis produzidos à frio foram utilizados para a encapsulação simultânea de compostos modelos de diferentes polaridades (curcumina e riboflavina). Foi verificado que a incorporação dos compostos provocou mudanças significativas na rede de gel, provocando tanto interações físicas quanto químicas. Por fim, objetivando uma rede mais estável frente ao processamento de alimentos, foi avaliada a influência da lecitina de soja no desenvolvimento de bigéis à frio para encapsulação dos extratos do hibisco. Foi observado que a lecitina promoveu maior organização da estrutura do bigel, provavelmente devido ao seu efeito surfactante, enquanto que os extratos a tornaram mais *soft*. De forma geral, além da valorização das folhas do hibisco, os resultados desse trabalho podem ajudar no avanço do estado-da-arte no desenvolvimento de sistemas gelificados mistos para veiculação de compostos bioativos em diferentes segmentos além da indústria de alimentos.

Palavras-chave: Compostos bioativos; fluido supercrítico; hibisco; digestibilidade; bigel

ABSTRACT

Hibiscus Sabdariffa L. is known for its calyx and flowers, which contain several compounds related to health benefits. Its leaves are also rich in different bioactives; however, they are usually wasted during processing. Alternative extraction technologies to conventional ones, as well as ways of delivering extracts that can protect its biological effects and enhance their bioavailability have been studied. Therefore, the objective of this work was to develop a bigel with sunflower oil, glycerol monostearate and whey protein isolate as a vehicle for bioactive compounds from the leaf of *Hibiscus Sabdariffa* L. obtained by high pressure. Firstly, the extracts were obtained by supercritical fluid (SFE) and pressurized liquid (PLE) extraction. Comparing the methods under optimized extraction conditions, it was noted that SFE showed better results in relation to the content of compounds, since the extracts were more concentrated. However, in terms of bioactive compounds' yield, PLE was superior, as it recovered a greater quantity of compounds, requiring less time and solvent. In the second stage, the bigels were developed through cold and hot gelation of the proteins. The results showed that the gelation process exerted an effect on the final structure of the bigels and, consequently, the mechanical properties. The hydrogel:oleogel ratio was also an important parameter, where the physical arrangements (O/W, W/O or bicontinuous) were also dependent on the protein gelling process. In general, heat-set bigels produced rubber gels with a higher elasticity modulus, while cold-set ones were more elastic and did not break. Then, the cold-set bigels were used for simultaneous encapsulation of model compounds of different polarities (curcumin and riboflavin). It was observed that the incorporation of the compounds caused significant changes in the gel network, causing both physical and chemical interactions. Finally, aiming at a more stable network for food processing, the influence of soy lecithin was evaluated in the development of cold-set bigels for encapsulation of hibiscus extracts. It was observed that lecithin promoted greater organization of the bigel structure, probably due to its surfactant effect, while the extracts made it softer. In general, in addition to the hibiscus leaves valorization, the results of this work can promote advances in the state-of-the-art of the development of hybrid gelled systems for delivering bioactive compounds in different areas besides the food industry.

Key-words: Bioactive compounds; supercritical fluid; hibiscus; digestibility; bigel,

LISTA DE FIGURAS

LISTA DE TABELAS

SUMÁRIO

CAPÍTULO 1.

INTRODUÇÃO, JUSTIFICATIVA, OBJETIVOS E ESRUTURA DA TESE

1. INTRODUÇÃO, JUSTIFICATIVA, OBJETIVOS E ESTRUTURA DA TESE

1.1 INTRODUÇÃO E JUSTIFICATIVA

Nos últimos anos é possível observar uma tendência dos consumidores por alimentos naturais ou que contenham em sua formulação ingredientes que, de alguma forma, promovam bem-estar ou atuem na prevenção de doenças. Além dessa demanda por bem-estar e saúde, a sociedade começa a estar mais atenta à proveniência do que consome e o impacto causado no meio ambiente durante sua cadeia produtiva. Nesse sentido, as indústrias de alimentos e a comunidade científica têm se mostrado comprometidas no desenvolvimento de novos produtos contendo compostos bioativos e na utilização de novas tecnologias que atendam a esse cenário.

As plantas, de forma geral, são reconhecidas por apresentarem uma enorme diversidade de compostos metabólitos secundários. Estes compostos podem desempenhar diversas funções, como por exemplo, atuar como conservantes e corantes e desempenhar efeitos farmacológicos e/ou nutracêuticos no corpo humano sendo, portanto, passíveis de serem utilizados como aditivos alimentares ou no desenvolvimento de novos fármacos e alimentos funcionais (CHEMAT et al., 2019; CVJETKO BUBALO et al., 2018). Devido ao apelo sustentável, nutricional e funcional, as publicações com extração de compostos de origem vegetal, tiveram um aumento de mais de 100 % na base de busca *Science Direct*, da editora Elsevier, em relação ao ano de 2016, partindo de 1201 para 2847 produções anuais em 2021, quando utilizados os termos "*bioactive*", "*extraction*" e *"vegetable".*

Entre as fontes vegetais que podem ser utilizadas como fontes de bioativos encontra-se a *Hibiscus Sabdariffa* L., que é uma planta herbácea disponível durante todo o ano e conhecida por possuir propriedades biológicas benéficas, com efeitos anti-hipertensivos e anticancerígenos (RAGHU; NAIDOO; DEWIR, 2019). Estes efeitos são decorrentes da presença de compostos bioativos como as antocianinas, flavonoides e ácidos orgânicos presentes na planta que também é rica em macronutrientes (JABEUR et al., 2017). O cálice e as flores são as partes mais estudadas; entretanto, as folhas correspondem a maior parte da planta e também são ricas em compostos antioxidantes (ZHEN et al., 2016) e outros bioativos, que fazem com que possuam propriedades com efeitos hipoglicêmico, antioxidante e hipolipidêmico (CHEN et al., 2013). Todavia, poucos estudos são encontrados em relação à parte folhosa da planta. Além disso, os estudos publicados geralmente utilizam processos convencionais de extração sólido-líquido (CHEN et al., 2013; ZHEN et al., 2016), apesar de também serem encontradas algumas publicações com extração assistida por ultrassom (WANG

et al., 2014; ZHEN et al., 2016). Os processos convencionais geralmente são associados com alto gasto energético e com a utilização de solventes orgânicos prejudiciais à saúde e ao meio ambiente, como o hexano e o metanol (CHEMAT et al., 2019). Portanto, para que o produto possa chegar ao consumidor esse solvente precisa ser retirado e, para isso, etapas de remoção precisam ser adicionadas ao processo. Tendo isso em vista, processos alternativos de extração e preservação das propriedades dos compostos têm sido estudados, visando o aumento da segurança para o consumidor e a minimização da utilização de recursos naturais e do impacto ambiental (GOULA et al., 2017; NÁTHIA-NEVES; VARDANEGA; MEIRELES, 2019; NIPORNRAM et al., 2018). Essas tecnologias são conhecidas como tecnologias sustentáveis, *eco-friendly* ou verdes e os solventes utilizados como quimicamente verdes.

Apesar de ser um tema discutido e estudado há mais de uma década, é possível observar um aumento de mais de 200 % nas publicações anuais em 2023, na base de busca *Science Direct*, utilizando os termos "*green technology*" e "*extraction*", em relação ao ano de 2016. Dentre as tecnologias em destaque, tem-se a extração assistida por micro-ondas (MAE) e tecnologias de alta pressão como extração com líquidos pressurizados (PLE) e fluido supercrítico (SFE). Essas técnicas têm sido utilizadas em diferentes matrizes vegetais e seus resíduos, como sementes de uva e maracujá; pele de tomate e jabuticaba; grãos de café (RAN et al., 2017); *Arctium lappa* (SOUZA et al., 2019); semente de guaraná (SANTANA et al., 2019); amora (MACHADO et al., 2014); feijoa (SANTOS et al., 2021) dentre outros. Os resultados mostram que essas tecnologias são capazes de extrair biocompostos de forma mais eficiente com menor utilização de recursos energéticos e solvente (LU et al., 2019). Dessa forma, o investimento e a continuidade dos estudos sobre essas tecnologias se fazem necessários, visando um aprimoramento contínuo, com melhoria de rendimento e aumento do seu caráter sustentável.

Além de novas técnicas de extração, formas de veiculação de compostos bioativos com o intuito de potencializar sua biodisponibilidade e seus efeitos nutricionais e farmacológicos têm sido foco de diversas pesquisas (BEHERA et al., 2015; LUPI et al., 2016; PINHEIRO et al., 2017; SAGIRI et al., 2014; SINGH et al., 2014). Dentre as diferentes formas inovadoras, encontram-se os géis mistos ou bigéis, que são misturas de hidrogel e oleogel (SINGH et al., 2014). Devido à alta estabilidade de sua estrutura de caráter anfifílico, os bigéis permitem a incorporação e proteção simultânea de compostos hidrofílicos e hidrofóbicos (BOLLOM; CLARK; ACEVEDO, 2020), além de atuarem como modificadores de textura. No entanto,

estes sistemas têm sido estudados quase exclusivamente para aplicações cosméticas e farmacêuticas, e apenas recentemente tem sido reportada a sua utilização em alimentos.

1.2 OBJETIVOS

1.2.1 Objetivo Geral

Extrair e caracterizar compostos bioativos da *Hibiscus Sabdariffa* L. através de extração a altas pressões (extração com líquido pressurizado e com fluido supercrítico) e veiculá-los em um gel misto a base de proteína do soro do leite, glicerol monostearato e óleo de girassol, desenvolvido visando aplicação em alimentos.

1.2.2 Objetivos específicos

1. Otimizar a extração de compostos bioativos da folha da *Hibiscus Sabdariffa* L. através de tecnologias com alta pressão, nomeadamente extração com fluido supercrítico e líquido pressurizado;
2. Extrair compostos bioativos da folha da *Hibiscus Sabdariffa* L. através de metodologia convencional (maceração) como forma de comparação com tecnologias alternativas;
3. Caracterizar os compostos presentes nos extratos obtidos por diferentes métodos de extração em relação a sua composição;
4. Desenvolver um gel misto a base de isolado proteico do soro do leite, glicerol monostearato e óleo de girassol, utilizando as técnicas de gelificação quente e fria das proteínas;
5. Avaliar as propriedades reológicas, mecânicas, termodinâmicas e estruturais dos géis mistos;
6. Veicular compostos modelos (curcumina e riboflavina) nas fases oleogel e hidrogel e avaliar sua influência nas propriedades mecânicas, termodinâmicas e estruturais dos géis mistos;
7. Avaliar a adição de surfactante (lecitina de soja) no aprimoramento das propriedades físico-químicas dos géis mistos;
8. Veicular um extrato selecionado da folha da *Hibiscus Sabdariffa* L. nos géis mistos aprimorados com surfactante;
9. Avaliar a liberação e estabilidade dos compostos veiculados quando submetidos às condições do sistema trato gastrointestinal.

1.3 ESTRUTURA DA TESE

Essa Tese de Doutorado está estruturada na forma de capítulos. O Capítulo 1 apresenta uma introdução e justificativa sobre o tema de pesquisa escolhido, o objetivo principal e objetivos específicos, bem como a estrutura da Tese.

No Capítulo 2 é apresentada uma revisão bibliográfica, objetivando contextualizar o leitor sobre os temas abordados nesse estudo, englobando as principais características da *Hibiscus Sabdariffa* L., assim como os possíveis compostos bioativos que podem ser obtidos, e as tecnologias sustentáveis utilizadas para obtenção desses compostos. Além destes temas, têm-se uma breve discussão sobre sistemas gelificados, incluindo hidrogéis, oleogéis e bigéis e suas respectivas características.

O Capítulo 3 refere-se ao primeiro artigo produzido, já publicado no *Journal of Supercritical Fluids*, abordando de forma detalhada as extrações com fluido supercrítico (SFE), líquido pressurizado (PLE) e convencional por maceração dos compostos bioativos das folhas de hibisco. Também foi realizada a caracterização dos extratos em relação à quantidade de compostos fenólicos, flavonoides, antocianinas, taninos e atividade antioxidante.

O Capítulo 4 refere-se ao segundo artigo submetido à revista *Food Research International*, que aborda a elaboração e caracterização dos bigéis a partir de oleogéis de glicerol monoestearato e óleo de girassol e hidrogéis de isolado protéico de soro do leite. A fase hidrogel foi gelificada através dos métodos de gelificação à quente e à frio. Dessa forma, pode-se relacionar a influência do mecanismo de gelificação nas propriedades reológicas, mecânicas, termodinâmicas e estruturais dos bigéis. Esse trabalho serviu de ponto de partida para a produção dos próximos trabalhos, que foram o aprimoramento dos bigéis através da adição de surfactantes, a veiculação de compostos modelos e dos extratos vegetais obtidos previamente.

Os Capítulos 5 e 6 referem-se aos artigos referentes à incorporação da curcumina e riboflavina, bem como dos extratos, ao bigel, respectivamente. Nestes, pode-se observar a influência dos compostos nas propriedades reológicas, mecânicas e estruturais dos bigéis, além da liberação controlada em simulante alimentar e no trato gastrointestinal. Por fim, o Capítulo 7 aborda, de forma geral, todos os resultados obtidos neste trabalho, e os trabalhos futuros que podem ser desenvolvidos. A Figura 1 apresenta esquematicamente os capítulos da Tese de Doutorado, de forma a facilitar a visualização dos resultados obtidos em concordância com os objetivos específicos deste trabalho.

Figura 1.1. Esquema das atividades descritas neste trabalho.

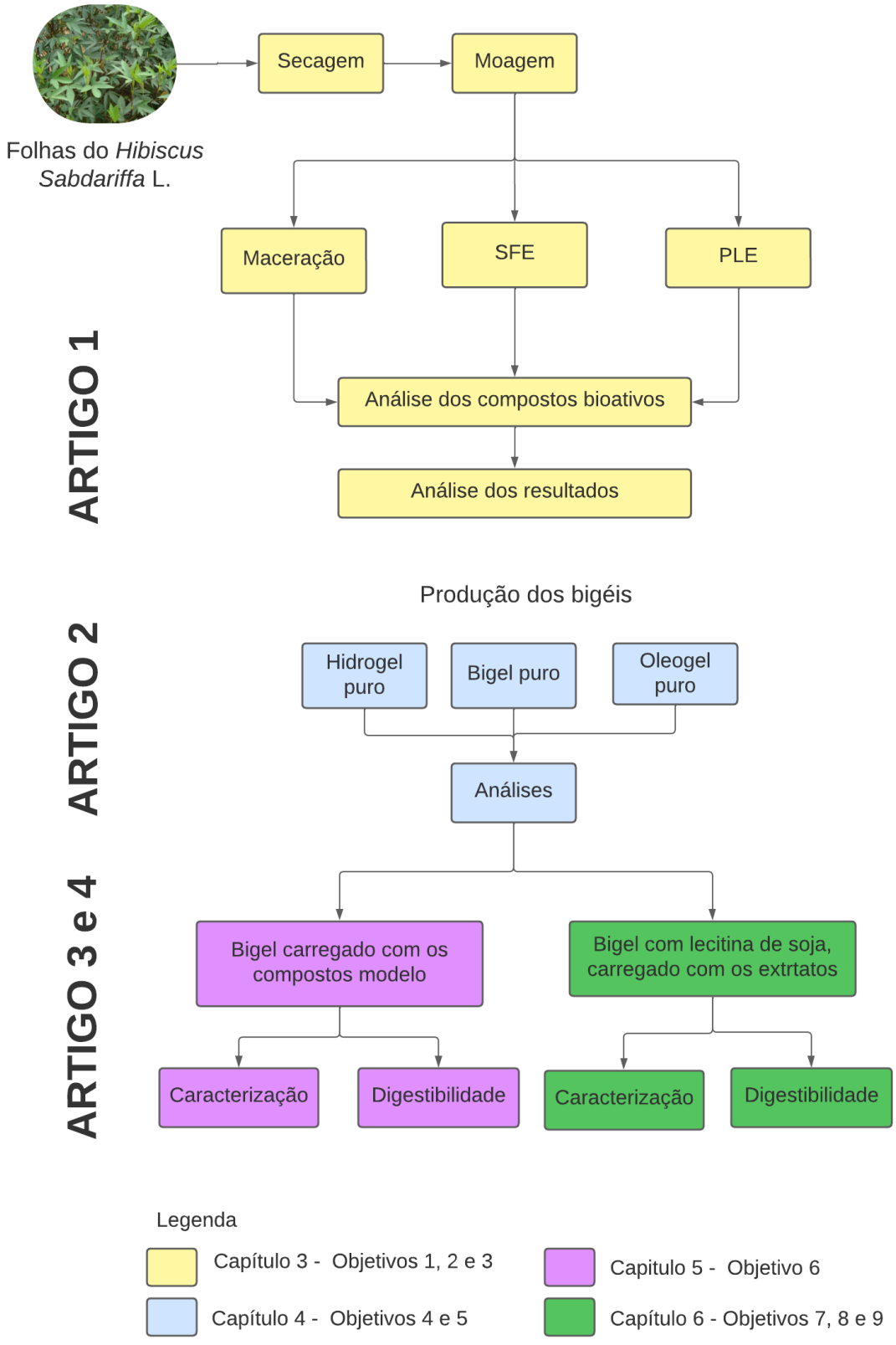

Fonte: Auto

CAPÍTULO 2.

REVISÃO BIBLIOGRÁFICA

2. REVISÃO BIBLIOGRÁFICA

2.1 HIBISCUS SABDARIFFA L.

A *Hibiscus sabdariffa* L., também conhecida como roselle, é uma planta herbácea pertencente à família Malvaceae. É amplamente cultivada em muitas áreas, incluindo América Central e África e pode ser dividida em três genótipos diferentes: verde, vermelho escuro e vermelho, variedade mais comumente utilizada (Figura 2.1) (JABEUR et al., 2017; KARAASLAN, 2019). É conhecida por possuir propriedades benéficas com efeitos anti-hipertensivos e anticancerígenos. Suas folhas possuem cores variadas indo do verde profundo ao vermelho, e suas flores tons amarelo pálido ou rosa claro com o centro vermelho (RAGHU; NAIDOO; DEWIR, 2019).

Figura 2.1. *Hibiscus sabdariffa* L.

Fonte: Autor

Seu cálice é comumente utilizado na culinária devido ao seu sabor exótico (ALAÑÓN et al., 2020), podendo ser encontrado seco ou *in natura*. Também é aplicado na preparação bebidas à base de plantas, bebidas quentes e frias, bebidas fermentadas, vinho, geleia, sorvetes, chocolates, aromatizantes, pudins e bolos (CLIMACO; VARDANEGA; FASOLIN, 2023); enquanto suas folhas são consumidas apenas como vegetal verde folhoso (JABEUR et al., 2017).

Dentre as partes da planta, o cálice e as flores são as partes mais estudadas, devido à sua maior carga nutricional, conteúdo de pectina, ácido ascórbico e málico, e compostos fenólicos (PERALTA et al., 2019). Entretanto, as folhas também possuem valor nutricional, medicinal e econômico para as indústrias alimentícia e farmacêutica, devido ao seu rico conteúdo de macro e micronutrientes, vitamina C e minerais (RASHEED et al., 2018). Contudo, os ácidos

orgânicos, antocianinas, polissacarídeos e flavonoides são os compostos mais estudados presentes nas folhas (MOURA et al., 2019).

A quantidade de compostos bioativos com atividade antioxidante presentes na folha é superior a outras matrizes vegetais reconhecidas pelo conteúdo desses compostos e em alguns casos, seu próprio cálice, dependendo da forma de extração (Tabela 2.1) (DA-COSTA-ROCHA et al., 2014). Sindi *et al* (2014), analisaram o cálice do hibisco através de um processo convencional utilizando água como solvente, e obtiveram valores superiores ao encontrado por Singh *et al.* (2011) para antocianinas nas folhas de hibisco. Porém, a atividade antioxidante dos compostos presentes nas folhas apresentou valores superiores ao encontrado no cálice (SINDI; MARSHALL; MORGAN, 2014), utilizando tanto o extrato aquoso (SINGH et al., 2011) quanto metanólico (SINGH et al., 2015).

Comparando com outras matrizes como a beterraba, uva e araçá; também é possível constatar valores inferiores na concentração de bioativos em comparação às folhas de hibisco. El-Beltagi *et al.* (2018) analisou a polpa da beterraba através de extração em *shaker* com etanol durante 24 horas, Schiassi *et al.*, (2018) analisou a polpa do araçá através de moagem com água, e González *et al*., (2020) analisou a polpa da uva através de extração assistida por ultrassom com solução hidroalcóolica (1:1 etanol:água). Dentre esses estudos, apenas os valores para antocianinas superam os encontrados em extrato aquoso da folha do hibisco.

Dessa forma, pode-se constatar que as folhas do hibisco são uma fonte promissora para recuperação de compostos bioativos. Entretanto, a falta de estudos sobre os compostos foliares dessa planta ainda é grande (ZHEN *et al*., 2016), uma vez que os trabalhos já publicados fazem uso, em sua maioria, apenas de tecnologias convencionais, como pode ser observado na Tabela 2.2. Isso provoca desperdício de compostos de alto valor agregado que poderiam ser utilizados para fins mais nobres, uma vez que a maior porcentagem da planta é composta por folhas (ZHEN *et al*., 2016).

Tabela 2.1. Compostos bioativos presentes em diferentes matrizes vegetais.

Matriz	Método	Antocianinas (mg/100 g)	Carotenoides (mg/100 g)	Fenólicos (mg/100 g)	Taninos (mg/100 g)	AA[4] (%)	Referência
Araçá – polpa *(Psidium g. Swartz)*[1]	Moagem com água	-	0,43±0,05	89,14±0,94	-	7,21	Schiassi *et al.*, (2018)
Beterraba – folha *(Beta vulgaris)*[2]	Moagem com metanol	423,8±6,2	225,3±4,7	250,0±4,5	467,1±8,4	93,5	Singh *et al.*, (2015)
Beterraba – polpa *(Beta vulgaris)*[2]	Shaker com etanol / 24h	63,73±0,03	1,72±0,08	133,5±1,05	5,13±0,081	70,35	El-Beltagi *et al.* (2018)
Beterraba – polpa *(Beta vulgaris)*[3]	Banho-maria	-	-	96,23	-	86,34	Kushwaha *et al.* (2017)
Hibisco – folha *(Hibiscus Sabdariffa* L.)[2]	Moagem com água	41,70±0,96	18,85±0,68	-	107,56±1,34	83,4	Singh *et al*., (2011)
Hibisco – folha *(Hibiscus Sabdariffa* L.)[1]	Moagem com metanol	79,0±3,5	694,6±4,6	235,5±3,0	519,4±5,1	87,4	Singh *et al.*, (2015)
Hibisco – cálice *(Hibiscus Sabdariffa* L.)[1]	Extrato aquoso	58,60±0,48	-	21,67±0,93	-	71,98	Sindi *et al.*, (2014)
Uva – pele *(Vitis Vinífera)*[2]	Ultrassom etanol 60 %	-	-	71,12±1,76	-	63,74	Milella *et al*. (2019)
Uva – polpa *(Vitis Vinífera)*[2]	Ultrassom etanol:água (1:1)	400,00±1,0	-	2160±3,8	-		González *et al*., (2020)

[1]expresso em g de matéria prima fresca; [2]expresso em g de matéria prima seca; [3]expresso em ml de extrato; [4]Atividade Antioxidante

Tabela 2.2. Compostos bioativos da folha do hibisco obtidos através de diferentes métodos de extração.

Método / Solvente	Compostos fenólicos[1]	Flavonoides[2]	Antocianinas[3]	Taninos[4]	Referência
Maceração com água	14,00	-	0,417	1,075	Singh *et al*., (2011)
Moagem com água	2,35	4,20	0,79	5,19	Singh *et al*., (2015)
Ultrassom com metanol	29,9	7,31	-	-	Zhen *et al* (2016)
Shaker com água +HCl	15,7	14,0	-	-	Karaaslan *et al*. (2019)
Extração com metanol, hexano e acetato de etila.	0,35	0,75	0,013	-	Chen *et al*. (2013)

[1]expresso mg de ácido gálico/g de extrato seco; [2]expresso em mg de catequina/g de extrato seco; [3]expressa em mg de cianidina-3-glicosídeo/g de extrato seco; [4]expresso em mg de ácido tânico/g de extrato seco.

É possível observar como o método de extração exerce grande influência na quantidade de compostos fenólicos presente nos extratos, sendo obtidos desde 2,35 mg/g de extrato seco através de moagem com água (SINGH et al., 2015), até 14 mg/g de extrato seco através de maceração com água (SINGH et al., 2011). Com a utilização de um *shaker* com solução ácida, tem-se também um rendimento ainda maior destes compostos (15,7 mg/g de extrato seco) (KARAASLAN, 2019) e, com a extração assistida por ultrassom utilizando metanol como solvente, esse valor se eleva quase 50 % (29,9 mg/g de extrato seco), o que foi observado também para o conteúdo de flavonóis (ZHEN et al., 2016).

Os extratos das folhas de hibisco obtidos por extração com metanol, hexano e acetato de etila foram ricos em polifenóis e apresentaram efeitos hipoglicêmicos, antioxidantes e hipolipidêmicos em quantidade equiparáveis com outras matrizes mais conhecidas (CHEN *et al*., 2013). Todavia, a presença dessas classes de compostos bioativos não assegura a funcionalidade ou atividade biológica do extrato. Essa característica é dependente das moléculas presentes no extrato. A Tabela 2.3 detalha os compostos identificados nas folhas de hibisco em diferentes métodos e condições de extração.

Em um estudo utilizando extrato aquoso das folhas do hibisco, realizado por Balogun *et al.* (2019), foi possível observar a presença de atividade anti-hipertensiva contra hipertensão induzida por carga de sal em ratos. Gosain *et al.* (2010) avaliaram o efeito hiperlipidêmico das folhas, através de extração em Soxhlet com etanol 95 % por 72 h, e constatou que a administração utilizada possibilitou a redução significativa do colesterol sérico, LDL, VLDL e nível sérico de triglicerídeos entre 15 % e 30 %, após quatro semanas de tratamento. Lin *et al.* (2012), por sua vez, avaliaram a atividade anticancerígena das folhas contra células de câncer de próstata humano in vitro e in vivo, e observaram efeito antiapoptótico tanto por vias intrínsecas quanto extrínseca, inibindo também o crescimento de tumor de próstata em camundongos.

Tabela 2.3. Diferentes métodos para análise da atividade antioxidante da folha do hibisco.

Método	A. Antioxidante		Compostos identificados	Referência
	ABTS[1]	DPPH[2]		
Maceração com água, etanol e acetona	-	79,70%	Ácido gálico, ácido ascórbico, cianidina-3-glicosídeo, ácido tânico, carotenoides, clorofila	Singh *et al*., (2011)
Extração com metanol (50 °C/3 h). O filtrado foi seco com evaporador rotativo a vácuo e o resíduo dissolvido em água (50°C) e extraído com hexano. A fase aquosa foi extraída com acetato de etila	-	70%	Ácido gálico, ácido protocatecuico (PCA), catequina, galato de epicatequina (ECG), ácido elágico, rutina, ácido q-cumárico, ácido ferúlico, quercetina, naringenina, ácido elágico, ácido ferúlico e quercetina	Chen *et al*. (2013)
Extração assistida por banho ultrassônico (500 W) com metanol 70% (v/v) por 30 min a temperatura ambiente	-	320 µg/ml	ácido neoclorogênico, ácido clorogênico, ácido criptoclorogênico, rutina e isoquercitrina	Wang *et al.*(2014)
Moagem da folha fresca, fervida por 5 min com água ou solução de NaCl 5% (1:1 p/v amostra: solvente)	-	96,0%	Ácido gálico, catequina, cianidina-3-glicosídeo, ácido tânico, carotenoides, clorofila, vit. C	Singh *et al*., (2015)
Maceração por 24 h em 300 mL de metanol à temperatura ambiente (1:6 p/v amostra: solvente)	-	44,98 µg/ml	Ácido gálico e catequina	Formagio *et al.*(2015)
Extração em *shaker* com água gelada (1:20 p/v amostra: solvente) durante 30 min	93,7%	-	Clorofila e ácido ascórbico	Kumar *et al.*(2015)
Extração com metanol 70% (v/v) e solução de ácido acético 0,1%. A solução foi colocada em banho-maria ultrassônico por 10 min seguido de agitação em temperatura ambiente durante a noite	152,5 molTE/g	-	5-(hidroximetil)furfurall, ácido neoclorogénico, ác. gálico, ác. clorogénico, ác. criptoclorogénico, ác. clorogênicos totais; quercetina; canferol	Zhen *et al* (2016)
Extração com etanol sob agitação contínua (150 min^{-1}) por 2-3 dias	-	65,19%	fitol, alfa-tocoferol, metil linolenato, etil palmitato e etil linolenato	Subhaswaraj *et al.* (2017)
Agitação em *shaker* por 1 h com solventes acidificados com HCl 0,1% em temperatura ambiente. Solventes utilizados: água, metanol, etanol, acetona e acetonitrila	33,2 mgTE/g	-	catequina, epicatequina, ácido clorogênico, ácido cafeico, ácido p-cumárico, naringina, hesperidina, floridzina, rutina, ácido elágico e miricetina	Karaaslan *et al*. (2019)

[1]ABTS: Atividade antioxidante por captura do radical 2,2´-azinobis(3-etilbenzotiazolina-6-ácido sulfônico); [2]DPPH: Atividade antioxidante por captura do radical 2,2-difenil-1-picril-hidrazil

Além das atividades descritas, a atividade antioxidante também é dependente dos compostos presentes no extrato e por isso pode mudar consideravelmente dependendo das condições de extração (Tabela 2.3). Subhaswaraj *et al.* (2017) avaliaram a atividade antioxidante das folhas através de agitação contínua com etanol, em período de 2 a 3 dias, e obtiveram um valor de 65,19 %. Por sua vez, Chen *et al*. (2013) avaliaram a extração com metanol a 50 ºC por 3 h e obtiveram resultado superior (70 %), enquanto a extração através da fervura das folhas em solução de NaCl 5 % (1:1 p/v amostra: água) por 5 min, levou a 90 % de atividade antioxidante pelo método DPPH (SINGH et al., 2015).

Um fator importante a ser avaliado é o tempo de extração, que também influencia no perfil e nas características dos compostos extraídos, dependendo do método e das condições utilizadas na obtenção do extrato. Na extração assistida por ultrassom, a aplicação das ondas sonoras por períodos mais longos, utilizando solução etanolica a 95 % (v/v) resultou em menores valores de atividade antioxidante (CHEW et al., 2021). De forma geral, tem-se a ideia que maiores tempos de extração resultam em maiores rendimentos de compostos e como consequência a atividade antioxidante. Entretanto, dependendo do processo pode ocorrer a degração dos compostos (MUHAMMAD et al., 2018), reduzindo assim não só a atividade antioxidante, mas também outras atividades biológicas, uma vez que o tempo de exposição tende a se relacionar com a temperatura, assim, tanto para o SFE, quanto PLE e MAE, a variação desses dois fatores podem causar efeitos adversos.

2.2 COMPOSTOS BIOATIVOS

2.2.1 Polifenóis

Dentre os metabólitos secundários presente nas plantas, os mais comumente presentes são os compostos fenólicos ou polifenóis, que são compostos amplamente estudados devido ao seu potencial antioxidante. Esses compostos são comumente encontrados em frutas, legumes, chá, café e vinho, e são responsáveis pelas características sensoriais dos alimentos, como sabor, cor e aroma (VARGAS-RAMELLA et al., 2021).

Eles apresentam em sua estrutura um ou mais anéis aromáticos acoplados a um ou mais grupos hidroxilas e podem variar desde estruturas mais simples, como os ácidos fenólicos, até estruturas complexas como os taninos (ALARA; ABDURAHMAN; UKAEGBU, 2021). Além desses, os compostos fenólicos também podem ser classificados em estilbenos e flavonoides, apresentando ainda subclasses na maioria dos casos (Figura 2.2) (ALARA; ABDURAHMAN; UKAEGBU, 2021).

Figura 2.2. Principais classes dos compostos fenólicos.

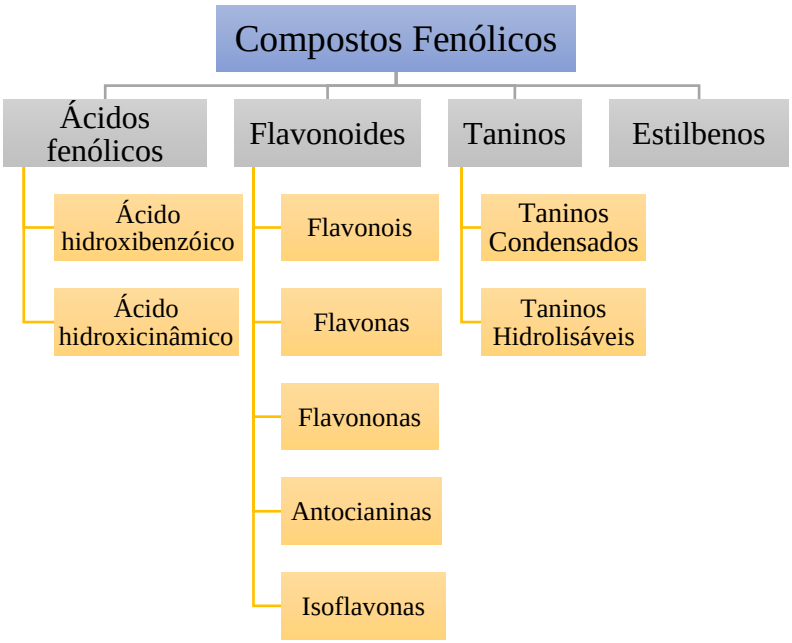

Fonte: Adaptado de Alara; Abdurahman e Ukaegbu (2021)

Os compostos fenólicos são diferenciados pela taxonomia biológica, sendo os ácidos fenólicos compostos por um anel benzeno ligado a uma cadeia carbônica (C_6-C_n), os flavonóis e estilbenos contendo dois anéis benzenos interligados por uma cadeia carbônica (C_6-C_n- C_6), e os taninos, que entram na classificação de fenóis poliméricos [$(C_6)_n$, $(C_6$-$C_3)_n$, e $(C_6$-C_3-$C_6)_n$] (TSIMOGIANNIS; OREOPOULOU, 2019). Dentre os compostos existentes, os mais comumente encontrados nas folhas do *Hibiscus Sabdariffa* L. são: ácido gálico, ácido protocatecuico (PCA), catequina, galato de epicatequina (ECG), ácido elágico, rutina, ácido q-cumárico, ácido ferúlico, quercetina e naringenina.

2.2.2 Ácidos fenólicos

Os ácidos fenólicos compõem o grupo mais proeminente dos polifenóis presentes nas plantas (RASHMI; NEGI, 2020). Eles dividem-se em dois grupos, os ácidos hidroxicinâmicos e os hidroxibenzoicos (Figura 2.3), sendo o primeiro grupo representado pelos ácidos cafeico, *p*-cumárico, ferúlico e sinápico, e presentes em várias matrizes vegetais, como frutas e cereais (OLIVEIRA; BASTOS, 2011). Já os ácidos hidroxibenzóicos constituem uma parte da complexa estrutura dos taninos, e se apresentam em menor quantidade nos vegetais consumidos por humanos; porém podem ser encontrados em alguns produtos fermentados como iogurte,

cerveja e vinho (OLIVEIRA; REIS, 2017). Os ácidos fenólicos são responsáveis por conferir cor, sabor, adstringência e aspereza, além de possuírem propriedades antioxidantes, anti-inflamatórias, imunorreguladoras, antialérgicas, antiaterogênicas, antimicrobianas, antitrombóticas, cardioprotetoras, anticancerígenas e antidiabéticas (RASHMI; NEGI, 2020).

Figura 2.3. Estrutura química dos ácidos fenólicos mais encontrados em matrizes vegetais.

Ácidos fenólicos	Estrutura química
Ácidos hidroxicinâmicos (HCAs)	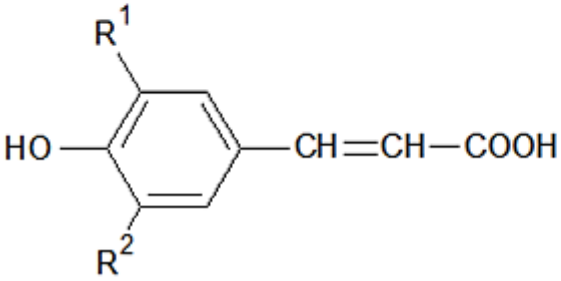

R_1	R_2	Composto
H	H	Ácido p-cumárico
OH	H	Ácido caféico
OCH_3	H	Ácido ferúlico
OCH_3	OCH_3	Ácido sinápico

Ácidos hidroxibenzóicos (HBAs)

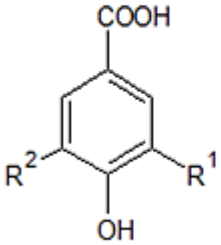

R_1	R_2	Composto
H	H	Ácidos p-hidroxibenzóicos
OH	H	Ácido protocatecuico
OCH_3	H	Ácido vanilico
OCH_3	OCH_3	Ácido Siringico
OH	OH	Ácido gálico

Fonte: Adaptado de Scalzini *et al*. (2021)

Vários autores já identificaram a presença desses compostos em matrizes alimentícias. Cruz *et al*. (2019) analisaram as folhas de yacon através do uso da tecnologia supercrítica utilizando etanol como cossolvente, e encontraram porções quantificáveis de ácido gálico; ácido protocatecuico; ácido clorogênico; ácido cafeico e ácido ferúlico. Nas folhas da manga também foram quantificados ácido gálico, ácido 3,4-diidroxibenzóico e galato de metila, através de extração com líquido pressurizado (FERNÁNDEZ-PONCE et al., 2015). Para as folhas do *Hibiscus sabdariffa* L., alguns autores identificaram a presença de diferentes ácidos fenólicos, como ácido gálico; ácido protocatecuico (PCA); ácido elágico; ácido q-cumárico e ácido ferúlico, através de maceração com etanol 50% durante 3 h (CHEN et al., 2013). Através

da extração assistida por ultrassom com metanol 70 % durante 30 min foram identificados os ácidos neoclorogênico, clorogênico e criptoclorogênico (WANG et al., 2014); enquanto que para maceração com metanol por 24 h (FORMAGIO et al., 2015) e moagem com água (SINGH et al., 2015) os autores quantificaram apenas o ácido gálico.

2.2.3 Flavonoides

Os flavonoides são os principais polifenóis da dieta humana. É uma categoria de compostos fenólicos amplamente distribuída em plantas vasculares, e possuem potentes propriedades antioxidantes e antimicrobianas (ZHANG et al., 2020); além de ações anti-hipertensivas, antiartríticas, anti-inflamatórias, anti-hepatotóxicas e anti-úlceras (ALEXANDRE et al., 2018). De forma geral, são compostos por um núcleo de flavan com 15 átomos de carbono dispostos em 3 anéis. Eles se subdividem em cinco subgrupos, nomeadamente flavonas, flavanonas, flavonóis, antocianinas e isoflavonas (Figura 2.4) (ALARA; ABDURAHMAN; UKAEGBU, 2021). Singh *et al.* (2015) encontraram quantidades consideráveis de flavonoides (402,2 mg/100 g de matéria prima) nas folhas do *Hibiscus Sabdariffa* L., extraídos a partir da folha fresca.

Figura 2.4. Estrutura química das principais classes dos flavonoides.

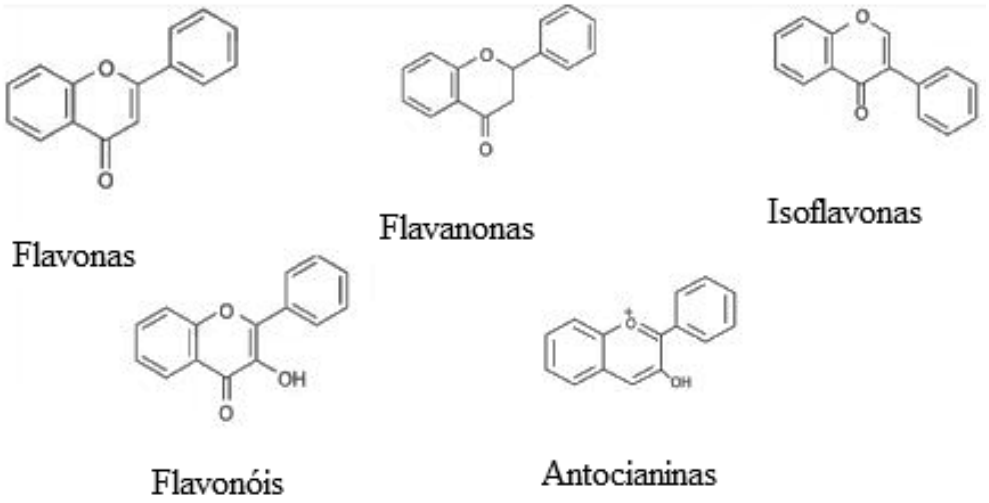

Fonte: Adaptado de Garavand *et al.* (2021)

Os flavonóis constituem a maior classe dos flavonoides, e geralmente apresentam propriedades com maior atividade farmacológica, tanto in vivo quanto in vitro, quando comparados com as outras classes (TONG et al., 2021). Dentre os flavonóis existentes, a quercetina (Figura 2.5) é o mais conhecido, difundido e estudado, estando presente em uma

infinidade de frutas e vegetais (BARRECA et al., 2021). Esse composto possui atividade anticarcinogênicas, antimicrobianas, antidiabéticas e anti-inflamatórias (DUAN et al., 2021). Além da quercetina, também são exemplos de flavonóis a fisetina, galangina, gossipetina, kaempferol, morina, miricetina, e viscidulina, que apresentam, de forma geral, atividades antitumoral, anti-inflamatória, antidiabética, antienvelhecimento, antimicrobiano, antioxidante e efeitos benéficos no sistema cardiovascular.

Figura 2.5. Estrutura química da quercetina.

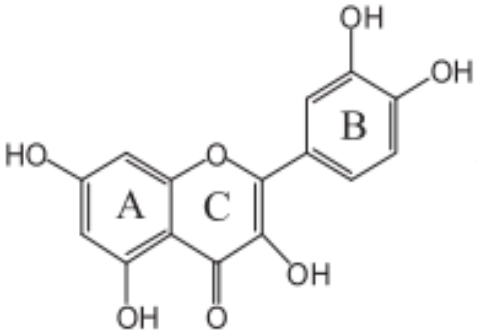

Fonte: Adaptado de Zhang *et al.* (2020)

Alguns autores avaliaram a capacidade antioxidante para extratos do cálice (JABEUR et al., 2017) e das folhas do *Hibiscus Sabdariffa* L., baseado no teor de quercetina (ZHEN et al., 2016). Zhen *et al.* (2016) reportaram ser o composto de maior quantidade nas folhas, quando comparado a outros como ácido neoclorogênico, ácido clorogênico, ácido criptoclorogênico e kaempferol. Karraslan *et al.* (2019) avaliaram o teor de flavonoides presentes nas folhas através de extração em *shaker*, com diferentes solventes acidificados. Os autores observaram resultados variando de 1,05 a 27,7 mg equivalente quercetina/g de extrato seco, sendo o extrato metanólico acidificado o mais rico nesses compostos.

As antocianinas, outra classe dos flavonoides, são as formas glicosídicas das antocianidinas, e responsáveis principalmente pela pigmentação de plantas (GARCIA; BLESSO, 2021), representando pigmentos hidrossolúveis baseados na estrutura do 2-fenilbenzofiril (ALEXANDRE et al., 2018). Analisando o hibisco como um todo (cálice, flores e folhas), diferentes tipos de antocianinas já foram encontrados, como cianidina 3-rutinosídeo, delfinidina 3-sambubiósido, cianidina 3-sambubiósido, cianidina 3-glicosídeo e delfinidina 3-glicosídeo (SINDI; MARSHALL; MORGAN, 2014). Suas estruturas podem ser observadas na Figura 2.6.

Figura 2.6. Estruturas químicas de antocianinas encontradas na *Hibiscus Sabdariffa* L.

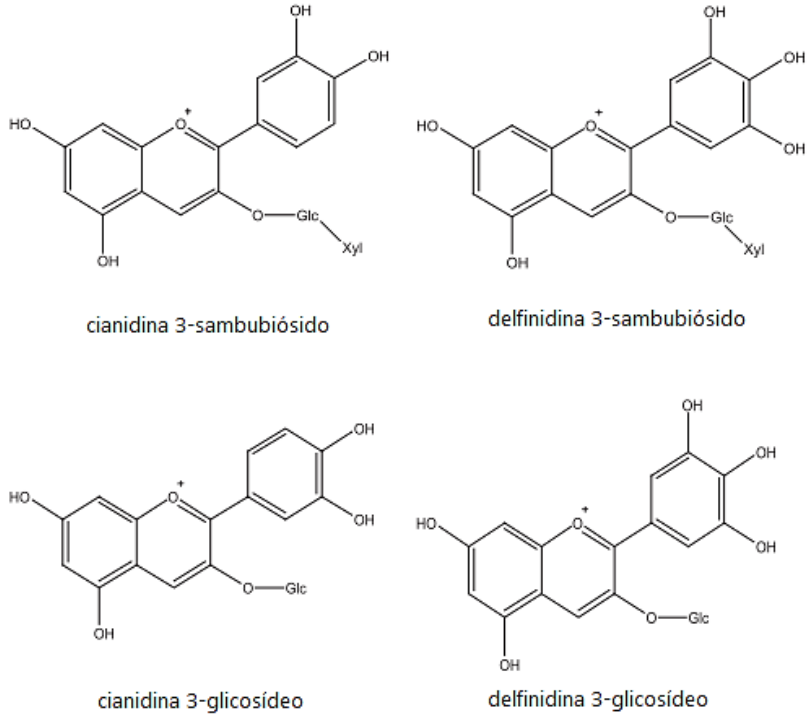

Fonte: Adaptado de Sindi *et al.* (2014)

A quantidade de antocianinas em extratos obtidos a partir das flores do *Hibiscus Sabdariffa* L., (MOURA et al., 2019) e de suas folhas (SINGH et al., 2011, 2015) também foi avaliada. Percebe-se que mesmo que a quantidade encontrada nas flores (0 a 21,03 mg/g de extrato seco) seja relativamente maior, as folhas (0,79 e 0,41 mg de cianidina-3-glicosídeo/g de extrato seco, respectivamente) também são passíveis de utilização.

2.2.4 Taninos

Os taninos são polifenóis adstringentes responsáveis pela precipitação das proteínas (TSIMOGIANNIS; OREOPOULOU, 2019), e são divididos em hidrolisáveis e condensados. Os taninos hidrolisáveis são heteropolímeros compostos por ácidos polifenólicos e seus derivados; enquanto os condensados são flavonoides poliméricos, sendo assim, insolúveis em água (DE HOYOS-MARTÍNEZ et al., 2019). São encontrados amplamente em frutas, sementes, flores e cascas; entretanto, apresentam-se em pequenas quantidades, dificultando assim sua obtenção (GUO et al., 2020).

Vários fatores podem influenciar na obtenção dos taninos, desde o tipo de matéria-prima, como folhas, raízes e sementes, até fatores ambientais como temperatura e luminosidade, atuando diretamente nos métodos de extração. Dessa forma, Lavado *et al.* (2021) analisaram a

quantidade de taninos nas folhas do sobreiro (*Quercus suber* L.) através de extração convencional em diferentes solventes e observaram que as maiores quantidades foram obtidas a partir de soluções hidroalcóolicas (1,35 mg de catequina/100 g de amostra para solução (1:1 água: etanol)). Já Guo *et al*. (2020) realizaram um delineamento experimental para obtenção de taninos a partir da *Coriaria nepalensis*, obtendo na condição ideal 42,81 %, com base na porção de sólidos solúveis absorvida por um padrão de couro cromado em pó. Para as folhas do *Hibiscus Sabdariffa* L. foram encontrados valores diferentes através de maceração (SINGH et al., 2011) e moagem (SINGH et al., 2015), ambos com água, sendo 1,075 e 5,19 mg de ácido tânico/100 g de extrato seco, respectivamente.

2.3 ATIVIDADE ANTIOXIDANTE

A oxidação é um importante processo da vida biológica dos seres vivos, pois atua como fonte de energia. Entretanto, a produção excessiva de radicais livres derivados do processo de oxidação pode danificar as células, provocando relaxamento tecidual, destruição de genes, envelhecimento precoce, além de estarem relacionados com diversas doenças relacionadas ao coração e fígado, doenças neurodegenerativas e câncer em seres humanos (WANG et al., 2022). Assim, como forma de equilibrar esse processo, os compostos antioxidantes atuam diretamente na prevenção do estresse oxidativo (SANTOS et al., 2021). Além disso, os antioxidantes também atuam prolongando a vida útil de um alimento, protegendo sua textura, cor e aroma.

De acordo com Miranda *et al.* (2014), os compostos antioxidantes podem se dividir em enzimáticos, representados pelas enzimas Superóxido Dismutase (SOD), Catalase (CAT) e Glutationa Peroxidase (GPx), e não enzimáticos, onde encontram-se os minerais, vitaminas e polifenóis (Figura 2.7). As plantas contêm uma gama desses compostos, podendo ser usados tanto no processamento e armazenamento dos alimentos além de ser uma forma de promover saúde e bem-estar no consumidor, objetivando o controle de reações oxidativas.

Atualmente, existem mais de 100 ensaios diferentes para determinação da atividade antioxidante. Entretanto, nenhum é capaz de avaliar essa atividade em sua totalidade, devido à complexidade de cada matriz; uma vez que cada método utiliza apenas um composto como rota específica de oxidação. Dessa forma, se faz necessário o uso de múltiplos ensaios para avaliar de forma geral o potencial antioxidante de extratos (HOFMANN, 2019).

Figura 2.7. Classificação dos compostos antioxidantes.

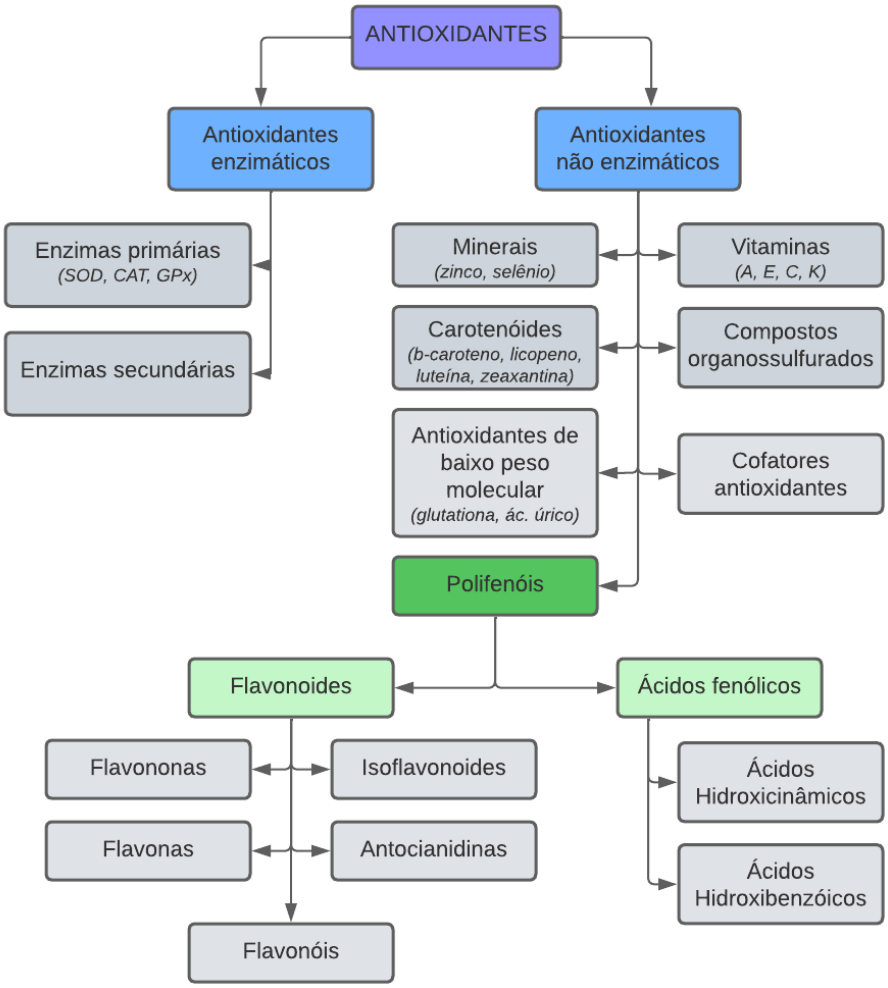

Autor: Adaptado de Miranda *et al.* (2014)

Dentre os ensaios mais comumente utilizados, têm-se os ensaios de eliminação de radicais de ácido 2,20-azino-bis-3-etilbenztiazolina-6-sulfônico (ABTS) e 1,1-difenil-2-picrilhidrazil (DPPH), ensaio de poder antioxidante redutor férrico (FRAP) e ensaio de capacidade de absorção de radicais de oxigênio (ORAC), que se baseam na eliminação de radicais e no potencial redox dos antioxidantes. Esses ensaios também se destacam por serem fáceis e rápidos de reproduzir (CHEDEA; POP, 2019).

Singh *et al.* (2015) observaram a atividade antioxidante por DPPH, das folhas do *Hibiscus Sabdariffa* L., em extratos obtidos por três métodos diferentes e obtiveram valores de até 96 %. Estes valores são considerados altos, quando comparados com outras matrizes ricas em antioxidantes, como uva e beterraba, por exemplo. Milella *et al.* (2019) analisaram a atividade antioxidante por DPPH da pele da uva (*Vitis vinifera* L.), através de extração assistida por ultrassom, e encontrou valores variando de 45 a 63%, e Kushwaha e colaboradores (2017)

encontraram valores variando de 50 a 86 %, aplicando extração aquosa convencional na polpa da beterraba, utilizando o mesmo método. Também para a beterraba, foi encontrada valores próximos a 70 % para a atividade antioxidante por DPPH através de extração etanólica sólido-líquido (EL-BELTAGI et al., 2018). Constata-se, portanto, que as folhas do *Hibiscus Sabdariffa* L., além de serem ricas em diferentes classes de compostos fenólicos, que estes também apresentam alta atividade antioxidante.

2.4 TÉCNICAS DE EXTRAÇÃO

A recuperação de compostos bioativos de matrizes vegetais é realizada através de processos de extração. Entretanto, os métodos convencionais comumente utilizados para a obtenção desses compostos fazem uso de equipamentos e procedimentos que, apesar de mais simples, podem tornar a qualidade dos extratos obtidos questionáveis (PANJA, 2018). Além disso, são geralmente extrações longas que fazem uso de grandes volumes de solventes orgânicos, aumentando o consumo de energia, e consequentemente provocando a degradação de compostos sensíveis, além de gerar elevado impacto ambiental (MENA-GARCÍA et al., 2019). Dentre os existentes, os mais difundidos são a maceração, Soxhlet e hidrodestilação, que ao longo do tempo vêm sendo substituídos por novas tecnologias, devido à busca por processos mais sustentáveis e ambientalmente amigáveis (AGREGÁN et al., 2021).

As novas tecnologias, também conhecidas como tecnologias verdes ou sustentáveis, baseiam-se na obtenção de um processo mais limpo, mais eficiente e menos prejudicial ao meio ambiente (GOULA et al., 2017). Dentre elas têm-se as extrações com alta pressão, como extração com fluido supercrítico (SFE) e extração com líquido pressurizado (PLE), além das extrações assistidas por micro-ondas (MAE), ultrassom (UAE) e enzimas (EAE) (MENA-GARCÍA et al., 2019). Essas tecnologias estão se difundindo largamente por apresentarem vantagens como a utilização de solventes verdes, como CO_2, etanol e água, em quantidades inferiores às convencionais; além de proporcionar alto rendimento em um tempo de operação reduzido (AGREGÁN et al., 2021).

2.4.1 Extração com fluido supercrítico - SFE

Como o próprio nome antecipa, a extração com fluido supercrítico, do inglês *supercritical fluid extraction* (SFE), se baseia na utilização de um fluido em condições de temperatura e pressão acima do seu ponto crítico (Figura 2.8), que é colocado em contato com a matriz contendo os compostos de interesse (CHEMAT et al., 2017).

Figure 2.8. Diagrama de fases esquemático.

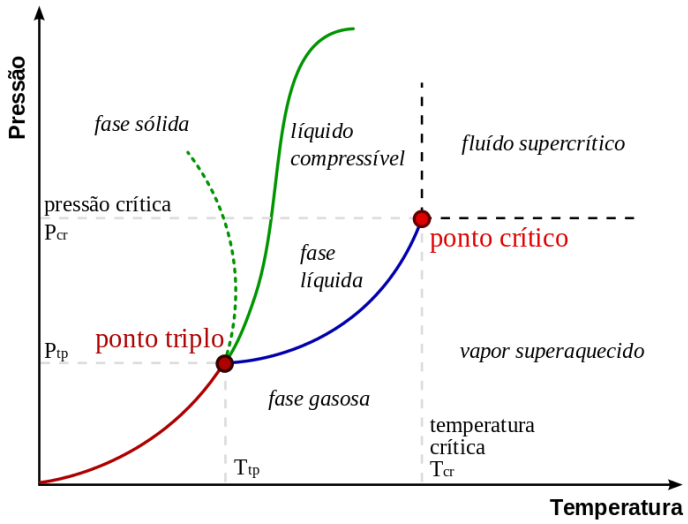

Fonte: Adaptado de Soquetta *et al*. (2018)

O fluido, quando no estado supercrítico alia propriedades de gases e líquidos, como baixa viscosidade, alta densidade e alta difusividade (SILVA; ROCHA-SANTOS; DUARTE, 2015). Essas características conferem aspectos vantajosos a essa técnica, pois possibilitam maior penetrabilidade na matriz e maior poder de solvatação dos compostos, proporcionando assim um maior rendimento em menor tempo. Entretanto, dependendo das condições utilizadas, pode ocasionar degradação de compostos termossensíveis, além de ser uma técnica de alto custo operacional (OKOLIE et al., 2019). Esse processo é dividido em duas etapas: a extração propriamente dita e a separação do soluto do solvente. Na Figura 2.9 observa-se um processo de extração simplificado utilizando CO_2 como fluido supercrítico.

Primeiramente a amostra é colocada no vaso extrator, seguida da preparação do fluido até sua condição supercrítica. O fluido supercrítico passa então pelo leito de extração em uma determinada vazão pelo tempo necessário. Após isso, é realizada a etapa de separação, onde o fluido supercrítico retorna ao estado original, condição na qual o extrato é insolúvel e facilmente separado. Após esse processo, o fluido pode ser descartado ou reciclado para uma nova extração, como demonstrado na Figura 2.9.

Figura 2.9. Esquema simplificado da instalação para extração utilizando CO_2 como fluido supercrítico, sendo (l) estado líquido, (g) estado gasoso e (sc) estado supercrítico.

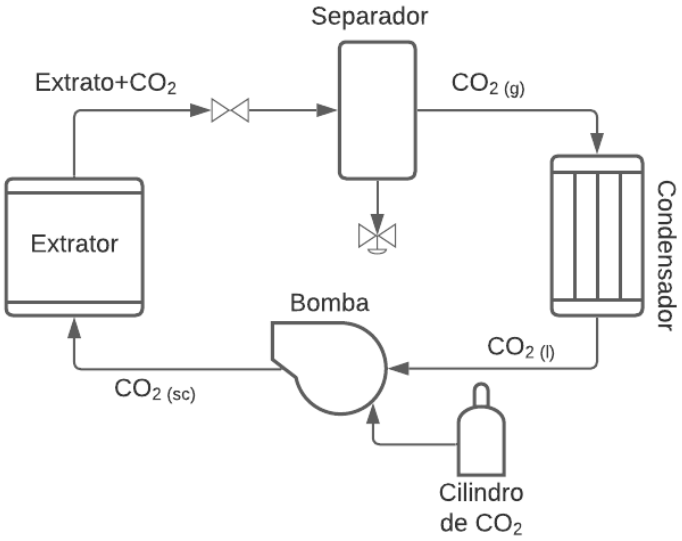

Fonte: Adaptado de Chemat *et al* (2017).

Essa técnica tem sido muito utilizada para extração de óleos voláteis e também para diferentes compostos bioativos, como catequinas de *Camellia Sinensis*, licopeno de tomate, e antocianinas e outros compostos fenólicos de uma grande variedade de plantas (GALLEGO; BUENO; HERRERO, 2019). Quando as substâncias de interesse são apolares ou de polaridade média, o uso de CO_2 supercrítico ($scCO_2$) tem sido bastante difundido. Uma das maiores vantagens da utilização de CO_2, é que a temperatura e pressão necessárias para alcançar o ponto crítico são relativamente brandas (T_c=31 ºC e P_c=7,38 MPa) (OKOLIE et al., 2019) quando comparadas com a da água (T_c=374 ºC e P_c=22,1 MPa), por exemplo (ZHANG et al., 2019). Além disso, é não reativo, não-tóxico, não-inflamável, possui bom poder de solvatação, além de apresentar facilidade de remoção do produto, segurança alimentar (GRAS) e baixo custo (KOVAČEVIĆ et al., 2018).

Contudo, por possuir baixa polaridade, o CO_2 é mais eficiente para extrair compostos apolares de baixo peso molecular (até 1000 g/mol), como carotenoides, triglicerídeos, ácidos graxos e óleos voláteis (CHEMAT et al., 2019). Entretanto, quando o composto de interesse é muito polar o uso de CO_2 é ineficiente, fazendo-se necessária a utilização de cossolventes como etanol e água, que atuam como modificadores de polaridade para aumentar o rendimento da extração (CHEMAT et al., 2019).

Existem na literatura diversos estudos para a obtenção de compostos bioativos de folhas de diferentes matrizes através da aplicação de tecnologias de extração com alta pressão como o

SFE (Tabela 2.4). Fazendo uma comparação entre os estudos que utilizaram folha da amora branca (*Morus Alba*) (SANTOS et al., 2020b) e ora-pro-nóbis (TORRES et al., 2022), é possível observar aproximadamente a mesma quantidade de rendimento global, sendo 1,11 %, a 60 ºC e 200 bar, e 1,78 % a 40 ºC e 250 bar, respectivamente, utilizando apenas CO_2 como solvente. Em outro estudo, fazendo uso do etanol como cossolvente, Cruz e colaboradores (2019) constataram que, na mesma condição (50 ºC e 200 bar), o rendimento global do extrato das folhas de yacon aumentou consideravelmente, partindo de 0,27 % (apenas CO_2) para 3,76 % (2:1 etanol:matéria seca), reforçando assim a ideia de que o mesmo processo pode proporcionar resultados diferentes dependendo não apenas da matriz, mas também das condições de operação, como a adição de cossolventes, que influenciam a densidade do solvente e consequentemente seu poder de solvatação e seletividade.

Outro exemplo dessa eficiência pode ser observado na quantidade de compostos fenólicos obtidos neste estudo (CRUZ et al., 2019), que variou de 16,60 mg EAG/g de extrato utilizando CO_2, para 34,09 mg EAG/g de extrato com CO_2+etanol (2:1 etanol:matéria seca). Entretanto, devido a variabilidade de cada matriz, faz se necessário um estudo mais profundo e individual, para avaliação do quanto uma extração com cossolvente pode ser mais eficaz.

Além disso, muitos trabalhos foram feitos para estudar a viabilidade dessa técnica em comparação com outras técnicas convencionais (CAVALCANTI et al., 2011; VARDANEGA et al., 2019; VARDANEGA; PRADO; MEIRELES, 2014). Extratos de folhas de Guayusa foram obtidos por Soxhlet usando hexano, acetato de etila e etanol como solventes, SFE usando $scCO_2$ e SFE usando $scCO_2$ combinado com etanol (CADENA-CARRERA et al., 2019). Eles observaram que o rendimento do extrato era maior usando Soxhlet ou SFE com $scCO_2$ + etanol. Porém, o primeiro demandou 6 horas de processo, em temperatura de ebulição para cada solvente, enquanto o SFE foi capaz de extrair em apenas 2 horas a 75 ºC. Resultado semelhante foi observado na extração de flavonoides e antioxidantes das folhas da Jujuba (*Ziziphus jujuba Mill.* cv. Junzao), onde o melhor resultado observado foi na utilização de $scCO_2$ + etanol quando comparado com extração por Soxhlet e ultrassom (SONG et al., 2019).

Contudo, além do rendimento da extração e parâmetros energéticos, essa técnica apresenta outras vantagens quando comparada com as convencionais, como o uso reduzido de tempo, solvente e do fator temperatura, que como não necessita ser elevada (dependendo do solvente), consequentemente facilita o manejo de compostos termossensíveis, além de ser um processo intrinsecamente estéril (CHEMAT et al., 2017).

Tabela 2.4. Trabalhos avaliando a quantidade de bioativos presentes em folhas de diferentes matrizes através de tecnologia com alta pressão.

Matéria-prima	Extração por SFE					Rendimento/Melhor condição	Referência
	T (ºC)	P (bar)	t (min)	Vazão	Solvente		
Amora branca *(Morus Alba)*	40-60	150 - 200	120	2 g/min	CO_2	R: 1,11 % (60 ºC e 200 bar) FT: 4,16 mg EAG/g (60 ºC e 200 bar)	Santos *et al*. (2020b)
Bardana *(Arctium lappa)*	80	150	150	2ml/min	CO_2	R: 12,78 % FT: 47,62 mg EAG/g	Souza *et al.* (2019)
Copaíba *(Copaifera sp)*.	40-60	100 - 300	150	4,99 g/min	CO_2	R: 4,00 % (60 ºC e 225 bar)	Botelho *et al.* (2014)
Cravo-da-índia *(Syzygium aromaticum)*	40-60	150 - 220	80	1,99 ml/min	CO_2	R: 1,08 % (40 ºC e 220 bar) FT: 347,37 mg EAG/g (40 ºC e 150 bar)	Frohlicha *et al.*(2019)
Ecalipto *(Eucalyptus)*	40	200; 300	180	12 g/min	CO_2 + Etanol 5 %	R: 3,16 % (200 bar)	Rodrigues *et al.* (2018)
Guayusa *(Ilex guayusa* Loes)	45-75	150 - 250	180	8,33 g/min	CO_2 + Etanol 7 %	R: 6,02 % (75 ºC e 250 bar) FT: 4,04 mg EAG/g (75 ºC e 250 bar)	Cadena-carrera *et al.*(2019)
Guanxuma *(Sida rhombifolia)*	40; 50	200; 300	120	32,33 g/min	CO_2 (etanol na amostra)	R: 1,61 % (50 ºC e 300 bar) FT: 16,46 mg EAG/g (50 ºC e 300 bar)	Ferro *et al*. (2019)
Mamão *(Carica papaya linn)*	40-60	180 - 300	60	3; 4,5; 6 ml/min	CO_2 + Etanol (3; 4 e 5 %)	R: 5,35 % (60 ºC e 180 bar)	Chai *et al*. (2020)
Ora-pro-nóbis	40-60	250	150	19,8 g/min	CO_2	R: 1,78 % (40 ºC)	Torres *et al.*(2022)

(Pereskia aculeata)						FT: 4,90 mg EAG/g (60 ºC)	
Rabanete *(Raphanus sativus)*	35-50	300; 400	180	10 g/min	CO_2 (etanol na amostra)	R: 20 % (35 ºC e 400 bar) FT: 14,55 mg EAG/g (40 ºC e 400 bar)	Goyeneche *et al.* (2018)
Oliveira *(Olea europea)*	55; 80	120; 200	120	10 g/min	CO_2 + Etanol 50 %	R: 9,35 % (55 ºC e 120 bar) FT: 1647,23 ppm (80 ºC e 120 bar)	Bastante *et al.* (2018)
Urtiga *(Urtica dioica)*	40; 60	100 - 300	300	3,33 g/min	CO_2	R: 4,00 % (60 ºC e 300 bar)	Durivc *et al.* (2022)

Matéria-prima	**Extração por PLE**					**Rendimento/Melhor condição**	**Referência**
	T (ºC)	**P (bar)**	**t (min)**	**Fluxo**	**Solvente (%)**		
Bardana *(Arctium lappa)*	80	150	240	2 ml/min	Água; Etanol	R: 40,35 % (Etanol 45 %) FT: 69,03 mg EAG/g (Etanol 45 %)	Reder *et al.* (2019)
Chá-verde *(Camellia sinensis)*	100	100	20	-	Lactato de etila Etanol	R: 20,7 % (Etanol)	Bermejo *et al.* (2015)
Espinheira santa *(Monteverdia aquifolia)*	40-60	100	30	2 ml/min	Etanol 50 Etil acetano n-Hexano	R: 5,3 % (60 ºC e Etanol) FT: 326 mg EAG/g (40 ºC e Etanol)	Alves *et al.* (2022)
Feijoa *(Acca sellowiana)*	40;80	100	50	3 ml/min	Etanol; Água	R: 31 % (80 ºC e Água) FT: 158 mg EAG/g (80 ºC e Água)	Santos *et al.*(2021)
Lúcia-lima *(Lippia citriodora)*	40-180	110	5-20	-	Etanol	R: 62,11	Leyva-Jiménez *et al.* (2018)

Mangaba *(Hancornia speciosa)*	25;60	100	180	1 ml/min	Etanol; Hexano Etil acetato	R: 40 % (60 ºC e Etanol) FT: 347 mg EAG/g (60 ºC e Etanol)	Barbosa *et al*. (2019)
Manga *(Mangifera indica L.)*	60-100	40-200	180	10 g/min	Água; Etanol	R: 38,7 % (Água)	Fernández-ponce *et al*. (2015)
Oliveira *(Olea europea)*	190	-	5	-	Etanol 60	R: 51,55 % FT: 0,339 mmol EAG/g	Lama-Muñoz *et al*.(2020)
Oliveira *(Olea europea)*	50-200	-	5-20	-	Etanol	R: 44% (200 ºC, 5 min, Etanol 50%) FT: 143 mg EAG/g (125 ºC, 20 min, Etanol)	Martín-garcía *et al*.(2020)
Vara-de-ouro *(Solidago virgaurea L.)*	70;140	103	15	-	Hexano; Acetona Água	R: 28,9 % (140 ºC e Etanol 80%) FT: 185 mg EAG/g (17 ºC e acetona)	Kraujaliene *et al*. (2017)

T – Temperatura (ºC); P – Pressão (bar); t – tempo (min); R: Rendimento global (%); FT: Fenólicos Totais; EAG - Equivalente a ácido gálico

2.4.2 Extração com Líquido Pressurizado – PLE

O PLE (do inglês *pressurized liquid extraction*) é outra técnica que surgiu com o objetivo de substituir as técnicas convencionais de extração (SOUZA et al., 2019). Essa técnica também é conhecida por extração acelerada por solvente (ASE), uma vez que permite uma extração mais rápida, utilizando menos solvente, sendo assim considerada como "verde" (MACHADO et al., 2014). Foi introduzida pela primeira vez pela *Dionex Corporation* na Conferência Pittcon em 1995, recebendo a aceitação como um método oficial da Agência de Proteção Ambiental dos EUA (USEPA) para poluentes orgânicos persistentes em amostras sólidas ambientais (ANDREU; PICÓ, 2019).

Para utilização dessa metodologia, faz-se necessário o uso de um equipamento, como demonstrado no esquema Figura 2.10, onde a amostra é disposta na célula extratora, e o sistema é iniciado com aquecimento da célula e pressurização. Assim que as condições de temperatura e pressão escolhidas são atingidas, a válvula pode ser aberta e assim começar a coleta do extrato. Cabe ressaltar que esse método pode ser realizado tanto no modo estático quanto no dinâmico, ou até uma combinação dos dois; não apresentando diferenças significativas quanto ao rendimento (VAZQUEZ-ROIG; PICÓ, 2015).

Figure 2.10. Esquema simplificado da instalação para extração com líquido pressurizado.

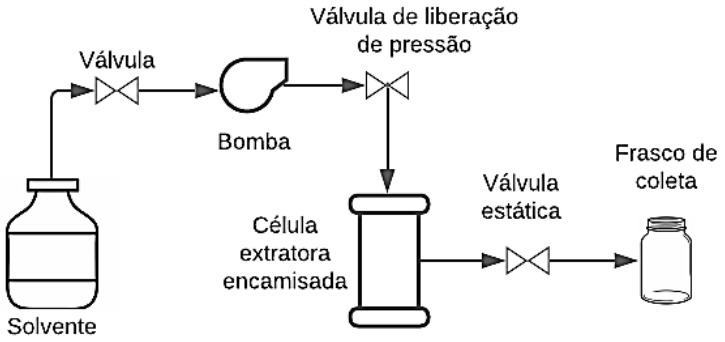

Fonte: Adaptado de Andreu e Picó (ANDREU; PICÓ, 2019)

Comumente são utilizados como solvente a água, metanol, acetona e hexano, em uma faixa de temperatura de 75 °C a 150 °C e uma pressão de 10,4 MPa (OREOPOULOU; TSIMOGIANNIS; OREOPOULOU, 2019), podendo variar até 20,5 MPa (VAZQUEZ-ROIG; PICÓ, 2015). Esses fatores são uma das principais vantagens desse processo, pois esses limites de temperatura e pressão facilitam a extração de compostos em matrizes complexas, exigindo menos tempo e solvente (OLEJAR et al., 2021). A otimização da extração por PLE se dá pela

união dessas duas variáveis de processo, que intensificam a transferência de massa, difusividade e solubilidade dos solutos, gerando quebra nas ligações e na tensão superficial do solvente, permitindo assim que o mesmo penetre na matriz com maior facilidade (HERBST et al., 2021). Entretanto, como a alta pressão é utilizada com o intuito de manter o fluido no seu estado líquido quando o mesmo se encontra acima do seu ponto de ebulição, ela pode se tornar um fator indiferente se a extração for realizada numa pressão suficientemente alta (ANDREU; PICÓ, 2019).

Vários trabalhos foram realizados utilizando essa técnica (Tabela 2.4). Comparando a extração com PLE de compostos das folhas da bardana (SOUZA et al., 2019) e mangaba (BARBOSA et al., 2019), é possível observar rendimento global semelhante, porém em condições diferentes, sendo 40,35 % de rendimento a 80 ºC, 150 bar e etanol 45 % (v/v) e 40 % de rendimento a 60 ºC, 150 bar e etanol puro, respectivamente Outro detalhe importante observado para a bardana, é que com o aumento da concentração do solvente para 88 % (v/v) de etanol, o rendimento teve uma redução de 7,3 %. Santos *et al*. (2021), analisaram a folha da feijoa (*Acca sellowiana*) com temperatura variando entre 40 ºC a 80 ºC, pressão de 10 MPa e utilizando água, etanol e solução etanol:água (50:50 v/v) como solventes. Os autores constataram que o melhor rendimento global (35,1 %) foi obtido à 80 ºC utilizando solução hidroalcoólica, sendo este um comportamento comum, uma vez que a solução possibilita uma maior solvatação dos compostos, quando comparado aos solventes puros (SANTOS et al., 2021). Por sua vez, Ferro *et al*. (2019) avaliaram o rendimento global e de compostos específicos das folhas da guanxuma (*Sida rhombifolia)* através de extração com Soxhlet (hexano), ultrassom (etanol 70 %), fluido supercrítico (CO_2) e líquido pressurizado (etanol 70%) e constataram que dentre as amostras puras, o maior rendimento global (12,34 %) e de compostos fenólicos (62,98 mg EAG/g), foi observado para extração com líquido pressurizado à 80 ºC e 10 MPa. Percebe-se, portanto, que as técnicas de alta pressão (SFE e PLE) são eficientes na recuperação de compostos bioativos de matrizes foliares, uma vez que permitem uma melhor solvatação dos compostos. Porém, as condições operacionais variam em cada caso a depender da matriz e do composto de interesse, sendo necessária uma avaliação mais profunda sobre as melhores condições a serem utilizadas.

2.4.3 Variáveis do processo

De forma geral, vários fatores podem influenciar o rendimento de uma extração realizada a alta pressão, como a temperatura, pressão, tempo de exposição, tamanho das partículas e tipo de solvente, sendo necessário um estudo aprofundado dessas condições em

relação aos compostos de interesse, para que seja obtido um máximo rendimento sem degradação dos compostos (OKOLIE et al., 2019).

Dentre as citadas, a pressão é uma das variáveis de grande importância para extrações com alta pressão. Para o SFE, essa variável se relaciona diretamente com a solubilidade dos compostos da matriz, elevando-a de forma diretamente proporcional, devido ao aumento da densidade do CO_2, conferindo assim um maior poder de solvatação dos compostos. Entretanto, em alguns casos, como para os óleos essenciais, o aumento demasiado da densidade do fluido pode extrair simultaneamente as ceras, dificultando a análise do resultado final (CVJETKO BUBALO et al., 2018). Dessa forma, a pressão e, consequentemente a densidade do fluido, deve ser avaliada para selecionar apenas compostos de interesse solúveis naquela condição. Já para o PLE, a pressão pode ser um fator com menor significância, pois ela é necessária apenas para manter o fluido no seu estado líquido quando ele se encontra acima do seu ponto de ebulição logo, pressões além deste ponto podem não apresentar influência no rendimento da extração (ANDREU; PICÓ, 2019).

Santos *et al.* (2020) estudaram a extração de óleo da semente da favela (*Cnidoscolus quercifolius*) por SFE e observaram que o aumento da pressão até 300 bar a temperatura constante de 60 °C ocasionou o maior rendimento de extração, chegando a 41%. Da mesma forma, à 40 ºC o rendimento partiu de 22,8% (200 bar) para 39,1% (300 bar). Outro trabalho, realizado por Reder *et al.* (2019), avaliou os dois métodos (SFE e PLE) para folha da bardana. Os autores observaram maior rendimento global (40,35 %) para PLE com solução etanólica (45 % v/v), quando comparado com SFE utilizando solução etanólica (1:8 v/v) como cossolvente (9,12 %). Entretanto, apesar da diferença entre o rendimento global, o mesmo não foi observado nos compostos fenólicos, que apresentaram teores semelhantes, sendo 69,03 e 72,32 mg EAG/g de extrato, para PLE e SFE respectivamente, demonstrando assim a maior seletividade do SFE.

A temperatura, por sua vez, pode desempenhar papéis antagônicos, visto que interfere em mais de uma propriedade simultaneamente (densidade, viscosidade e pressão de vapor). Um aumento da temperatura pode aumentar a solubilidade devido ao aumento da pressão de vapor do soluto ocasionado pelo aumento da mobilidade e fricção entre as moléculas. Além disso, provoca também a redução da viscosidade do solvente, proporcionando uma maior difusividade entre as moléculas com consequente aumento do rendimento. Contudo, esse aumento também pode ser prejudicial ao processo de extração, pois uma redução muito intensa da densidade do solvente reduz o poder de solvatação dos compostos. Dessa forma, não é trivial prever sua influência principalmente quando combinada ao efeito da pressão (AHANGARI et al., 2021;

CVJETKO BUBALO et al., 2018). Além disso, temperaturas elevadas podem ocasionar degradação dos compostos, diminuindo a qualidade do extrato obtido (VAZQUEZ-ROIG; PICÓ, 2015). Como pode ser observado no estudo nas folhas da guayusa (*Ilex guayusa Loes.*), onde foi possível quantificar uma maior quantidade de compostos fenólicos a 75 ºC do que 45 ºC, utilizando CO^2 + Etanol como cossolvente. Outro exemplo é a análise das folhas da jujuba (*Ziziphus jujuba Mill*.) por tecnologia supercrítica, na qual o rendimento dos flavonoides cresce com o aumento da temperatura até 55 ºC, e decresce em temperaturas superiores (SONG et al., 2019).

Para análises utilizando líquido pressurizado, as temperaturas mais comumente utilizadas variam entre 50 e 150 ºC, sendo 100 ºC a mais utilizada, pois situa-se acima do ponto de ebulição da maioria dos solventes orgânicos, além de não ser alta o suficiente para danificar os compostos durante a extração (ANDREU; PICÓ, 2019). Um exemplo é o trabalho realizado por Herbst *et al.* (2021) na análise do resíduo da cerveja, na qual os melhores rendimentos foram observados na maior temperatura (120 ºC), mesmo variando as proporções de etanol:água. Resultado similar também foi observado por Santos *et al.* (2021) com as folhas da feijoa, onde foi possível constatar que o aumento da temperatura de 40 ºC para 80 ºC, utilizando etanol, água ou a combinação dos dois como solventes, durante 50 min, proporcionou aumento no rendimento global. Esse aumento pode ser justificado pela redução da viscosidade e tensão de superfície do solvente, que facilita a penetração do solvente na matriz e remoção dos compostos, aumentando assim a taxa de transferência de massa.

A vazão ou fluxo de solvente também é de grande importância, pois sendo muito alto, pode ocorrer uma percolação preferencial, ou seja, o solvente flui em alta velocidade ao redor da matriz, reduzindo assim o contato necessário entre o solvente e os compostos (GALLEGO; BUENO; HERRERO, 2019). Por outro lado, vários autores reportaram que fluxos baixos permitem um maior tempo de residência, ou seja, maior tempo de contato do solvente com a matriz; porém, taxas extremamente baixas geram uma quantidade de solvente insuficiente para extração dos compostos de interesse, resultando assim numa extração insuficiente, tanto utilizando fluido supercrítico (ESSIEN; YOUNG; BAROUTIAN, 2020), quanto líquido pressurizado (ANDRADE et al., 2021).

Em relação ao solvente utilizado, este necessita ter uma polaridade semelhante à dos compostos, para que a extração se torne mais eficiente (VAZQUEZ-ROIG; PICÓ, 2015), pois para o SFE, o CO_2 sendo apolar, a captura de compostos polares seria facilitada apenas com a adição de um cossolvente de polaridade semelhante, como pode ser observado no trabalho de

Herbst *et al.* (2021) com extração por PLE do resíduo da produção de cerveja. Os autores realizaram um ensaio preliminar em Soxhlet, durante 6 h, com o objetivo de avaliar a água, etanol, acetato de etila, n-hexano e acetona como possíveis solventes. Os autores constataram que o rendimento global foi maior, quando realizado uma extração sequencial de água e etanol, variando de 9,6 % a 10,5 % em peso. Isso ocorreu pois houve um aumento da polaridade do solvente, quando comparado com os outros solventes utilizados. Esse resultado foi comparado com extração com líquido pressurizado variando temperatura (60 - 120 ºC) proporção de etanol:água (25 – 75 %) e fluxo (2 – 6 ml/min), observando que o maior rendimento (19,3 %) foi obtido na condição de 120 ºC, 50 % e 6 ml/min.

Após avaliar todos os fatores listados, entender como funciona a cinética da extração é de grande importância, pois atua diretamente na otimização das condições do processo (SANTOS; DA SILVA; DA SILVA, 2020), principalmente quando se objetiva aumento de escala e análise de custos (ESSIEN; YOUNG; BAROUTIAN, 2020). De acordo com Santana *et al.* (2019), a cinética pode se dividir em até 3 fases (Figura 2.11), a primeira é chamada de taxa de extração constante (CER) e representa a transferência de massa constante, controlada pela convecção entre o composto e o solvente.

Figure 2.11. Cinética da extração com fluido supercrítico representada por diferentes curvas de extração geral.

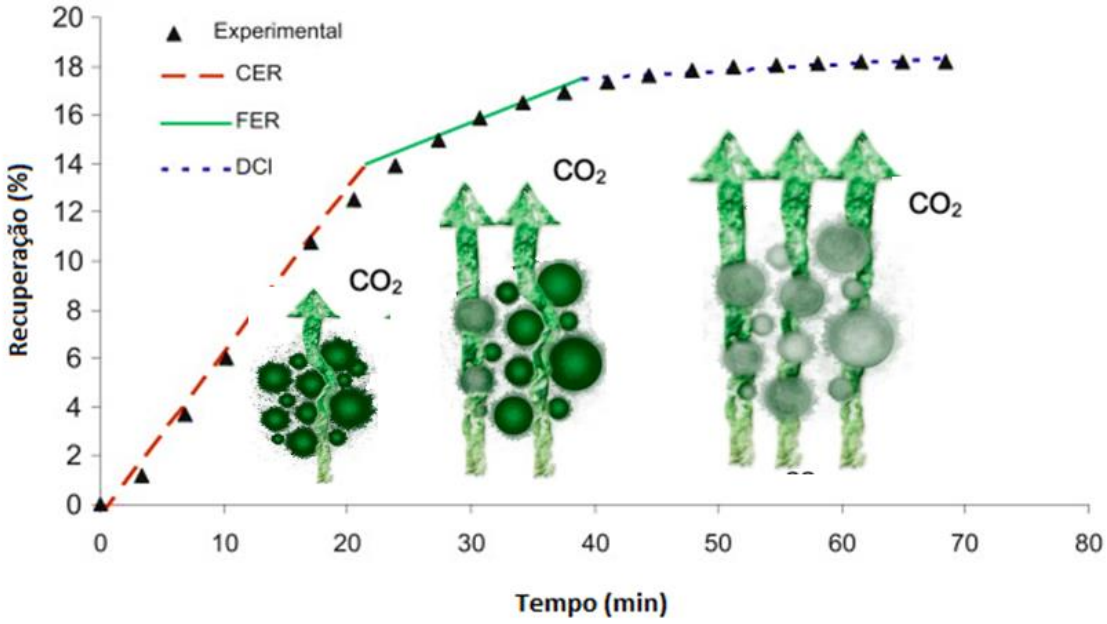

Fonte: Adaptado de Cavalcanti *et al*. (2012) e Silva *et al*. (2015)

A fase CER é seguida pela taxa de extração decrescente (FER), que representa a redução na taxa de obtenção do extrato, ocorrendo tanto transferência de massa interna como externa. Por último, têm-se a fase difusional (DCI), onde a extração se limita apenas à difusão e o solvente encontra-se no interior da célula (SANTOS et al., 2020b).

Além dos que foi citado anteriormente, a curva da cinética pode apresentar inclinações diferentes, como consequência da interação entre o soluto e solvente, e do tamanho das partículas, pois diâmetros pequenos permitem uma melhor transferência de massa do soluto para o solvente, uma vez que possuem uma área de contato maior e os compostos estão mais expostos do que nas partículas maiores, que podem resultar numa penetração ineficiente do solvente (SANTOS et al., 2015). Assim, é de suma importância o conhecimento prévio sobre a influência de cada fator no sistema, bem como a matriz a ser utilizada e os compostos de interesse, uma vez que as interações entre estes podem ocasionar resultados diferentes.

2.5 GEL MISTO (BIGEL)

Sistemas gelificados são utilizados frequentemente na indústria de alimentos como agentes de textura, normalmente fazendo uso de um polissacarídeo ou proteína (BOLLOM; CLARK; ACEVEDO, 2020). Dependendo da fase gelificada, os géis podem ser caracterizados como um hidrogel (solvente polar: água), organogel/oleogel (solvente apolar: líquidos orgânicos e óleos vegetais), ou ainda uma mistura dos dois, conhecida como gel misto, bifásico ou bigel (SAGIRI *et al*., 2014).

2.5.1 Hidrogel

Os hidrogéis apresentam diferentes vantagens pois, além da solubilidade em água, apresentam compatibilidade com uma gama de solventes e por isso, têm sido bastante estudados como veículo para sistemas de liberação de compostos (MARTINS et al., 2019) e modificador de textura (HE et al., 2021). Dentre os agentes gelificantes mais utilizados estão as proteínas do leite, (BOURBON; CERQUEIRA; VICENTE, 2016), como o isolado proteico do soro do leite (do inglês *Whey Protein Isolate* -WPI), que vem sendo estudado ao longo dos anos por diversos autores (BOLLOM; CLARK; ACEVEDO, 2020; KUHN; CAVALLIERI; CUNHA, 2011; SHISHIR et al., 2018).

O WPI é um subproduto oriundo da produção de queijo, e amplamente utilizado na indústria de alimentos devido seu alto valor nutricional, sendo composto principalmente por β-lactoglobulina (β-lg,~65 %) e α-lactalbumina (α-la,~25 %) (JIANG et al., 2021). Além disso, possui propriedades gelificantes, emulsificantes e espumantes, possibilitando a formação de

uma matriz estrutural capaz de reter água, sabores, probióticos e ingredientes alimentares (HE et al., 2021).

O processo de gelificação utilizando WPI pode ser realizado de duas formas, por gelificação à frio e à quente (KUHN; CAVALLIERI; CUNHA, 2011). A gelificação à frio é realizada em duas etapas, tendo primeiro a preparação da solução estoque de WPI, com armazenamento por 24h, para total desnaturação das proteínas, e depois adição de sal ou ajuste de pH, para formação do gel (KUHN; CAVALLIERI; CUNHA, 2011). Dessa forma, as proteínas do soro do leite são desnaturadas em valores de pH distantes do ponto isoelétrico (pI) e em baixa força iônica, e para formação do gel necessitam de complementação – adição de sal ou ajuste de pH - de forma a provocar a ligação entre as proteínas (HAZRATI; MADADLOU, 2021).

O método a quente é realizado em uma etapa, onde é formado uma solução aquosa de WPI, contendo ou não cloreto de sódio, seguido de aquecimento (80ºC) e armazenamento durante 24 h, para assim ser formada a rede de gel (YANG; CHEN; MERCADÉ-PRIETO, 2021). Assim, devido a divisão do processo em duas fases, a gelificação à frio proporciona um gel mais homogêneo, em relação à gelificação a quente, quando no mesmo teor de pH e/ou sal, permitindo também o encapsulamento de compostos sensíveis ao calor (HAZRATI; MADADLOU, 2021).

Além do método, o pH afeta diretamente a formação do gel, podendo gerar uma estrutura opaca, quando formados próximos do ponto isoelétrico (pI), na qual a estrutura consiste de partículas esféricas com diâmetro de várias centenas de nanômetros, ou transparentes, quando situados abaixo ou acima do pI da proteína, onde pode haver formação de fios reticulados (WAGNER et al., 2021).

Diante disso, muitos autores vêm estudando essa matéria-prima visando aplicação em alimentos. Seiwert e colaboradores (2021) estudaram a produção de filmes comestíveis utilizando WPI, e observaram que suas propriedades melhoram com adição de xilana, possibilitando a produção de uma embalagem a partir de dois subprodutos residuais, já Bollom e colaboradores (2020) avaliaram a produção de um bigel utilizando WPI e lecitina de soja e constataram que à baixas concentrações, o hidrogel à base de WPI interage sinergicamente com o oleogel, possibilitando assim futuras aplicações. Hazrati e Madadlou (2021) avaliaram a utilização de bioativos, associados com o WPI, para atuar como gelificantes, e constatou que os ácidos fosfórico, gálico e cítrico provocam alterações na rede de gel, modificando propriedades como tensão compressiva, força e de penetração e capacidade de retenção de água.

2.5.2 Oleogel

Os oleogéis têm recebido bastante atenção na substituição da gordura animal em produtos alimentícios (MARTÍNEZ-MALDONADO et al., 2020; SANTOS et al., 2020a) com intuito de melhorar o seu perfil lipídico e valor nutricional (MARTINS et al., 2019). Além disso, apresentam propriedades físico-químicas interessantes como a termo reversibilidade (CERQUEIRA et al., 2017). Podem ser formados por dois métodos, o direto e indireto. O primeiro consiste na adição do gelificante diretamente na fase oleosa, em temperaturas acima do ponto de derretimento do gelificante, e o segundo, também chamado de método de troca de solventes, é realizado através da modificação da polaridade da fase orgânica, substituindo a fase contínua já existente, pela nova fase, ou seja, substituindo a fase aquosa por uma fase oleosa usando um solvente específico que tenha afinidade tanto para óleo quanto para água, como a acetona, por exemplo (SHAKEEL et al., 2021).

A rede de gel pode ser formada basicamente por dois tipos de gelificantes, os de baixo peso molecular (LMOGs), que foram uma rede de cristal que liga o óleo, e os de alto peso molecular (HMOGs), que são formados por reações químicas e interações físicas(HWANG, 2020), sendo o primeiro a classe onde se encontra o glicerol monostearato (GM) (ZENG et al., 2021).

O GM tem sido utilizado como agente gelificante para a estruturação de óleos comestíveis para uso alimentício, por ser econômico e eficiente em baixas concentrações (TRUJILLO-RAMÍREZ et al., 2018). Além disso, é considerado GRAS pela Administração de Alimentos e Medicamentos dos EUA (CFR 21 - Seção 182.1324) e aprovado pela União Europeia para uso alimentício (EUROPEAN, 2018).

Diante disso, muitos autores vêm estudando esse agente visando aplicação em alimentos. Zheng e colaboradores (2020) avaliaram a produção de um bigel de grau alimentício utilizando k-carragenina e GM, para transporte de β-caroteno. Esse estudo revelou que as propriedades do bigel foram grandemente afetadas pela presença do oleogel, aumentando suas propriedades mecânicas e estabilidade térmica, além de promover uma maior liberação de β-caroteno durante a digestão simulada, sugerindo assim que esses sistemas podem ser boas alternativas para entrega de bioativos lipofílicos.

Outro estudo utilizando GM verificou a sua eficiência, comparando com Sorbitano monostearato (SM), para a produção de um oleogel a base de óleo da semente de chia, e perceberam que as propriedades reológicas e de textura afirmaram que o GM apresenta redes mais fortes e mais resistentes à deformação, do que o SM, fornecendo assim base para a

formulação de oleogéis com propriedades diferentes, de acordo com a aplicação desejada (TRUJILLO-RAMÍREZ et al., 2018).

2.5.3 Bigéis

Os bigéis, por sua vez, são definidos pela literatura como uma mistura de hidrogel e oleogel, podendo apresentar estruturas óleo-em-água, água-em-óleo, mistura de géis coloidais interpenetrados, ou até um gel bicontínuo com características diferentes em cada fase (SHAKEEL *et al*., 2019). Estes sistemas apresentam alta estabilidade, não apresentando separação das fases em armazenamento à temperatura ambiente por longos períodos (LUPI *et al*., 2016), devido ao aprisionamento das fases através de uma complexa rede de gel tridimensional (SINGH *et al*., 2014). Além disso, outro aspecto interessante é a de apresentar simultaneamente as características e propriedades físico-químicas dos dois sistemas formadores (SAGIRI *et al*., 2014), possibilitando o transporte de compostos com diferentes polaridades (BOLLOM; CLARK; ACEVEDO, 2020).

De acordo com Samui *et al.* (2021) os bigeis podem ser formados a partir de dois métodos, podendo ser uma mistura direta do hidrogel com oleogel, seguido de agitação mecânica de baixo e alto cisalhamento, durante determinado tempo, como também a mistura dos dois géis após a preparação, e antes da total gelificação, levando a uma emulsificação à quente das duas fases, usando também agitação mecânica.

Independente da forma de produção do bigel, vários fatores podem influenciar na sua qualidade final, sendo eles o tipo de solvente, tipo e estrutura do hidro-gelificante, concentração dos gelificantes, natureza do óleo-gelificante e a razão hidrogel:oleogel, sendo este o fator de maior importância uma vez que cada combinação formada pode resultar numa rede com propriedades reológicas diferentes (SHAKEEL et al., 2021). Zheng *et al* (2020) analisaram diferentes formulações de bigéis utilizando hidrogel de κ-carragena e oleogéis de monoglicerídeo e observaram que a rigidez e tensão de fratura teve um aumento diretamente proporcional a porcentagem da fase oleosa. Porém, em outro estudo utilizando hidrogel de alginato e oleogéis de cera de abelha, foi constatado que o aumento da fase oleosa no bigel provocou uma redução nos valores de firmeza e espalhabilidade (MARTINS et al., 2019). Logo, constata-se que cada gelificante possui uma forma de atuação diferente, devendo então ser analisado de acordo com o objetivo de produção.

Vários estudos têm sido realizados na área de fármacos e cosméticos visando a liberação controlada de compostos através da utilização de bigéis (BEHERA *et al*., 2015; SAGIRI *et al*., 2014; SINGH *et al*., 2014). Entretanto, só recentemente as pesquisas começaram a explorar o

uso dos géis mistos para aplicações em alimentos. Zheng e colaboradores (2020), desenvolveram géis mistos de grau alimentício com hidrogéis de κ-carragena e oleogéis de monoglicerídeo. Fasolin *et al.* (2021) desenvolveram bigéis a base de goma gelana e gliceril monostearato, possibilitando o uso em alimentos como substitutos de gordura. Outro estudo com bigéis formados a partir de concentrado protéico de soro do leite e combinações de lecitina-ácido esteárico, mostrou a importância da estrutura formada na funcionalidade e estabilidade da estrutura final (BOLLOM; CLARK; ACEVEDO, 2020). No entanto, apesar dos resultados promissores, ainda são necessários estudos para desenvolver e avaliar sistemas para estas aplicações.

REFERÊNCIAS

AGREGÁN, R. et al. Recent advances in the extraction of polyphenols from eggplant and their application in foods. **LWT**, v. 146, n. March, p. 111381, 2021.

AHANGARI, H. et al. Supercritical fluid extraction of seed oils – A short review of current trends. **Trends in Food Science and Technology**, v. 111, n. February, p. 249–260, 2021.

ALARA, O. R.; ABDURAHMAN, N. H.; UKAEGBU, C. I. Extraction of phenolic compounds: A review. **Current Research in Food Science**, v. 4, n. March, p. 200–214, 2021.

ALAÑÓN, M. et al. A novel sustainable approach for the extraction of value-added compounds from Hibiscus sabdariffa L. calyces by natural deep eutectic solvents. **Food Research International,** v. 137, September, 2020.

ALEXANDRE, E. M. C. et al. Emerging technologies to extract high added value compounds from fruit residues: Sub/supercritical, ultrasound-, and enzyme-assisted extractions. **Food Reviews International**, v. 34, n. 6, p. 581–612, 2018.

ALVES, T. P. et al. Improved extraction of bioactive compounds from *Monteverdia aquifolia* leaves by pressurized-liquid and ultrasound-assisted extraction: Yield and chemical composition. **The Journal of Supercritical Fluids**, v. 181, n. March 2021, 2022.

ANDRADE, T. A. et al. Ultrasound-assisted pressurized liquid extraction of anthocyanins from Aronia melanocarpa pomace. **Separation and Purification Technology**, v. 276, n. April, 2021.

ANDREU, V.; PICÓ, Y. Pressurized liquid extraction of organic contaminants in environmental and food samples. **TrAC - Trends in Analytical Chemistry**, v. 118, p. 709–721, 2019.

BALOGUN, M. E. et al. Ameliorative effect of aqueous extract of hibiscus sabdariffa (roselle) on salt-induced hypertension in wistar rats. **PharmacologyOnLine**, v. 2, n. August, p. 247–258, 2019.

BARBOSA, A. M. et al. Separation and Purification Technology Separation of antibacterial biocompounds from *Hancornia speciosa* leaves by a sequential process of pressurized liquid extraction. **Separation and Purification Technology**, v. 222, n. April, p. 390–395, 2019.

BARRECA, D. et al. Food flavonols: Nutraceuticals with complex health benefits and functionalities. **Trends in Food Science and Technology**, n. September 2020, 2021.

BASTANTE, C. C. et al. Characterization of olive leaf extract polyphenols loaded by supercritical solvent impregnation into PET / PP food packaging films. **The Journal of Supercritical Fluids**, v. 140, n. March, p. 196–206, 2018.

BEHERA, B. et al. Physical and mechanical properties of sunflower oil and synthetic polymers based bigels for the delivery of nitroimidazole antibiotic – A therapeutic approach for controlled drug delivery. **European Polymer Journal**, v. 64, p. 253–264, 2015.

BERMEJO, D. V. et al. High catechins/low caffeine powder from green tea leaves by pressurized liquid extraction and supercritical antisolvent precipitation. **Separation and Purification Technology**, v. 148, p. 49–56, 2015.

BOLLOM, M. A.; CLARK, S.; ACEVEDO, N. C. Development and characterization of a novel soy lecithin-stearic acid and whey protein concentrate bigel system for potential edible applications. **Food Hydrocolloids**, p. 105570, 2020.

BOTELHO, J. R. S. et al. Copaíba (*Copaifera sp*.) leaf extracts obtained by CO2 supercritical fluid extraction: Isotherms of global yield, kinetics data, antioxidant activity and neuroprotective effects. **The Journal of Supercritical Fluids**, 2014.

BOURBON, A. I.; CERQUEIRA, M. A.; VICENTE, A. A. Encapsulation and controlled release of bioactive compounds in lactoferrin- glycomacropeptide nanohydrogels: curcumin and caffeine as model compounds**. Journal of Food Engineering**, 2016.

CADENA-CARRERA, S. et al. Biological activity of extracts from guayusa leaves (Ilex guayusa Loes.) obtained by supercritical CO_2 and ethanol as cosolvent. **The Journal of Supercritical Fluids**, v. 152, 2019.

CAVALCANTI, R. N. et al. Supercritical fluid extraction with a modifier of antioxidant compounds from jabuticaba (*Myrciaria cauliflora*) by- products: economic viability. **Procedia Food Science**, v. 1, p. 1672–1678, 2011.

CAVALCANTI, R. N.; MEIRELES, M. A. A. **Fundamentals of Supercritical Fluid Extraction**. [s.l.] Elsevier, 2012. v. 2

CERQUEIRA, M. A. et al. Structural and mechanical properties of organogels: Role of oil and gelator molecular structure. **Food Research International**, v. 96, p. 161–170, 2017.

CHAI, Y. H. et al. Supercritical fluid extraction and solubilization of *Carica papaya linn* . leaves in ternary system with CO_2 + ethanol solvents. **Chemical Engineering Research and Design**, v. 156, p. 31–42, 2020.

CHEDEA, V. S.; POP, R. M. Total Polyphenols Content and Antioxidant DPPH Assays on Biological Samples. In: **Polyphenols in Plants**. 2. ed. [s.l.] Elsevier Inc., 2019. p. 169–183.

CHEMAT, F. et al. Review of Green Food Processing techniques - Preservation, transformation, and extraction. **Innovative Food Science and Emerging Technologies**, v. 41, p. 357–377, 2017.

CHEMAT, F. et al. Green extraction of natural products. Origins, current status, and future challenges. **TrAC - Trends in Analytical Chemistry**, v. 118, p. 248–263, 2019.

CHEN, J. et al. Hibiscus sabdariffa leaf polyphenolic extract inhibits LDL oxidation and foam cell formation involving up-regulation of LXRa / ABCA1 pathway. **Food Chemistry**, v. 141, n. 1, p. 397–406, 2013a.

CHEW, S. Y. et al. Optimization of ultrasonic extraction condition for maximal antioxidant, antimicrobial, and antityrosinase activity from *Hibiscus cannabinus* L. leaves by using the single factor experiment. **Journal of Applied Research on Medicinal and Aromatic Plants**, v. 25, n. 1, p. 100321, 2021.

CLIMACO, G. N; VARDANEGA, R.; FASOLIN, L. H. *Hibiscus sabdariffa* L. leaves as an alternative source of bioactive compounds obtained through high pressure technologies. **The Journal of Supercritical Fluids**, v. 200, n. May, 2023.

CRUZ, P. N. et al. Antioxidant activity and fatty acid profile of yacon leaves extracts obtained by supercritical CO_2 + ethanol solvent. **The Journal of Supercritical Fluids**, v. 146, n. January, p. 55–64, 2019.

CVJETKO BUBALO, M. et al. New perspective in extraction of plant biologically active compounds by green solvents. **Food and Bioproducts Processing**, v. 109, p. 52–73, 2018.

DA-COSTA-ROCHA, I. et al. *Hibiscus sabdariffa L.* – A phytochemical and pharmacological review. **Food Chemistry**, v. 165, p. 424–443, 2014.

DE HOYOS-MARTÍNEZ, P. L. et al. Tannins extraction: A key point for their valorization and cleaner production. **Journal of Cleaner Production**, v. 206, p. 1138–1155, 2019.

DUAN, Y. et al. Genotypic variation of flavonols and antioxidant capacity in broccoli. **Food Chemistry**, v. 338, n. August 2020, 2021.

ĐUROVIC, S. et al. Recovery of biologically active compounds from stinging nettle leaves part I: Supercritical carbon dioxide extraction. **Food Chemistry**, v. 373, n. August 2021, 2022.

EL-BELTAGI, H. S. et al. Evaluation of some chemical constituents, antioxidant, antibacterial and anticancer activities of *beta Vulgaris* L. Root. **Fresenius Environmental Bulletin**, v. 27, n. 9, p. 6369–6378, 2018.

ESSIEN, S. O.; YOUNG, B.; BAROUTIAN, S. Recent advances in subcritical water and supercritical carbon dioxide extraction of bioactive compounds from plant materials. **Trends in Food Science and Technology**, v. 97, n. January, p. 156–169, 2020.

EUROPEAN, C. Commission Regulation of the European Parliament and of the Council as regards food category 17 and the use of food additives in food supplements. No 1333/2008 of 8 October 2018. **Official Journal of the European Union**, n. October, p. 20–30, 2018.

FASOLIN, L. H. et al. Modulating process parameters to change physical properties of bigels for food applications. **Food Structure**, v. 28, n. June 2019, p. 100173, 2021.

FERNÁNDEZ-PONCE, M. T. et al. Use of high-pressure techniques to produce Mangifera indica L. leaf extracts enriched in potent antioxidant phenolic compounds. **Innovative Food Science and Emerging Technologies**, v. 29, p. 94–106, 2015.

FERRO, D. M. et al. Integrated extraction approach to increase the recovery of antioxidant compounds from *Sida rhombifolia* leaves. **The Journal of Supercritical Fluids**, v. 149, p. 10–19, 2019.

FORMAGIO, A. S. N. et al. Phenolic compounds of Hibiscus sabdariffa and influence of organic residues on its antioxidant and antitumoral properties. **Brazilian Journal of Biology**, v. 75, n. 1, p. 69–76, 2015.

FROHLICHA, P. C. et al. Evaluation of the effects of temperature and pressure on the extraction of eugenol from clove (*Syzygium aromaticum*) leaves using supercritical CO_2. **The Journal of Supercritical Fluids**, v. 143, n. September 2018, p. 313–320, 2019.

GALLEGO, R.; BUENO, M.; HERRERO, M. Sub- and supercritical fluid extraction of bioactive compounds from plants, food-by-products, seaweeds and microalgae – An update. **TrAC - Trends in Analytical Chemistry**, v. 116, p. 198–213, 2019.

GARAVAND, F. et al. Encapsulation of phenolic compounds within nano/microemulsion systems: A review. **Food Chemistry**, v. 364, n. April, p. 130376, 2021.

GARCIA, C.; BLESSO, C. N. Antioxidant properties of anthocyanins and their mechanism of action in atherosclerosis. **Free Radical Biology and Medicine**, v. 172, n. March, p. 152–166, 2021.

GONZÁLEZ, M. et al. Ultrasound assisted extraction of bioactive compounds in fresh and freeze-dried *Vitis vinifera cv Tannat* grape pomace. **Food and Bioproducts Processing**, v. 124, p. 378–386, 2020.

GOSAIN, S. et al. Hypolipidemic effect of ethanolic extract from the leaves of *Hibiscus sabdariffa L*. in hyperlipidemic rats. **Acta Poloniae Pharmaceutica**, v. 67, n. 2, p. 179–184, 2010.

GOULA, A. M. et al. Green ultrasound-assisted extraction of carotenoids from pomegranate wastes using vegetable oils. **Ultrasonics Sonochemistry**, v. 34, p. 821–830, 2017.

GOYENECHE, R. et al. Supercritical CO_2 extraction of bioactive compounds from radish leaves: Yield, antioxidant capacity and cytotoxicity. **The Journal of Supercritical Fluids**, v. 135, n. January, p. 78–83, 2018.

GUO, L. et al. Optimization of tannin extraction from *Coriaria nepalensis* bark as a renewable resource for use in tanning. **Industrial Crops and Products**, v. 149, n. January, p. 112360, 2020.

HAZRATI, Z.; MADADLOU, A. Gelation by bioactives: Characteristics of the cold-set whey protein gels made using gallic acid. **International Dairy Journal**, v. 117, p. 104952, 2021.

HE, Z. et al. Heat-induced gel formation by whey protein isolate - *Lycium barbarum* polysaccharides at varying pHs. **Food Hydrocolloids**, v. 115, n. January, 2021.

HERBST, G. et al. Pressurized liquid extraction of brewer's spent grain: Kinetics and crude extracts characterization. **Journal of Industrial and Engineering Chemistry**, v. 102, p. 370–383, 2021.

HOFMANN, T. Structure and Antioxidant Efficiency of Beech (Fagus sylvatica L.) Bark Polyphenols Unraveled by High-Performance Liquid Chromatography/Photodiode Array Detection/Multistage Electrospray Mass Spectrometry and Chemometrics. In: **Polyphenols in Plants**. [s.l: s.n.]. p. 83–109.

HWANG, H.-S. A critical review on structures, health effects, oxidative stability, and sensory properties of oleogels. **Biocatalysts and Agricultural Biotechnology**, v. 26, n. March, p. 101657, 2020.

JABEUR, I. et al. Hibiscus sabdariffa L. as a source of nutrients, bioactive compounds and coloring agents. **Food Research International**, v. 100, n. August, p. 717–723, 2017.

JIANG, L. et al. Acid / alkali shifting of Mesona chinensis polysaccharide-whey protein isolate gels: Characterization and formation mechanism. **Food Chemistry**, v. 355, n. March, p. 129650, 2021.

KARAASLAN, N. M. A comprehensive study about Hibiscus sabdariffa leaves: antioxidant activity, polyphenol profile and macro- and micro-element content. **Chemical Papers**, v. 73, n. 4, p. 791–799, 2019.

KOVAČEVIĆ, D. B. et al. Innovative technologies for the recovery of phytochemicals from *Stevia rebaudiana* Bertoni leaves: A review. **Food Chemistry**, v. 268, n. March, p. 513–521, 2018.

KRAUJALIENE, V.; PUKALSKAS, A.; VENSKUTONIS, P. R. Biorefining of goldenrod (*Solidago virgaurea* L.) leaves by supercritical fluid and pressurized liquid extraction and evaluation of antioxidant properties and main phytochemicals in the fractions and plant material. **Journal of Functional Foods**, v. 37, p. 200–208, 2017.

KUHN, K. R.; CAVALLIERI, Â. L. F.; CUNHA, R. L. DA. Cold-set whey protein-flaxseed gum gels induced by mono or divalent salt addition. **Food hydrocolloids**, v. 25, n. 5, p. 1302–1310, 2011.

KUMAR, S. S. et al. Effect of different drying methods on chlorophyll, ascorbic acid and antioxidant compounds retention of leaves of Hibiscus sabdariffa L. **Journal of the Science of Food and Agriculture**, v. 95, n. 9, p. 1812–1820, 2015.

KUSHWAHA, R. et al. Optimization of Different Variable for Eco-friendly Extraction of Betalains and Phytochemicals from Beetroot Pomace. **Waste and Biomass Valorization**, 2017.

LAMA-MUÑOZ, A. et al. Content of phenolic compounds and mannitol in olive leaves extracts from six Spanish cultivars: Extraction with the Soxhlet method and pressurized liquids. **Food Chemistry**, v. 320, n. September 2019, p. 126626, 2020.

LAVADO, G.; LADERO, L.; CAVA, R. Cork oak (*Quercus suber L.*) leaf extracts potential use as natural antioxidants in cooked meat. **Industrial Crops and Products**, v. 160, n. July 2020, p. 1–9, 2021.

LEYVA-JIMÉNEZ, F. J. et al. Comparative study of conventional and pressurized liquid extraction for recovering bioactive compounds from *Lippia citriodora* leaves. **Food Research International**, v. 109, n. March, p. 213–222, 2018.

LIN, H. H. et al. Hibiscus sabdariffa leaf induces apoptosis of human prostate cancer cells in vitro and in vivo. **Food Chemistry**, v. 132, n. 2, p. 880–891, 2012.

LUPI, F. R. et al. A rheological and microstructural characterization of bigels for cosmetic and pharmaceutical uses. **Materials Science & Engineering**, v. 69, p. 358–365, 2016.

MACHADO, A. P. DA F. et al. Pressurized liquid extraction of bioactive compounds from blackberry (*Rubus fruticosus* L.) residues: a comparison with conventional methods. **FRIN**, p. 9, 2014.

MARTÍN-GARCÍA, B. et al. Box-Behnken experimental design for a green extraction method of phenolic compounds from olive leaves. **Industrial Crops & Products**, v. 154, n. June, p. 112741, 2020.

MARTÍNEZ-MALDONADO, M. A. et al. Effect of high pressure processing on heat-induced gelling capacity of blue crab (*Callinectes sapidus*) meat. **Innovative Food Science and Emerging Technologies**, v. 59, n. May 2019, p. 102253, 2020.

MARTINS, A. J. et al. Hybrid gels: Influence of oleogel/hydrogel ratio on rheological and textural properties. **Food Research International**, v. 116, n. July, p. 1298–1305, 2019.

MENA-GARCÍA, A. et al. Green techniques for extraction of bioactive carbohydrates. **TrAC Trends in Analytical Chemistry**, v. 119, p. 115612, 2019.

MILELLA, R. A. et al. Optimized ultrasonic-assisted extraction of phenolic antioxidants from grape (*Vitis vinifera* L.) skin using response surface methodology. **Journal of Food Science and Technology**, v. 56, n. 10, p. 4417–4428, 2019.

MIRANDA, R. C. DE; SCHIEFERDECKER, M. E. M.; SCHMIDT, S. T. Uso de inquéritos alimentares na avaliação da ingestão de antioxidantes. **Nutrire**, v. 39, n. 1, p. 154–165, 2014.

MOURA, S. C. S. R. DE et al. Release of anthocyanins from the hibiscus extract encapsulated by ionic gelation and application of microparticles in jelly candy. **Food Research International**, v. 121, n. December 2018, p. 542–552, 2019.

MUHAMMAD, U. et al. Effects of Extraction Variables on Pharmacological Activities of Vine Tea Extract (*Ampelopsis grossedentata*). **International Journal of Pharmacology**, v. 14, p. 495–505, 2018.

OKOLIE, C. L. et al. Influence of conventional and recent extraction technologies on physicochemical properties of bioactive macromolecules from natural sources: A review. **Food Research International**, v. 116, p. 827–839, 2019.

OLEJAR, K. J. et al. Thermo-chemical conversion of cannabis biomass and extraction by pressurized liquid extraction for the isolation of cannabidiol. **Industrial Crops and Products**, v. 170, n. April, p. 113771, 2021.

OLIVEIRA, D. M. DE; BASTOS, D. H. M. BIODISPONIBILIDADE DE ÁCIDOS FENÓLICOS. **Química Nova**, v. 34, n. 6, p. 1051–1056, 2011.

OLIVEIRA, P. H. R. DE; REIS, R. R. Ácido Benzóico (CAS 65-85-0). **Revista Virtual de Quimica**, v. 9, n. 6, p. 2673–2687, 2017.

OREOPOULOU, A.; TSIMOGIANNIS, D.; OREOPOULOU, V. Extraction of Polyphenols From Aromatic and Medicinal Plants: An Overview of the Methods and the Effect of Extraction Parameters. In: **Polyphenols in Plants**. 2. ed. [s.l.] Elsevier Inc., 2019. p. 243–259.

PANJA, P. Green extraction methods of food polyphenols from vegetable materials. **Current Opinion in Food Science**, v. 23, p. 173–182, 2018.

PERALTA, J. et al. Aqueous hibiscus extract as a potential natural pH indicator incorporated in natural polymeric films. **Food Packaging and Shelf Life**, v. 19, n. December 2018, p. 47–55, 2019.

RAGHU, K.; NAIDOO, Y.; DEWIR, Y. H. Secretory structures in the leaves of Hibiscus sabdariffa L. **South African Journal of Botany**, v. 121, p. 16–25, 2019.

RASHEED, D. M. et al. Comparative analysis of Hibiscus sabdariffa (roselle) hot and cold extracts in respect to their potential for α -glucosidase inhibition. **Food Chemistry**, v. 250, n. January, p. 236–244, 2018.

RASHMI, H. B.; NEGI, P. S. Phenolic acids from vegetables: A review on processing stability and health benefits. **Food Research International**, v. 136, n. April, p. 109298, 2020.

RODRIGUES, V. H.; MELO, M. M. R. DE; SILVA, C. M. Extraction of Eucalyptus leaves using solvents of distinct polarity. Cluster analysis and extracts characterization. **The Journal of Supercritical Fluids**, v. 135, n. January, p. 263–274, 2018.

SAGIRI, S. S. et al. Stearate organogel-gelatin Hydrogel based bigels: Physicochemical, thermal, mechanical characterizations and in vitro drug delivery applications. **Journal of the Mechanical Behavior of Biomedical Materials**, 2014.

SAMUI, T. et al. The development and characterization of novel in-situ bigel formulation. **Food Hydrocolloids**, v. 113, n. June 2020, p. 106416, 2021.

SANTANA, Á. L. et al. Pressurized liquid- and supercritical fluid extraction of crude and waste seeds of guarana (*Paullinia cupana*): Obtaining of bioactive compounds and mathematical modeling. **Food and Bioproducts Processing**, v. 117, p. 194–202, 2019.

SANTOS, M. DOS et al. Emulsion gels based on pork skin and dietary fibers as animal fat replacers in meat emulsions: An adding value strategy to byproducts. **LWT**, v. 120, n. August 2019, p. 108895, 2020a.

SANTOS, K. A. et al. Extraction of Morus alba leaves using supercritical CO2 and ultrasound-assisted solvent: Evaluation of β-sitosterol content. **Journal of Supercritical Fluids**, v. 159, 2020b.

SANTOS, K. A.; DA SILVA, E. A.; DA SILVA, C. Supercritical CO_2 extraction of favela (*Cnidoscolus quercifolius*) seed oil: Yield, composition, antioxidant activity, and mathematical modeling. **Journal of Supercritical Fluids**, v. 165, 2020.

SANTOS, P. et al. Supercritical carbon dioxide extraction of capsaicinoids from malagueta pepper (*Capsicum frutescens* L.) assisted by ultrasound. **Ultrasonics Sonochemistry**, v. 22, p. 78–88, 2015.

SANTOS, P. H. et al. Antioxidant and antibacterial compounds from feijoa leaf extracts obtained by pressurized liquid extraction and supercritical fluid extraction. **Food Chemistry**, v. 344, n. April 2020, p. 128620, 2021.

SCALZINI, G. et al. Effect of withering process on the evolution of phenolic acids in winegrapes: A systematic review. **Trends in Food Science & Technology**, v. 116, n. August, p. 545–558, 2021.

SCHIASSI, M. C. E. V. et al. Fruits from the Brazilian Cerrado region: Physico-chemical characterization, bioactive compounds, antioxidant activities, and sensory evaluation. **Food Chemistry**, v. 245, p. 305–311, 2018.

SEIWERT, K. et al. Development and characterization of whey protein isolate and xylan composite films with and without enzymatic crosslinking. **Food Hydrocolloids**, v. 120, n. May, 2021.

SHAKEEL, A. et al. Key characteristics and modelling of bigels systems: A review. **Materials Science & Engineering**, v. 97, n. February 2018, p. 932–953, 2019.

SHAKEEL, A. et al. Bigels and multi-component organogels: An overview from rheological perspective. **Food Hydrocolloids**, v. 111, n. July 2020, p. 106190, 2021.

SHISHIR, M. R. I. et al. Advances in micro and nano-encapsulation of bioactive compounds using biopolymer and lipid-based transporters. **Trends in Food Science & Technology**, 2018.

SILVA, R. P. F. F.; ROCHA-SANTOS, T. A. P.; DUARTE, A. C. Supercritical fluid extraction of bioactive compounds. **Trends in Analytical Chemistry**, 2015.

SINDI, H. A.; MARSHALL, L. J.; MORGAN, M. R. A. Comparative chemical and biochemical analysis of extracts of Hibiscus sabdariffa. **Food Chemistry**, v. 164, p. 23–29, 2014.

SINGH, S. et al. Estimation of proximate composition, micronutrients and phytochemical compounds in traditional vegetables from Andaman and Nicobar Islands. **International Journal of Food Science and Nutrition**, v. 62, n. November, p. 765–773, 2011.

SINGH, S. et al. Changes in phytochemicals, anti-nutrients and antioxidant activity in leafy vegetables by microwave boiling with normal and 5% NaCl solution. **Food Chemistry**, v. 176, p. 244–253, 2015.

SINGH, V. K. et al. Preparation and characterization of novel carbopol based bigels for topical delivery of metronidazole for the treatment of bacterial vaginosis. **Materials Science and Engineering**, v. 44, p. 151–158, 2014.

SONG, L. et al. Supercritical CO2 fluid extraction of flavonoid compounds from Xinjiang jujube (*Ziziphus jujuba Mill*.) leaves and associated biological activities and flavonoid compositions. **Industrial Crops & Products**, v. 139, n. June, p. 111508, 2019.

SOQUETTA, M. B.; TERRA, L. DE M.; BASTOS, C. P. Green technologies for the extraction of bioactive compounds in fruits and vegetables. **CYTA - Journal of Food**, v. 16, n. 1, p. 400–412, 2018.

SOUZA, A. R. C. DE et al. Assessment of composition and biological activity of *Arctium lappa* leaves extracts obtained with pressurized liquid and supercritical CO_2 extraction**. The Journal of Supercritical Fluids**, v. 152, p. 104573, 2019.

SUBHASWARAJ, P. et al. Determination of antioxidant activity of *Hibiscus sabdariffa* and *Croton caudatus* in *Saccharomyces cerevisiae* model system. **Journal of Food Science and Technology**, v. 54, n. 9, p. 2728–2736, 2017.

TONG, C. et al. Shining natural flavonols in sensing and bioimaging. **TrAC - Trends in Analytical Chemistry**, v. 137, p. 116222, 2021.

TORRES, T. M. S. et al. Neuroprotective potential of extracts from leaves of ora-pro-nobis (*Pereskia aculeata*) recovered by clean compressed fluids. **The Journal of Supercritical Fluids**, v. 179, n. May 2021, 2022.

TRUJILLO-RAMÍREZ, D. et al. Cooling rate, sorbitan and glyceryl monostearate gelators elicit different microstructural, viscoelastic and textural properties in chia seed oleogels. **Food Research International**, n. October, p. 0–1, 2018.

TSIMOGIANNIS, D.; OREOPOULOU, V. Classification of Phenolic Compounds in Plants. In: **Polyphenols in Plants**. [s.l.] Elsevier Inc., 2019. p. 263–284.

VARDANEGA, R. et al. Selective extraction of bioactive compounds from annatto seeds by sequential supercritical CO_2 process. **The Journal of Supercritical Fluids**, v. 150, p. 122–127, 2019.

VARDANEGA, R.; PRADO, J. M.; MEIRELES, M. A. A. Adding value to agri-food residues by means of supercritical technology. **The Journal of Supercritical Fluids**, 2014.

VARGAS-RAMELLA, M. et al. Impact of pulsed light processing technology on phenolic compounds of fruits and vegetables. **Trends in Food Science & Technology**, v. 115, n. April, p. 1–11, 2021.

VAZQUEZ-ROIG, P.; PICÓ, Y. Pressurized liquid extraction of organic contaminants in environmental and food samples. **Trends in Analytical Chemistry**, v. 71, p. 55–64, 2015.

WAGNER, J. et al. Effect of ethanol on the microstructure and rheological properties of whey proteins: Acid-induced cold gelation. **LWT**, v. 139, n. November 2020, p. 110518, 2021.

WANG, F. et al. Research on structure and antioxidant activity of polysaccharides from Ginkgo biloba leaves. **Journal of Molecular Structure**, v. 1252, p. 132185, 2022.

WANG, J. et al. Antioxidant activity of leaf extracts from different *Hibiscus Sabdariffa* accessions and simultaneous determination five major antioxidant compounds by LC-Q-TOF-MS. **Molecules**, v. 19, n. 12, p. 12226–12238, 2014.

YANG, B.; CHEN, X. D.; MERCADÉ-PRIETO, R. Stress relaxation of particulate whey protein hydrogels. **Food Hydrocolloids**, v. 118, n. March, 2021.

ZENG, L. et al. Recent advances of organogels: from fabrications and functions to applications. **Progress in Organic Coatings**, v. 159, n. March, p. 106417, 2021.

ZHANG, J. et al. Recent advances in the extraction of bioactive compounds with subcritical water: A review. **Trends in Food Science & Technology**, 2019.

ZHANG, N. et al. Structure and functional properties of active packaging films prepared by incorporating different flavonols into chitosan-based matrix. **International Journal of Biological Macromolecules**, v. 165, p. 625–634, 2020.

ZHEN, J. et al. Phytochemistry, antioxidant capacity, total phenolic content and anti-inflammatory activity of *Hibiscus sabdariffa* leaves. **Food Chemistry**, v. 190, p. 673–680, 2016.

ZHENG, H. et al. Development of food-grade bigels based on κ-carrageenan hydrogel and monoglyceride oleogels as carriers for β-carotene: Roles of oleogel fraction. **Food Hydrocolloids**, v. 105, n. February, p. 105855, 2020.

CAPÍTULO 3.

Hibiscus Sabdariffa L. leaves as an alternative source of bioactive compounds obtained through high pressure technologies

Artigo publicado na revista *Journal of Supercritical Fluids, v.200 (2023), 105968*

3. *HIBISCUS SABDARIFFA* L. LEAVES AS AN ALTERNATIVE SOURCE OF BIOACTIVE COMPOUNDS OBTAINED THROUGH HIGH PRESSURE TECHNOLOGIES

Gabrielli Nunes Clímaco[1], Renata Vardanega[2]; Luiz Henrique Fasolin[1,*]

[1]Department of Food Engineering and Technology, School of Food Engineering, University of Campinas, CEP 13083-862, Campinas, SP, Brazil
[2]Centre of Biological Engineering, University of Minho, 4710-057 Braga, Portugal

[*]Corresponding author: lfasolin@unicamp.br

ABSTRACT

The aim of the present study was to obtain bioactive compounds from hibiscus leaves through supercritical fluid extraction (SFE) and pressurized liquid extraction (PLE). For SFE, temperature, pressure, and co-solvent were evaluated on extraction yield (X0), content of bioactive compounds and antioxidant activity (AA). For PLE, temperature and solvent composition were evaluated on the same responses. The highest X0 was observed at 60 °C, 300 bar and 15% of co-solvent for SFE, and at 100 °C and ethanol 75% for PLE. For bioactive compounds, different results were observed. For SFE, the best condition was at 60 ºC, 100 bar and 15% of co-solvent, and for PLE at 80 ºC with ethanol 99.5%. Regarding AA, SFE extracts presented highest values at 60 ºC, 100 bar and 5% of co-solvent while PLE presented better results at 60 °C and 99.5%. Chlorogenic acid and quercetin were the main compounds identified in the extracts.

Keywords: Hibiscus; supercritical fluid extraction; pressurized liquid extraction; antioxidant activity; phenolic compounds

3.1 INTRODUCTION

Hibiscus (*Hibiscus sabdariffa* L.) is an herbaceous plant available during the whole year and widely cultivated in many areas, including Central America and Africa. The hibiscus calyx is commercialized dried or in natura and it is known for having beneficial biological properties, such as antihypertensive and anticancer effects [1]. Due to its exotic flavor, the hibiscus calyxes are used in different food products, such as wine, jam, ice cream, chocolates, puddings, and cakes besides the preparation of herbal drinks, hot, cold or fermented drinks [2]. On the other hand, its leaves are consumed only as a green leafy vegetable and are considered a by-product [1], despite they correspond to the majority of the plant [3] and may have significant or even higher amounts of bioactive compounds when compared to the calyx and flowers [4]. The use of hibiscus leaves as a source of bioactive compounds can meet the growing demand for natural additives in functional products, in addition to the advantage of being a low-cost material [5].

Several authors quantified phenolic compounds from hibiscus leaves using different methods. Aqueous extraction by milling resulted in an extract containing 2.35 mg of gallic acid equivalent (GAE)/g of dry extract [6] against 14 mg GAE/g of dry extract obtained by maceration with water [7]. When an acidic solution was used as solvent for the extraction using a shaker, it was observed an improvement on the content these compounds (15.7 mg GAE/g of dry extract) [8]. Moreover, for ultrasound-assisted extraction using methanol as solvent, the phenolic compounds content reached 29.9 mg GAE/g of dry extract [3].

The main phenolic compounds found in the hibiscus leaves extracts include protocatechuic acid (PCA), catechin, epicatechin gallate (ECG), quercetin, naringenin, [9], chlorophyll, ascorbic acid [10], neochlorogenic acid, gallic acid, chlorogenic, and cryptochlorogenic [3]. In addition, tannins have been reported as a prevailing fraction among the phenolic compounds present in the hibiscus leaves [6,7]. The presence of these bioactive compounds confers antioxidant, hypoglycemic and hypolipidemic effects to the hibiscus leaves extract [9]. Moreover, it was observed higher antioxidant activity in the leaves when compared with the calyx [11]. Besides that, comparing with other food matrices such as beet [12], grape [13] and araçá [14], the hibiscus leaves also present higher antioxidants activity, mainly related to the high content of phenolic compounds and tannins [6].

Such secondary metabolites composition and their biological activity meets consumers' desire for natural products, which, in some way, promote health and well-being [5]. Furthermore, the use of by-products to obtain such bioactive compounds is advantageous for

the environment once the levels of residue disposed is reduced. In this way, the biorefinery concept has emerged in recent years to promote the complete exploration of a raw material. The use of all fractions of the food matrices is of great importance, since it allows obtaining a wide variety of value-added products, in addition to reducing waste generation [15]. Promoting the biorefinery concept corroborates the United Nations Sustainable Development Goals (SDGs) [16] that have a great appeal to overcome the sustainably challenges, since one of its objectives include the use of sustainable patterns of production and consumption (SGD 12). Moreover, in 2011 the water-energy-food nexus (WEF) proposal was discussed for the first time in Bonn, Germany. This nexus aims to improve the study of the interactions of the subsystems of water, energy and food, from the consequences observed in the climate change to the food production chain [17].

Thus, the recovery of compounds from hibiscus leaves represents a way of fully explore the raw material, however, there are still few studies about the utilization of the leaves as a source of bioactive compounds, reporting only the use of conventional solid-liquid extraction processes [3,9]. Alternative processes of extraction and preservation of the properties of the bioactive compounds have been studied in the last decade, aiming at increasing safety for the consumer and minimizing the environmental impact [18–20]. These new processes, also known as green or sustainable technologies, are based on achieving a process that is cleaner, more efficient and less harmful to the environment [18]. Among them, high pressure techniques such as supercritical fluid extraction (SFE) and pressurized liquid extraction (PLE) have raised as promising alternatives to the conventional ones.

SFE is based on the use of a fluid in conditions of temperature and pressure above its critical point [21]. At this condition, the supercritical fluid combines properties of gases and liquids, such as low viscosity, high density and, improved diffusivity [22]. Therefore, the mixture of these qualities found in gases and liquids promotes a fluid with density and diffusivity capable of greater penetration into the matrix and solvation of the compounds, thus providing greater yield in less time. This technique has been widely used for the extraction of volatile oils and also for different bioactive compounds, such as catechins from Camellia Sinensis [23], lycopene from tomato [24], and anthocyanins and other phenolic compounds from a wide variety of plants. [25].

One of the most commonly used fluids in SFE is CO_2, since it is non-reactive, non-toxic, non-flammable, has good solvating power, is easy to remove from the product, is generally recognized as safe (GRAS) and has low cost [26]. In addition, the temperature and

pressure required to reach the critical point are relatively mild (Tc=31 °C and Pc=7.38 MPa) [22] when compared to other solvents. However, due to its low polarity, CO_2 is more efficient to extract nonpolar compounds of low molecular weight (up to 1000 g/mol), such as carotenoids, triglycerides, fatty acids and volatile oils [27]. Thus, in order to obtain polar compounds, it is necessary to use co-solvents such as ethanol and water, which act as polarity modifiers to increase the extraction yield [27].

PLE is another technique that emerged with the aim of replacing conventional extraction techniques [28]. It is a continuous process that allows faster extraction using less solvent [29]. This technique works at high temperatures that combined with high pressure, provide the extraction of compounds from complex matrices, requiring less time and solvent [30,31]. The optimization of the extraction by PLE occurs by the union of these two variables, which intensify the mass transfer, diffusivity, and solubility of the solutes. These severe conditions promote interactions inside the cell to reduce the surface tension of the solvent, thus allowing it to easier penetrate the matrix [32]. Several works have been carried out using this technique to obtaining bioactive compounds from different matrices, such as burdock [33], mangaba [34] and feijoa leaves [35]. A comparison between the overall yield and phenolic compounds of guanxuma (Sida rhombifolia) leaves through extraction with Soxhlet (hexane), ultrasound (70% ethanol), supercritical fluid (CO_2) and pressurized liquid (70% ethanol) found that the best results were observed for extraction with pressurized liquid at 80 ºC and 10 MPa [36]. So, regardless of the extractive method, operating conditions may vary in each case depending on the matrix and the compound of interest, requiring a deeper evaluation of the best conditions to be used.

Therefore, the aim of this work was to explore hibiscus leaves as a potential source of bioactive compounds, extracted by sustainable high-pressure techniques, namely SFE and PLE. The extracts were characterized regarding the extraction yield, chemical composition, and antioxidant activity, in addition to the identification of some of the bioactive compounds of the extracts.

3.2 MATERIALS AND METHODS

Raw materials

Fresh hibiscus (*Hibiscus sabdariffa* L.) leaves were obtained from the Centro de Abastecimento de Campinas – CEASA (Campinas, Brazil), washed with tap water, sanitized in 200 ppm chlorinated water and dried at room temperature with forced air circulation for 48 h.

After drying, the leaves were ground in a knife mill (Marconi, MA-340, Piracicaba, Brazil), stored at -18 °C in hermetical bags and protected from light. The solvents used in the extractions were CO2 (99.95% purity, White Martins, São Paulo, Brazil), 99.95% absolute ethanol (Sinergia, São Paulo, Brazil) and distilled water.

Raw material characterization

Moisture was determined by the distillation method with xylol immiscible solvent (JACOBS, 1973), due to the possible presence of volatile compounds. For determination, 25 g of ground material and 100 ml of xylol (P.A., Ecibra, Brazil) were used in a 250 ml volumetric flask. The system was boiled and refluxed for 15 h. After cooling, the volume of water in the collection tube was measured. The experiment was performed in duplicate. The material moisture, expressed as a percentage (% wet basis), was calculated by Equation 1.

$$U = \frac{V_{H_2O} * \rho_{H_2O}}{m} \qquad \text{Equation 1}$$

where V_{H2O} is the volume of water in the collection tube, ρ_{H2O} is the density of water, and m is the mass of the ground sample.

The particle size distribution of the milled leaves was determined by separating particles from 50 g of sample. For this, a set of sieves from the Tyler series (W.S. Tyler, USA) with openings of meshes 10 (2.00 mm), 14 (1.41 mm), 18 (1.00 mm), 25 (0. 71 mm), 50 (0.297 mm) and 80 (0.180 mm) were used with mechanical agitation in a magnetic stirrer (Marconi, MA420, Brazil), for 15 min. The mean particle diameter was determined according to the methodology recommended by the American Society of Agricultural Engineers ASAE (1993) (Equation 2).

$$d_{gw} = log^{-1}\left(\frac{\sum_{i=1}^{n} w_i log\, D_i}{\sum_{i=1}^{n} w_i}\right) \qquad \text{Equation 2}$$

where $D_i = (d_i * d_{i+1})^{0,5}$; d_i is nominal opening of the i-th sieve (mm); $d_{(i+1)}$ nominal sieve opening greater than the i-th sieve (mm); w_i is the mass of material retained on the i-th sieve.

The determination of the real density (d_r) was performed using helium gas pycnometry technique. The bed apparent density (d_a) was determined by the ratio between the amount of sample (M_t) necessary to completely fulfill the extractor cell and the volume of the extractor cell (V_t) (Equation 3). The porosity of the bed (ε) was calculated from the data on the actual density of the particles and the bed apparent density (Equation 4).

$$d_a = \frac{M_t}{V_t} \quad \text{Equation 3}$$

$$\varepsilon = 1 - \left(\frac{d_a}{d_r}\right) \quad \text{Equation 4}$$

Maceration

For maceration, 10 g of ground sample was mixed with 60 mL of 99.5% ethanol, macerated for 3 min at room temperature and left to rest for 24 h. Afterwards, the extracts were filtered through filter paper and stored at -18 °C for further analysis. The overall extraction yield (X_0) and content of specific compounds (phenolics, flavonoids, and tannins) and antioxidant activity were evaluated as response variables.

Supercritical Fluid Extraction – SFE

All SFE experiments were performed in the laboratory scale SFE unit (MV-10 ASFE System, Waters, USA). A 2 × 4 × 2 full factorial design was carried out totaling 16 experiments. The independent variables were temperature (40 and 60 ºC), pressure (100, 175, 250 and 300 bar) and proportion of co-solvent (5% and 15% ethanol). The extraction time (187 min) was defined after determining the total mass needed to pack the extraction vessel (approximately 15 g of sample), with the S/F ratio set at 25 (g/g). The CO_2 flow rate was 1.9 g/min and 1.7 g/min and the ethanol flow rate was adjusted to 0.1 g/min and 0.3 g/min for 5% and 15% of co-solvent, respectively. The X_0 and content of bioactive compounds (phenolics, flavonoids, and tannins) and antioxidant activity were the dependent answers of the experimental design. X_0 was obtained by the ratio between the mass of the extract and the dry raw material.

Pressurized Liquid Extraction – PLE

The PLE assays were performed in a customized system set up at the Laboratory of Supercritical Technology: Extraction, Fractionation and Identification of Plant Extracts – LASEFI, described in detail by Náthia-Neves, Vardanega and Meireles [19]. To define the extraction time, a preliminary kinetic test was carried out at 100 bar, 100 ºC, and a mixture of ethanol-water (70% ethanol, v/v), with a volumetric flowrate of 3.47 mL/min, using 3.0 g of raw material, based on literature data [39]. The extraction time was defined as 60 min.

To evaluate the effect of the PLE variables on the dependent variables, a 3 × 3 full factorial design was carried out in duplicate, where the independent variables were temperature (60, 80 and 100 °C) and solvent composition (mixtures of ethanol-water with different

proportions of ethanol set as 50, 75 and 99.5% v/v). For each assay, 3.0 g of raw material were used, the solvent flow rate was defined according to the proportions of each ethanolic solution in order to maintain a constant mass flow rate of 1.5 g/min. All assays were performed in duplicate. The extracts were collected in amber glass vials and stored under at −18 ºC for further analysis.

Kinetics study

The extraction conditions used to obtain the overall extraction curves were determined based on the highest content of the compounds of interest. For SFE, the kinetic curves were performed in the SFE unit (Spe-ed SFE unit, Applied Separations, 7071, USA), equipped with a 300 mL extraction vessel containing 45.0 g of sample and the remaining avoid space was filled with glass beads. A co-solvent proportion of 15% was used and the total flow rate was kept in 6 g/min (being 0.9 g/min of ethanol and 5.1 g/min of CO_2) at 200 bar and 60 ºC. For PLE, the kinetic curves were performed in the same customized system previously described in section 2.5, using 3.0 g of sample, ethanol 99.5% at 80 ºC and 100 bar, with a solvent flow of 3 mL/min (2.37 g/min). To obtain the overall extraction curves, 8 or more experimental points were collected at predetermined times until reaching the diffusional period. The experimental data from the overall extraction curves were fitted to a spline model using three straight lines, performed in RStudio software, adjusted to the models proposed by Meireles [40]. The first line is the CER stage, that corresponds to the period of constant extraction rate, the second, FER stage, corresponds to the period of decreasing extraction rate and third, DC, represents the diffusional period:

For $t \leq t_{CER}$ (CER period)

$$y = b_0 + b_1 t \qquad \text{Equation 5}$$

For $t_{CER} \leq t \leq t_{FER}$ (FER period)

$$y = (b_0 + C_1 b_2) + (b_1 + b_2)t \qquad \text{Equation 6}$$

For $t \geq t_{FER}$ (DC period)

$$y = (b_0 + C_1 b_2 + C_2 b_3) + (b_1 + b_2 + b_3)t \qquad \text{Equation 7}$$

where y being the response variable; b_0 is the linear coefficient (order zero term) from CER line; b_1, b_2 and b_3 are the inclinations (first order terms) from CER, FER e DC lines, respectively; C_1 is the time interval of CER and C_2 is the final period FER, t_{CER} is the CER time e t_{FER} is the final of FER period.

Characterization of extracts

Total phenolic compounds

The amount of total phenolic compounds was determined according to the Folin-Ciocalteu method [41] using gallic acid as standard. In each test tube 1 ml of sample or standard, 6 ml of distilled water and 0.5 ml of Folin-Ciocalteu reagent were mixed and incubated at room temperature for 3 min. Then, 1.5 ml of 20% Na_2CO_3 solution and 1.9 ml of distilled water were added, and the mixture was incubated in the dark for 2 h at room temperature. The absorbance was read at 760 nm using a UV-Vis spectrophotometer (FEMTO 800XI, Brazil). The assays were performed in triplicate and were expressed as mg of gallic acid equivalent (GAE) per g of dry extract (mg GAE/g of dry extract).

Total flavonoid compounds

The flavonoids content was determined according to Veggi et al. [42], using catechin as standard. In a volumetric flask of 10 ml, containing 4 ml of distilled water, 1 ml of the sample with known dilution was added. At time zero, 0.3 ml of 5% (w/v) $NaNO_2$ was added to the flask. After 5 min, 0.3 ml of 10% (w/v) $AlCl_3$ was added. Then, after 6 min, 2 ml of 1M NaOH (w/v) were added to the mixture, and immediately, 2.4 ml of distilled water were added to the flask and the solution was mixed vigorously. The absorbance of the mixture was determined at 510 nm in a UV-Vis spectrophotometer (FEMTO 800XI, Brazil). The assays were performed in triplicate and the total flavonoids content expressed in mg equivalent of catechin/g of dry extract (mg CE/g of dry extract).

Total tannins

The content of total tannins present in the extracts was determined by the difference between the total phenolic compounds and the residual phenolic compounds, from the complexation of tannins with casein through the tannin-protein bond, using gallic acid as standard [43]. For this purpose, 6 mL of extract, 10 mL of distilled water and 1 g of bovine casein were mixed in an Erlenmeyer flask and kept under stirring for 3 h. Then, the contents

were filtered, and the volume was measured in a 25 mL volumetric flask. Subsequently, residual phenolic compounds were determined according to the Folin-Ciocalteau method (see previous section) (SINGLETON; ORTHOFER; LAMUELA-RAVENTÓS, 1999). Finally, the tannin content determined by difference and the result expressed in milligram equivalent of gallic acid (GAE) per gram of dry extract (mg GAE/g).

Antioxidant activity

The antioxidant activity was evaluated using ABTS and FRAP methods. The ABTS method was performed based on the procedure described by Re et al. [44]. For this, the ABTS radical was diluted in ethanol until reaching an absorbance of 0.70 ± 0.02 at 734 nm. A 30 µL aliquot of each diluted extract was transferred to test tubes with 3.0 mL of the ABTS radical. Absorbance was determined at 734 nm using a UV-Vis spectrophotometer (FEMTO 800XI, Brazil) after 6 min of reaction. The value of the antioxidant capacity of each sample was calculated as TEAC (Trolox equivalent antioxidant capacity). Assays were performed in triplicate and the result expressed as mg Trolox/g dry extract (mg TE/g dry extract).

The FRAP method was performed based on the methodology described by Bendif et al. [45]. The FRAP reagent was prepared by mixing 25 mL of acetate buffer (300 mM; pH 3.6), 2.5 mL of TPTZ solution (10 mM TPTZ (Fluka) in 40 mmol/L HCl) and 2.5 mL of 20 mM solution. FeCl3, in a ratio of 10:1:1 (v:v:v) mixed at the time of use. After mixing, the FRAP reagent was heated to 37 °C before use. For the reaction, 0.5 ml of each sample, blank or standard was added to 2 ml of FRAP reagent. Absorbance was measured at 595 nm using a UV-Vis spectrophotometer (FEMTO 800XI, Brazil) after 40 minutes. Assays were performed in triplicate and the result expressed as mg Trolox/g dry extract (mg TE/g dry extract)

High Pressure Liquid Chromatography (HPLC)

The extracts were analyzed by an HPLC-DAD (Waters, Alliance E2695, Milford, USA) according to Sanches et al. [46] to quantify chlorogenic acid and quercetin, with some modifications. To quantify the compounds, a calibration curve (20-200ppm) was made, and the UV/Vis spectra chromatograms were registered between 280 and 520 nm. Compounds were separated in a C18 column (Kinetex, 100 × 4.6 mm; 2.6 µm; Phenomenex, Torrance, USA) using a mobile phase of milli-Q water acidified with 1% of formic acid (A) and acetonitrile (B) in the following gradient: 0 min, 97 % A; 3 min, 94 % A; 6 min, 90 % A, 14 min, 87 % A, 16

min, 85 % A, 18 min, 80 % A, 19 min, 75 % A, 21 min, 70 % A, 26 min, 50 % A, 30 min, 70 % A, 34 min, 97 % A. The temperature and flow rate were 29 °C and 1.0 mL/min, respectively.

Statistical Analysis

The effect of the parameters for both extraction methods was determined by analysis of variance (ANOVA) and Tukey's test, using Minitab 19.1 (Minitab Ltd., State College, PA, USA) with a 95% confidence level ($\alpha = 0.05$).

3.3 RESULTS AND DISCUSSION

Characterization of the raw material

The moisture content of the dried raw material was 9.6 ± 0.7%, similar to that found by Peng [47] for hibiscus calyx. This parameter is of great importance, since it acts directly on the overall yield. The amount of water present in the raw material can impair the solvent flow due to changes that may occur in surface tension and in the contact angle during the interaction of the solute with the solvent, thus reducing the amount of compounds extracted [22]. Because of this, the moisture content recommended for raw material that are aimed to be extracted by supercritical fluids is less than 18% [48].

The mean diameter of the particles obtained was 0.38 ± 0.01 mm. Santos et al. [49] performed a study evaluating the influence of particle diameter on SFE and observed an increase on the overall extraction yield proportional to the reduction in particle diameter in the range from 1.43 mm to 0.26 mm. However, very small particles can aggregate forming preferential paths that can facilitate the passage of fluid without necessarily completely penetrating the sample, thus causing a reduction in yield [50]. The real density was 1.55 ± 0.01 g/mL, while the apparent density was 0.6 g/mL, and the bed porosity was 0.612.

Overall extraction Yield (X_0)

Figure 3.1 presents the X_0 results of hibiscus leaves extraction using SFE and PLE. For SFE, the X_0 values ranged from 1.47 to 26.26 g extract /100 g of dried raw material and the highest value was obtained at 60 ºC and 300 bar, using 15% of co-solvent (Figure 3.1A). Regarding the analysis of variance (ANOVA), for all extractions the R^2 presented values above 75%, showing that the model satisfactorily adjusted to the data (Table 3.1 and Table 3.2).

Temperature, co-solvent and pressure presented significant effect on X_0 ($p<0.05$). As it can be seen in Figure 3.1A, pressure increases leaded to increases of X_0 values. Such effect was

more pronounced when higher percentages of co-solvent were used, which can be explained by the increase in solvent density caused by the higher pressure, resulting in greater solubility of the compounds and consequent higher yield [51]. Moreover, since ethanol can recover more polar compounds, the increase of the co-solvent proportion can also reflect on the increase of X_0. Similar behavior was found for the SFE extraction of bioactive compounds from the radish (*Raphanus sativus* L.) leaves using CO_2 and ethanol as co-solvent [51].

Figure 3.1. Results of overall extraction yield (X0) for the extraction of hibiscus leaves by SFE (A) and PLE (B) at different extraction conditions.

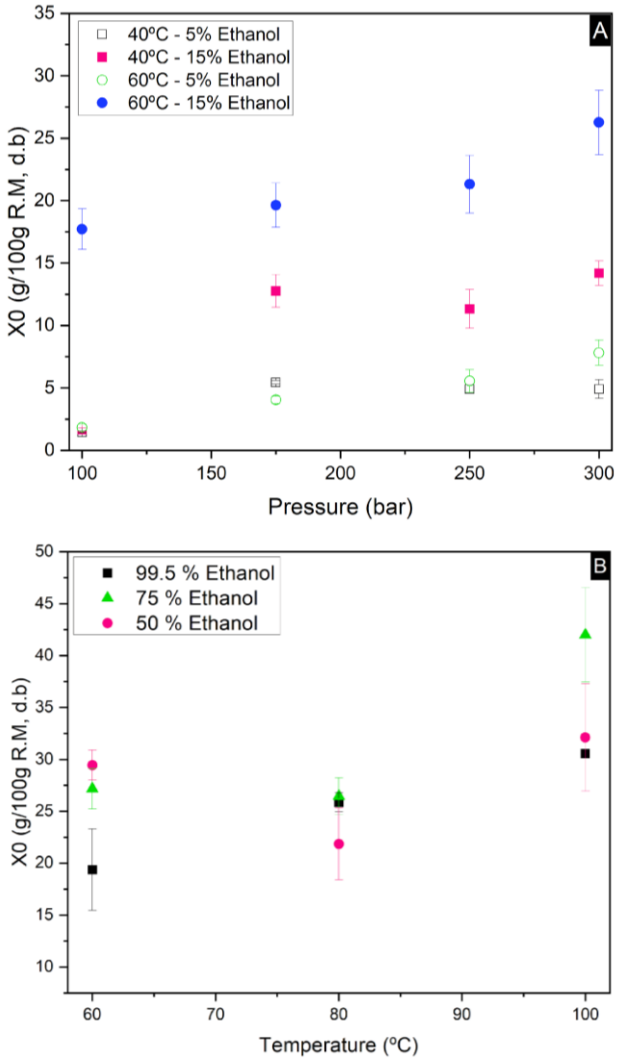

The temperature effect on X_0 is not trivially described, since it is involved in a complex relationship with between the solubility and solvent temperature and density, which can lead to the observation of retrograde effect [52]. This phenomenon, also called as crossover effect, occurs when, at a fixed pressure, the solubility decreases with increasing temperature close to the critical point due to a decrease in the density of the solvent but increase with increasing the

temperature far from the critical point due to increased vapor pressure of the solute [52,53]. This crossover effect was observed at 250 bar when 5% of co-solvent was used. For higher co-solvent concentration, the increase of vapor pressure of the solutes caused by the temperature increase had a predominant effect resulting in higher yields obtained at 60 °C, which were almost the double than the valued obtained at 40 °C.

For PLE, the X_0 values ranged from 19.4 to 42.0 g extract/100 g of dry raw material and the highest value was found at 100 °C using ethanol 75% (v/v) as solvent (Figure 3.1B). In this case, only the temperature was statistically significant ($p < 0.05$) (Table 3.1). Although the solvent composition had no significant difference at 95% confidence level, the p-value was 0.088, which means that by reducing the confidence level to 90%, the proportion of solvent becomes significant as well.

Table 3.1. ANOVA for extracts obtained by PLE.

OVERALL YIELD	**DF**	**SS (Aj.)**	**MS (Aj.)**	**F-value**	**P-value**
(A) Temperature	2	381.7	190.86	10.24	0.005
(B) Solvent	2	120.4	60.20	3.23	0.088
A*B	4	143.2	35.79	1.92	0.191
Error	9	167.8	18.64		
R^2	79.37				
PHENOLICS	**DF**	**SS (Aj.)**	**MS (Aj.)**	**F-value**	**P-value**
(A) Temperature	2	10202.6	5101.31	64.87	0.000
(B) Solvent	2	3896.5	1948.25	24.77	0.000
A*B	4	791.6	197.89	2.52	0.054
Error	45	3538.8	78.64		
R^2	80.80				
FLAVONOLS	**DF**	**SS (Aj.)**	**MS (Aj.)**	**F-value**	**P-value**
(A) Temperature	2	1611.2	805.62	25.68	0.000
(B) Solvent	2	3686.4	1843.21	58.76	0.000
A*B	4	852.3	213.07	6.79	0.001
Error	27	847.0	31.37		
R^2	87.90				
TANNIN	**DF**	**SS (Aj.)**	**MS (Aj.)**	**F-value**	**P-value**
(A) Temperature	2	6946.6	3473.28	43.34	0.000
(B) Solvent	2	2700.9	1350.43	16.85	0.000
A*B	4	617.8	154.44	1.93	0.135
Error	27	2164.0	80.15		
R^2	82.59				
ANTIOXIDANT ACTIVITY	**DF**	**SS (Aj.)**	**MS (Aj.)**	**F-value**	**P-value**
(A) Temperature	2	175671	87836	558.86	0.000
(B) Solvent	2	64223	32111	204.31	0.000
A*B	4	893615	223404	1421.43	0.000
Error	27	4244	157		
R^2	99.63				

Table 3.2. ANOVA for the results of extracts obtained by SFE at different temperatures and pressures with ethanol as co-solvent.

OVERALL YIELD	**DF**	**SS (Aj.)**	**MS (Aj.)**	**F-value**	**P-value**
Model	15	1868,08	124,54	4018,59	0,000
(A) Temperature	1	294,21	294,21	9493,62	0,000
(B) Pressure	3	246,67	82,22	2653,21	0,000
(C) %Solvent	1	1004,53	1004,53	32413,94	0,000
A * B	3	37,55	12,52	403,91	0,000
A * C	1	233,77	233,77	7543,13	0,000
B * C	3	34,87	11,62	375,10	0,000
A * B * C	3	16,47	5,49	177,18	0,000
Error	16	0,50	0,03		
R2	31	1868,58			
PHENOLICS	**DF**	**SS (Aj.)**	**MS (Aj.)**	**F-value**	**P-value**
Model	15	153696	10246,4	1487,45	0,000
(A) Temperature	1	10904	10903,7	1582,87	0,000
(B) Pressure	3	18000	6000,0	871,00	0,000
(C) %Solvent	1	13413	13413,1	1947,14	0,000
A * B	3	31919	10639,8	1544,55	0,000
A * C	1	16145	16145,4	2343,79	0,000
B * C	3	30747	10248,9	1487,80	0,000
A * B * C	3	32568	10856,1	1575,95	0,000
Error	32	220	6,9		
R^2	99,86				
FLAVONOLS	**DF**	**SS (Aj.)**	**MS (Aj.)**	**F-value**	**P-value**
(A) Temperature	1	5710	5710,1	320,74	0,000
(B) Pressure	3	11178	3726,1	209,30	0,000
(C) %Solvent	1	3983	3983,1	223,73	0,000
A * B	3	39370	13123,4	737,14	0,000
A * C	1	17151	17151,0	963,37	0,000
B * C	3	52163	17387,6	976,66	0,000
A * B * C	3	30260	10086,8	566,58	0,000
Error	32	570	17,8		
R^2	99,64				
TANNIN	**DF**	**SS (Aj.)**	**MS (Aj.)**	**F-value**	**P-value**
(A) Temperature	1	6680,3	6680,26	3070,36	0,000
(B) Pressure	3	11363,3	3787,76	1740,91	0,000
(C) %Solvent	1	8213,4	8213,42	3775,02	0,000
A * B	3	19394,4	6464,81	2971,33	0,000
A * C	1	8970,5	8970,46	4122,97	0,000
B * C	3	18223,3	6074,45	2791,91	0,000
A * B * C	19	19039,0	1002,05		
Error	79,28				
ANTIOXIDANT ACTIVITY	**DF**	**SS (Aj.)**	**MS (Aj.)**	**F-value**	**P-value**
(A) Temperature	1	0,105340	0,105340	113,44	0,000
(B) Pressure	3	0,494889	0,164963	177,64	0,000
(C) %Solvent	1	0,020000	0,020000	21,54	0,000
A * B	3	0,258614	0,086205	92,83	0,000
A * C	1	0,001568	0,001568	1,69	0,212
B * C	3	0,008751	0,002917	3,14	0,054
A * B * C	3	0,0129	0,0043	4,64	0,016
Error	16	0,01485	0,000929		
R^2	98,38				

Herbst et al. [32] carried out a study of PLE from beer residue and observed that the highest X_0 was obtained at 120 ºC and ethanolic solution 50% (v/v), and Martín-García et al. [54] found similar result obtaining maximum X0 in the condition of 200 ºC and ethanolic solution 50% (v/v), for the PLE from olive tree leaves. This increase can be explained by the fact that mixing water with ethanol provides an increase in solvent polarity, increasing the desorption of the analyte, facilitating the breakdown of hydrogen bonds in the matrix and thus, providing better recovery of the compounds [28]. In addition, an increase in yield can be seen with increasing temperature, for the proportions of ethanol 75% and 99.5% (v/v).

Comparing the extractions, it is evident that PLE had better X_0 results than SFE. However, one must keep in mind that not only the amount of extract obtained matters, but its quality aligned with the desired application need to be considered. The higher selectivity of the SFE can result in a purer extract, but the use of water and ethanol together can result in a greater content of bioactive compounds, depending on the extraction conditions [25].

Chemical composition of the extracts

The chemical composition of the extracts obtained by SFE and PLE are shown in Table 3.3 and 3.4, respectively. The ANOVA presented R^2 values above 79% for all compounds, showing that the model satisfactorily adjusted to the data (Table 3.1 and Table 3.2). For SFE, all the factors temperature, co-solvent and pressure were significant ($p < 0.05$). The highest temperature and co-solvent proportion had a positive effect on the bioactive compounds content, while the pressure increase had a negative effect, i.e, the higher contents of bioactive compounds were obtained at 60 ºC, 15% of co-solvent and 100 bar. For PLE extracts, both factors, temperature and solvent composition, also presented a significant effect ($p < 0.05$) for all compounds. The increase of ethanol proportion in the solvent had a positive effect, but the temperature increase had a negative effect. Thus, the best PLE condition was obtained at 80 °C and 99.5% ethanol.

Although the pressure increase directly affects solvation power of CO^2 favoring the recovery of bioactive compounds from the matrix, it is a non-polar solvent, which makes necessary the addition of co-solvents to improve the recovery of phenolic compounds [55]. The co-solvent addition to the CO^2 can cause modifications in the matrix, making it possible to obtain better yield at lower pressures [56].

Table 3.3. Results of the bioactive compounds content and antioxidant activity of the extracts obtained by SFE.

Temperature (ºC)	Pressure (bar)	Co-solvent (% v/v)	Phenolic[1]	Flavanols[2]	Tannin[1]	Antioxidant Activity	
						ABTS[3]	FRAP[3]
40	100	5	10 ± 2	6 ± 1	9 ±1	0.21 ± 0.001	0.5 ± 0.04
		15	6.5 ± 0.01	14 ±1	5.6 ± 0.02	0.08 ± 0.01	0.4 ±0.01
	175	5	23 ± 0.6	77 ± 3	27 ± 0.6	0.14 ± 0.07	7.87 ± 0.07
		15	23 ± 3	22 ± 0.2	23 ± 3	0.03 ±0.001	1 ± 0.01
	250	5	20 ± 0.7	42 ± 3	19 ± 0.7	0.05 ± 0.001	4.4 ± 0.001
		15	20 ± 0.3	28.6 ± 0.5	20 ± 0.3	0.06 ± 0.02	2.63 ± 0.01
	300	5	19 ± 2	42 ± 0.01	18 ±2	0.07 ± 0.01	4.6 ± 0.2
		15	17 ± 0.3	25 ± 0.1	16.8 ± 0.3	0.041 ± 0.001	0.4 ± 0.003
60	100	5	6 ± 0.01	16.5 ± 0.5	5 ± 0.01	0.6 ± 0.04	3 ± 0.2
		15	246 ± 3	261 ± 3	237 ± 3	0.06 ± 0.04	2 ± 0.01
	175	5	16 ± 0.07	35 ± 0.2	7.8 ± 10.4	0.11 ±0.01	3 ± 2
		15	19 ±0.03	22 ± 0.4	18.5 ± 0.03	0.044 ± 0.001	0.9 ± 0.002
	250	5	22 ± 1	37 ± 1	21.2 ± 0.9	0.14 ± 0.06	3.0 ± 0.2
		15	32 ±2	21 ± 4	31 ± 2	0.05 ± 0.001	0.03 ± 0.01
	300	5	12 ±1	23 ± 0.01	12 ± 1	0.04 ± 0.01	1 ± 0.04
		15	29 ± 2	21 ± 2	28 ± 2	0.17 ± 0.001	0.1 ± 0.02

[1]mg GAE/g extract (d.b.); [2]mg CE/g g extract (d.b.); [3]mg TE/g extract (d.b.).

On the other hand, temperature can play antagonistic roles, since it interferes with more than one property simultaneously (density, viscosity and vapor pressure) [57]. Thus, higher temperatures can promote the solubility due to the increase in the vapor pressure of the solute. In addition, there is a reduction in the viscosity of the solvent, allowing a greater diffusivity between the molecules and consequently increasing the extraction yield [55,58]. However, very high temperatures can cause degradation of the compounds, reducing the quality of the extract obtained [28].

For the phenolic compounds, the SFE resulted in extracts with a content ranging from 6.00 ± 0.01 to 246 ± 3 mg GAE/g of dry extract, while for PLE, it ranged from 58 ± 3 to 107 ± 10 mg GAE/g of dry extract, with the maximum value at 80 ºC and 99.5% ethanol. For maceration, the content of phenolic compounds was 7.1 ± 0.2 mg GAE/g of dry extract. By comparing these results, it is noted that the conventional maceration extraction resulted in a lower recovery than both high pressure techniques.

Table 3.4. Results of the bioactive compounds content and antioxidant activity of the extracts obtained by PLE.

	Temperature (ºC)	Ethanol (% v/v)	Phenolic[1]	Flavanols[2]	Tannin[1]	Antioxidant Activity	
						ABTS[3]	FRAP[3]
PLE	100	99.5	67 ± 6^{de}	31 ± 10^{b}	62 ± 6^{cd}	0.051 ± 0.001^{f}	2 ± 0.08^{bcd}
		75	58 ± 3^{e}	24 ± 1^{bc}	55.0 ± 0.4^{d}	0.170 ± 0.001^{a}	0.6 ± 0.07^{d}
		50	75 ± 3^{cd}	22 ± 3^{bc}	73 ± 3^{bcd}	0.06 ± 0.01^{ef}	0.6 ± 0.1^{d}
	80	99.5	107 ± 10^{a}	60 ± 11^{a}	104 ± 12^{a}	0.100 ± 0.001^{c}	4 ± 2^{ab}
		75	89 ± 10^{bc}	33 ± 2^{b}	86 ± 11^{ab}	0.040 ± 0.001^{g}	1.0 ± 0.1^{cd}
		50	102 ± 12^{ab}	32 ± 2^{b}	100 ± 12^{a}	0.150 ± 0.001^{b}	0.6 ± 0.4^{d}
	60	99.5	88 ± 16^{bc}	50 ± 2^{a}	84 ± 16^{ab}	0.060 ± 0.001^{e}	5 ± 3^{a}
		75	56 ± 3^{e}	17 ± 3^{c}	54 ± 3^{d}	0.040 ± 0.001^{g}	2.9 ± 0.3^{abc}
		50	80 ± 6^{cd}	25 ± 5^{bc}	78 ± 4^{bc}	0.070 ± 0.001^{d}	0.6 ± 0.4^{d}

[1]mg GAE/g extract (d.b.); [2]mg CE/g extract (d.b.); [3]µg TE/g extract (d.b.). Means with the same letters in the same column do not differ significantly by the Tukey Test at 5% of confidence level.

Comparing these results with those obtained for hibiscus calyx extracts obtained by conventional extraction with methanol and aqueous methanolic solution 50% (v/v), it is possible to observe that hibiscus calyx extracts showed lower phenolic compounds content (14.24 and 51.72 mg GAE/g of extract, respectively) [59] when compared to high pressure techniques, but it is higher than that obtained by maceration. On the other hand, extracts from hibiscus calyx obtained by SFE at 50 °C, 250 bar and 16.7% (v/v) ethanol as co-solvent, presented phenolic compounds content in the same range of those observed in the present study (113 mg GAE/g extract), but for PLE of hibiscus calyx, the results obtained at 200 °C and ethanolic solution 50% (v/v) reported by Pimentel-Moral [60] (135 mg GAE/g extract) was slightly higher. Probably, it occurred due to the higher temperature used, that can increase the content of compounds due to the enhance of solubility, caused by the increase of vapor pressure [55,58].

It was not found in the literature studies of pressurized extractions of hibiscus leaves, but Chen *et al*. [9] reported a content of 0.354 g GAE/g of dry extract for the extract obtained by maceration. In terms of phenolic compounds yield, i.e., mg GAE/g raw material, SFE and PLE processes resulted in up to 16.38 and 36.07 mg GAE/g of raw material, respectively, overcoming the results obtained by Singh *et al* [6], 2.41 mg GAE/g of raw material for the extraction of hibiscus leaves using maceration with methanol.

The flavonoids content of the extracts obtained by SFE ranged from 7 ± 1 to 261 ± 3 mg CE/g of dry extract. For PLE, the flavonoids content ranged from 17 ± 3 to 60 ± 11 mg CE/g of dry extract, and for maceration, a value of 5.2 ± 0.6 mg CE/g of dry extract was obtained. Similarly to observed for the phenolic compounds, the maceration resulted in extracts with lower flavonoids content than the two high pressure techniques. Although the flavonoids content of the PLE extracts was lower than those obtained for the SFE extracts, they were still higher than the results reported for the extracts obtained from the hibiscus calyx by SFE (0.53 mg CE/g of dry extract) [60]. In addition, the flavonoids content of the hibiscus leaves extracts obtained in the present work were higher than those reported for ethanolic extracts obtained by microwave from Vernonia amygdalina leaves (91.12 mg QE/g of dry extract) [61] and from *Cissus sicyoides* L. extracts (leaves and steam) obtained by SFE with ethanol as co-solvent (5% v/v) (8.06 QE/g of dry extract) [62]. Regarding the flavonoids yield, SFE and PLE extracts resulted in 17.41 and 20.11 mg CE/g of raw material, respectively, which were both higher than the results reported by Singh *et al*. [6] for fresh hibiscus leaves extracts obtained by maceration with methanol (3.64 mg/g of raw material), and were similar to the results reported by Goyeneche *et al*. [51] for radish leaves extracts obtained by SFE-CO_2 (21.8 mg QE/g raw material).

The tannins content ranged from 4.80 ± 0.01 to 237 ± 3 mg GAE/g of dry extract for SFE extracts, while PLE extracts presented a tannins content between 54 ± 3 and 104 ± 12 mg GAE/g of dry extract. For maceration, a value of 6.5 ± 0.2 mg GAE/g of dry extract was obtained, which is lower than the values reported for SFE and PLE. These values were superior than those reported by Samadi and Fard [63] for extracts obtained by maceration with ethanol from black tea, green tea and hibiscus calyx, resulting in values of 25.02, 64.3 and 17.18 mg tannic acid/g of dry extract, respectively. Regarding the tannins yield, the highest value for SFE extracts was 15.80 mg GAE/g of raw material and for PLE was 1.60 mg GAE/g of raw material. Singh et al. [6] reported a value of 4.51 mg tannic acid/g of fresh sample for the extracts obtained from fresh hibiscus leaves. It is interesting to note that the tannins content obtained in the present work corresponds to almost 100% of the total phenolic compounds quantified.

Thus, both SFE and PLE technologies were effective in the recovery of phenolic compounds from hibiscus leaves, surpassing amounts obtained by conventional technologies and with similar results observed for the calyx, mostly because the effectiveness of matrix penetration that enabled the extraction of a greater content of compounds in lower conditions of temperature and pressure. Besides that, the use of leaves to obtain bioactive compounds can

be a promising way for by-products reuse, since it allows obtaining a greater variety of bioactive compounds in addition to reducing waste generation.

Antioxidant Activity

The ABTS and FRAP antioxidant activities of the extracts obtained by SFE and PLE are presented in Tables 3.3 and 34, respectively. Both antioxidant activity methodologies showed different optimal conditions for the maximum value from those observed for the compounds content evaluated. For SFE extracts, the maximum value (0.6 ± 0.04 mg TE/g of dry extract) was obtained at 60 ºC, 100 bar and 5% of co-solvent for the ABTS method, and for the FRAP radical method, the maximum value (7.87 ± 0.07 mg TE/g of dry extract), was observed at 40 ºC, 175 bar and 5% of co-solvent. For PLE extracts, the maximum value of 0.17 ± 0.01 mg TE/g of dry extract observed by the ABTS method was obtained at 100 ºC and 75% ethanol and the maximum value of 5 ± 3 mg TE/g observed by the FRAP radical was obtained at 60 °C and 99.5% ethanol. For maceration, a value of 3.00 ± 0.02 µg TE/g of dry extract was obtained for ABTS method, and for the FRAP radical method, the value was 1.30 ± 0.01 mg TE/g of dry extract.

The differences observed between the methods can be explained by the site of action of each one. ABTS methodology is based on the ability of the antioxidants present in the matrix to capture the ABTS●+ cation, whereas FRAP causes the conversion of the ferric-tripyridyltriazine complex (FeIII-TPZ) in ferrous complex (FeII-TPZ), depending on the presence of an antioxidant and under acidic conditions [64]. Both methods fit as chain-breaking antioxidants, but act in two different pathways, being hydrogen atom transfer for ABTS, while FRAP involves a single electron transfer and is strongly solvent-dependent [65]. So, it is common to observe such differences between these methods, since the ABTS have a greater propensity to capture hydrophilic compounds [44] as the phenolic acids, while FRAP can have a better recovery for lipophilic compounds, such as flavanols, that also has sensibility to high temperatures [66]. Besides that, the difference in the maximum conditions of compounds and antioxidant activity can be due to the solvent, because when there is a mixture (ethanol and water) the solvent polarity is reduced, promoting a greater recovery of antioxidant compounds, since single-carbon-chain compounds to polyphenols [67].

Regarding the ABTS method, the results observed in the present study are superior to those reported by Zhen *et al*. [3] for extracts of hibiscus leaves from various locations obtained by ultrasound-assisted extraction using methanolic solution as solvent, resulting in values

between 0.027 and 0.038 mg TE/g dry extract. In terms of raw material, SFE extracts presented 13.2 and 52.78 mg TE/g of raw material for ABTS and FRAP, respectively, while PLE extracts presented 5.46 and 158.2 mg TE/g of raw material for ABTS and FRAP, respectively. The antioxidant activity measured by FRAP for PLE extracts was higher, corroborating the results reported by Santana *et al*. [68], who evaluated both the guarana seed and its residue, and observed that PLE at temperatures of 40-60 ºC and 50% ethanol solution (v/v) was better than SFE.

These results demonstrate that both SFE and PLE enables to obtain a great content of bioactive compounds with high antioxidant activity when compared with conventional and non-conventional technologies, such as ultrasound. Besides that, both technologies are important, since each one was capable to recover different compounds that reacts with ABTS radical for SFE and FRAP radical for PLE. Indeed, it could be said that PLE probably can recover most alcohol soluble compounds once the maximum conditions were observed when ethanol 99.5% were used, and SFE the both water and lipid-soluble antioxidants, but without a specific solubility.

Furthermore, it demonstrates the potential of hibiscus leaves as source of these bioactive compounds, since it presented similar and/or greater amounts than other known plant matrices (e.g. beet, grape, radish). However, depending on the application of the extract, it is worth mentioning that not only the quantity of the compounds of interest matters, but the quality of the extract obtained, because although PLE was more efficient to recover the compounds, the extract obtained is more diluted than those obtained by SFE, which can facilitate its application.

Compounds identification

The extracts from hibiscus leaves obtained by SFE and PLE were also analyzed by HPLC to identify some of the phenolic compounds. Chlorogenic acid and quercetin were identified by comparison with authentic standards, as well as by retention time and UV-VIS characteristics (Figure 1S). By analyzing the UV-VIS characteristics of the peaks 1, 3 and 4, it was found that peak 1 was very similar to chlorogenic acid, while peaks 3 and 4 were similar to quercetin, thus enabling the identification of peak 1 as chlorogenic acid isomer and peaks 3 and 4 as quercetin isomers. The analysis of a methanolic extract from hibiscus leaves performed by Zhen *et al.* [3] also identified 3 different isomers of chlorogenic acid, being neochlorogenic acid (5-O-caffeoylquinic acid), chlorogenic acid (3-O- caffeoylquinic acid), and cryptochlorogenic acid (4-O- caffeoylquinic acid).

Table 3.5 presents the compounds identified in the extracts. For SFE, the maximum chlorogenic acid content (35 ± 2 mg/g of extract) was obtained at 60 ºC, 200 bar and 15% ethanol, and quercetin (26 ± 0.8 mg/ g of extract) at 40 ºC, 175 bar and 5% ethanol, and both are in agreement with the conditions of maximum antioxidant activity obtained. In relation to PLE, the maximum chlorogenic acid content (47 ± 5 mg/g of extract) was obtained with 50% of ethanolic solution (v/v) and quercetin (32 ± 10 mg/ g of extract) with 99.5%, both at 80 ºC, also in agreement with the maximum antioxidant activity observed. The same behavior was observed for the other peaks partially identified.

Table 3.5. HPLC identification and quantification of the phenolic compounds (mg/g of dry extract) of the hibiscus leaves extract obtained by SFE and PLE.

	Temperature (ºC)	Ethanol (%)	Chlorogenic Acid (I)	Chlorogenic Acid	Quercetin (I)	Quercetin (II)	Quercetin
PLE	100	99.5	63±13^{c}	32±1^{ab}	6±13^{ab}	10±2^{abc}	24±4^{abc}
		75	59±17^{c}	24±11^{b}	55±12^{ab}	9±2^{abc}	16±0^{bc}
		50	81±8^{bc}	31±2^{ab}	53±2^{ab}	9±0^{bc}	19±1^{abc}
	80	99.5	78±4^{bc}	41±5^{ab}	73±4^{ab}	12±2^{ab}	32±10^{a}
		75	67±1^{bc}	35±6^{ab}	62±15^{ab}	12±0^{ab}	27±5^{abc}
		50	122±14^{a}	47±5^{a}	77±7^{a}	13±1^{a}	31±1^{ab}
	60	99.5	79±3^{bc}	38±6^{ab}	70±6^{ab}	11±0^{abc}	23±0^{abc}
		75	48±6^{c}	23±0.1^{b}	42±2^{b}	7±0^{bc}	11±0^{c}
		50	102±4^{ab}	39±1^{ab}	67±0^{ab}	12±0^{ab}	24±3^{abc}

	Temperature (ºC)	Pressure (bar)	Co-solvent (%)	Chlorogenic Acid (I)	Chlorogenic Acid	Quercetin (I)	Quercetin (II)	Quercetin
SFE	40	100	5	*ND*	*ND*	*ND*	*ND*	*ND*
			15	*ND*	*ND*	*ND*	*ND*	*ND*
		175	5	18.1	19	64	18	25
			15	16.1	*ND*	*ND*	*ND*	*ND*
		200	5	12.6	14	16	6	16
			15	25	18	2,72	1,47	2
		300	5	*ND*	*ND*	*ND*	*ND*	*ND*
			15	27	19	4	2	2
	60	100	5	*ND*	*ND*	*ND*	*ND*	*ND*
			15	28	19	13	1	*ND*
		175	5	71	10	9	9	7
			15	39	30	16	4	5
		200	5	*ND*	*ND*	*ND*	*ND*	*ND*
			15	61	35	42	10	12
		300	5	*ND*	*ND*	0,20	0,30	*ND*
			15	4	18	44	16	1

Chlorogenic Ac. (Isomer)^{a} and Chlorogenic Ac.^{b}: UV-Vis 325; Quercetin (Isomer 1)^{c}, Quercetin (Isomer 2)^{d} and Quercetin^{e}: UV-Vis 330; *ND*-Non detected

These results suggest that antioxidant activity measured by ABTS is mainly related to the content of chlorogenic acid, while the antioxidant activity measured by FRAP is mainly related to quercetin content. This is probably due to the characteristic of each compound, once quercetin has low solubility in water [69], consequently the best condition to recover it used 99.5% of ethanol as solvent, similarly to observed for the FRAP measurement. On the contrary, aqueous solutions has a better effect in the recovery of chlorogenic acid [70], which could influence the final results for ABTS, since it can measure the activity of both water and lipid-soluble antioxidants [44].

Zhen *et al*. [3] observed that quercetin was the major compound of the methanolic extract obtained from hibiscus leaves, representing about 26% of the total identified compounds, which was different from the results observed in this work, where chlorogenic acid presented higher amounts than quercetin. Several authors discuss the variability of compounds in relation to the various genotypes of hibiscus, and neochlorogenic acid is reported as one of the major compounds of *Hibiscus Sabdariffa* L. [71]. The presence of this compounds must be highlighted since they are related to different biological activities [3], such as antihypertensive, antimutagenic, chemopreventive, antioxidant, anticonvulsant, anti-inflammatory and hypoglycemic action [72,73]. Besides that, a study performed by Sargin [74] reported that quercetin and chlorogenic acid are a potent antiviral agent and the most effective natural compounds against the influenza virus. Thus, it is noted that the PLE extracts were superior than the SFE extracts regarding the recovery of these phenolic acids, despite the selectivity of SFE mentioned above.

Overall Extraction Curves – OEC

Based on the content obtained for the classes of compounds, it was possible to select the operational conditions of SFE and PLE for the kinetic study. The SFE condition selected was 60 ºC, 100 bar and 15% of co-solvent, and PLE condition was 80 ºC with ethanol 99.5%. The extraction of solutes from plant matrices is not a linear function of extraction time and may present up to three characteristic extraction periods. The first one, CER stage, corresponds to the period of constant extraction rate, the second, FER stage, corresponds to the period of decreasing extraction rate and third, DC, represents the diffusional period. Thus, from the construction of the overall extraction curves (OEC) (Figure 3.2) in addition to describing the kinetic behavior of the extraction it is possible to obtain necessary information for the calculation of the kinetic parameters of the extraction processes.

Figure 3.2. OEC of hibiscus leaf as a function of extraction time by SFE (A) and PLE (B).

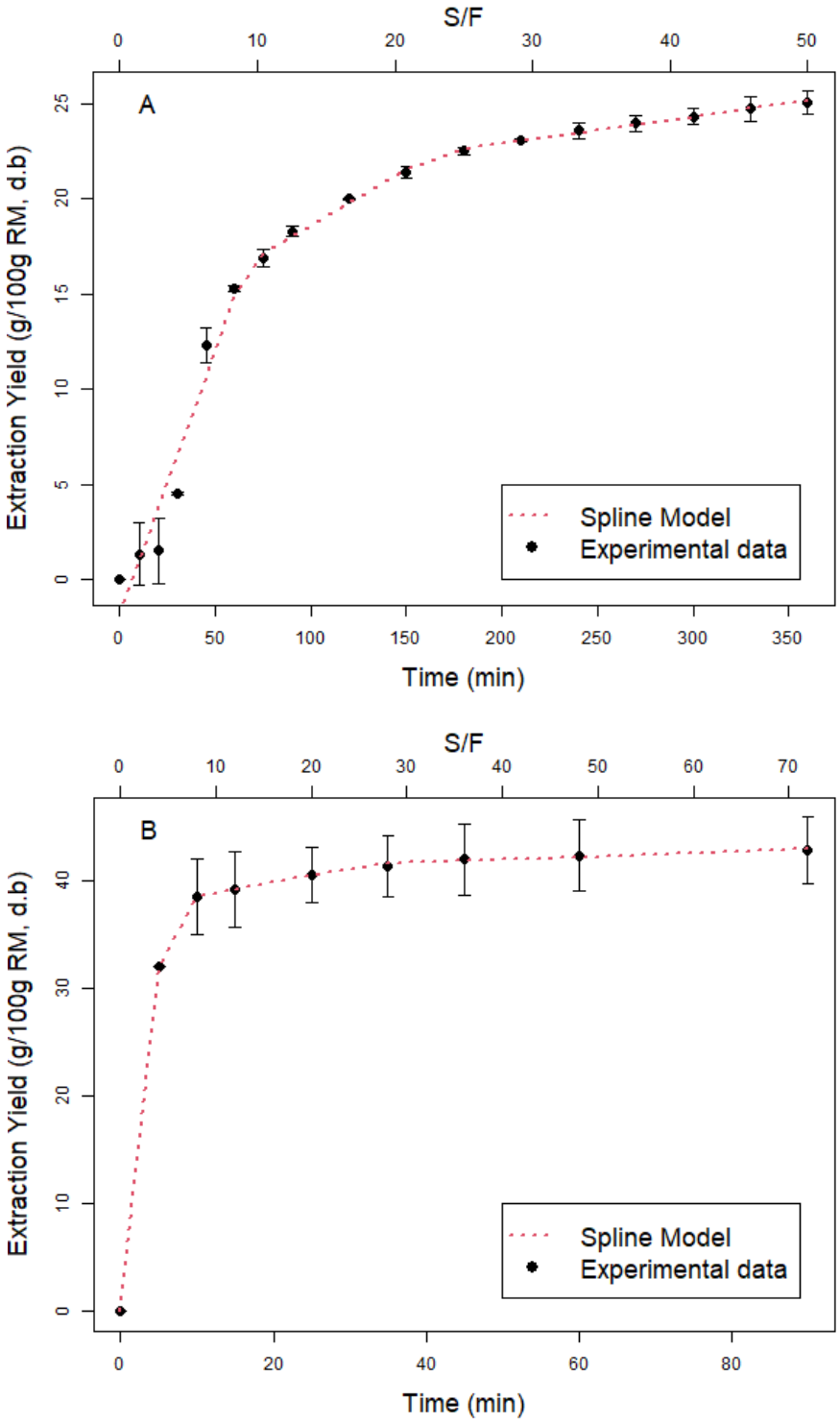

For the SFE, an extraction yield of approximately 25 g extract /100 g of dry raw material was obtained in 360 min with a S/F = 48, and for the PLE, approximately 40 g extract /100 g of dry raw material was obtained in 90 min with an S/F = 71. Thus, the SFE process enabled a recovery of 0.52 g extract/g solvent, while PLE resulted in a recovery of 0.56 g extract/g solvent, which means that the PLE was more efficient that SFE, even considering the time that

the sample was exposed to the solvent, that was lower for PLE. The slope of the first line represents the mass transfer rate (M_{CER}) of the CER step. The time that dictates the intersection of the first two straight lines is the t_{CER} (75.22 and 5.95 for SFE and PLE respectively), which represents the end of the CER stage; the intersection time between the second and third lines is the t_{FER} (164.41 and 39.03 for SFE and PLE respectively) [40]. Lastly, RCER is the extraction yield obtained in the CER step (16.67 and 32.24 for SFE and PLE respectively).

For SFE, the fraction of extract recovered in the CER period referring to the total extracted was 68.18%, which represents the extract recovered with low resistance to mass transfer, probably due to the easy availability of the compounds and high solubility of the extract in the solvent, since in this phase, the solvent does not need to fully diffuse into the matrix to perform the extraction. It was also observed for PLE, with a recovery of approximately 95%, showing that most of the extract was obtained in this phase. As a consequence, for the FER phase, lower yields were obtained, being 30.9% for SFE and 5% for PLE.

Another factor that should be noted is the duration of the CER phase, which for SFE corresponded to approximately 1/5 of the total time (75.22 min) with an S/F = 10.0, while for PLE corresponds to 1/12 of the total time (5.92 min) with an S/F = 4.7, i.e, with a considerably shorter time and less consumption of solvent, PLE was able to recover a greater amount of extract. Thus, the importance of optimizing the extraction parameters is perceived, as too much time can increase operating costs, without significant changes in the overall extraction yield.

3.4 CONCLUSION

The results of the present study demonstrate that hibiscus leaves are a potential source of bioactive compounds, presenting yields comparable or superior to those observed for hibiscus calyx and flowers or even to other plant matrices. Both SFE and PLE technologies were efficient to obtain extracts rich in compounds that can be use by food, pharmaceutical and cosmetic industries, being an alternative to conventional technologies. Indeed, SFE and PLE showed higher recovery for all compound evaluated (total phenolic, tannins and flavonoids) in comparison to maceration. The best SFE condition was 60 ºC, 100 bar and 15% ethanol, resulting in the highest extraction yield and content of bioactive compounds. For PLE, the highest X_0 (42.12%) was obtained at 100 ºC and 75% ethanol. However, for the bioactive compounds, the best condition was 80 ºC and 99.5% ethanol. In relation to the antioxidant activity best SFE condition was at 60 ºC and 100 bar, with a co-solvent proportion of 5% ethanol for ABTS and 15% ethanol for FRAP. For PLE, the antioxidant activity measured by ABTS

showed the maximum at the same maximum yield point (100 ºC and 75% ethanol), and for FRAP, in the condition of 60 ºC and 99.5% ethanol. The maximum antioxidant activity measured by ABTS and FRAP corroborates with the best conditions obtained for chlorogenic acid and quercetin, respectively. Comparing the two extraction methods, it can be noted that the SFE allowed a better result in terms of compounds content, since it results more concentrated extracts, but in terms of compounds yield PLE was superior, allowing the recovery of a greater amount of the compounds demanding less time and solvent.

ACKNOWLEDGMENTS

This research received financial support of São Paulo Research Foundation (FAPESP) (Brazil, Grants 2019/27354-3, and 2021/07639-3). G. Nunes Clímaco thanks Coordenação de Aperfeiçoamento de Pessoal de Nível Superior - Brasil (CAPES) - Finance Code 001 for a Ph.D. fellowship. Renata Vardanega thanks European Union's Horizon 2020 research and innovation programme under the Marie Sklodowska-Curie grant agreement No 101062938 for the postdoctoral fellowship.

REFERENCES

[1] I. Jabeur, E. Pereira, L. Barros, R.C. Calhelha, M. Sokovi, M.B.P.P. Oliveira, I.C.F.R. Ferreira, Hibiscus sabdariffa L. as a source of nutrients, bioactive compounds and coloring agents, Food Res. Int. 100 (2017) 717–723. https://doi.org/10.1016/j.foodres.2017.07.073.

[2] I. Da-costa-rocha, B. Bonnlaender, H. Sievers, I. Pischel, M. Heinrich, Hibiscus sabdariffa L. – A phytochemical and pharmacological review, Food Chem. 165 (2014) 424–443. https://doi.org/10.1016/j.foodchem.2014.05.002.

[3] J. Zhen, T.S. Villani, Y. Guo, Y. Qi, K. Chin, M.H. Pan, C.T. Ho, J.E. Simon, Q. Wu, Phytochemistry, antioxidant capacity, total phenolic content and anti-inflammatory activity of Hibiscus sabdariffa leaves, Food Chem. 190 (2016) 673–680. https://doi.org/10.1016/j.foodchem.2015.06.006.

[4] A.S.N. Formagio, D.D. Ramos, M.C. Vieira, S.R. Ramalho, M.M. Silva, N.A.H. Zárate, M.A. Foglio, J.E. Carvalho, Phenolic compounds of Hibiscus sabdariffa and influence of organic residues on its antioxidant and antitumoral properties, Brazilian J. Biol. 75 (2015) 69–76. https://doi.org/10.1590/1519-6984.07413.

[5] B. Kumari, B.K. Tiwari, M.B. Hossain, N.P. Brunton, D.K. Rai, Recent Advances on Application of Ultrasound and Pulsed Electric Field Technologies in the Extraction of

Bioactives from Agro-Industrial By-products, Food Bioprocess Technol. 11 (2018) 223–241. https://doi.org/10.1007/s11947-017-1961-9.

[6] S. Singh, S. Swain, D.R. Singh, K.M. Salim, D. Nayak, S.D. Roy, Changes in phytochemicals, anti-nutrients and antioxidant activity in leafy vegetables by microwave boiling with normal and 5% NaCl solution, FOOD Chem. 176 (2015) 244–253. https://doi.org/10.1016/j.foodchem.2014.12.068.

[7] S. Singh, D.R. Singh, K.M. Salim, A. Srivastava, L.B. Singh, R.C. Srivastava, Estimation of proximate composition, micronutrients and phytochemical compounds in traditional vegetables from Andaman and Nicobar Islands, Int. J. Food Sci. Nutr. 62 (2011) 765–773. https://doi.org/10.3109/09637486.2011.585961.

[8] N.M. Karaaslan, A comprehensive study about Hibiscus sabdariffa leaves: antioxidant activity, polyphenol profile and macro- and micro-element content, Chem. Pap. 73 (2019) 791–799. https://doi.org/10.1007/s11696-018-0629-x.

[9] J. Chen, C. Wang, C. Wang, J. Sheu, C. Lin, H. Lin, Hibiscus sabdariffa leaf polyphenolic extract inhibits LDL oxidation and foam cell formation involving up-regulation of LXRa / ABCA1 pathway, Food Chem. 141 (2013) 397–406. https://doi.org/10.1016/j.foodchem.2013.03.026.

[10] S.S. Kumar, P. Manoj, N.P. Shetty, P. Giridhar, Effect of different drying methods on chlorophyll, ascorbic acid and antioxidant compounds retention of leaves of Hibiscus sabdariffa L., J. Sci. Food Agric. 95 (2015) 1812–1820. https://doi.org/10.1002/jsfa.6879.

[11] H.A. Sindi, L.J. Marshall, M.R.A. Morgan, Comparative chemical and biochemical analysis of extracts of Hibiscus sabdariffa, FOOD Chem. 164 (2014) 23–29. https://doi.org/10.1016/j.foodchem.2014.04.097.

[12] H.S. El-Beltagi, H.I. Mohamed, B.M.H. Megahed, M. Gamal, G. Safwat, Evaluation of some chemical constituents, antioxidant, antibacterial and anticancer activities of beta Vulgaris L. Root, Fresenius Environ. Bull. 27 (2018) 6369–6378.

[13] R.A. Milella, T. Basile, V. Alba, M. Gasparro, M.A. Giannandrea, G. Debiase, R. Genghi, D. Antonacci. Optimized ultrasonic-assisted extraction of phenolic antioxidants from grape (Vitis vinifera L.) skin using response surface methodology, J. Food Sci. Technol. 56 (2019) 4417–4428. https://doi.org/10.1007/s13197-019-03946-9.

[14] M.C.E.V. Schiassi, V.R. de Souza, A.M.T. Lago, L.G. Campos, F. Queiroz, Fruits from the Brazilian Cerrado region: Physico-chemical characterization, bioactive compounds,

antioxidant activities, and sensory evaluation, Food Chem. 245 (2018) 305–311. https://doi.org/10.1016/j.foodchem.2017.10.104.

[15] F.J. Barba, Z. Zhu, M. Koubaa, A. De Souza, S. Ana, V. Orlien, Green alternative methods for the extraction of antioxidant bioactive compounds from winery wastes and by-products: A review, Trends Food Sci. Technol. (2016). https://doi.org/10.1016/j.tifs.2016.01.006.

[16] U. Nations, Trasnforming our world: 2030 agenda for sustainable development, 2017. https://doi.org/10.1057/978-1-137-45443-0_24.

[17] L. Sun, D. Niu, M. Yu, M. Li, X. Yang, Z. Ji, Integrated assessment of the sustainable water-energy-food nexus in China: Case studies on multi-regional sustainability and multi-sectoral synergy, J. Clean. Prod. 334 (2022) 130235. https://doi.org/10.1016/j.jclepro.2021.130235.

[18] A.M. Goula, M. Ververi, A. Adamopoulou, K. Kaderides, Green ultrasound-assisted extraction of carotenoids from pomegranate wastes using vegetable oils, Ultrason. Sonochem. 34 (2017) 821–830. https://doi.org/10.1016/j.ultsonch.2016.07.022.

[19] G. Náthia-Neves, R. Vardanega, M.A.A. Meireles, Extraction of natural blue colorant from Genipa americana L. using green technologies: Techno-economic evaluation, Food Bioprod. Process. 114 (2019) 132–143. https://doi.org/10.1016/j.fbp.2018.12.004.

[20] S. Nipornram, W. Tochampa, P. Rattanatraiwong, R. Singanusong, Optimization of low power ultrasound-assisted extraction of phenolic compounds from mandarin (Citrus reticulata Blanco cv. Sainampueng) peel, Food Chem. 241 (2018) 338–345. https://doi.org/10.1016/j.foodchem.2017.08.114.

[21] F. Chemat, N. Rombaut, A. Meullemiestre, M. Turk, S. Perino, A.S. Fabiano-Tixier, M. Abert-Vian, Review of Green Food Processing techniques - Preservation, transformation, and extraction, Innov. Food Sci. Emerg. Technol. 41 (2017) 357–377. https://doi.org/10.1016/j.ifset.2017.04.016.

[22] R.N. Cavalcanti, M.A.A. Meireles, Fundamentals of Supercritical Fluid Extraction, Elsevier, 2012. https://doi.org/10.1016/B978-0-12-381373-2.10039-0.

[23] D.V. Bermejo, E. Ibáñez, G. Reglero, C. Turner, T. Fornari, I. Rodriguez-meizoso, High catechins / low caffeine powder from green tea leaves by pressurized liquid extraction and supercritical antisolvent precipitation, Sep. Purif. Technol. 148 (2015) 49–56. https://doi.org/10.1016/j.seppur.2015.04.037.

[24] M.S. Lenucci, M. De Caroli, P.P. Marrese, A. Iurlaro, L. Rescio, V. Böhm, G. Dalessandro, G. Piro, Enzyme-aided extraction of lycopene from high-pigment tomato cultivars by supercritical carbon dioxide, Food Chem. 170 (2015) 193–202. https://doi.org/10.1016/j.foodchem.2014.08.081.

[25] R. Gallego, M. Bueno, M. Herrero, Sub- and supercritical fluid extraction of bioactive compounds from plants, food-by-products, seaweeds and microalgae – An update, TrAC - Trends Anal. Chem. 116 (2019) 198–213. https://doi.org/10.1016/j.trac.2019.04.030.

[26] D.B. Kovačević, M. Maras, F.J. Barba, D. Granato, S. Roohinejad, K. Mallikarjunan, D. Montesano, J.M. Lorenzo, P. Putnik, Innovative technologies for the recovery of phytochemicals from Stevia rebaudiana Bertoni leaves: A review, Food Chem. 268 (2018) 513–521. https://doi.org/10.1016/j.foodchem.2018.06.091.

[27] F. Chemat, M. Abert-Vian, A.S. Fabiano-Tixier, J. Strube, L. Uhlenbrock, V. Gunjevic, G. Cravotto, Green extraction of natural products. Origins, current status, and future challenges, TrAC - Trends Anal. Chem. 118 (2019) 248–263. https://doi.org/10.1016/j.trac.2019.05.037.

[28] P. Vazquez-Roig, Y. Picó, Pressurized liquid extraction of organic contaminants in environmental and food samples, Trends Anal. Chem. 71 (2015) 55–64. https://doi.org/10.1016/j.trac.2015.04.014.

[29] A.P. da F. Machado, J.L. Pasquel-reátegui, G.F. Barbero, J. Martínez, Pressurized liquid extraction of bioactive compounds from blackberry (Rubus fruticosus L.) residues: a comparison with conventional methods, FRIN. (2014) 9. https://doi.org/10.1016/j.foodres.2014.12.042.

[30] K.J. Olejar, J. Hatfield, C.J. Arellano, A.T. Gurau, D. Seifried, B. Vanden Heuvel, C.A. Kinney, Thermo-chemical conversion of cannabis biomass and extraction by pressurized liquid extraction for the isolation of cannabidiol, Ind. Crops Prod. 170 (2021) 113771. https://doi.org/10.1016/j.indcrop.2021.113771.

[31] A. Oreopoulou, D. Tsimogiannis, V. Oreopoulou, Extraction of Polyphenols From Aromatic and Medicinal Plants: An Overview of the Methods and the Effect of Extraction Parameters, in: Polyphenols in Plants, 2nd ed., Elsevier Inc., 2019: pp. 243–259. https://doi.org/10.1016/B978-0-12-813768-0.00025-6.

[32] G. Herbst, F. Hamerski, M. Errico, M. L. Corazza, Pressurized liquid extraction of brewer's spent grain: Kinetics and crude extracts characterization, J. Ind. Eng. Chem. 102 (2021) 370–383. https://doi.org/10.1016/j.jiec.2021.07.020.

[33] A.R.C. de Souza, S. Stefanov, M.C.M. Bombardelli, M.L. Corazza, R.P. Stateva, Assessment of composition and biological activity of Arctium lappa leaves extracts obtained with pressurized liquid and supercritical CO2 extraction, J. Supercrit. Fluids. 152 (2019) 104573. https://doi.org/10.1016/j.supflu.2019.104573.

[34] A.M. Barbosa, K.S. Santos, G.R. Borges, A.V.C.S. Muniz, F.M.R. Mendonça, M.S. Pinheiro, E. Franceschi, C. Dariva, F.F. Padilha, Separation and Purification Technology Separation of antibacterial biocompounds from Hancornia speciosa leaves by a sequential process of pressurized liquid extraction, Sep. Purif. Technol. 222 (2019) 390–395. https://doi.org/10.1016/j.seppur.2019.04.022.

[35] P.H. Santos, J.C. Kammers, A.P. Silva, J.V. Oliveira, H. Hense, Antioxidant and antibacterial compounds from feijoa leaf extracts obtained by pressurized liquid extraction and supercritical fluid extraction, Food Chem. 344 (2021) 128620. https://doi.org/10.1016/j.foodchem.2020.128620.

[36] D.M. Ferro, S. Mazzutti, L. Vitali, C.M.O. Müller, S.R.S. Ferreira, Integrated extraction approach to increase the recovery of antioxidant compounds from Sida rhombifolia leaves, J. Supercrit. Fluids. 149 (2019) 10–19. https://doi.org/10.1016/j.supflu.2019.03.013.

[37] M.B. Jacobs, Determination of moisture, in: Chem. Anal. Foods Food Prod., 3th ed., Van Nostrand Reinhold, New York, 1973: pp. 22–23. https://doi.org/10.1021/ed016p100.1.

[38] A.S. of A.E. ASAE, ASAE Standards: Standards, Engineering Practices and Data Adopted by the American Society of Agricultural Engineers, American Society of Agricultural Engineers, 1993. https://books.google.com.br/books?id=GrYdAQAAMAAJ.

[39] J. Viganó, I.Z. Brumer, P.A. de C. Braga, J.K. da Silva, M.R. Maróstica Júnior, F.G. Reyes Reyes, J. Martínez, Pressurized liquids extraction as an alternative process to readily obtain bioactive compounds from passion fruit rinds, Food Bioprod. Process. 100 (2016) 382–390. https://doi.org/10.1016/j.fbp.2016.08.011.

[40] M.A.A. Meireles, Extraction of bioactive compounds from latin american plants, CRC Press - Taylor & Francis Group, Boca Raton, 2008. https://doi.org/10.1201/9781420006513.

[41] V.L. Singleton, R. Orthofer, R.M. Lamuela-Raventós, Analysis of Total Phenols and Other Oxidation Substrates and Antioxidants by Means of Folin-Ciocalteu reagente, Polyphenols and Flavonoids. 299 (1999) 152–178.

[42] P.C. Veggi, R.N. Cavalcanti, M.A.A. Meireles, Production of phenolic-rich extracts from Brazilian plants using supercritical and subcritical fluid extraction: Experimental data and

economic evaluation, J. Food Eng. 131 (2014) 96–109. https://doi.org/10.1016/j.jfoodeng.2014.01.027.

[43] E.L.C. Amorim, J.E. Nascimento, J.M. Monteiro, T.A.S. Peixoto-Sobrinho, T.J.S. Araújo, U.P. Albuquerque, A simple and accurate procedure for the determination of tannin and flavonoid levels and some applications in ethnobotany and ethnopharmacology. Functional Ecosystems and Communities, v. 2, n. 1, p. 88–94, 2008., Funct. Ecosyst. Communities. 2 (2008) 88–94.

[44] R. Re, N. Pellegrini, A. Proteggente, A. Pannala, M. Yang, C. Rice-Evans, Antioxidant activity applying an improved abts radical cation decolorization assay, Free Radic. Biol. Med. 26 (1999) 1231–1237.

[45] H. Bendif, K. Adouni, M.D. Miara, R. Baranauskienė, P. Kraujalis, P.R. Venskutonis, S.M. Nabavi, F. Maggi, Essential oils (EOs), pressurized liquid extracts (PLE) and carbon dioxide supercritical fluid extracts (SFE-CO2) from Algerian Thymus munbyanus as valuable sources of antioxidants to be used on an industrial level, Food Chem. 260 (2018) 289–298. https://doi.org/10.1016/j.foodchem.2018.03.108.

[46] V.L. Sanches, T.A. Cunha, J. Viganó, L.M. de Souza Mesquita, L.H. Faccioli, M.C. Breitkreitz, M.A. Rostagno, Comprehensive analysis of phenolics compounds in citrus fruits peels by UPLC-PDA and UPLC-Q/TOF MS using a fused-core column, Food Chem. X. 14 (2022). https://doi.org/10.1016/j.fochx.2022.100262.

[47] W.L. Peng, H. Mohd-Nasir, S.H.M. Setapar, A. Ahmad, D. Lokhat, Optimization of process variables using response surface methodology for tocopherol extraction from Roselle seed oil by supercritical carbon dioxide, Ind. Crops Prod. 143 (2020) 111886. https://doi.org/10.1016/j.indcrop.2019.111886.

[48] M.A.A. Meireles, Supercritical extraction from solid: process design data (2001 – 2003), Curr. Opin. Solide State Mater. Sci. 7 (2003) 321–330. https://doi.org/10.1016/j.cossms.2003.10.008.

[49] P. Santos, A.C. Aguiar, G.F. Barbero, C.A. Rezende, J. Martínez, Supercritical carbon dioxide extraction of capsaicinoids from malagueta pepper (Capsicum frutescens L.) assisted by ultrasound, Ultrason. Sonochem. 22 (2015) 78–88. https://doi.org/10.1016/j.ultsonch.2014.05.001.

[50] Y.C. Yang, M.C. Wei, A combined procedure of ultrasound-assisted and supercritical carbon dioxide for extraction and quantitation oleanolic and ursolic acids from Hedyotis corymbosa, Ind. Crops Prod. 79 (2016) 7–17. https://doi.org/10.1016/j.indcrop.2015.10.038.

[51] R. Goyeneche, A. Fanovich, C. Rodriguez, M. Celeste, K. Di, Supercritical CO2 extraction of bioactive compounds from radish leaves: Yield, antioxidant capacity and cytotoxicity, J. Supercrit. Fluids. 135 (2018) 78–83. https://doi.org/10.1016/j.supflu.2018.01.004.

[52] M.L. Cygnarowiczt, W.D. Seider, Effect of Retrograde Solubility on the Design Optimization of Supercritical Extraction Processes, Ind. Eng. CHem. Res; 28 (1989) 1497–1503.

[53] N.R. Foster, G.S. Gurdial, J.S.L. Yun, K.K. Liong, K.D. Tilly, S.S.T. Ting, H. Singh, J.H. Lee, Significance of the Crossover Pressure in Solid-Supercritical Fluid Phase Equilibria, Ind. Eng. Chem. Res; 30 (1991) 1955–1964.

[54] B. Martín-garcía, S. Pimentel-moral, A.M. Gómez-caravaca, D. Arráez-román, A. Segura-carretero, Box-Behnken experimental design for a green extraction method of phenolic compounds from olive leaves, Ind. Crop. Prod. 154 (2020) 112741. https://doi.org/10.1016/j.indcrop.2020.112741.

[55] M. Cvjetko Bubalo, S. Vidović, I. Radojčić Redovniković, S. Jokić, New perspective in extraction of plant biologically active compounds by green solvents, Food Bioprod. Process. 109 (2018) 52–73. https://doi.org/10.1016/j.fbp.2018.03.001.

[56] S. Cadena-carrera, D. Parolo, A. Bella, R. Cé, B. Cruz, J. Miguel, H. Hense, Biological activity of extracts from guayusa leaves (Ilex guayusa Loes.) obtained by supercritical CO2 and ethanol as cosolvent, J. Supercrit. Fluids. 152 (2019). https://doi.org/10.1016/j.supflu.2019.104543.

[57] S. Đurovic, S. Sorgic, S. Popov, L. Pezo, P. Maskovic, S. Blagojevic, Z. Zekovic, Recovery of biologically active compounds from stinging nettle leaves part I: Supercritical carbon dioxide extraction, Food Chem. 373 (2022). https://doi.org/10.1016/j.foodchem.2021.131724.

[58] H. Ahangari, J.W. King, A. Ehsani, M. Yousefi, Supercritical fluid extraction of seed oils – A short review of current trends, Trends Food Sci. Technol. 111 (2021) 249–260. https://doi.org/10.1016/j.tifs.2021.02.066.

[59] M. Singh, T. Thrimawithana, R. Shukla, B. Adhikari, Extraction and characterization of polyphenolic compounds and potassium hydroxycitrate from Hibiscus sabdariffa, Futur. Foods. 4 (2021) 100087. https://doi.org/10.1016/j.fufo.2021.100087.

[60] S. Pimentel-Moral, I. Borrás-Linares, J. Lozano-Sánchez, D. Arráez-Román, A. Martínez-Férez, A. Segura-Carretero, Supercritical CO 2 extraction of bioactive compounds

from Hibiscus sabdariffa, J. Supercrit. Fluids. 147 (2019) 213–221. https://doi.org/10.1016/j.supflu.2018.11.005.

[61] O.R. Alara, N.H. Abdurahman, O.A. Olalere, Ethanolic extraction of flavonoids, phenolics and antioxidants from Vernonia amygdalina leaf using two-level factorial design, J. King Saud Univ. - Sci. 32 (2020) 7–16. https://doi.org/10.1016/j.jksus.2017.08.001.

[62] M.A.R. Salazar, J.V. Costa, G.R.O. Urbina, V.M.B. Cunha, M.P. Silva, P. do N. Bezerra, W.B.S. Pinheiro, W. Gomes-Leal, A.S. Lopes, R.N. Carvalho Junior, Chemical composition, antioxidant activity, neuroprotective and anti-inflammatory effects of cipó-pucá (Cissus sicyoides L.) extracts obtained from supercritical extraction, J. Supercrit. Fluids. 138 (2018) 36–45. https://doi.org/10.1016/j.supflu.2018.03.022.

[63] S. Samadi, F. Raouf Fard, Phytochemical properties, antioxidant activity and mineral content (Fe, Zn and Cu) in Iranian produced black tea, green tea and roselle calyces, Biocatal. Agric. Biotechnol. 23 (2020) 101472. https://doi.org/10.1016/j.bcab.2019.101472.

[64] N.R. Sucupira, A.B. da Silva, G. Pereira, J.N. da Costa, Métodos Para Determinação da Atividade Antioxidante de Frutos, UNOPAR Cientifíca. Ciências Biológicas e Da Saúde. 14 (2012) 263–270.

[65] B. Ou, D. Huang, M. Hampsch-Woodill, J.A. Flanagan, E.K. Deemer, Analysis of antioxidant activities of common vegetables employing oxygen radical absorbance capacity (ORAC) and ferric reducing antioxidant power (FRAP) assays: A comparative study, J. Agric. Food Chem. 50 (2002) 3122–3128. https://doi.org/10.1021/jf0116606.

[66] M.S. Sammani, S. Clavijo, V. Cerdà, Recent, advanced sample pretreatments and analytical methods for flavonoids determination in different samples, TrAC - Trends Anal. Chem. 138 (2021). https://doi.org/10.1016/j.trac.2021.116220.

[67] A.P.D.F. Machado, A.L.D. Pereira, G.F. Barbero, J. Martínez, Recovery of anthocyanins from residues of Rubus fruticosus, Vaccinium myrtillus and Eugenia brasiliensis by ultrasound assisted extraction, pressurized liquid extraction and their combination, Food Chem. 231 (2017) 1–10. https://doi.org/10.1016/j.foodchem.2017.03.060.

[68] Á.L. Santana, L.D. Queirós, J. Martínez, G.A. Macedo, Pressurized liquid- and supercritical fluid extraction of crude and waste seeds of guarana (Paullinia cupana): Obtaining of bioactive compounds and mathematical modeling, Food Bioprod. Process. 117 (2019) 194–202. https://doi.org/10.1016/j.fbp.2019.07.007.

[69] S. Rathod, S. Arya, S. Kanike, S.A. Shah, P. Bahadur, S. Tiwari, Advances on nanoformulation approaches for delivering plant-derived antioxidants: A case of quercetin, Int. J. Pharm. 625 (2022) 122093. https://doi.org/10.1016/j.ijpharm.2022.122093.

[70] C.A. Rice-Evans, N.J. Miller, G. Paganga, Structure-antioxidant activity relationships of flavonoids and phenolic acids, Free Radic. Biol. Med. 20 (1996) 933–956. https://doi.org/10.1016/0891-5849(95)02227-9.

[71] P.M. Kapepula, N. Kabamba Ngombe, P. Tshisekedi Tshibangu, C. Tsumbu, T. Franck, A. Mouithys-Mickalad, D. Mumba, D. Tshala-Katumbay, D. Serteyn, M. Tits, L. Angenot, P.D.T. Kalenda, M. Frédérich, Comparison of metabolic profiles and bioactivities of the leaves of three edible Congolese Hibiscus species, Nat. Prod. Res. 31 (2017) 2885–2892. https://doi.org/10.1080/14786419.2017.1305382.

[72] S. Gosain, R. Ircchiayab, P.C. Sharma, S. Thareja, A. Kalra, A. Deep, T.R. Bhardwaj, Hypolipidemic effect of ethanolic extract from the leaves of Hibiscus sabdariffa L. in hyperlipidemic rats, Acta Pol. Pharm. 67 (2010) 179–184.

[73] I. Da-Costa-Rocha, B. Bonnlaender, H. Sievers, I. Pischel, M. Heinrich, Hibiscus sabdariffa L. - A phytochemical and pharmacological review, Food Chem. 165 (2014) 424–443. https://doi.org/10.1016/j.foodchem.2014.05.002.

[74] S.A. Sargin, Potential anti-influenza effective plants used in Turkish folk medicine: A review, J. Ethnopharmacol. 265 (2021) 113319. https://doi.org/10.1016/j.jep.2020.113319.

SUPLEMENTARY MATERIAL

Figure 1S. Chromatographic profile of phenolic compounds from extracts by SFE (A) and PLE (B).

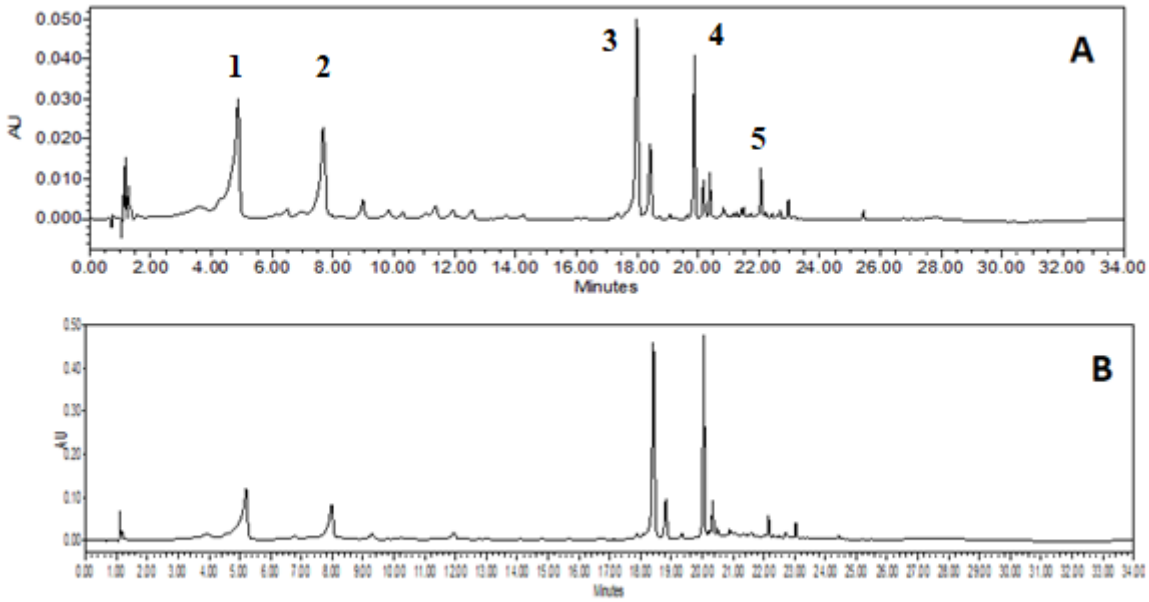

CAPÍTULO 4.

Effect of the gelling mechanism on the physical properties of bigels based on whey protein isolate

Artigo submetido à revista *Food Research International*

4. EFFECT OF THE GELLING MECHANISM ON THE PHYSICAL PROPERTIES OF BIGELS BASED ON WHEY PROTEIN ISOLATE

Gabrielli Nunes Clímaco [a]; Luiz Henrique Fasolin [a],*

[a] Department of Food Engineering and Technology, School of Food Engineering, University of Campinas, CEP 13083-862, Campinas, SP, Brazil

ABSTRACT

The effect of the cold-set and heat-set gelling mechanism of whey protein isolate on bigel production was assessed. For this purpose, hydrogel phase was produced with whey protein isolated (10% w/v) and for oleogel sunflower oil and glycerol monostearate (7.5% w/v) were used. Bigels were produced by hot emulsification of different hydrogel:oleogel ratios (from 90:10 up to 10:90). For cold-set bigels (CSB) NaCl (200 mM) was added to the aqueous phase prior to the emulsification and the emulsion was cooled to promote the 3D network formation. On the other hand, heat-set bigels (HSB) were produced by heating the emulsion (80 °C, 60 min). Bigels were evaluated through microscopy, FTIR, thermal and texture analyzes. Results showed that depending on the hydrogel:oleogel ratio and gelling mechanism different structures organization were obtained. CSB were more organized, showing that the rate of gelation was the mechanism responsible for the structure. However, for HSB the heat treatment destabilized the emulsion and disorganized structures were observed for high oleogel content. FTIR corroborates the visual observation and showed that the arrangement was purely physical. In addition, the structural arrangement led to different mechanical properties. In general, HSB produced gels with rubber-like behavior, higher elasticity modulus and the presence of a breaking point. In contrast, CSB behaves as squeezing gel, with no breaking point and lower values of elasticity modulus. Moreover, for O/W bigels the dispersed oleogel particles disrupted the WPI network decreasing the gel strength in comparison to pure hydrogels. However, for systems where oleogel was the continuous phase, the gel strength was recovered due to the metastable and dynamic character of these systems. Thus, results showed that the gelling mechanism of the protein exerted an effect on the physical properties of bigels. In addition, the mechanical properties also can be modulated according to the bigel composition, allowing its application in products with different sensorial characteristics.

Keywords: hybrid gel; hydrogel; oleogel; cold-set; heat-set; gelation;

4.1 INTRODUCTION

Bigels are defined as a mixture of hydrogel and oleogel, which can be organized as oil-in-water, water-in-oil, a mixture of interpenetrated colloidal gels, or even a bicontinuous structure with different bulk physicochemical properties (Shakeel et al., 2019). They can be produced by either cold or hot emulsification of the oily and aqueous phases. The first one is characterized by the mixture of the pure hydrogels and oleogels (after the gelled network

formation). On the other hand, for the hot emulsification, the liquid solutions containing the dispersed gelling agents are submitted to the emulsification process prior to the gelation (Samui et al., 2021). However, regardless of the production process, several factors can influence the physicochemical properties of bigels, such as the shear applied, type of solvent, type, structure and concentration of the gelling agents and the hydrogel:oleogel ratio. The last one being the most important factor since each combination can result in a network with different rheological properties (Fasolin et al., 2021; Shakeel et al., 2021).

These systems have shown high stability, with no phase separation during storage at room temperature for long periods, due to the complex three-dimensional gelled network (Lupi et al., 2016; Singh et al., 2014). In addition, the simultaneous presence of the oily and aqueous gelled phase confers unique texture properties (Sagiri et al., 2014) and also allows the incorporation of compounds with different polarities (Bollom et al., 2020; Fasolin et al., 2021). However, despite the increasing number of studies in the last decade, most of the publications in this subject are focused on cosmetic and pharmaceutical applications and only recently these structures have been explored by food scientists. Some of the recent works focused in improve the texture of foods and their nutritional value, through encapsulations of compounds using GRAS ingredients, such as ethylcellulose and starch (Ghiasi and Golmakani, 2022), beeswax (Martins et al., 2019; Zhai et al., 2022), soy lecithin and whey protein (Bollom et al., 2020), gellan gum and glycerol monostearate (Fasolin et al., 2021), candelilla wax and gelatin (Xie et al., 2023), k-carageenan and glyceride (Zheng et al., 2020), rice bran wax and gums (Nutter et al., 2023) and xanthan gum (Zheng et al., 2022). Recently, bigels have been developed and modulated for different applications, according to their physicochemical properties. The main applications are related to the fortification of food products, controlled delivery and fat replacement. Butter (Hashim et al., 2023), yogurt (Zuangh et al., 2021), cheese (Machado et al., 2023; Tian et al., 2023) and fermented sausages (Siachou et al., 2023) are examples of food application developed in the las years.

The oleogel phase can be produced by different methods, mainly classified as direct and indirect methods. For the direct methods, the gelling agent is dispersed in the oil and solubilized at high temperatures. The gel network can be formed by two types of gelling agents, namely high molecular weight (HMOGs) and low molecular weight (LMOGs). For HMOGs, the 3D network is formed by covalent interactions and entanglement among the macromolecules. On the other hand, the LMOGs are molecules self-organized into a 3D network that trap the oil by capillarity (Hwang, 2020). Glyceryl monostearate (GM) is a LMOG that has been widely used

as a gelling agent for structuring edible oils for food application, since it is efficient at low concentrations and present low cost (Trujillo-Ramírez et al., 2018). In addition, it is considered GRAS by the US Food and Drug Administration (CFR 21 - Section 182.1324) and approved by the European Union for food application (European, 2018). Several authors used GM along with other compounds to produce edible bigels, such as gellan gum (Fasolin et al., 2021; Zhu et al., 2021), gelatin (Samui et al., 2021) and k-carrageenan and whey protein concentrate (Habibi et al., 2022). In all of these studies, GM improved the oleogel network and the bigel texture, conferring higher firmness.

Concerning the aqueous phase, several authors have already studied the effects of different polysaccharides for bigel production, such as gellan gum (Zhu et al., 2021), k-carrageenan (Zheng et al., 2020), alginate (Martins et al., 2019), and also proteins like whey protein isolate (WPI) (Hazrati and Madadlou, 2021; Rodrigues et al., 2020). WPI is a product derived from the cheese production and is widely used in the food industry due to its high nutritional value (Jiang et al., 2021). It is one of the most used gelling agents, and has been studied over the years by several authors (Bollom et al., 2020; Kuhn et al., 2011; Shishir et al., 2018). WPI can be divided into four main individual protein components, namely β-lactoglobulin (β-LG), α-lactalbumin (α-LA), bovine serum albumin (BSA), and lactoferrin (LF) (Falsafi et al., 2022). This protein presents interesting gelling, emulsifying and foaming properties, enabling the formation of a structural matrix capable of retaining water, flavors, probiotics and food ingredients (He et al., 2021). Regarding the gelling ability, these globular proteins can form gels through two different processes, generally called heat- and cold-set gelation (Yang et al., 2021) and different molecular interaction can be involved (e.g., steric and van der Waals; hydrophobic; electrostatic interaction and hydrogen and disulfide bonds) (Bryant and McClements, 1998).

The heat-set gelation is performed in one step, where an aqueous solution of WPI is heated to promote the protein denaturation (McClements and Keogh, 1995; Yang et al., 2021). The unfolding of the native proteins led to exposure of non-polar amino acids, thereby increasing the hydrophobic attraction between them. At this point, the unfolded protein molecules are charged and may remain separated due to the electrostatic repulsion. However, in the presence of salts the charged sites present in the protein are screened, favoring the intermolecular hydrophobic interaction and gel formation. In addition, the heat treatment also led to the exposure of the thiol group (SH) of the cysteine residues mainly present in the β-lactoglobulin fraction. Thus, in addition to the aggregation promoted by the hydrophobic forces

disulfide bonding also plays an important role in the gel aggregation and strengthening (Hongsprabhas and Barbut, 1997). In fact, Hongsprabhas and Barbut (1997) demonstrated that disulfide bonds were mainly involved in the polymerization step prior to gelation and assisted in maintaining the network structure. The thiol group of the cysteine residue is especially important for the aggregation behavior of β-lg. Moreover, it is worth mentioning that for this method, WPI must be above the critical protein concentration to promote protein interaction and gel formation (Martins et al., 2018).

On the other hand, for cold-set gels the same gelation mechanisms, i.e., molecular interactions are present. However, they occur in two different steps. At first, the WPI solution (below critical concentration) is partially denatured at high temperatures, pH values far from the isoelectric point (pI) and at low ionic strength. In these conditions the gel formation did not occur due to the low protein concentration and the electrical repulsion. After the solution cooling, the salt is added and acts as counter-ions, which shield the electrostatic repulsion between the electrically charged protein filaments and cause them to aggregate (Bryant and McClements, 1998; Hazrati and Madadlou, 2021; Kuhn et al., 2011).

Based on these gelation mechanisms, some authors have observed that cold-set gels; generally, promote the formation of hydrogels with improved physicochemical properties (Babaei et al., 2022). The slow rate gelation led to a more organized structure that led to higher water holding capacity and mechanical strength with greater stability. (He et al., 2021; Kuhn et al., 2011; Rodrigues et al., 2020; Yang et al., 2021). However, to our knowledge, WPI bigels have been produced only by heat-set method. Therefore, the aim of this work was to produce GRAS bigels for food application with WPI, sunflower oil and GM through heat and cold-set protein gelation in order to evaluate the influence of the gelling process on physicochemical properties.

4.2 MATERIALS AND METHODS

Materials

Whey Protein Isolate (WPI) powder (Lacprodan DI-9212, 91% protein concentrate), kindly supplied by Arla Foods Ingredients (Viby, Denmark) and NaCl (Merck, Germany) was used for the hydrogels production. Oleogels were produced with glyceryl monostearate (GM) (> 95%) from Alfa Aesar (Tewksbury, Massachusetts) and commercial sunflower oil (LIZA, 10% saturated fat).

Methods

Pure gels production

Oleogels (OG) were prepared by heating the mixture of gelling agent (GM) at three different concentration (2%, 5% e 7.5% (w/v)) and sunflower oil at 80 °C during 30 min under magnetic stirring (Heidolph, Magnetic stirrer Hei-Tec) (500 min^{-1}) in order to solubilize the gelling agent (Cerqueira et al., 2017). The solution was put in appropriate molds and stored at 25 ± 2 °C for 24 h for complete oleogel formation.

Hydrogels were produced with WPI through heat and cold-set gelation, according to the methodology described by Yang et al. (2021) and Rodrigues et al. (2020). Heat-set hydrogels (HH) were produced with WPI (7.5 and 10 % (w/v)) dispersed into a 0.1 M sodium chloride solution. The mixtures were magnetically stirred for 2-3 h until the protein was completely dissolved and the pH was adjusted to 7.0 using NaOH (1 M). The gels were put in Falcon tubes and subject to heat treatment at 80 °C during 30 min. Then, the WPI hydrogels were stored during the night before characterization.

For cold-set hydrogel (CH), the WPI (7.5 and 10 % (w/v)) were dispersed in distillate water under magnetic stirring for 2 hours at room temperature (25 °C) and kept overnight, for complete hydration and protein solubilization. The solutions (pH 7.0, adjusted using NaOH (1 M)) were subject to heat treatment at 90 °C during 10 min. Then, the partially denatured WPI was cooled to 55 °C, and the ionic strength was adjusted with NaCl 5 M solution (25 ºC) until a final concentration of 200 mM. The mixtures were quickly put in Falcon tubes, homogenized in vortex and stored at 25 ± 2 °C for 24 h. Both hydrogels and oleogels were submitted to analyses of microscopy, mechanical properties, infra-red spectrophotometry (FTIR) and differential scanning calorimetry (DSC).

Bigels production

The bigels were produced by mixing pure hydrogel (CH or HH gels) and oleogel at different hydrogel:oleogel ratio (90:10, 70:30, 50:50, 30:70 and 10:90). Heat-set bigels (HSB) were prepared as follows: after the gelling agent solubilization, the oleogel solution was cooled to 55 °C, while WPI solution without heat treatment was heated to the same temperature. The both solutions were mixed and then emulsified at 18.000 min^{-1} for 2 min, using Ultra Turrax (T18, IKA, Germany). The emulsions were put in cylindrical molds (diameter = 22 mm), heated at 80 °C for 60 min in a water bath and then cooled at room temperature (25 ± 2 °C). For the cold-set bigels (CSB), the oleogel solution and the WPI solution (after heat treatment) were cooled to 55 °C, adjusted with NaCl 5 M solution (25 ºC) until a final concentration of 200 mM,

mixed and emulsified at the same conditions (18.000 min^{-1}, 2 min). The solutions were put in cylindrical molds (diameter = 22 mm) and stored at room temperature (25 ± 2 °C) to gel formation. The bigels were submitted to analyses of microscopy, mechanical properties, infra-red spectrophotometry (FTIR) and differential scanning calorimetry (DSC).

Optical Microscope

The bigels were put in a glass slide immediately after preparation, covered by a coverslip, and stored at 25 °C during 24 h before analyses. The images were obtained under a microscope optic (Leica – DM2000) loaded with a digital camera EC3 (Leica Microsystems, Heerburg, Suíça).

Particle size distribution and the organization of the oil and water phases were observed. The size of the particles was analyzed using the ImageJ 1.53t software (National Institutes of Health, USA). At least 500 particles were used to calculate the mean diameter and particle size distribution. The volume-surface mean diameters (d_{32}) were calculated using Eq. 1.

$$d_{32} = \frac{\sum n_i d_i^3}{\sum n_i d_i^2} \quad (1)$$

where n_i was the number of particles with diameter d_i.

Scanning electron microscopy (SEM)

The samples (cylinders of 14 mm × 20 mm) were frozen using liquid nitrogen, lyophilized (Terroni - ENTERPRISE I, São Carlos, Brasil) and fractured. The fractured samples were fixed in a sample holder with double-sided carbon adhesive tape, metallized with gold (K450- Sputter Coater) and taken to the equipment for observation. At least three images of typical structures were recorded at a magnification of 30×, 250× and 1.000× using Quattro SEM, TermoFisher Scientific (Waltham, USA) microscope operating at 10 kV.

Confocal microscopy

A Leica TCS SP5 confocal laser scanning microscope (CLSM), was operated in fluorescence mode with a 63× oil-immersion objective. The protein phase was stained with FITC, and the oil phase with Nile Red. The samples were stained with Nile Red (0.1 g/L) and FITC (0.2 g/L) at 1:10 ratio (dye:sample, v/v), which enabled the oil particles to become visible. The samples were then placed onto a microscope slide with a cavity and covered by a coverslip. The CLSM images were recorded using a He–Ne laser with an excitation wavelength of 517

nm for FITC and 636 nm for Nile Red. All measurements were performed at 25 ºC and the experiments were carried out at least in duplicate.

Infra-red spectrophotometry (FTIR)

FTIR spectra was used to evaluate the possible interactions between the gel's compounds, following the methodology described by Sagiri et al. (2014). The spectrums of FTIR were measured using one spectrophotometer (FTIR – MID/FAR Agilent 660), operated in attenuated total reflectance mod (ATR). The measures were between 4000 and 400 cm^{-1} in resolution of 1 cm^{-1}.

Mechanical Proprieties

The mechanical properties were determined by uniaxial compression measurements in a TA. XTplus Texture Analyzer (Stable Micro Systems, United Kingdom) equipped with a 40 mm diameter plate. Cylindrical gels (diameter: 22 mm) were compressed to 80% of the initial height with crosshead speed of 1 $mm.s^{-1}$. The force x height data were transformed into Hencky stress (σ_H) and Hencky deformation (ε_H) (Eq. 2 and 3) (Fasolin et al., 2013; Rodrigues et al., 2020). Stress x deformation curves were used to evaluate the rupture point (first maximum point of the curve), while elasticity or Young's modulus (*E*) was calculated as the slope of the linear region.

$$\sigma_H = F(t)\left[\frac{H(t)}{H_0 A_0}\right] \quad (2)$$

$$\varepsilon_H = -ln\ ln\left[\frac{H(t)}{H_0}\right] \quad (3)$$

where *F(t)* being the force (N) in time *t*, A_0 (m^2) and H_0 (m) are the sample area and initial high, respectively e *H(t)* is the high (m) in time *t*. The stress (σ_H) and strain (ε_H) at rupture were calculated considering the rupture point as the maximum point of the stress–strain curve.

Differential Scanning Calorimetry (DSC)

DSC measurements were performed in a Mettler Toledo DSC1 equipment (Schwerzenbach, Switzerland). Approximately 10 mg of each bigel sample was sealed in aluminum pans previously weighed, and an empty aluminum pan without sample was set as reference. A heating and cooling ramp was performed, under an inert nitrogen atmosphere. Samples were cooled to 15°C and held at that temperature for 15 min before being heated to 90

°C (5 °C min^{-1}), and held at that temperature for 15 min. After this period, they were cooled again to 15 °C at the same temperature rate.

Statistical Analysis

The effect of both methods was determined by analysis of variance (ANOVA) and Tukey's test, using Minitab 19.1 (Minitab Ltd., State College, PA, USA) with a 95% confidence level ($\alpha = 0.05$).

4.3 RESULTS AND DISCUSSION

Properties of pure oleogels and hydrogels

The formation of the network that promotes a self-sustainable gel is directly related to the type and concentration of the gelling agent. Visual observation was used to verify the self-supported gels by tube flipping (Figure 4.1S). Oleogel's formulations were self-supported and visual changes were also observed for oleogels that became opaque with GM concentration increase. Also, it was reported that for oleogels produced with high-oleic sunflower oil at least 3% (w/w) GM was needed and the structure is denser and stronger with the increase in oleogelator increase (Cerqueira et al., 2017).

FTIR spectra were similar for both GM concentration (Figure 4.6). Two very defined peaks were observed at 2922 cm^{-1} and 2853 cm^{-1}. In addition, two very significant peaks were observed at 1745 cm^{-1} and 1162 cm^{-1}, which may be related to the stretching vibrations of C=O triglycerides (Fasolin et al., 2021; Zheng et al., 2020). They are characteristic of the asymmetrical and symmetrical stretching vibrations of methylene and also of the methyl groups (Fasolin et al., 2021). Besides, mechanical properties show that the maximum stress observed increases from 1.4 kPa to 3 kPa, for the 5 % and 7.5 % formulations, respectively (Figure 4.2S). Moreover, it is also important to highlight the Young's modulus (*E*). The greater the value of *E*, the smaller the deformation observed when the same magnitude was applied. So, for the hardest oleogel (7.5% (w/v) GM), *E* was higher, 17 kPa, in comparison to the oleogel with 5% (w/v) GM (10 kPa) (Figure 2S).

For hydrogels, visual analysis showed that for both CH and HH produced with WPI 7.5 % (w/v) it was observed syneresis, which means that the 3D network was not enough to entrap all the water content. Indeed, it was reported that for salt-induced WPI hydrogels the protein concentrations must be around 10%, and a reduction in protein concentration (up to 6%) during preheating has been shown to reduce gel strength and water holding capacity (Nicolai et al.,

2011). Moreover, CH gels were more translucid and HH opaquer, as reported by other authors (Figure 1S) (Bryant and McClements, 1998; McClements and Keogh, 1995).

Besides the WPI concentration, the gelling mechanism (heat or cold-set gelation) can exert influence on the arrangement and formation of protein intermolecular bonds. FTIR analysis verifies the presence of functional groups and did not show any difference among the spectra, i.e., despite the different gelling mechanism there was no change regarding the interactions between protein molecules (Figure 4.6). For both the hydrogels (HH and CH), a broad band between 3500 and 3000 cm^{-1} was observed, which may be related to the arrangement of water present in the system (Cheng et al., 2013). For this reason, it was not possible to observe the characteristic peaks like the stretching vibrations of -OH linked to $-NH_2$ that occur around 3268 cm^{-1} (Gbassi et al., 2012). The high intensity of this band masked the other characteristic peaks of the protein. For example, it is possible to observe very small peaks related to amide II (around 1537 cm^{-1}) and amide III (between 1400 and 1200 cm^{-1}). However, it was possible to identify a peak at 1648 cm^{-1} that can be related to the amide I (Popescu et al., 2021).

However, despite the absence of chemical interactions that could promote changes in the functional groups of the protein network, it was possible to observe a great difference in the physical organization of the protein network as a result of the gelation mechanism, i.e., heat- and cold-set. Thermal gelation (heat-set gels) occurred due to the unfolding of the protein molecules under heat in the presence of salt. The unfolded protein exposes hydrophobic amino acid residues and the thiol group (SH), promoting protein aggregation through mainly hydrophobic interactions and disulfide bonds (Hoffmann and Van Mil, 1997; Babaei et al., 2022). The molecular interactions are enhanced by the salt that reduces the electrostatic repulsion between the charged protein molecules. In summary, the denaturation and molecular interaction happen simultaneously, producing particulate gels (Bryant and McClements, 1998).

In turn, for cold-set gelation, the protein is partially unfolded and the formation of the 3D network is induced by the salt addition after the heat treatment. At this point, the unfolded protein filaments are charged and dispersed in the aqueous medium. Then, the salt addition binds the charged groups, decreasing the electrostatic repulsive forces between protein molecules and inducing gelation by promoting the same molecular interactions, i.e., hydrophobic interactions and disulfide bonds (Kuhn et al., 2011). This two step process produces an organized filamentous gel with different physicochemical properties (Bryant and McClements, 1998; McClements and Keogh, 1995).

As a consequence of the gelation mechanism, heat-gelled hydrogels presented a more disorganized network with larger porous in comparison to the cold-set ones, probably due to the faster network formation mechanism (Figure 4.1). On the other hand, cold-set gelation allows slower organization of the 3D network, thus generating a more organized and uniform structure. However, both have a honeycomb structure, characteristic of globular protein hydrogels (Joshi et al., 2014).

Figure 4.1. Scanning electron microscopy images of cold-set (CH) and hot-set (HH) hydrogel under a magnification of 30x (left) and 250x (right).

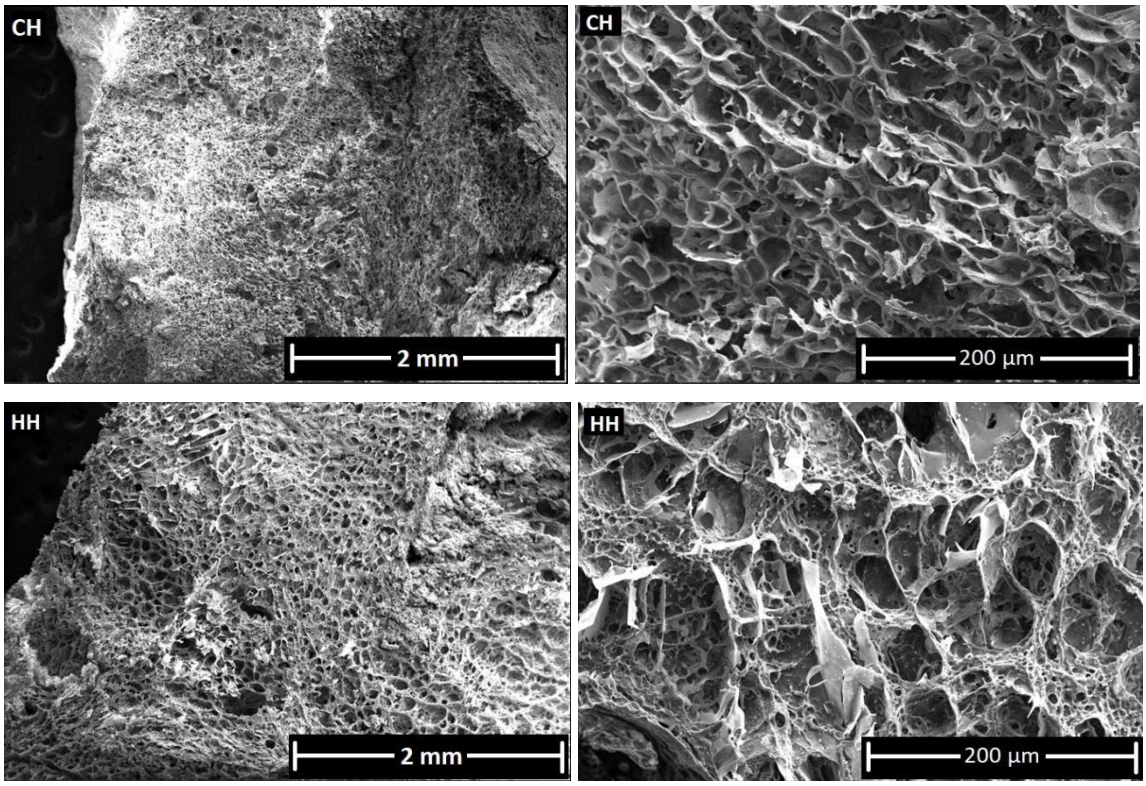

Differences in the network consequently led to different mechanical behavior. HH presented a rubber-like behavior in the stress-strain curves and a maximal stress or a "breaking point" was observed before the final stress (Bryant and McClements, 2000). However, CH did not show this "breaking point" until the maximum deformation evaluated (80% deformation), being characterized as a squeezing gel, which means that the gel spreads until the maximal deformation applied (Fasolin et al., 2013) (Figure 4.2). The aforementioned CH's organized structure observed in Figure 4.1 promotes a network more ductile and elastic, since the aggregates at the start of the cold gelation were formed at different conditions and resulted in a filamentous gel (Nicolai et al., 2011, Bryant and McClements, 1998). Similar result was observed for a cold-set oat starch-WPI hydrogel, where could be observed a honeycomb porous

structure, that resemble as interconnected tunnels, being responsible for gel elasticity, and the density degree of these voids indicates the strength of the gel (Kumar et al., 2022), while the heat-set also forms a honeycomb structure, but not uniformly, thus impairing the elasticity of the gel.

Figure 4.2. Representative stress-strain behavior for 10% heat-set (HH) and cold-set (CH) WPI hydrogels.

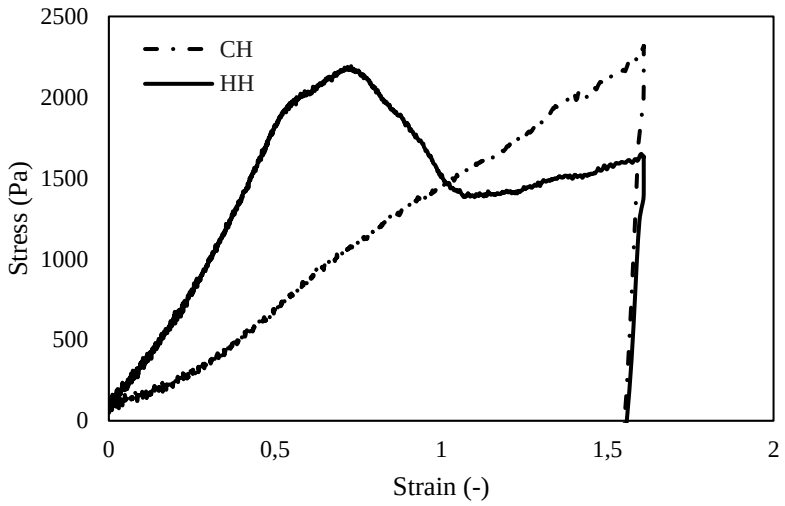

Figure 4.3 shows the mechanical properties of HH and CH hydrogels. The deformation observed at the maximum stress corroborates the gel behavior (rubber or squeezing gel). As mentioned before, squeezing gels spread until the maximal deformation applied, while rubber gels present a maximal stress in the rupture or breaking point. Thus, HH gels showed higher resistance to fracture and became more brittle gels. This structure has a higher ability to store the energy of the applied stress with lower deformation degree. However, higher stress values promote the structure breakdown. On the other hand, CH gels showed lower *E* values, being more elastic or more deformable gels.

Figure 4.3. Mechanical properties of hydrogels produced with WPI though heat-set (HH) and cold-set (CH) gelation (A) Maximum stress, (B) Strain at maximum stress, (C) Young's Modulus.

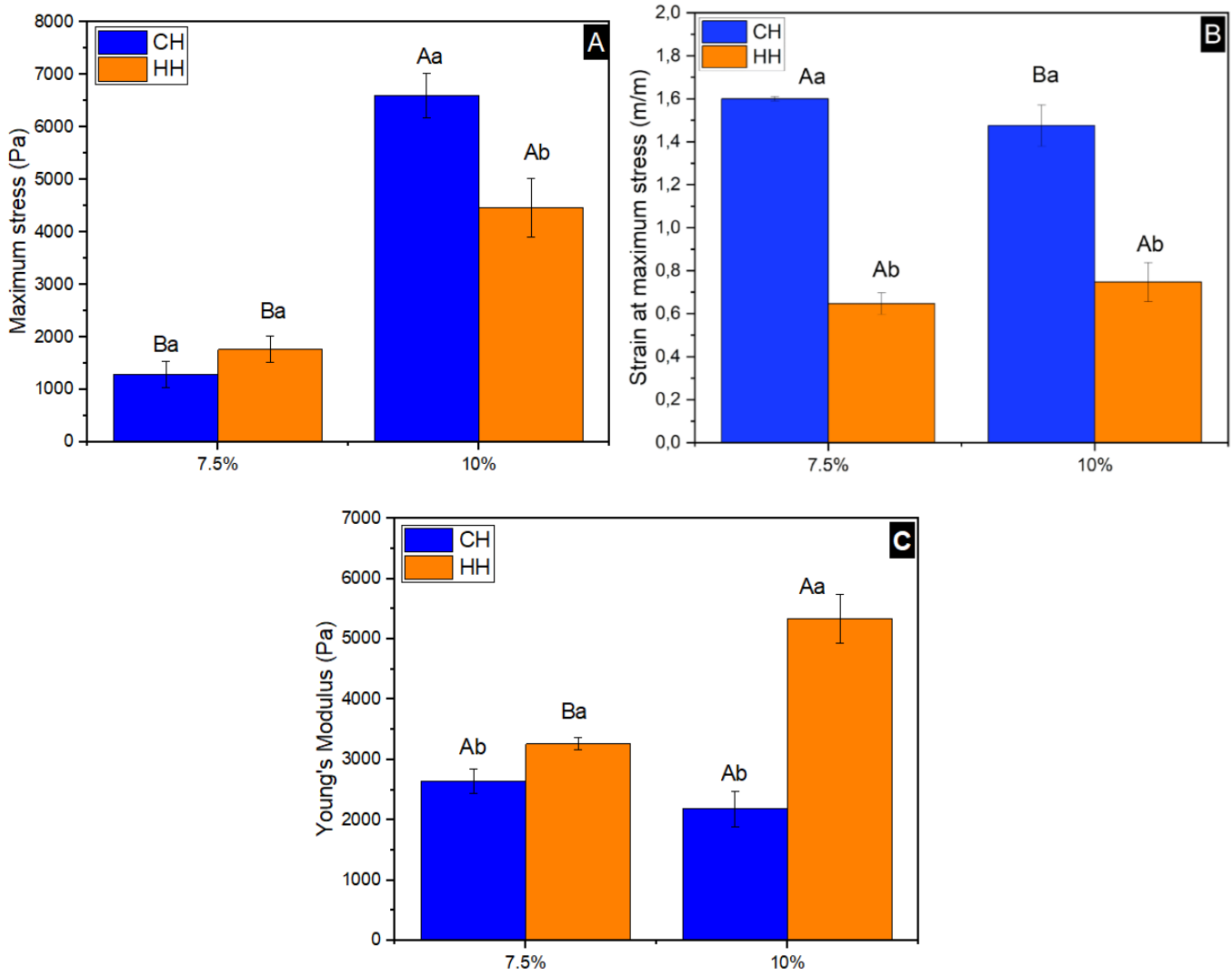

Values in the same set of bars (CH or HH) followed by different capital letters are significantly different by Tukey's test ($p < 0.05$); Values followed by different lowercase letters are significantly different by Tukey's test ($p < 0.05$).

General proprieties of bigels

Since WPI 7.5% (w/v) gels showed some syneresis degree, bigels were produced with 10% (w/v) for both heat and cold-set methods. The oleogel phase was produced with the minimum GM amount required for the production of self-sustainable systems within the range evaluated (7.5% (w/v)). All formulations of bigels produced self-sustainable gels, except for HSB 10:90, probably due to prolonged heating during gelation, where the structure can't remain stable, thus causing definitive phase separation.

It is possible to verify that the CSB 90:10, that contains a higher percentage of hydrogel (90 % (w/w)), seems like a hard gel (Figure 4.4A). Through visual observation and during

manipulation, it was observed that with the increase of the oleogel content in the formulation, the structure changes and the gel becomes softer, with a texture that corresponds to an ointment or a cream.

Optical microscopy showed structural differences between the CSB formulations (Figure 4.4A). O/W structures were observed for CSB from 90:10 to 50:50 along with the increase of the particle's size until CSB 30:70. After this point, the system seems to change from O/W to W/O. A study with beeswax and hydroxypropylmethylcellulose (HPMC) bigels showed similar results, where the number of particles increased when the proportion of oleogel increased from 20% to 50%. Furthermore, in a similar work, it was observed that when the amount of oleogel exceeded 60%, it was possible to observe the phase conversion, where the oil became the continuous phase (Chen et al., 2023). In relation to the heat-set bigels, it wasn't possible to capture the images, because after gelation, the network was completely structured, making it impossible to obtain a thin layer to analyze.

The oil particles had a homogeneous distribution in the bigels formulated with 10% and 30% oleogel, and D_{32} was 45.3 μm for CSB 70:30. For the 90:10 system, it wasn't possible to observe the oil particles, even with a high zoom, since they were too small. For this reason, particle size analysis was carried out for this system using the confocal images (Figure 4.4B). The approximate diameter for 90:10 oleogel particles was approximately 4.4 μm for CSB. It is worth mentioning that this analysis was carried out only to get an idea of the magnitude of the particles since the techniques used to obtain the images were different. In the bigels with 50% oleogel, the particle size showed a D_{32} increase to approximately 66 μm. As mentioned before, the crystallization of the oleogel occurs at temperatures slightly below 50 °C (Fasolin et al., 2018). Moreover, after the emulsification and during the cooling process the system was probably not able to stabilize the O/W emulsion. Thus, there was some coalescence of the oil phase until reach the crystallization onset temperature prevented this phenomenon. For W/O bigels, we must look in the opposite direction. Bigels with 90% oleogel showed a $D_{32} = 88$ μm and the hydrogel increase led to larger particles (~100 μm). However, these bigels did not clearly demonstrate the spherical shape of the particles.

Confocal microscopy (Figure 4.4B) could be performed for both bigels and improved the insights of the optical microscopy. For CSB the images also showed a more organized system in the CSB 90:10 and 10:90 bigels. For these systems there were very defined continuous and dispersed phases and it was possible to observe the small oleogel particles in CSB 90:10. Furthermore, the phase inversion from O/W to W/O in CSB 10:90 was clearly

observed through the inversion of colors of continuous and dispersed phase. However, for equal proportions of water and oil (50:50 system), the network was disorganized, with particles of different sizes and expressive coalescence.

Figure 4.4. A) Visual appearance and microscopic images of cold-set bigels (CSB) with different hydrogel:oleogel ratios and B) confocal images of cold-set (CSB) and heat-set (HSB) bigels with different hydrogel:olegel ratios.

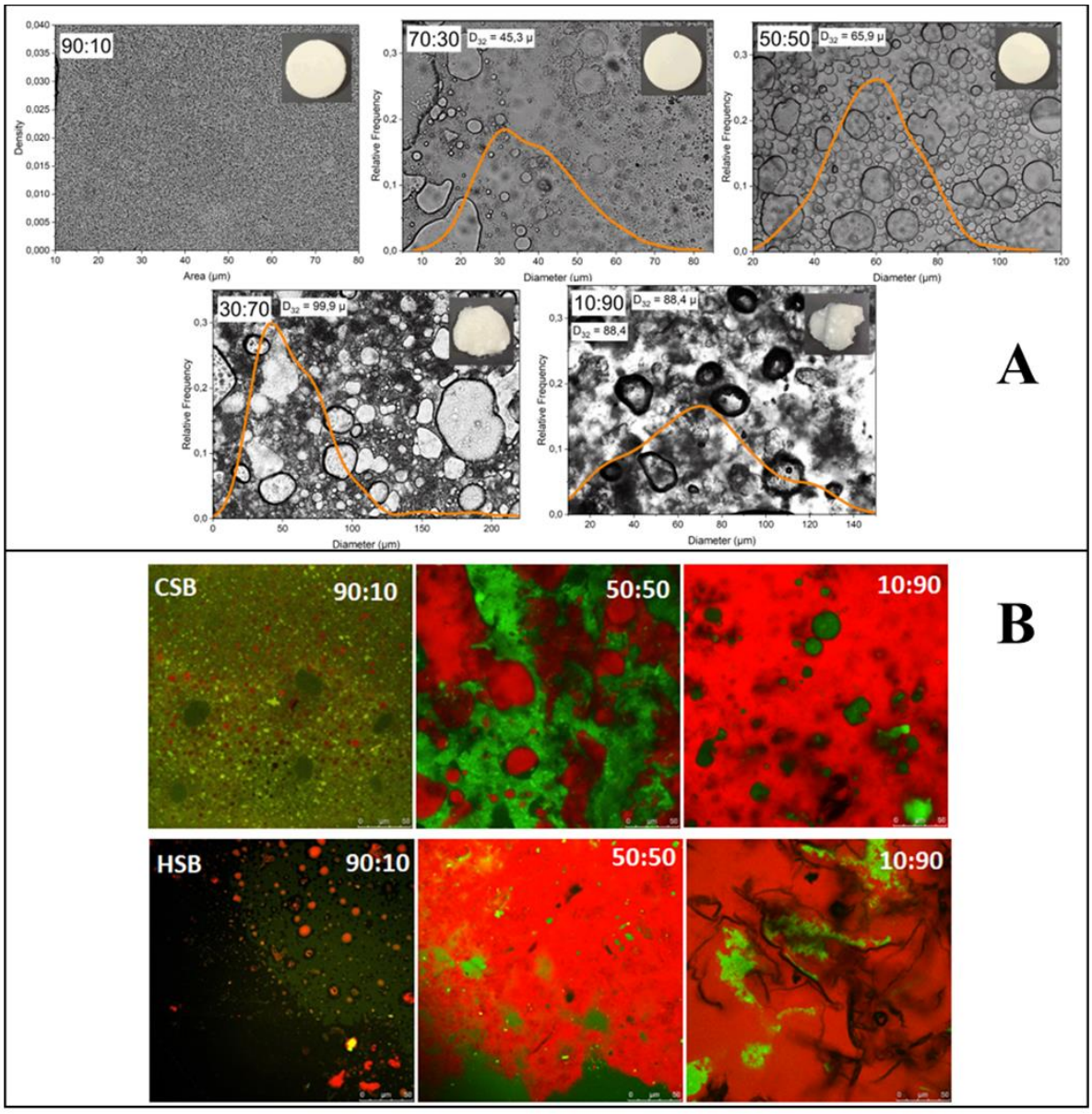

On the other hand, the HBS bigels structures were different from CBS and the effect of temperature on the oil-water interface during the gelation process can be observed. In the 90:10 gel, the heat process led to the formation of larger oil particles in comparison to CBS ones (approximately 6.9 μm). The temperature increase reduces the interfacial tension and the

viscosity of the continuous phase (Gaonkar, 1992; Okasha, 2018), allowing the drops coalescence. As the oil phase increased, this effect was more pronounced and emulsion was destabilized. This result also explains the destabilization and no gel formation for the 90:10 system.

To evaluate these structural differences, it is important once again to understand the kinetics of the gelation mechanism that led to the structural differences observed between CSB and HSB. The final CSB structure was only dependent on the gelation kinetics of both oleogel and hydrogel phases. The cold-set hydrogel has a slower gelling rate in comparison to the oleogel phase. Thus, for O/W CSB (90:10) the viscosity of the continuous phase prevents the coalescence of the oil droplets before the gelation process. Moreover, since the oleogel droplets gelled before the hydrogel, the well-defined continuous phase and dispersed spherical particles were maintained. On the other hand, for W/O CSB (10:90), the viscosity of the continuous phase was not enough to prevent coalescence of the hydrogel droplets. Thus, the simultaneous and dynamic process of droplets coalescence and gelation, plus the fast gelation rate of the oil continuous phase led to the well-defined separate phases, but with undefined shaped particles. However, for HSB the temperature increase reduces the interfacial tension and the viscosity as mentioned before, allowing the drops coalescence and emulsion destabilizing.

Regarding the protein 3D network, SEM shows that bigels resemble the respective pure gels, with cold gelling providing a more organized network than heat gelling (Figure 4.5). For both cold- and heat-set 90:10 bigels, it was possible to observe that the oleogel particles were dispersed in the porous of the protein network as part of the structure. Moreover, the 50:50 formulation showed more noticeable differences between the cold- and heat-set mechanisms. For CSB bigels smaller oil particles were observed in the protein network in comparison to the HSB, as mentioned before and observed in the confocal images (Figure 4.4B). However, the droplets are still intertwined in the protein network. This “oleogel interconnected network” is a characteristic of GM oleogelator, that promotes gels with a lot of protrusions, representing the oil particles entrapped in the gel network (Chen et al., 2020).

Figure 4.5. Scanning electron microscopy images of cold-set (CSB) and heat-set (HSB) bigels in the hydrogel:oleogel ratio of 90:10 and 50:50 under a magnification of 30x (left) and 250x (right).

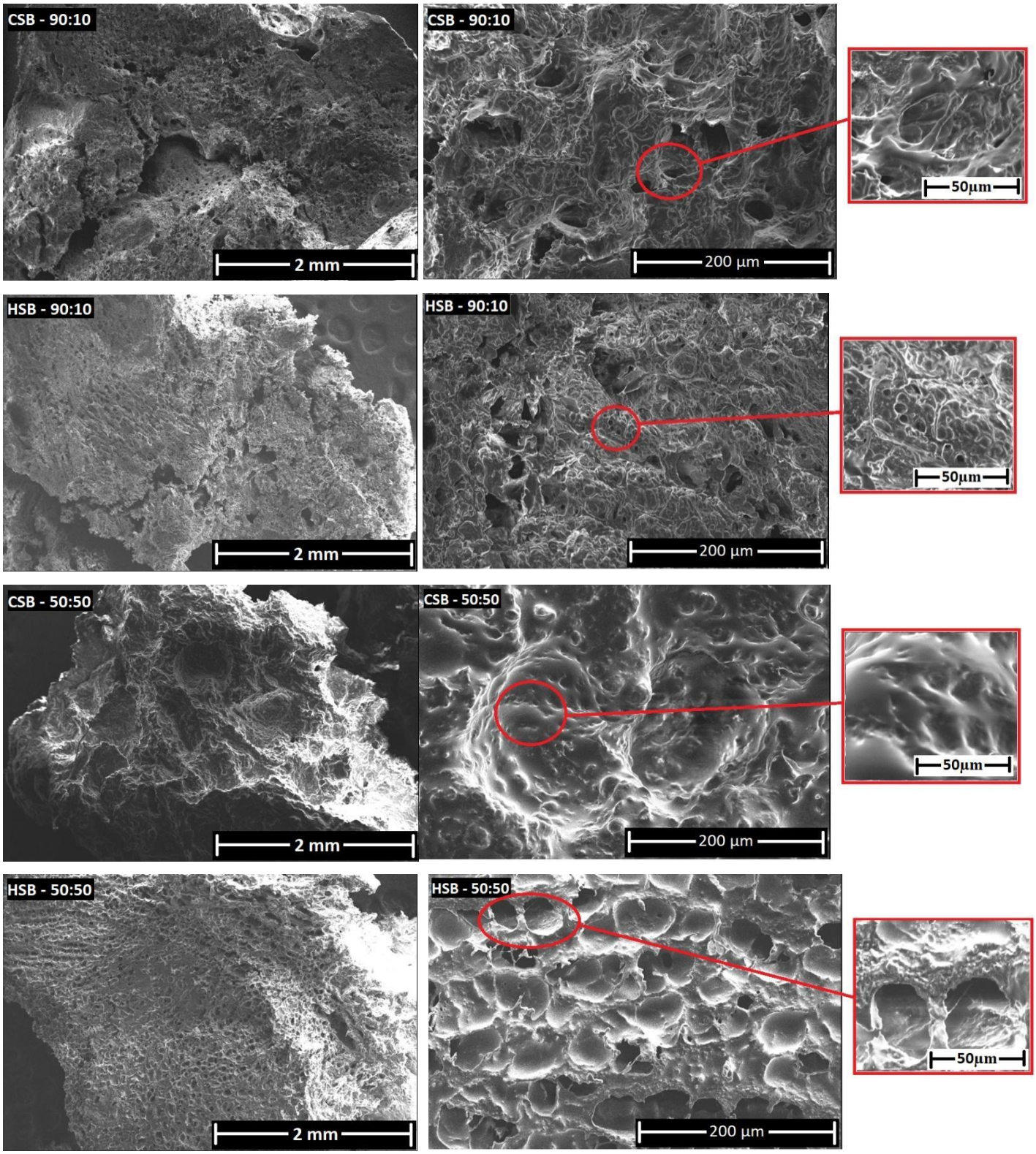

FTIR analysis for the bigels (Figure 4.6) corroborates the microscopy analysis with new insights about the structure organization. Figure 6 shows the maintenance of the same characteristic peaks of hydrogel and oleogel, which means that the arrangement of hydrogel and oleogel was purely physical, without any chemical interaction. For cold-set bigels with hydrogel prevailing (90:10 and 70:30), the spectra were similar to pure hydrogels, and the same happened when there is a predominance of oleogel. However, the bigel spectra undergo changes as the percentage of oleogel in the system increases. At 70% (w/w) oleogel (CSB 30:70) it is possible to observe the characteristic peaks for both oleogel and hydrogel simultaneously.

Figure 4.6. FTIR spectra of oleogel (OG), heat-set (HH) and cold-set (CH) WPI hydrogels, and cold-set (CSB) and heat-set (HSB) bigels.

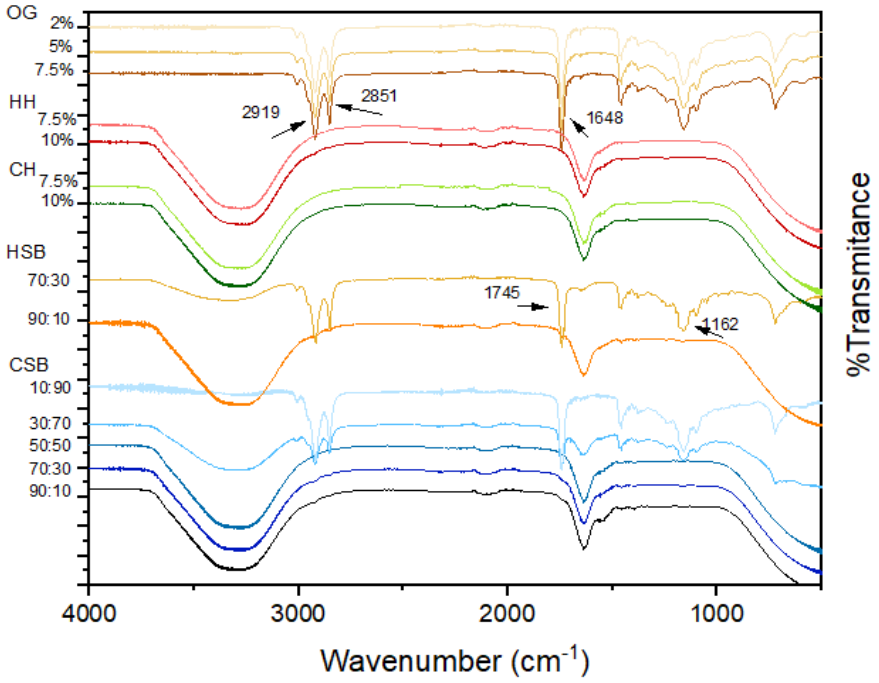

However, when the system changed from O/W to W/O i.e., oleogel became the continuous phase, the peaks between 3500 and 3000 cm^{-1} (Kazemi-Taskooh and Varidi, 2021; Vergara et al., 2022), were completely replaced by the two peaks present at 2919 cm^{-1} and 2851 cm^{-1}, referring to oil and GM, characterizing the vibrations of asymmetric and symmetrical stretching of methylene (Fasolin et al., 2021). In addition, the well-defined peak for the hydrogel at 1648 cm^{-1}, characteristic of the C=O bond also disappears, giving rise to peaks at 1745 cm^{-1} and 1162 cm^{-1}, when the bigel has 90% oleogel (Fasolin et al., 2021; Zheng et al., 2020). Thus, it seems that the formulations have the characteristics of the continuous phase, which means that CBS from 90:10 to 50:50 are O/W and CBS 10:90 W/O bigels, as

observed in Figures 4.5 and 4.6. On the other hand, CSB 30:70 is probably transitioning between O/W and W/O structures, showing a more complex arrangement.

For the HSB, the formulation HSB 90:10 is very similar to CSB 90:10, presenting more characteristics of the hydrogel than the oleogel, as expected. However, HSB 70:30, which still has a prevailing of hydrogel than the oleogel in its formulation, showed a pattern mainly related to oleogel, with the most significant peaks at 2919 cm^{-1}, 2851 cm^{-1}, 1745 cm^{-1} and 1162 cm^{-1}. This behavior may have occurred due to the different organization of the network observed in SEM and confocal micrographs (Figure 4.4B and 4.5). The aforementioned effect of heat treatment destabilized the system and allowed the oil to disperse through the protein network, promoting a more complex and disorganized network than cold-set bigels.

Such structural differences directly reflect on the mechanical behavior of the bigels (Figure 4.7). In general, the CSB and HSB stress-strain behavior were similar to their respective CH and HH pure hydrogels (squeezing and rubber gels, respectively). For this reason, no major differences were observed in the deformation where the maximum stress occurred. However, Young's modulus behavior was only similar to pure hydrogels for O/W bigels, i.e. HSB 90:10 and CSB 90:10 and 70:30. With oleogel increase, HSB *E* values became smaller than CSB ones, which can be related with the more disorganized structure observed for HSB with high oil content. However, *E* values for both CSB and HSB increased with the prevailing oleogel content.

Such behavior shows that the oil-water organization exerted effect on the mechanical properties, namely gel strength and maximal stress support. In addition, the effect was different depending on the structure organization. For both heat- and cold-set O/W bigels, the oil particles negatively affected these properties, which means that their magnitude was smaller than pure hydrogels. Increasing the oleogel proportion caused a more pronounced reduction in the gel strength. In fact, the force required to reach maximum stress decreases drastically between formulation 90:10 and 50:50 (Figure 4.7). The oleogel particles are dispersed as interconnected channels, disrupting the continuity of the WPI network (Figure 4.6) and consequently decreasing the strength and the rigidity of the system. Such behavior was also reported for bigels produced with alginate and k-carrageenan, where the authors observed that the addition of oleogel weakened the gel structure, promoting a more fluid and less organized network (Martins et al., 2019; Zheng et al., 2020). Moreover, such behavior could be intensified due to the absence of chemical interactions in the interface between oil and aqueous phase (Zheng et al., 2020). In addition, the authors reinforce that this behavior is not necessarily undesirable.

However, when this structure changes to W/O, for ratios over 50% oleogel, the gel recovers its strength. The W/O bigels showed a firmer gel with higher maximum stress, since the oleogel is a metastable and dynamic structure that self-organizes until it reaches stability, i.e., the organization of the oleogel structure is time-dependent (Fasolin et al., 2021). Bollom; Clark and Acevedo (2020) reported similar behavior for cold-set bigels produced with WPC80, stearic acid and soy lecithin. They observed improved mechanical properties when the hydrogel fraction increases in the bulk oleogel.

Figure 4.7. Effect of the type of gelation on cold-set (CSB) and heat-set (HSB) bigels with different hidrogel:oleogel ratios. Maximum stress (A), strain at maximum stress (B) and Young Modulus (C).

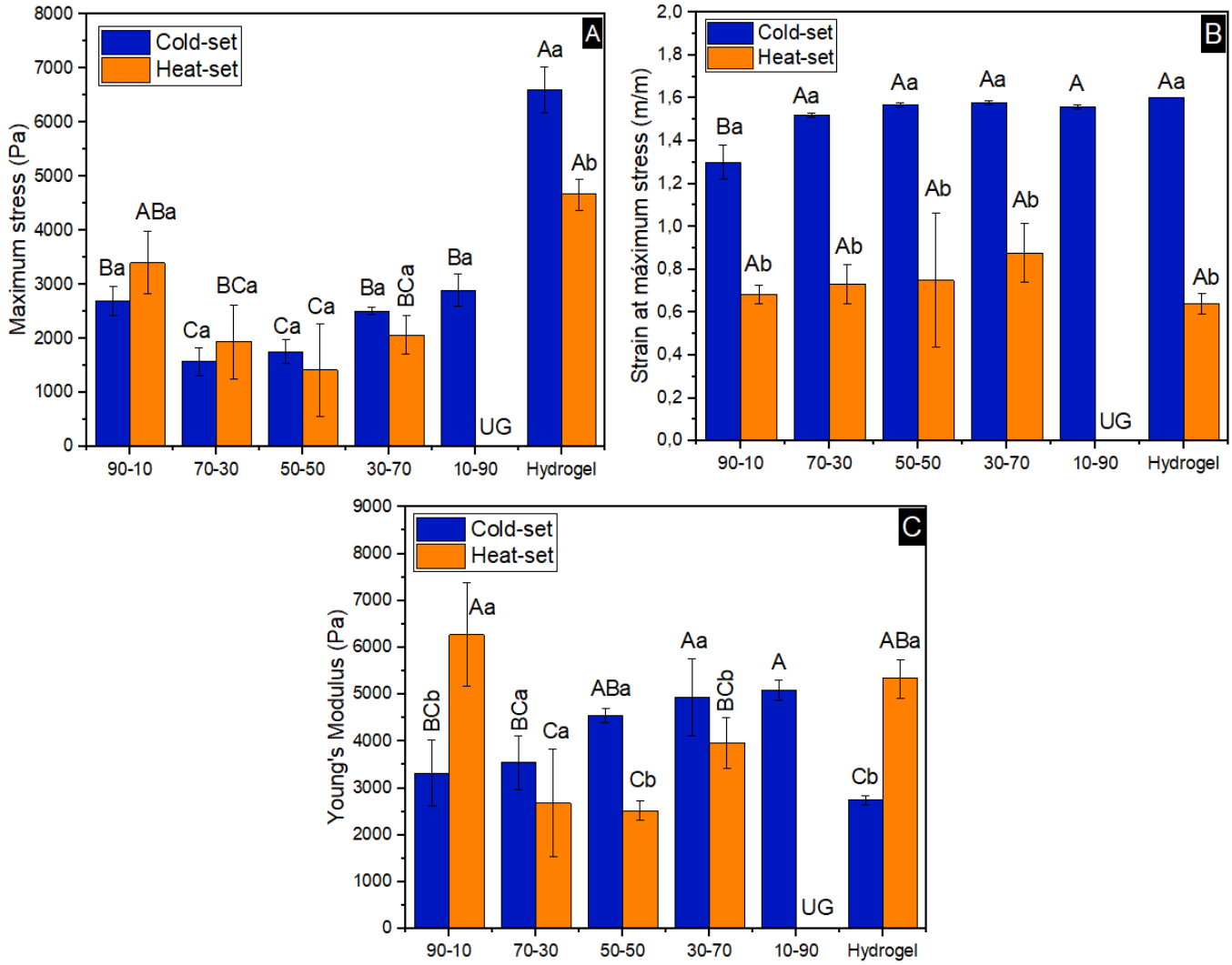

Values in the same set of bars for bigels (Cold-set or Heat-set) followed by different capital letters are significantly different by Tukey's test ($p < 0.05$). Values for each formulation (90:10, 70:30, 50:50, 30:70 and hydrogel) followed by different lowercase letters are significantly different by Tukey's test ($p < 0.05$); UG: unformed gel

The divergence of the mechanical properties shows that the application of the material must be evaluated. Modulating the mechanical properties is extremely important in product

development. Changes in process parameters and gel composition can produce systems with different physicochemical characteristics (Martins et al., 2023; Hashemi et al., 2024). These properties will dictate whether bigel is more suitable for specific applications, such as a texturing agent, vehicle for protection and delivery of compounds, fat replacement, etc. In fact, Fasolin et al. (2021) showed through principal component analysis (PCA) that bigels formulated with the same ingredients can have a similar behavior to creams, lotions, or foods depending on the hydrogel:olegel ratio, gelator concentration and velocity of mixing. Thus, in addition to these variables, protein gelation mechanisms can also modulate the physicochemical properties of bigels and improve the possibility of application of bigels.

Thermal profiles (Figure 4.8), shows that pure oleogel has a melting (62.89 ºC) and a crystallization (48.83 ºC) point. On the other hand, hydrogels did not show sol-gel transition. For this reason, bigels showed a similar DSC curve to oleogel phase and the intensity of the enthalpy was proportional to the oleogel content (Table 4.1S). Besides, the melting and crystallization temperatures for both HSB and CSB had slight differences among the different compositions that did not exceed approximately 1 ºC. This result shows that regardless of the composition, the thermal behavior was not influenced, which was expected, since the transition temperature of the oleogel is a consequence of its composition that was constant in this work. The enthalpy presented a greater difference between the formulations, ranging from 11.86 mJ to 323.16 mJ for CSB and 14.36 mJ to 380.83 mJ for HSB in the melting step, and 1.52 mJ to 138.57 mJ for CSB and 4.58 mJ to 172.83 mJ for HSB in the cooling step, while the pure oleogel presented an enthalpy of 333.51 mJ for melting and 143.26 mJ for cooling (Table 4.1S). However, the difference is related with the amount of oleogel present in the bigel used for the analysis. For example, 90:10 bigels had less oleogel than 10:90 interfering with the signal captured by the equipment. For the same reason the enthalpy observed for 10:90 bigels were closer to pure oleogels. DSC results reinforce that thermal events were only related to the system composition, i.e hydrogel:oleogel fractions.

Figure 4.8. DSC (exo up) melting and crystallization profiles of pure oleogel and hydrogel and cold- (CSB) and heat-set (HSB) bigels with different hydrogel:oleogel fractions.

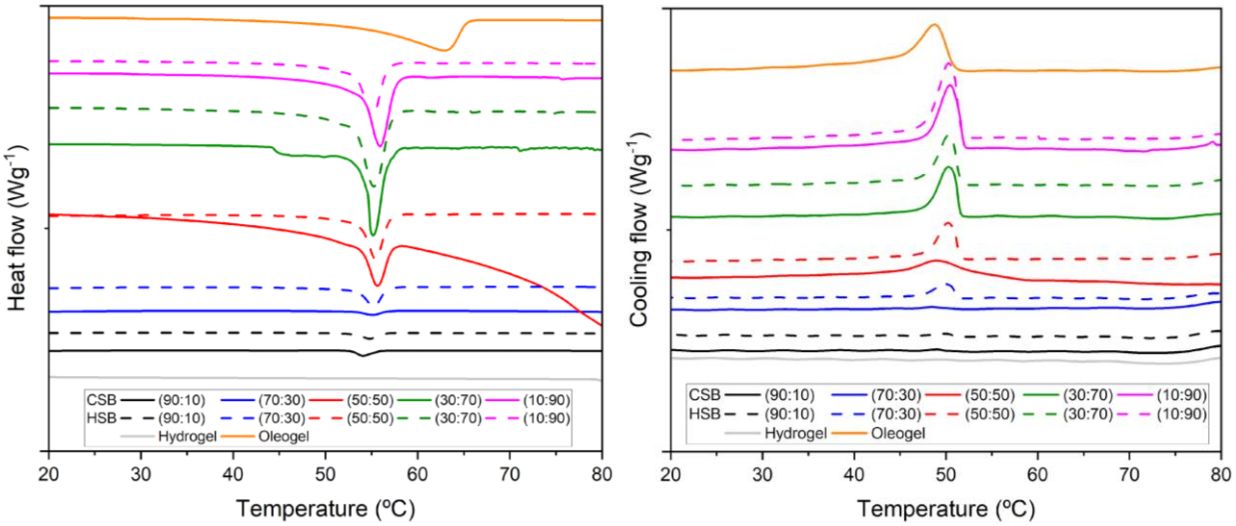

4.4 CONCLUSION

It was observed that both cold-set and heat-set gelation methods and the hydrogel:olegel ratio led to different structural organization during the bigel production and exerted effect on the mechanical properties. For HSB and CSB 90:10 a very well defined oleogel dispersed phase was observed and a protein honeycomb structure similar to pure hydrogels. However, oleogel did not form isolated particles, instead they interconnect and intertwine in the protein network as part of the structure. Such organization decreased the magnitude of the mechanical properties and gel strength in comparison to pure hydrogels. With oleogel concentration increasing up to 50:50, bigels became weaker, but some differences were observed between HSB and CSB. CSB was able to maintain the O/W structure, while for HSB the network was disorganized, with particles of different sizes and expressive coalescence, making the system unstable and even weaker. For oleogel concentration above 50:50 the bigel changed to W/O structures and recovered its strength due to the ability of the oleogel to self-organize. However, only CSB still showed an organized structure. Structural differences were strictly related to the protein gelation mechanism. The final CSB structure was only dependent on the gelation kinetics of both oleogel and hydrogel phases, i.e., the cooling process triggers the crystallization process that prevents high coalescence degree. Thus, well-defined O/W or W/O structures were observed. On the other hand, HSB is produced at high temperatures that reduces the interfacial tension between oil and water phase, allowing the drops coalescence and emulsion destabilizing. Therefore, evidence shows that the use of different gelling methods allows

modulating the structure and consequently the mechanical properties of bigels formulated with WPI. However, the choice of the bigel formulation for any food application must be carefully chosen, to mimic desirable texture properties providing stability.

ACKNOWLEDGMENTS

This research received financial support of São Paulo Research Foundation (FAPESP) (Brazil, Grants 2019/27354–3, and 2021/ 07639–3). G. Nunes Clímaco Thanks Coordenação de Aperfeiçoamento de Pessoal de Nível Superior - Brasil (CAPES) - Finance Code 001 for a Ph.D. fellowship.

REFERENCES

Babaei, J., Khodaiyan, F., Mohammadian, M., and Sheikhi, M. (2022). In vitro digestibility and functional attributes of the whey protein heat-induced hydrogels reinforced by various polysaccharides and CaCl2. *Journal of Food Measurement and Characterization*, *16*(1), 19–28. https://doi.org/10.1007/s11694-021-01142-y

Bollom, M. A., Clark, S., and Acevedo, N. C. (2020). Development and characterization of a novel soy lecithin-stearic acid and whey protein concentrate bigel system for potential edible applications. *Food Hydrocolloids*, 105570.

Bryant, C. M., and McClements, D. J. (1998). Molecular basis of protein functionality with special consideration of cold-set gels derived from heat-denatured whey. T*rends in Food Science & Technology*, *9*(4), 143-151. https://doi.org/10.1016/S0924-2244(98)00031-4

Bryant, C. M., and McClements, D. J. (2000). Influence of NaCl and CaCl2 on cold-set gelation of heat-denatured whey protein. *Journal of Food Science*, *65*(5), 801–804. https://doi.org/10.1111/j.1365-2621.2000.tb13590.x

Cerqueira, M. A., Fasolin, L. H., Picone, C. S. F., Pastrana, L. M., Cunha, R. L., and Vicente, A. A. (2017). Structural and mechanical properties of organogels: Role of oil and gelator molecular structure. *Food Research International*, *96*, 161–170. https://doi.org/10.1016/j.foodres.2017.03.021

Chen, H., Mao, L., Hou, Z., Yuan, F., and Gao, Y. (2020). Roles of additional emulsifiers in the structures of emulsion gels and stability of vitamin E. *Food Hydrocolloids*, *99*(September 2019), 105372. https://doi.org/10.1016/j.foodhyd.2019.105372

Chen, Z., Bian, F., Cao, X., Shi, Z., and Meng, Z. (2023). Novel bigels constructed from oleogels and hydrogels with contrary thermal characteristics: Phase inversion and 3D

printing applications. *Food Hydrocolloids*, *134*(June 2022), 108063. https://doi.org/10.1016/j.foodhyd.2022.108063

Cheng, F., Cao, Q., Guan, Y., Cheng, H., Wang, X., and Miller, J. D. (2013). FTIR analysis of water structure and its influence on the flotation of arcanite (K_2SO_4) and epsomite ($MgSO_4 \cdot 7H_2O$). *International Journal of Mineral Processing*. https://doi.org/10.1016/j.minpro.2013.04.007.

European, C. (2018). Commission Regulation of the European Parliament and of the Council as regards food category 17 and the use of food additives in food supplements. No 1333/2008 of 8 October 2018. *Official Journal of the European Union*, *October*, 20–30. https://doi.org/http://eur-lex.europa.eu/pri/en/oj/dat/2003/l_285/l_28520031101en00330037.pdf

Falsafi, S. R., Karaca, A. C., Deng, L., Wang, Y., Li, H., Askari, G., and Rostamabadi, H. (2022). Insights into whey protein-based carriers for targeted delivery and controlled release of bioactive components. *Food Hydrocolloids*, *133*(July). https://doi.org/10.1016/j.foodhyd.2022.108002

Fasolin, L. H., Cerqueira, M. A., Pastrana, L. M., Vicente, A. A., and Cunha, R. L. (2018). Thermodynamic, rheological and structural properties of edible oils structured with lmogs: influence of gelator and oil phase. *Food Structure*. https://doi.org/10.1016/j.foostr.2018.03.003

Fasolin, L. H., Martins, A. J., Cerqueira, M. A., and Vicente, A. A. (2021). Modulating process parameters to change physical properties of bigels for food applications. *Food Structure*, *28*(June 2019), 100173. https://doi.org/10.1016/j.foostr.2020.100173

Fasolin, L. H., Picone, C. S. F., Santana, R. C., and Cunha, R. L. (2013). Production of hybrid gels from polysorbate and gellan gum. *Food Research International*, *54*(1), 501–507. https://doi.org/10.1016/j.foodres.2013.07.026

Gaonkar, A. G. (1992). Effects of salt, temperature, and surfactants on the interfacial tension behavior of a vegetable oil/water system. *Journal of Colloid and Interface Science*, *149*(1), 256–260. https://doi.org/10.1016/0021-9797(92)90412-F

Gbassi, G.; Yolou, F.; Sarr, S.; Atheba, P.; Amin, C. and Ake, M. (2012). Whey proteins analysis in aqueous medium and in artificial gastric and intestinal fluids. *International Journal of Biological and Chemical Sciences*. 6, 1828-1837. https://doi.org/10.4314/ijbcs.v6i4.38

Ghiasi, F., and Golmakani, M. T. (2022). Fabrication and characterization of a novel biphasic

system based on starch and ethylcellulose as an alternative fat replacer in a model food system. *Innovative Food Science and Emerging Technologies*, *78*(March), 103028. https://doi.org/10.1016/j.ifset.2022.103028

Habibi, A., Kasapis, S., and Truong, T. (2022). Effect of hydrogel particle size embedded into oleogels on the physico-functional properties of hydrogel-in-oleogel (bigels). *Lwt*, *163*(May), 113501. https://doi.org/10.1016/j.lwt.2022.113501

Hashemi, B., Assadpour, E., Jafari, S. M. (2024). Bigels as novel carriers of bioactive compounds: Applications and research trends. *Food Hydrocolloids*, *147*, Part B, https://doi.org/10.1016/j.foodhyd.2023.109427

Hashim, A. F., El-Sayed, S. M., & El-Sayed, H. S. (2023). Bigel formulations based on sesame oleogel with probiotics alginate hydrogel: A novel structure for nutritious spreadable butter. International Journal of Biological Macromolecules, *242*, 124782. https://doi.org/10.1016/J.IJBIOMAC.2023.124782

Hazrati, Z., and Madadlou, A. (2021). Gelation by bioactives: Characteristics of the cold-set whey protein gels made using gallic acid. *International Dairy Journal*, *117*, 104952. https://doi.org/10.1016/j.idairyj.2020.104952

He, Z., Ma, T., Zhang, W., Su, E., Cao, F., Huang, M., and Wang, Y. (2021). Heat-induced gel formation by whey protein isolate- Lycium barbarum polysaccharides at varying pHs. *Food Hydrocolloids*, *115*(January).

Hoffmann, M., & van Mil, P.J. (1997). Heat-Induced Aggregation of β-Lactoglobulin: Role of the Free Thiol Group and Disulfide Bonds. *Journal of Agricultural and Food Chemistry, 45*, 2942-2948.

Hongsprabhas P., Barbut S. (1997). Ca2+-Induced cold gelation of whey protein isolate: effect of two-stage gelation, *Food Research International*, *30* (August), https://doi.org/10.1016/S0963-9969(98)00010-6.

Hwang, H.-S. (2020). A critical review on structures, health effects, oxidative stability, and sensory properties of oleogels. *Biocatalysis and Agricultural Biotechnology*, *26*(March), 101657. https://doi.org/10.1016/j.bcab.2020.101657

Jiang, L., Zhang, J., Ren, Y., Shen, M., Yu, Q., Chen, Y., Zhang, H., and Xie, J. (2021). Acid / alkali shifting of Mesona chinensis polysaccharide-whey protein isolate gels : Characterization and formation mechanism. *Food Chemistry*, *355*(March), 129650. https://doi.org/10.1016/j.foodchem.2021.129650

Joshi, M., Aldred, P., Panozzo, J. F., Kasapis, S., and Adhikari, B. (2014). Rheological and

microstructural characteristics of lentil starch-lentil protein composite pastes and gels. *Food Hydrocolloids*, *35*, 226–237. https://doi.org/10.1016/j.foodhyd.2013.05.016

Kazemi-Taskooh, Z., and Varidi, M. (2021). Designation and characterization of cold-set whey protein-gellan gum hydrogel for iron entrapment. *Food Hydrocolloids*, *111*(June 2020), 106205. https://doi.org/10.1016/j.foodhyd.2020.106205

Kuhn, K. R., Cavallieri, Â. L. F., and Cunha, R. L. da. (2011). Cold-set whey protein-flaxseed gum gels induced by mono or divalent salt addition. *Food Hydrocolloids*, *25*(5), 1302–1310. https://doi.org/10.1016/j.foodhyd.2010.12.005

Kumar, L., Brennan, M., Brennan, C., and Zheng, H. (2022). Influence of whey protein isolate on pasting, thermal, and structural characteristics of oat starch. *Journal of Dairy Science*, *105*(1), 56–71. https://doi.org/10.3168/jds.2021-20711

Lupi, F. R., Shakeel, A., Greco, V., Oliviero, C., Baldino, N., and Gabriele, D. (2016). A rheological and microstructural characterisation of bigels for cosmetic and pharmaceutical uses. *Materials Science & Engineering C*, *69*, 358–365. https://doi.org/10.1016/j.msec.2016.06.098

Machado, M., Sousa, S. C., Rodríguez-Alcalá, L. M., Pintado, M., & Gomes, A. M. (2023). Functional lipid enriched probiotic cheese: Gastrointestinal stability and potential health benefits. International Dairy Journal, 144, 105700. https://doi.org/10.1016/J.IDAIRYJ.2023.105700

Martins, A. J., Silva, P., Maciel, F., Pastrana, L. M., Cunha, R. L., Cerqueira, M. A., and Vicente, A. A. (2019). Hybrid gels: Influence of oleogel/hydrogel ratio on rheological and textural properties. *Food Research International*, *116*(July), 1298–1305. https://doi.org/10.1016/j.foodres.2018.10.019

Martins, A. J., Guimarães, A., Fuciños, P., Sousa, P., Venâncio, A., Pastrana, L. M., Cerqueira, M. A. (2023). Food-grade bigels: Evaluation of hydrogel:oleogel ratio and gelator concentration on their physicochemical properties. *Food Hydrocolloids*, 143. https://doi.org/10.1016/j.foodhyd.2023.108893.

Martins, J. T., Bourbon, A. I., Pinheiro, A. C., Fasolin, L. H., and Vicente, A. A. (2018). Protein-Based Structures for Food Applications: From Macro to Nanoscale. *Frontiers in Sustainable Food Systems*, *2*(November), 1–18. https://doi.org/10.3389/fsufs.2018.00077

McClements, D. J., and Keogh, M. K. (1995). Physical properties of cold-setting gels formed from heat-denatured whey protein isolate. *Journal of the Science of Food and Agriculture*, *69*(1), 7–14. https://doi.org/10.1002/jsfa.2740690103

Nicolai, T., Britten, M., and Schmitt, C. (2011). β-Lactoglobulin and WPI aggregates: Formation, structure and applications. *Food Hydrocolloids*, *25*(8), 1945–1962. https://doi.org/10.1016/j.foodhyd.2011.02.006

Nutter, J., Shi, X., Lamsal, B., and Acevedo, N. C. (2023). Designing and characterizing multicomponent, plant-based bigels of rice bran wax, gums, and monoglycerides. *Food Hydrocolloids*, *138*(December 2022), 108425. https://doi.org/10.1016/j.foodhyd.2022.108425

Okasha, T. M. (2018). Investigation of the effect of temperature and pressure on interfacial tension and wettability. *International Symposium of the Society of Core Analysts*. Trondheim, Norway, 27-30 (August 2018).

Popescu V., Molea A., Moldovan M., Lopes P. M., Mazilu Moldovan A., Popescu G.L. (2021). The Influence of Enzymatic Hydrolysis of Whey Proteins on the Properties of Gelatin-Whey Composite Hydrogels. *Materials* ;14(13):3507. https://doi.org/10.3390/ma14133507.

Rodrigues, R. M., Fasolin, L. H., Avelar, Z., Petersen, S. B., Vicente, A. A., and Pereira, R. N. (2020). Effects of moderate electric fields on cold-set gelation of whey proteins – From molecular interactions to functional properties. *Food Hydrocolloids*, *101*(November 2019). https://doi.org/10.1016/j.foodhyd.2019.105505

Sagiri, S. S., Singh, V. K., Kulanthaivel, S., Banerjee, I., Basak, P., Battachrya, M. K., and Pal, K. (2014). Stearate organogel-gelatin Hydrogel based bigels: Physicochemical, thermal, mechanical characterizations and in vitro drug delivery applications. *Journal of the Mechanical Behavior of Biomedical Materials*. https://doi.org/10.1016/j.jmbbm.2014.11.026

Samui, T., Goldenisky, D., Rosen-Kligvasser, J., and Davidovich-Pinhas, M. (2021). The development and characterization of novel in-situ bigel formulation. *Food Hydrocolloids*, *113*(September 2020), 106416. https://doi.org/10.1016/j.foodhyd.2020.106416

Shakeel, A., Farooq, U., Gabriele, D., Marangoni, A. G., and Lupi, F. R. (2021). Bigels and multi-component organogels: An overview from rheological perspective. *Food Hydrocolloids*, *111*(July 2020), 106190. https://doi.org/10.1016/j.foodhyd.2020.106190

Shakeel, A., Farooq, U., Iqbal, T., Yasin, S., Lupi, F. R., and Gabriele, D. (2019). Key characteristics and modelling of bigels systems: A review. *Materials Science & Engineering C*, *97*(February 2018), 932–953. https://doi.org/10.1016/j.msec.2018.12.075

Shishir, M. R. I., Xie, L., Sun, C., Zheng, X., and Chen, W. (2018). Advances in micro and

nano-encapsulation of bioactive compounds using biopolymer and lipid-based transporters. *Trends in Food Science & Technology*. https://doi.org/10.1016/j.tifs.2018.05.018

Siachou C, Zampouni K, Katsanidis E. (2023). Bigels as Fat Replacers in Fermented Sausages: Physicochemical, Microbiological, Sensory, and Nutritional Characteristics. *Gels*. 9(*4*):340. https://doi.org/10.3390/gels9040340

Singh, V. K., Anis, A., Banerjee, I., Pramanik, K., Bhattacharya, M. K., and Pal, K. (2014). Preparation and characterization of novel carbopol based bigels for topical delivery of metronidazole for the treatment of bacterial vaginosis. *Materials Science and Engineering C*, *44*, 151–158. https://doi.org/10.1016/j.msec.2014.08.026

Tian, W.; Huang, Y.; Song, Z.; Abdullah, Dr.; Yu, Y.; Liu, J.; Cao, Y. and Xiao, J. (2023). Flexible Control of Bigel Microstructure for Enhanced Stability and Flavor Release during Oral Consumption. *Food Research International. 174*.http://doi.org/10.1016/j.foodres.2023.113606.

Trujillo-ramírez, D., Lobato-calleros, C., Vernon-carter, E. J., and Alvarez-ramirez, J. (2018). Cooling rate, sorbitan and glyceryl monostearate gelators elicit different microstructural, viscoelastic and textural properties in chia seed oleogels. *Food Research International*, *October*, 0–1. https://doi.org/10.1016/j.foodres.2018.10.066

Vergara, D., Loza-Rodríguez, N., Acevedo, F., Bustamante, M., and López, O. (2022). Povidone-iodine loaded bigels: Characterization and effect as a hand antiseptic agent. *Journal of Drug Delivery Science and Technology*, *72*(November 2021). https://doi.org/10.1016/j.jddst.2022.103427

Xie, D., Hu, H., Huang, Q., and Lu, X. (2023). Development and characterization of food-grade bigel system for 3D printing applications: Role of oleogel / hydrogel ratios and emulsifiers. *Food Hydrocolloids*, *139*(September 2022), 108565. https://doi.org/10.1016/j.foodhyd.2023.108565

Yang, B., Chen, X. D., and Mercadé-Prieto, R. (2021). Stress relaxation of particulate whey protein hydrogels. *Food Hydrocolloids*, *118*(March). https://doi.org/10.1016/j.foodhyd.2021.106786

Zhai, X., Sun, Y., Cen, S., Wang, X., Zhang, J., Yang, Z., Shi, J., Huang, X., Zou, X., Gong, Y., and Holmes, M. (2022). Anthocyanins-encapsulated 3D-printable bigels: A colorimetric and leaching-resistant volatile amines sensor for intelligent food packaging. *Food Hydrocolloids*, *133*(March), 107989.

https://doi.org/10.1016/j.foodhyd.2022.107989

Zheng, H., Mao, L., Cui, M., Liu, J., and Gao, Y. (2020). Development of food-grade bigels based on κ-carrageenan hydrogel and monoglyceride oleogels as carriers for β-carotene: Roles of oleogel fraction. *Food Hydrocolloids*, *105*(February), 105855. https://doi.org/10.1016/j.foodhyd.2020.105855

Zheng, R., Chen, Y., Wang, Y., Rogers, M. A., Cao, Y., and Lan, Y. (2022). Microstructure and physical properties of novel bigel-based foamed emulsions. *Food Hydrocolloids*, 108097. https://doi.org/10.1016/j.foodhyd.2022.108097

Zhuang X, Clark S, Acevedo N. (2021). Bigels-oleocolloid matrices-as probiotic protective systems in yogurt. *J Food Sci*. (November). 86(11):4892-4900. doi:10.1111/1750-3841.15928

Zhu, Q., Gao, J., Han, L., Han, K., Wei, W., Wu, T., Li, J., and Zhang, M. (2021). Development and characterization of novel bigels based on monoglyceride-beeswax oleogel and high acyl gellan gum hydrogel for lycopene delivery. *Food Chemistry*, *365*. https://doi.org/10.1016/j.foodchem.2021.130419

SUPLEMENTARY MATERIAL

Figure 4.1S. Visual observation of self-supported cold-set hydrogel (CH) heat-set hydrogel (HH) and oleogel (OG) in different proportions of gelling agent.

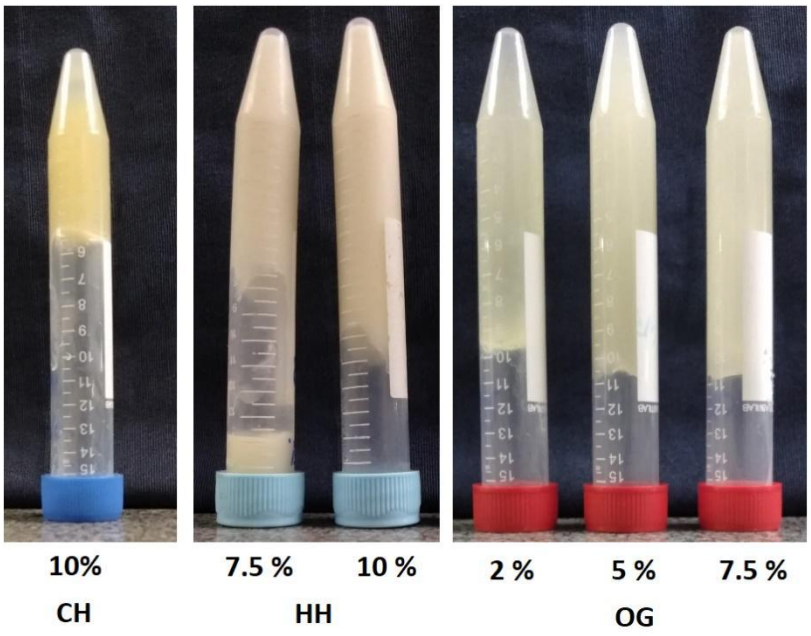

Figure 4.2S Mechanical properties of oleogel with 5% and 7.5% of GM.

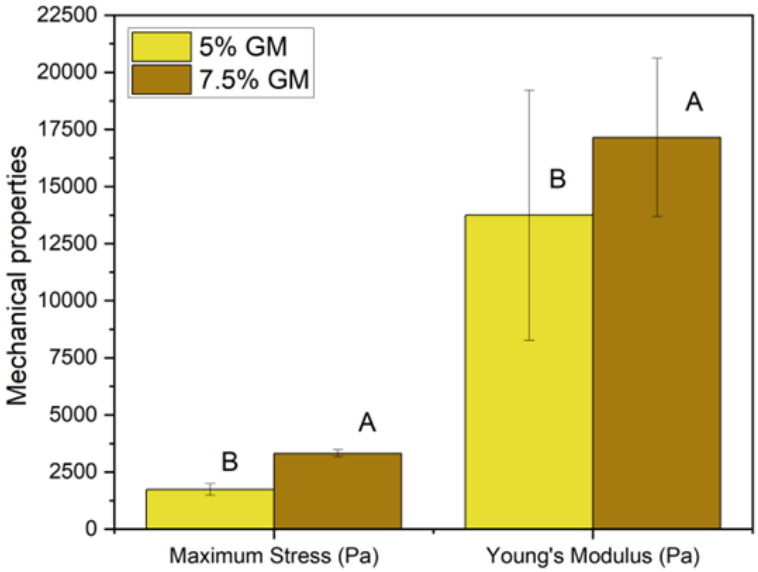

Table 4.1S. Thermal properties of pure oleogel and cold- (CSB) and heat-set (HSB) bigels with different hydrogel:oleogel fractions.

Sample	T_{onset} (ºC) (Heat flow)	T_{peak} (ºC)	Enthalpy (mJ)	T_{onset} (ºC) (Cooling flow)	T_{peak} (ºC)	Enthalpy (mJ)
Oleogel	53.43	62.89	-333.51	50.86	48.83	143.26
CSB (90:10)	52.77	54.09	-11.86	49.92	48.98	1.52
CSB (70:30)	53.33	55.09	-12.47	49.77	48.48	2.04
CSB (50:50)	53.94	55.64	-120.09	54.41	49.01	99.27
CSB (30:70)	54.17	55.17	-207.94	51.62	50.33	91.24
CSB (10:90)	53.73	55.99	-323.16	52.00	50.39	138.57
HSB (90:10)	52.91	54.83	-14.36	51.24	49.90	4.58
HSB (70:30)	53.42	55.24	-70.56	51.25	49.89	29.80
HSB (50:50)	53.59	55.41	-145.20	51.57	50.29	60.01
HSB (30:70)	53.08	55.03	-212.80	51.59	50.22	96.46
HSB (10:90)	53.02	55.21	-380.83	51.67	50.34	172.83

Values in the same group (CSB or HSB) followed by different capital letters are significantly different by Tukey's test ($p < 0.05$); Values followed by different lowercase letters are significantly different by Tukey's test ($p < 0.05$)

CAPÍTULO 5.

Cold-set WPI bigels for simultaneous vehiculation of curcumin and riboflavin

5. COLD-SET WPI BIGELS FOR SIMULTANEOUS VEHICULATION OF CURCUMIN AND RIBOFLAVIN

Gabrielli Nunes Clímaco[a]; Raquel F.S Gonçalves[b]; Jean-Michel Fernandes[b]; Ana C. Pinheiro[b]; António A Vicente[b]; Luiz Henrique Fasolin[a]

[a]Department of Food Engineering and Technology, School of Food Engineering, University of Campinas, CEP 13083-862, Campinas, SP, Brazil
[b]CEB- Centre of Biological Engineering, University of Minho, 4710-057 Braga, Portugal

ABSTRACT

The influence of curcumin (model hydrophobic compound) and riboflavin (model hydrophilic compound) on the structure and physicochemical properties of cold-set bigels was assessed. For this purpose, hydrogel phase was produced with whey protein isolated (11% w/v) and oleogel sunflower oil and glycerol monostearate (10% w/v) were used. Curcumin (0.03 mg/ml) was added to the oil phase and riboflavin (0.5 mg/ml) in the water phase. Bigels were produced by hot emulsification (18.000 min^{-1}, 2 min, 55 °C) of different hydrogel:oleogel ratios (90:10, 50:50 and 10:90). NaCl (200 mM) was added to the aqueous phase prior the emulsification. Bigels were evaluated through microscopy, XRD, FTIR, viscoelastic, texture, release kinetics and *in vitro* digestion analyzes. XRD and FTIR showed that the addition of compounds led to some possible structural differences in the gel structure. Microscopy images showed an increase of oil droplets proportionally to the amount of oil present, and predominantly oily network in bigel 10:90, due a conversion of the structure from oil in water (O/W) to water in oil (W/O). The structural differences led to different mechanical behavior. The bigels with the isolated compounds, had an improvement in the gel network, making it more structured, according to the phase that is being added. Riboflavin, when exposed to light, reacted with protein molecules, causing an increase in strength and stiffness. Curcumin, on the other hand, did not show such evident effect, but there was an increase in rigidity proportional to the increase of oleogel in the sample. In addition, the interaction curcumin-protein may have occurred due to the amphiphilic character of protein, increasing the hardness of the gel. Regarding controlled release, higher values for the 90:10 formulation was observed, for both compounds due to the matrix erosion. In relation to the bioaccessibility, curcumin showed similar values for 90:10 and 10:90 bigels. Riboflavin showed a growing bioaccessibility, with lower values for bigel 90:10, once the addition of riboflavin intensifies the strength of the gel, causing stronger protein bonds, which prevented the release of the compound during the digestion steps.

Key-words: Bigel; hydrogel; oleogel; bioaccessibility, digestion

5.1 INTRODUCTION

The demand for healthier products with a higher nutritional and functional content to guarantee or supplement dietary needs has grown over the years. This trend has gained the attention of the scientific community and food industries. They have been working on the development of innovative structures that can act as vehicles for the protection and delivery of bioactive compounds without, however, compromising the physical and sensory properties of the food (FALSAFI et al., 2022; GONÇALVES; VICENTE; PINHEIRO, 2023; MACHADO et al., 2019; MADALENA et al., 2016; NICOLAI; BRITTEN; SCHMITT, 2011; SIMÕES et al., 2020a; SINGH et al., 2014).

Bigels or hybrid gels are a class of soft materials initially developed for application in cosmetic and pharmaceutical products (LUPI et al., 2016; VERGARA et al., 2022). However, in the recent years, food scientists have been exploring the potential of these systems for food application (MARTINS et al., 2019; NUTTER et al., 2023; SAMUI et al., 2021; XIE et al., 2023). Bigels are a mixture of hydrogels and oleogels that can be organized into different structures, such as hydrogel in oleogel (W/O), oleogel in hydrogel (O/W) or even a more complex structure (SHAKEEL et al., 2019; ZHU et al., 2021). However, several factors can influence the bigels' structure and consequently their properties e.g., the type of solvent, structure and concentration of the hydro and oil gelling agents, and the hydrogel:oleogel ratio (SHAKEEL et al., 2021; ZHU et al., 2021).

The oleogel network can be formed by direct and indirect method. The indirect method can be classified as emulsion-templated, foam-templated, hydrogel-templated, and coated microcapsule-templated approaches, in which water or other polar solvents are needed. On the other hand, the direct method is performed by the direct solubilizations of the gelling agents in the oil phase (SABET et al., 2023). In the direct method, the gelling agents can be high molecular weight (HMOGs) and low molecular weight (LMOGs). HMOGs form a 3D network by covalent interactions, and the LMOGs by non-covalent interactions, both being able to trap the oil by capillarity (HWANG, 2020). One of the most used LMOGs is the glycerol monostearate (GM), an amphiphilic lipid molecule, as they have one fatty acyl chain linked to a glycerol backbone, being able to self-assemble with both water and oil, depending on the temperature and concentration (WANG; MARANGONI, 2015). For this reason, they can act as a gelling agent for edible oils that can be used for food application, (TRUJILLO-RAMÍREZ et al., 2018). Moreover, GM is able to form sustainable gels in a concentration from 4 % (LU et al., 2022). In addition, it presents low cost, is considered GRAS by the US Food and Drug

Administration (CFR 21 - Section 182.1324) and is approved by the European Union for food use (EUROPEAN, 2018).

The hydrogel network of the bigels can be produced using different biopolymers. Polysaccharides, such as gellan gum (ZHU et al., 2021), k-carrageenan (ZHENG et al., 2020), alginate (MARTINS et al., 2019), and also proteins such as whey protein isolate (WPI) (HAZRATI; MADADLOU, 2021) have been already used for this purpose. The last one has been studied over the years by several authors and is widely used in the food industry due to its technological properties and high nutritional value (JIANG et al., 2021; BOLLOM; CLARK; ACEVEDO, 2020; KUHN; CAVALLIERI; CUNHA, 2011; SHISHIR et al., 2018). This protein is divided into β-lactoglobulin (β-LG), α-lactalbumin (α-LA), bovine serum albumin (BSA), and lactoferrin (LF) (FALSAFI et al., 2022), and presents interesting gelling, emulsifying, and foaming properties, besides being capable to retain water, flavors, probiotics and food ingredients (HE et al., 2021).

The WPI gelled 3D network can be formed by heat or cold gelation. The first one is obtained by heating the protein solution, which promotes the biopolymer denaturation and gel formation (BABAEI et al., 2022; HE et al., 2021; NICOLAI; BRITTEN; SCHMITT, 2011). On the other hand, cold-set gels are carried out in two steps. The first step consists in the partial denaturation of the protein at high temperatures and pH far from the isoelectric point (pI), followed by the formation of the gel network with the addition of salt or pH adjustment towards the pI (BRYANT; MCCLEMENTS, 2000; WU et al., 2023).

Depending on the oleogel and hydrogel combination and processing, the physicochemical properties of bigels can be modulated. However, these systems stand out for presenting high stability for long periods, which is attributed to their complex three-dimensional gelled network in comparison with other oil+water systems as emulsions and emulgels (LUPI et al., 2016; SINGH et al., 2014). Bigels can be used to replace and reduce solid fat, mimicking their properties in foods or even conferring unique texture properties (SAGIRI et al., 2014; SILVA et al., 2022). Besides, due to the presence of the gelled oil and aqueous phase, they also allow the delivery of hydrophilic and hydrophobic compounds simultaneously (BOLLOM; CLARK; ACEVEDO, 2020; FASOLIN et al., 2021). However, the simultaneous use of bioactive compounds with different polarities was little explored. Lu et al. (2022) was able to evaluate the simultaneous encapsulation of epigallocatechin gallate (EGCG) and curcumin in bigels of gelatin, corn oil and GM. They observed that the increase in the percentage of GM

inhibited the release of curcumin, however, it did not present effects on the EGCG, indicating that the structure of the bigels can be easily modified by the gelling agent.

Therefore, this work proposes to produce WPI + sunflower oil + GM bigels by cold gelation of proteins, and evaluate their viability in the simultaneous delivery of compounds. For this curcumin and riboflavin were used as a model. Curcumin is a lipophilic, widely known to have antioxidant, anti-inflammatory, and anticancer action (GONÇALVES; VICENTE; PINHEIRO, 2023; YAN et al., 2023). However, its effect is limited due to its low stability and solubility in aqueous media (BOURBON; CERQUEIRA; VICENTE, 2016). So, several authors have been studying its effects into different systems, such as gelatin hydrogels (YAN et al., 2023), nanogels (HE et al., 2022), cellulose nanofibers (KUMARI; RAZA; MEENA, 2021) and lipid-based nanostructures (GONÇALVES et al., 2021).

Riboflavin, also known as vitamin B2, is highly soluble in water, however, it also has low stability, mainly in relation to light, thus limiting its use in different products (ZHU et al., 2022). Several authors studied its effect in different systems, such as β-lactoglobulin nanostructures (MADALENA et al., 2016), micro and nano β-Lactoglobulin structures (SIMÕES et al., 2020a), pea protein hydrogels (DJOULLAH; SAUREL, 2021) and wheat bran arabinoxylans and pea protein isolates cold-set hydrogel (ZHU et al., 2022). Therefore, the incorporation of these compounds in bigels, can be an alternative to promote higher solubility and stability, conferring nutraceutical assets to food properties. So, the objective of this work was to assess the influence of curcumin (model hydrophobic compound) and riboflavin (model hydrophilic compound) on the structure and physicochemical properties of bigels. Moreover, the release profile of the bioactives in food simulants and in vitro digestion were evaluated.

5.2 MATERIALS AND METHODS

Materials

Whey Protein Isolate (WPI) powder (Lacprodan DI-9224, 90% protein concentrate Arla Foods Ingredients, Viby, Denmark), glyceryl monostearate (Alfa Aesar, Kandel, Germany), NaCl (AppliChen, Darmstadt, Germany), commercial sunflower oil, distillate water and curcumin and riboflavin from Sigma-Aldrich (St. Louis MO, USA) were used for the production of the bigels. Pepsin from porcine gastric mucosa (1735.8 $U.mg^{-1}$), bile extract porcine, pancreatin from porcine pancreas (39 $U.mg^{-1}$), Pefabloc® SC, salts used to prepare

oral, gastric and intestinal electrolyte solutions and chloroform obtained from Fisher Scientific (NJ, USA) were used for in vitro digestibility assays.

Methods

Bigel production

Oleogel (OG) was prepared by heating the mixture of gelling agent (GM) 10% (w/w) and sunflower oil at 80 °C during 30 min under magnetic stirring (500 min^{-1}) (Heidolph, Magnetic stirrer Hei-Tec) in order to solubilize the gelling agent (CERQUEIRA et al., 2017). Then, the solution was cooled to 55 °C. Hydrogel (CH) was produced with WPI 11% (w/w) through cold-set gelation, according the methodology describe by Rodrigues et al. (2020). Briefly, WPI were dispersed in distillate water under magnetic stirring for 2 hours at room temperature (25 °C) and kept overnight, for complete hydration and protein solubilization. The solutions were subject to heat treatment at 90 °C during 10 min under magnetic stirring (500 min^{-1}). Then, the partially thermal denatured WPI was cooled to 55 °C using an ice bath, and the ionic strength was adjusted to 0.2 M with NaCl 5 M solution (25 ºC).

For bigels' production the OG and CH solutions were emulsified (18.000 min^{-1}, 2 min, at 55 °C) using Ultra Turrax (T18, IKA, Germany) at different CH:OG ratios (90:10, 50:50 and 10:90). The emulsions were put in cylindrical molds (diameter = 22 mm) and stored at room temperature (25 °C) to gel formation. Bigels containing bioactive compounds were produced with the same methodology. Curcumin was added to the oil phase after the GM solubilization, in the concentration of 0.03 mg/ml (GONÇALVES et al., 2021). On the other hand, 0.5 mg/ml riboflavin (ZHU et al., 2022) was added to WPI solution in the cooling step, right before the addition of NaCl solution.

Confocal Microscopy

A Leica TCS SP5 confocal laser scanning microscope (CLSM), was operated in fluorescence mode with a 63× oil-immersion objective. The protein phase was stained with FITC, and the oil phase with Nile Red. The samples were stained with Nile Red (0.1 g/L) and FITC (0.2 g/L) at 1:10 ratio (dye:sample, v/v), which enabled the oil droplets to become visible. The samples were then placed onto a microscope slide with a cavity and covered by a coverslip. The CLSM images were recorded using a He–Ne laser with an excitation wavelength of 517 nm for FITC and 636 nm for Nile Red. For curcumin and riboflavin, was used a laser to promote de compound reflection, once the excitation wavelength was in the same range of the

fluorescent compounds. All measurements were performed at 25 ºC and the experiments were carried out at least in duplicate.

Mechanical Proprieties

The mechanical proprieties were determined by uniaxial compression measurements in a TA XTplus Texture Analyzer (Stable Micro Systems, United Kingdom) equipped with a 7 cm of diameter plate. The gels (diameter = 14 mm) were compressed to 80% of the initial height with crosshead speed of 1 mm s^{-1}. The force x height data were transformed into Hencky stress (σ_H) and Hencky deformation (ε_H) (Equation 1 and 2) (FASOLIN et al., 2013; RODRIGUES et al., 2020).

$$\sigma_H = F(t)\left[\frac{H(t)}{H_0 A_0}\right] \quad (1)$$

$$\varepsilon_H = -ln\ ln\left[\frac{H(t)}{H_0}\right] \quad (2)$$

were *F(t)* being the force (N) in time *t*, A_0 (m^2) and H_0 (m) are the sample area and initial high, respectively and *H(t)* is the high (m) in time *t*. Stress x deformation curves were used to evaluate the breaking point (first maximum point of the curve), while elasticity or Young's modulus (*E*) was calculated as the slope of the linear region.

Rheological analyses

Viscoelastic properties of the bigels were evaluated with a Discovery HR1 rheometer (TA Instruments, Crawley, UK) equipped with a cone plate (60 mm, 2º angle, truncation 64 μm). Approximately 2 g of the sample was placed on the surface of rheometer plate for the test. Linear viscoelastic region (LVR) of the samples was firstly determined by dynamic strain sweep test at the strain range of 0.01%–100%. Temperature (90 to 25 ºC at a heating rate of 5 ºC/min) sweeps were performed within the LVR (0.5% strain). Both storage modulus (G') and loss modulus (G'') were recorded.

Infra-red spectrophotometry (FTIR)

FTIR spectra was performed to evaluated the possible interactions among the gels and the bioactives, following the methodology describe by Sagiri et al. (2014). The spectrums of FTIR were measured using one spectrophotometer (FTIR – MID/FAR Agilent 660), operated

in attenuated total reflectance mod (ATR). The measures were between 4000 and 400 cm^{-1} in resolution of 1 cm^{-1}.

X-Ray Diffraction (XRD)

XRD patterns of bigels were taken using an X-ray diffractometer (Bruker D8 Discover, USA), equipped with an X-ray tube Cu source (λ = 1.54056 Å) operated at 45 kV and 40 mA, with calibration offset to 2θ = -0.0372°, and with sweeps ranging from 5.0 to 50° (2θ) (step 0.050 °C/s), at room temperature, for 174s (FASOLIN et al., 2021).

Release kinetics

The release kinetics of curcumin (0.03 mg/ml) and riboflavin (0.5 mg/ml) in food simulants was evaluated by the dissolution test following the methodology described in Simões et al. (2020a) with some modifications. Two food simulant solutions, composed of 10 and 50% ethanol, were used to simulate hydrophilic and hydrophobic food matrices, respectively, in accordance with Commission Regulation (EU) No. 10/2011 of January 14, 2011 (2011), and were conducted at 25°C (simulating room temperature).

The gels containing the bioactive compounds were prepared inside a syringe (5ml) with the cap removed and left to rest for 24 hours before analysis, for complete gelation. Afterwards, the syringes were placed vertically immersed in a reactor with 30 ml of the simulant solution, under continuous magnetic stirring at 200 min^{-1}. At appropriate time intervals, 0.25 mL of supernatant was removed and replaced by the same amount of original solution, in order to keep the volume constant. Curcumin and riboflavin concentration was determined by UV-Vis spectrophotometry at 425 nm and 455, respectively.

The compounds release profile was evaluated using an equation that considers the effects of Fickian and Case II transport in hydrophilic matrices (KATIME; MENDIZÁBAL, 2010).

$$\frac{M_t}{M_\infty} = k_F * t^n \quad (1)$$

were M_t is the mass released at time t, M_∞ is the mass release at equilibrium, K_f is the Fickian diffusion rate constant and n is a characteristic exponent of the transport mode. Depending on the polymer diffusion and relaxation rates, three different classes of mechanisms can be observed: 1) Case I or Fickian diffusion, in which the diffusion rate is much lower than the relaxation rate (n = 0.50), 2) Diffusion case II, in which diffusion is superior to the relaxation

process (n = 1), and 3) non-Fickian or anomalous diffusion that occurs when diffusion and relaxation rates are comparable ($0.50 < n < 1$).

In vitro digestion

Only the bigels containing both compounds were subjected to in vitro digestion process using the harmonized static in vitro digestion model described by Minekus *et al*. (2014), that simulates the mouth, stomach and intestinal phases. For this purpose, 3 standard fluids were used, being Simulated Salivary Fluid (SSF) (KCl 15.1 mM, KH_2PO_4 3.7 mM, $NaHCO_3$ 13.6 mM, $MgCl_2(H2O)_6$ 0.15 mM, $(NH_4)_2CO_3$ 0.06 mM and HCl 1.1 mM), Simulated Gastric Fluid (SGF) (KCl 6.9 mM, KH_2PO_4 0.9 mM, $NaHCO_3$ 25 mM, NaCl 47.2 mM, $MgCl_2(H_2O)_6$ 0.12 mM, $(NH_4)_2CO_3$ 0.5 mM and HCl 15.6 mM, and Simulated Intestinal Fluid (SIF) (KCl 6.8 mM, KH_2PO_4 0.8 mM, $NaHCO_3$ 85 mM, NaCl 38.4 mM, $MgCl_2(H_2O)_6$ 0.33 mM and HCl 8.4 mM).

The oral phase consisting of simulated salivary fluid (SSF), $CaCl_2(H_2O)_2$ 0.3 M (in order to achieve 0.75 mM at the final mixture) and Milli-Q water (in order to make up the final volume) was added to 5 g of sample. The mixture was incubated at 37 ºC for 2 min under orbital agitation at 120 min^{-1}. α-amylase was not used as samples did not contain starch (SARKAR; GOH; SINGH, 2009). For the gastric phase, simulated gastric fluid (SGF), $CaCl_2(H_2O)_2$ 0.3 M (in order to achieve 0.075 mM at the final mixture) and pepsin solution (with final activity of 40.000 U/mL in the final mixture) were added to the previous mixture. The pH was adjusted to 3.0 with HCl 1 M and Milli-Q water was added to make up the final volume. The samples were incubated for 2 h at 37 ºC under orbital agitation at 120 min^{-1}. Finally, the intestinal phase containing simulated intestinal fluid (SIF), $CaCl_2(H_2O)_2$ 0.3 M (in order to achieve 0.3 mM at the final mixture), bile salts (in order to achieve 10 mM at the final mixture) and pancreatin solution (with final activity of 800 U/mL in the final mixture) were added to the solution. The pH was adjusted to 7.0 with NaOH 1 M or HCl 1 M and then Milli-Q water was added to achieve the final volume. The samples were incubated during 2 h at 37 ºC under orbital agitation at 120 min^{-1}. At the end of digestion, the reaction was stopped adding enzyme inhibitor Pefabloc® (1 mM) (10 µL for each 1 mL of sample), and after that, samples were collected. All the samples were tested in triplicate.

Curcumin and riboflavin's bioaccessibility

Curcumin and riboflavin bioaccessibility were determined at the end of the digestion based on the methodology described by Gonçalves *et al*. (2021). The digesta (10 mL) was

centrifuged (Allegra 64R, Beckman Coulter Inc., USA) at 18.700 g at room temperature for 30 min, and the supernatant (which was assumed as the micelle phase) was collected. For curcumin, micelle phase samples (5 mL) were mixed with 5 mL of chloroform using a vortex and centrifuged at 700 g at room temperature for 10 min. The bottom layer was collected, and the top layer was subjected again to the extraction procedure. The second bottom layer was combined with the first one and analyzed. For riboflavin, direct analysis was performed with the micelle phase collected (supernatant). Both samples were analyzed in an UV–VIS spectrophotometer (V-560, Jasco, USA) at 425 nm for curcumin and 455 for riboflavin. Curcumin concentration was determined through a calibration curve in chloroform, and riboflavin was determined through a calibration curve in water.

5.3 RESULTS AND DISCUSSION

All pure bigels produced were self-supporting, as well as the bigels with the bioactive compounds. Despite the visual differences, the bioactives also can interact with the oleogel and/or hydrogel matrix, changing the network at microscopic level and consequently its physicochemical properties. X-ray diffraction evaluates the crystalline-amorphous state of materials. In general, amorphous materials produce a broad and non-defined peak, being the opposite of crystalline materials that present a series of sharp peaks (MACHADO et al., 2019). XRD spectra (Figure 5.1) shows a very broad peak, indicating that the bigels shows non-crystalline structure, when compared to oleogels, which is typical of amorphous materials. However, there were differences in relation to the hydrogel:oleogel ratio. A flatter formation with a broad band around 30º 2θ was observed when the hydrogel phase prevailed (90:10), which is a characteristic of WPI spectra (HAZRATI; MADADLOU, 2021; ZHONG et al., 2023). On the other hand, with the oleogel content increase there was a peak at 20º 2θ and its intensity increased proportionally to the oleogel content. This increase in intensity may be due to the GM spectrum, which has sharp peaks at 19.6◦ and 23.7º 2θ and may result from a different molecular packaging (CARRILLO-NAVAS et al., 2014) et al., 2021).

The presence of curcumin and/or riboflavin exerted different effects on the XRD spectra, and this effect was also dependent on the hydrogel:oleogel ratio. In general, the presence of the two compounds simultaneously causes more effects on the structure. For 90:10 formulation a broad band was still observed around 30º 2θ for bigel with curcumin and riboflavin isolated, which was similar to pure bigel. However, when the two compounds were incorporated at the same time, another small peak was observed around 20º 2θ. Formulation

50:50 presents no effect in relation to the addition of the compounds. However, formulation 10:90 present some differences related to intensity of the peak. The presence of riboflavin slightly increases the intensity, while the curcumin decrease, but the effect of the two compounds together promotes a great reduction on intensity, showing that there is a synergistic effect between the compounds. Curcumin and riboflavin have a several peaks between 10º 2θ and 27.4º 2θ, due to its highly crystalline state (FENG et al., 2021; ZHONG et al., 2023). There was a predominance of the continuous phase and for this reason it as observed only an amorphous state, characteristic of the protein, or a peak around 20º 2θ characteristic of the GM.

Figure 5.1. X-ray scattering profile of cold-set bigels loaded with curcumin and riboflavin. CR means bigel with curcumin and riboflavin. Pure bigel (A), bigel 90:10 (B), bigel 50:50 (C) and bigel 10:90 (D).

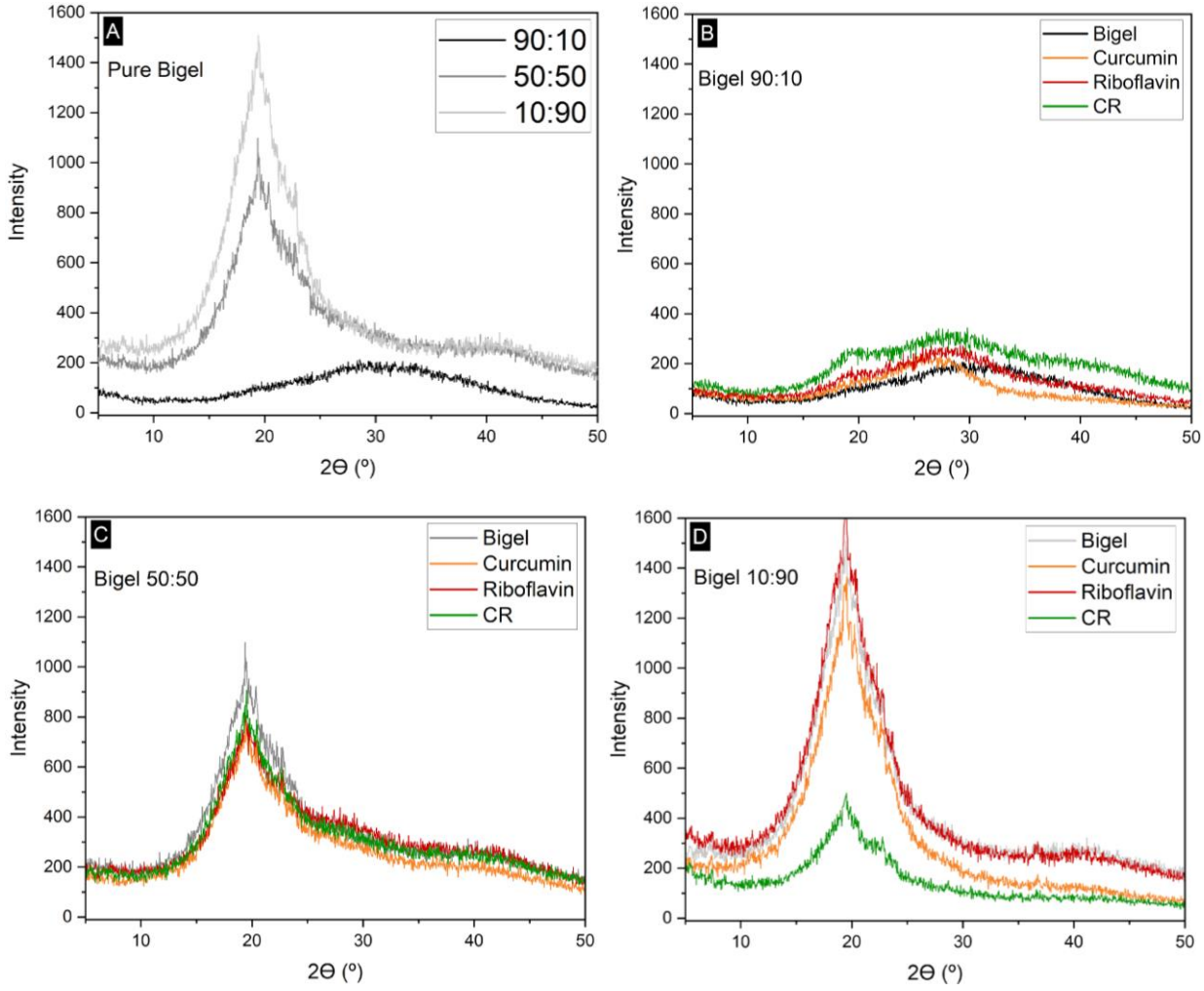

FTIR analysis was performed to verify interactions among the hydro/oleogelators and the bioactive compounds through changes in the functional groups. However, Figure 5.2A did not show much difference among the spectra, i.e., despite the different ratios of

hydrogel:oleogel, there was not different interactions between the molecules, showing that the role of the fillers (hydrogel and oleogel) was purely physical, without any chemical interaction.

For all formulations (Figure 5.2), a broad band between 3500 and 3000 cm^{-1} was observed, which may be related to O-H stretching vibrations participating in the hydrogen bond within the hydrogel, and a peak at 1650 cm^{-1} characteristic of the C=O bond (VERGARA et al., 2022). However, this broad band was reduced as the percentage of oil in the sample increases. Also, peaks for bigel around 1660 cm^{-1}, characteristic of the C=O bond, undergoes reduction when oil was added to the formulation.

Figure 5.2. FTIR spectra of cold-set bigels loaded with the compounds. Pure bigel (A), bigel with curcumin (B), bigel with riboflavin (C) and bigel with both compounds (D).

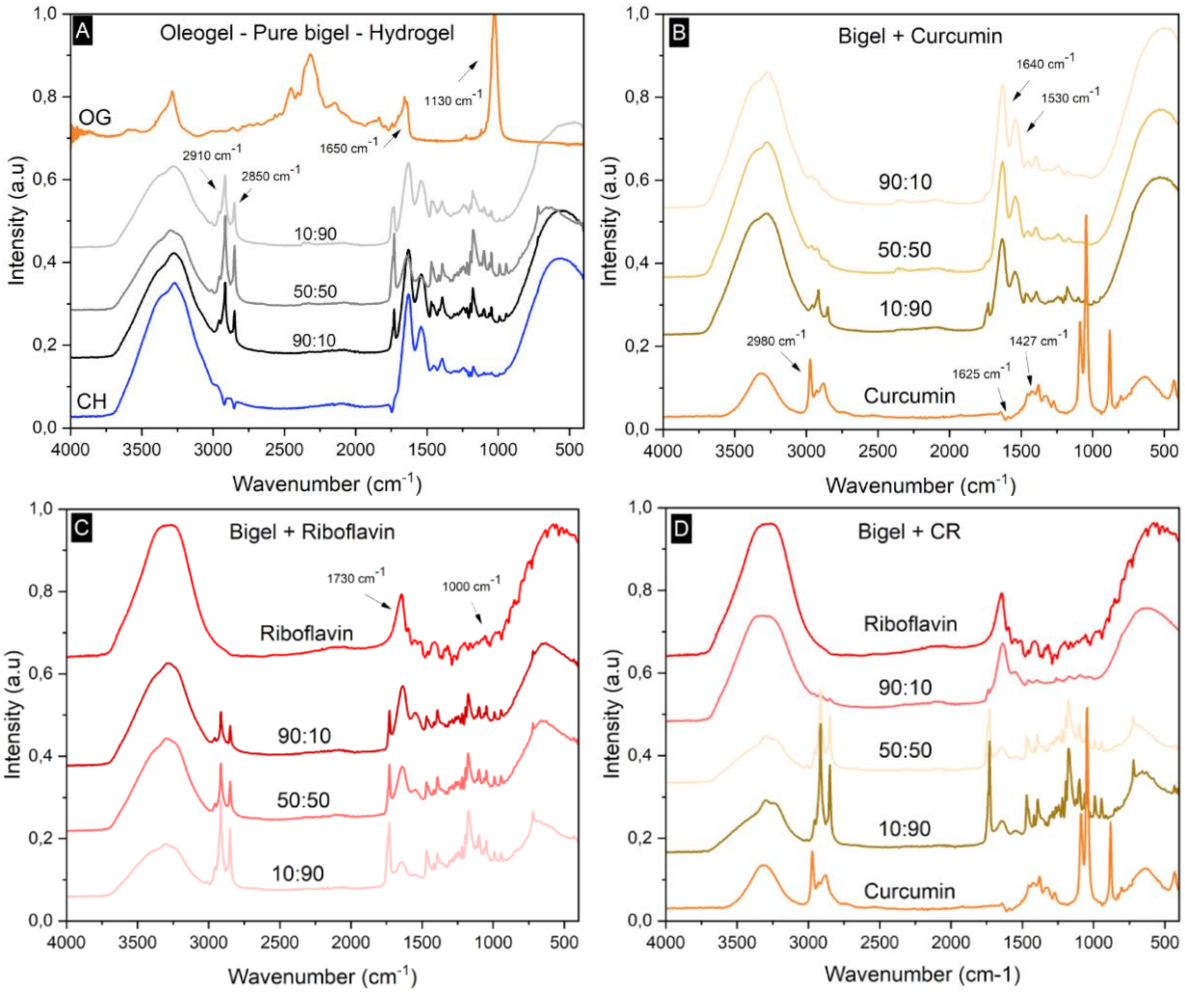

In bigels loaded with curcumin, the peaks at 2910 cm^{-1}, 2850 cm^{-1}, associated with the stretching of C-H, observed in all pure bigels disappear in the formulations 90:10 and 50:50. Curcumin present peaks only at 3516 cm^{-1}, 2980 cm^{-1} and multiple sharp peaks at 1625, 1504,

and 1427 cm^{-1}, related to its various functional groups such as aromatic rings (ZHONG et al., 2023), so these modifications are expected to happen when there is interaction between the components. However, as curcumin is in smaller amounts when compared to the other components of bigel, it has little effect on the structure, as previously reported by Chuesiang et al. (2022) in curcumin-loaded hydroxypropyl methylcellulose (HPMC) oleogels and by Yallapu et al. (2010) in a β-Cyclodextrin-curcumin self-assembly.

For riboflavin bigels, a series of peaks between 1000 and 1750 cm^{-1}, characteristic of riboflavin was observed. They are associated with C–OH (1150 cm^{-1}), C=N (1550 cm^{-1}), C=C (1580 cm^{-1}) and C=O (1650 cm^{-1}) (ANWAR et al., 2023). Some of these are also characteristic of the bigels. For this reason, it was not possible to observe great modifications. However, the intensity of the peaks may have been affected by the interaction of riboflavin with the bigel compounds, as also observed by Anwar et al. (2023) on alginate-riboflavin nanoparticles, in which the intensity and displacement of some peaks clearly indicated the conjugation of riboflavin on the surface of the particles. In relation to the bigels loaded with both compounds, the overlapping of the peaks observed for the encapsulation of the compounds in isolation was clearly observed.

Confocal images show differences between the formulations (Figure 5.3), in which the oil particles increased proportionally to the amount of oil present. Moreover, in bigel 50:50, it was possible to observe some coalescence and, with the oleogel prevailing content (10:90) a conversion of the structure from oil-in-water (O/W) to a bicontinuous system. This phase conversion was probably due the inability of the system to stabilize the W/O emulsion during the cooling process, causing the oil droplets to coalesce until their total crystallization.

Curcumin, being a lipophilic compound, was almost entirely bound to the oleogel, inside the particles, in system 90:10. However, in 50:50 system, several oleogel particles without curcumin were also observed, showing that the dispersion of the compounds did not happen uniformly. Regarding riboflavin, since it is characterized by being a hydrophilic compound, most of it was dispersed in the aqueous phase, in a form of rod-like crystals, as also observed by Djoullah et al. (2021) in riboflavin encapsulation into microparticles of pea protein.

However, when the two compounds were simultaneously encapsulated, some differences could be observed. Bigel 90:10 presented a well-defined structure, where each compound settled in its proper place, i.e., curcumin in the oleogel and riboflavin in the hydrogel network. As for bigel 50:50, a small part of riboflavin was found in the oil phase, as well as curcumin in the aqueous phase. This behavior became more visible in bigel 10:90. The large

amount of oleogel in the 10:90 sample and the high energy during the emulsification step could have promoted the aggregation of curcumin with the hydrophobic sites of the protein, which can basically be performed by hydrophobic interactions and hydrogen bonds (LEI et al., 2023). As for riboflavin, despite being vehiculate in the aqueous phase, the temperature increase promoted by the emulsification process reduced the oil viscosity and also prevented the interaction with protein molecules, thus facilitating its migration to the oil phase. Such phenomenon was observed by Bou et al. (2014) in the encapsulation of riboflavin in double emulsions with different types of oils.

Figure 5.3. Confocal scanning laser micrographs of bigels with curcumin and riboflavin. The samples are labeled according to the hydrogel:oleogel ratio. Hydrogel, oleogel, curcumin and riboflavin are presented in green, red, blue and orange rod-like crystals, respectively, under a magnification of 63x.

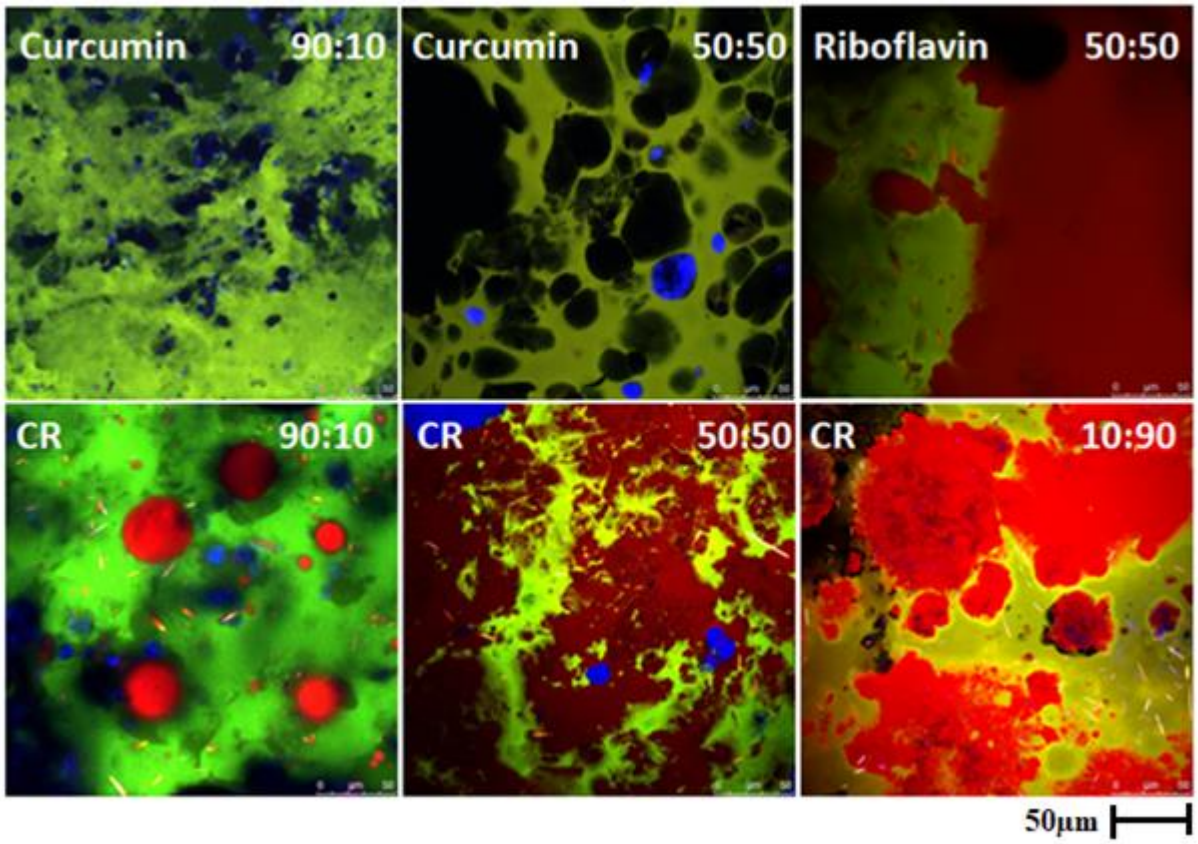

The structural differences reflected directly on the mechanical properties of bigels. In general, the pure bigels 90:10 and 10:90 behave as rubber gels, with higher Young's modulus, when compared with 50:50, that showed a squeezing gel behavior (Figure 5.1S). Such difference was probably due to a more disorganized structure, as observed in confocal images (Figure 5.3). However, no major differences were observed in the deformation where the

maximum stress occurred. Such behavior shows that the presence of oil directly affects the mechanical properties. The increase up to 50% caused a reduction in the gel strength (Figure 5.4A), showing that the oil particles disrupted the continuity of the WPI network and consequently decreased the rigidity of the system, which means that their magnitude was smaller than pure hydrogels. In fact, the force required to reach 80% of deformation decreased drastically between formulation 90:10 and 50:50. However, for ratios over 50%, when this structure changes to W/O, the gel recovers its strength. The W/O bigels showed a firmer gel with a maximum stress value, since the oleogel is a metastable and dynamic structure that self-organizes until it reaches stability (FASOLIN et al., 2021).

The addition of curcumin and riboflavin promoted different performances (Figure 5.4). The bigels with the isolated compounds, had an improvement in the gel strength. For bigel 90:10, it is possible to observe a great effect of riboflavin. When exposed to light, riboflavin produces free radicals and oxidative species, which react with protein molecules, forming covalent bonds that cause an increase in strength and stiffness (HEO et al., 2016). This behavior was quite evident in the study carried out by Ahearne et al. (2016) in the application of UVA-riboflavin crosslinking to enhance the mechanical properties of essential extracellular matrix (ECM) derived hydrogels. The authors tested several tissues such as porcine cornea, ovine liver and ovine heart, in addition to different concentrations of riboflavin, and found that the mechanical properties were improved with the addition of up to 0.1% of riboflavin, as well as with exposure to light for 60 minutes. In the system 50:50 and 10:90 riboflavin also exerted a positive effect on the gel strength, increasing the rigidity of the network. However, as the percentage of hydrogel decreases, the maximum tension also decreases, demonstrating that the hardness of the gel is directly correlated with the effect of the interaction between the hydrogel and riboflavin.

Regarding the encapsulation of curcumin, a similar behavior is observed, in which the rigidity increased proportionally to the amount of oleogel in the sample. However, its effect was lower in comparison to riboflavin. For bigel 10:90, once the oil has become the continuous phase and the network was more structured when compared to a bicontinuous gel, the curcumin was able to act in a way to improve intramolecular bonds, increasing the strength of the gel. Furthermore, as previously observed in the confocal images and FTIR, a curcumin-protein interaction may have occurred, increasing the hardness of the gel, and consequently improving resistance to deformation.

As for the encapsulation of the two compounds simultaneously, the greatest effect was observed in the 10:90 system, where an interaction between curcumin and protein may have occurred, as previously mentioned. In addition, despite being present in smaller amounts, riboflavin still had its cross-linking effect, and may have helped the curcumin to increase the strength and rigidity of the gel.

Figure 5.4. Effect of hydrogel:oleogel ratio and the presence of different compounds on bigels formulations being Maximum stress (A), Strain at maximum stress (B), Young Modulus (C) and Behavior of gels in the 90:10 ratio (D).

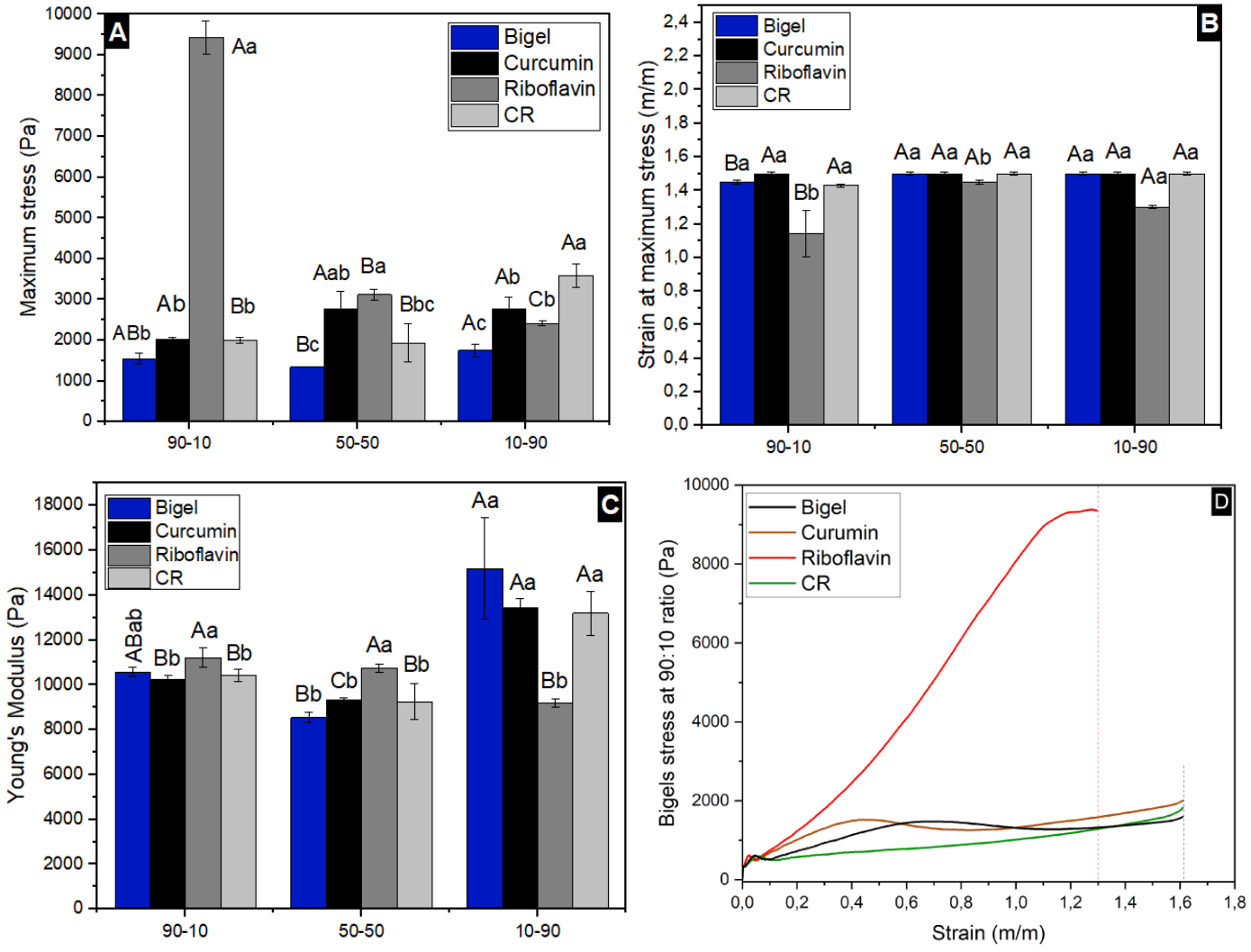

Values in the same set of bars (Bigel, Curcumin, Riboflavin or CR) followed by different capital letters are significantly different by Tukey's test ($p < 0.05$); Values in the same formulation (90-10, 50-50 and 10-90) followed by different lowercase letters are significantly different by Tukey's test ($p < 0.05$)

Besides texture, hydrogel:oleogel ratio and the encapsulations of curcumin and riboflavin also affect the rheological properties. From the temperature sweep test (Figure 5.5A), it was noticed that at higher temperatures (>85 °C) the bigels 50:50 and 10:90 do not have a fully structured network, with G' and G" almost overlapping. The oleogel, presented instability

at high temperatures (> 55ºC), which was already expected, since the oleogel of sunflower oil and GM has a melting peak around 50 ºC (FASOLIN et al., 2018) and the glycerol monostearate around 60 ºC (CERQUEIRA et al., 2017). However, as the temperature was reduced, it was observed a more structured gel network for 10:90, with higher G', due to the crystallization of the system. The temperature at which each network begins to be structured (crystallization point) depended on the ratio of hydrogel:oleogel in the sample. For bigel 10:90 is around 60 ºC and bigel 50:50 approximately 55°C, being the lowest crystallization temperature, corroborating the texture analysis, that this formulation has a weaker network.

On the other hand, no structural changes occurred in the temperature range evaluated for bigel 90:10. This behavior shows that the non-hydrophobic interactions are the main forces present in the stabilization of the protein, since the hydrophobic forces decrease with cooling. In addition, the hydrogen bonds and van der Waals forces become more resistant with temperature reduction, consequently promoting greater rigidity to the gel in the cooling step (MCCLEMENTS; KEOGH, 1995).

Figure 5.5. Rheological properties of cold-set bigels (A) and bigels with curcumin and riboflavin (B) with different oleogel fractions during temperature sweep (cooling) tests.

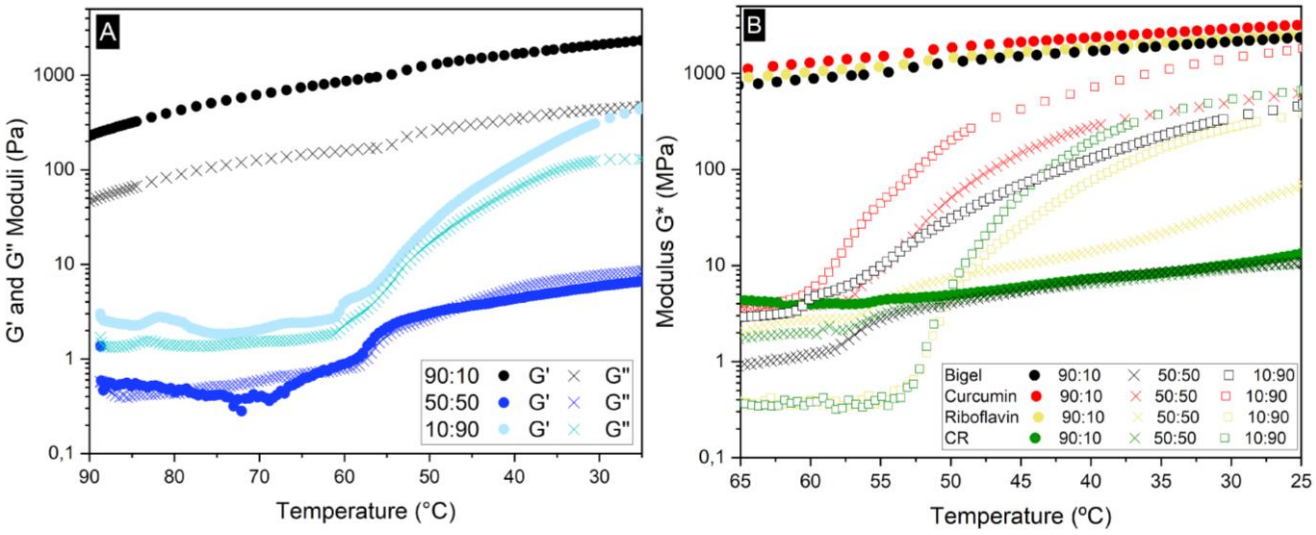

CR - Bigel with curcumin and riboflavin

In relation to the addition of compounds, the same behavior of the texture analysis was observed, with an improvement in the gel properties with the addition of compounds. However, significant differences were observed in relation to each compound. For bigel 90:10, the addition of curcumin and riboflavin separately caused an increase in G* moduli. On the other hand, the addition of both simultaneously led to a large reduction (Figure 5.5B). Even at low concentrations, curcumin was able to improve the gel network, promoting an increase in the

viscoelasticity of the bigel, probably due to the two hydrophobic phenolic rings present in the curcumin structure, making it possible to withstand higher tensions and loads (WU et al., 2023). Regarding the encapsulation of riboflavin, similar behavior is observed, since cross-linking of riboflavin with proteins causes improvements in the gel (HEO et al., 2016). A study carried out with a collagen bioink directly showed that the light incidence on the sample with riboflavin, during a rheological test, greatly increased its elastic and viscous molecules (DIAMANTIDES et al., 2017). For bigel 50:50, the encapsulation of curcumin resembles the pure one, with an evident phase change at approximately 60 °C. The other two show a more linear change. For bigel 10:90, the bigel with curcumin remains similar to the pure one, and the other two also show an evident phase change, but late, close to 53°C.

Release kinetics

During release trials in food simulant, no release of curcumin was observed in a simulant with 10% ethanol, since, due to its lipophilic nature, it is difficult to partition in aqueous solutions. The same behavior was observed for riboflavin in the 50% ethanol simulant. Table 5.1S shows that for all bigels evaluated the release rate by relaxation was greater than by diffusion ($n<0.5$). Besides, the model fitted well to data, with a $R^2 > 0.80$ for most samples, indicating that this model was suitable to describe the release mechanisms of riboflavin and curcumin from cold-set bigels. However, the percentage of release was affected by the structure of the gel. The model used is common to evaluate the diffusive behavior of water into hydrogels, as well as the release of hydrophilic compounds (KATIME; MENDIZÁBAL, 2010), therefore, it did not show such a good fit for curcumin encapsulation, since the way in which it is arranged in the matrix (inside the oil particles) differs from the way in which riboflavin is dispersed in the protein matrix, thus differentiating the surface area conducive to release.

Figure 5.6 shows that bigel 90:10 has a gel network more favorable to the release of the compounds when isolated, regardless of the phase in which it is bound. For these bigels exposed to 50% ethanol solution, it was noted that curcumin had a release of almost 80% and this amount decreased with the increase of oleogel in the system. This behavior can be justified by O/W structure observed in the 90:10 bigels. The oil particles are dispersed in the matrix and present a large surface area available for the release of curcumin. In addition, the protein network erodes facilitating the access of the solvent to the oil droplets. However, when the structure are bicontinuous or the oil became the continuous phase, the surface area was drastically reduced. Moreover, the GM 3D network did not swell or erode in the presence of the simulant. Also, the hydrogen bonds formed by GM molecules makes difficult for the bioactive migrate to the

simulant (SINGH et al., 2014). For these reasons the curcumin is entrapped into the oleogelator network, impairing the release. Similar result was observed by Zheng et al. (2020) in the analysis of bigels formulated with κ-carrageenan hydrogel and monoglyceride oleogels as carriers for β-carotene. The formulation with the highest percentage of oleogel (75%) was the one that showed the greatest resistance to the release of the bioactive. Lu et al. (2022) evaluated the release of curcumin from gelatin-GM bigels and also noticed that the increase in the percentage of GM, which consequently increased the hardness of the gel, negatively influenced the release of curcumin in the gastrointestinal tract.

Figure 5.6. Release profile of cold-set bigels loaded with curcumin and riboflavin through two different food simulants. Bigels release in simulant 50% (A) and simulant 10% (B).

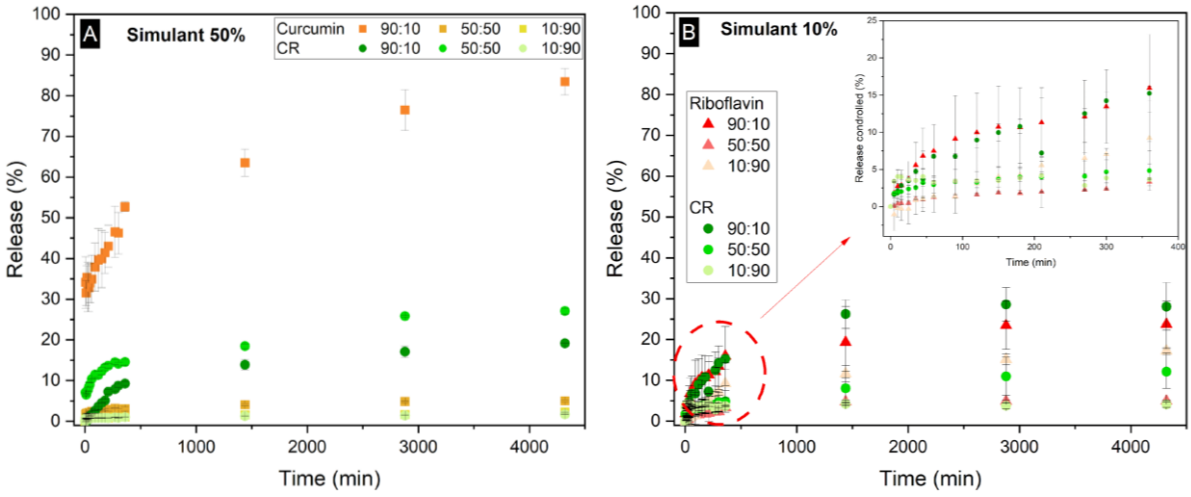

Regarding the formulation where the oleogel and hydrogel phases are in equal proportions (50:50), approximately 5% of curcumin were released. In these bigels, the water and oil phases were organized as a bicontinuous structure. This complex organization may have allowed the formation of small clumps that were able to encapsulate the compounds, preventing its release. This behavior was also observed by Kodela et al. (2017) in the study of ciprofloxacin hydrochloride release from bigels produced with agar, stearyl alcohol and rice bran oil. The authors observed that the increase in oleogel up to 25% favored the release, however, an additional increase in the proportion of oleogel up to 50%, and consequent formation of a bicontinuous system, resulted in a decrease in drug release. For bigel 10:90, the low release observed is a result of the formed gel structure, since a higher percentage of oleogel can impair the release in food simulants.

When the bigels were exposed to 10% ethanol solution the riboflavin release content was evaluated. It was noted that riboflavin had a recovery of 20% in bigel 90:10, followed by

15% for the bigel 10:90. Furthermore, in the 10:90 system, migration of riboflavin to the oleogel may have occurred, as observed in the confocal micrographs (Figure 5.3), facilitating release when compared to the 50:50 system. In general, as observed in the microstructure and texture analysis, the riboflavin strongly bound to the protein network, strengthening the structure and consequently being not available to be released.

However, when the curcumin and riboflavin were vehiculate simultaneously some differences were observed. In bigel 90:10, riboflavin improves the strength of the protein network being more difficult to undergo erosion, thus preventing the simulant from accessing the encapsulated curcumin, resulting in a lower recovery (approximately 20%). Riboflavin, on the other hand, has a similar result to that when encapsulated alone, leading to the belief that curcumin did not have major effects on the gel network in order to hinder the release of compounds. For the 50:50 bigel, the release of curcumin (~20% in simulant 50%) and riboflavin (~12% in simulant 10%) were higher in comparison to systems with only one compound. As previously mentioned, the protein network is easily eroded, which may have allowed the access of the food simulant to the oleogel drops that encapsulated the curcumin, and due to the cross-linking effect of riboflavin, despite the erosion of the network, riboflavin was not as available for release in the simulant.

In vitro digestion

Figure 5.7 shows the bioaccessibility of compounds encapsulated simultaneously, at the end of the in vitro digestion process. For curcumin, it was possible to observe a bioaccessibility of 45% for bigel 90:10, 15% for bigel 50:50 and 50% for bigel 10:90. This similar bioaccessibility observed in the 90:10 and 10:90 system may be correlated with the structure in which it was encapsulated. For an O/W system, the oil particles were smaller with a larger surface area. The larger contact area allows the lipase adherence in the oil phase besides interactions with bile salts. Such mechanism increased the degree of lipid digestion, producing micelles, favoring the release and migration of the bioactive (GONÇALVES et al., 2021). Such behavior was observed in the encapsulations of curcumin into solid lipid nano- particles (SLN) and nanostructured lipid carriers (NLC), that resulted in 87% and 40% of bioaccessibility, respectively (GONÇALVES; VICENTE; PINHEIRO, 2023) and also from the study of soy protein nanogels with curcumin, which resulted in a bioaccessibility of 80% (HE et al., 2022). As for the W/O system, the curcumin is solubilized in the continuous matrix, so despite the

hydrogen bonds making release difficult, the fact that the oil is the continuous phase facilitates lipid digestion, promoting the release of the bioactive (ZHENG et al., 2020).

Figure 5.7. Bioaccessibility of bigels with curcumin and riboflavin load simultaneously, after in vitro digestion process. Error bars represent the standard deviation of n = 3 replications.

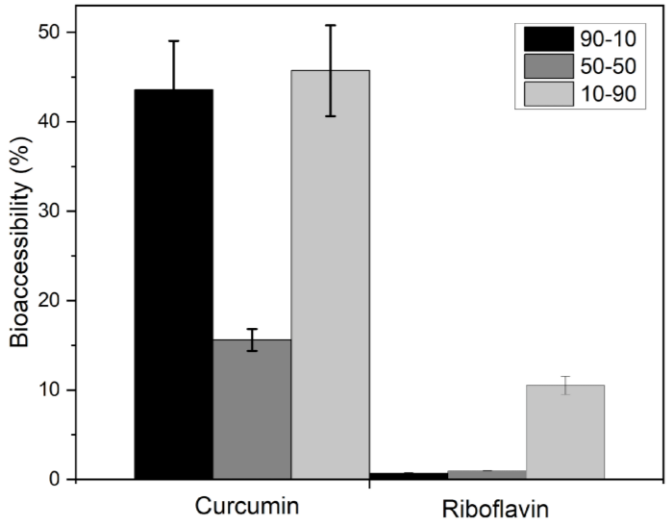

For riboflavin, it was possible to observe a growing bioaccessibility ranging from approximately 1% for bigel 90:10, 1.5% for bigel 50:50 and 10% for bigel 10:90. As aforementioned, riboflavin acted in such a way as to promote stronger protein bonds and intensifying the strength of the gel. The stronger network prevented the release of the compound during the digestion steps. Simões et al. (2020b) evaluated the release of riboflavin in its free form and through β-Lg micro- and nanostructures and noticed that at the end of digestion, 100% of the riboflavin that reaches the intestinal phase can be potentially absorbed, which differs from our results. Another work encapsulating riboflavin into zein-sodium alginate nanoparticles show that its bioaccessibility was up to 80% at the end of digestion (GE et al., 2023). This difference may be due to the structure, since the greater the available surface area, the greater the compound release rate. So, besides the structure of the studied bigels, the hydrogen bonds and electrostatic interactions, may be responsible for inhibiting pepsin permeation in order to reduce the rate of riboflavin release (YANG et al., 2022). For bigel 10:90 a curcumin-like behavior was observed. The highest percentage observed may be related to the arrangement of the oily network (in greater quantity in this case) that allowed greater availability, since the proteins are more dispersed in the matrix, and have a larger surface area conducive to the release of the bioactive. Regarding the 50:50 System, a low bioaccessibility was observed for both

compounds, probably due to the previously discussed bicontinuous structure, since the coexistence of the two phases impairs the release of the compounds (KODELA et al., 2017).

5.4 CONCLUSION

The incorporation of model compounds into cold-set WPI bigels exerted a great effect, leading to considerable changes in their structure. For pure bigels, XRD spectra showed a very broad peak, indicating that the bigels shows non-crystalline structure, being more crystalline with oleogel increase. The presence of riboflavin slightly increases the intensity of the peaks, while the curcumin decrease. However, the effect of the two compounds together promotes a great reduction on intensity. FTIR analysis did not presented any difference among the spectra of the pure gels, showing that the hydrogel and oleogel organization was purely physical. However, the addition of compounds promoted some changes, evidencing the presence of physical and chemical interactions. The microscopy images showed a conversion of the structure from oil in water (O/W) to water in oil (W/O), in the 10:90 formulation, which directly affected the mechanical properties. Besides, the formulation 90:10 and 10:90 presented as rubber gels, with higher Young's modulus, when compared with the 50:50, that had a squeezing gel behavior, probably due to a more disorganized structure. The addition of curcumin and riboflavin promoted different performances. The bigels with the isolated compounds, had an improvement in the gel network, making it more structured, according to the phase that is being added. For bigel 90:10, it was possible to observe a greater effect of riboflavin, while for bigel 10:90, the greater effects were observed for encapsulation of curcumin and both compounds simultaneously. Riboflavin, when exposed to light, reacted with protein molecules, causing an increase in strength and stiffness. Curcumin, on the other hand, did not show such evident effect, but there was an increase in rigidity proportional to the increase of oleogel in the sample. In relation to release kinetics, 90:10 was the best system for the release of isolated compounds, in both simulants, where there is ease erosion of the matrix. Therefore, increasing the amount of oleogel impaired the release of compounds. Regarding curcumin bioaccessibility, similar behavior was observed in the 90:10 and 10:90. As for riboflavin, it was possible to observe an increasing bioaccessibility with a maximum for bigel 10:90. As seen in the texture analyses, the 90:10 system was to be very hard gel, which may have prevented the release of the compound during the digestion steps. The results showed that it is, in fact, possible to incorporate hydrophilic and hydrophobic compounds in bigels simultaneously. However, the

effect can be very different depending on the composition. The interactions and synergisms between compounds and different structural components need to be further explored.

REFERENCES

AHEARNE, M.; COYLE, A. Application of UVA-riboflavin crosslinking to enhance the mechanical properties of extracellular matrix derived hydrogels. Journal of the Mechanical Behavior of Biomedical Materials, v. 54, p. 259–267, 2016.

ANWAR, Z. et al. Photochemical preparation, characterization and formation kinetics of riboflavin conjugated silver nanoparticles. Journal of Molecular Structure, v. 1289, n. March, p. 135863, 2023.

BABAEI, J. et al. In vitro digestibility and functional attributes of the whey protein heat-induced hydrogels reinforced by various polysaccharides and CaCl2. Journal of Food Measurement and Characterization, v. 16, n. 1, p. 19–28, 2022.

BOLLOM, M. A.; CLARK, S.; ACEVEDO, N. C. Development and characterization of a novel soy lecithin-stearic acid and whey protein concentrate bigel system for potential edible applications. Food Hydrocolloids, p. 105570, 2020.

BOU, R.; COFRADES, S.; JIM, F. Physicochemical properties and riboflavin encapsulation in double emulsions with different lipid sources. LWT - Food Science and Technology, v. 59, p. 621–628, 2014.

BOURBON, A. I.; CERQUEIRA, M. A.; VICENTE, A. A. Encapsulation and controlled release of bioactive compounds in lactoferrin- glycomacropeptide nanohydrogels: curcumin and caffeine as model compounds. Journal of Food Engineering, 2016.

BRYANT, C. M.; MCCLEMENTS, D. J. Influence of NaCl and CaCl2 on cold-set gelation of heat-denatured whey protein. Journal of Food Science, v. 65, n. 5, p. 801–804, 2000.

CARRILLO-NAVAS, H. et al. Inertial effects of adsorbed glycerol monostearate crystals on the shear rheology of water / canola oil interfaces. Journal of Food Engineering, v. 125, p. 112–118, 2014.

CERQUEIRA, M. A. et al. Structural and mechanical properties of organogels: Role of oil and gelator molecular structure. Food Research International, v. 96, p. 161–170, 2017.

CHEN, Z. et al. Novel bigels constructed from oleogels and hydrogels with contrary thermal characteristics: Phase inversion and 3D printing applications. Food Hydrocolloids, v. 134, n. June 2022, p. 108063, 2023.

CHUESIANG, P. et al. Observation of curcumin-loaded hydroxypropyl methylcellulose (HPMC) oleogels under in vitro lipid digestion and in situ intestinal absorption in rats. International Journal of Biological Macromolecules, v. 208, n. January, p. 520–529, 2022.

DIAMANTIDES, N. et al. Correlating rheological properties and printability of collagen bioinks: The effects of riboflavin photocrosslinking and pH. Biofabrication, v. 9, n. 3, 2017.

DJOULLAH, A.; SAUREL, R. Controlled release of riboflavin encapsulated in pea protein microparticles prepared by emulsion-enzymatic gelation process. Journal of Food Engineering, v. 292, n. July 2020, 2021.

EUROPEAN, C. Commission Regulation of the European Parliament and of the Council as regards food category 17 and the use of food additives in food supplements. No 1333/2008 of 8 October 2018. Official Journal of the European Union, n. October, p. 20–30, 2018.

EUROPÉIA, C. Regulamento (UE) No 10/2011 da Comissão de 14 de janeiro de 2011. Jornal Oficial das Comunidades Europeias, p. 1–89, 2011.

FALSAFI, S. R. et al. Insights into whey protein-based carriers for targeted delivery and controlled release of bioactive components. Food Hydrocolloids, v. 133, n. July, 2022.

FASOLIN, L. H., PICONE, C. S. F., SANTANA, R. C., AND CUNHA, R. L. Production of hybrid gels from polysorbate and gellan gum. Food Research International, v. 54, n.1, p. 501–507. 2013.

FASOLIN, L. H. et al. Modulating process parameters to change physical properties of bigels for food applications. Food Structure, v. 28, n. June 2019, p. 100173, 2021.

FENG, G. et al. Temperature and pH dual-responsive supramolecular hydrogels based on riboflavin sodium phosphate and 2, 6-Diaminopurine with thixotropic and fluorescent properties. Colloids and Surfaces A: Physicochemical and Engineering Aspects, v. 630, n. September, p. 127548, 2021.

GE, X. et al. The thermal resistance and targeting release of zein-sodium alginate binary complexes as a vehicle for the oral delivery of riboflavin. Journal of Food Science and Technology, v. 60, n. 1, p. 92–102, 2023.

GONÇALVES, R. F. S. et al. Lipid-based nanostructures as a strategy to enhance curcumin bioaccessibility: Behavior under digestion and cytotoxicity assessment. Food Research International, v. 143, n. March, 2021.

GONÇALVES, R. F. S.; VICENTE, A. A.; PINHEIRO, A. C. Incorporation of curcumin-loaded lipid-based nano delivery systems into food: Release behavior in food simulants and a case study of application in a beverage. Food Chemistry, v. 405, n. July 2022, 2023.

HAZRATI, Z.; MADADLOU, A. Gelation by bioactives: Characteristics of the cold-set whey protein gels made using gallic acid. International Dairy Journal, v. 117, p. 104952, 2021.

HE, M. et al. Fabrication of soy protein isolate-succinic anhydride-dextran nanogels: Properties, performance, and controlled release of curcumin. Lwt, v. 160, n. October 2021, p. 113259, 2022.

HE, Z. et al. Heat-induced gel formation by whey protein isolate- Lycium barbarum polysaccharides at varying pHs. Food Hydrocolloids, v. 115, n. January, 2021.

HEO, J. et al. Riboflavin-induced photo-crosslinking of collagen hydrogel and its application in meniscus tissue engineering. Drug Delivery and Translational Research, v. 6, n. 2, p. 148–158, 2016.

HWANG, H.-S. A critical review on structures, health effects, oxidative stability, and sensory properties of oleogels. Biocatalysis and Agricultural Biotechnology, v. 26, n. March, p. 101657, 2020.

JIANG, L. et al. Acid / alkali shifting of Mesona chinensis polysaccharide-whey protein isolate gels: Characterization and formation mechanism. Food Chemistry, v. 355, n. March, p. 129650, 2021.

KATIME, I.; MENDIZÁBAL, E. Swelling Properties of New Hydrogels Based on the Dimethyl Amino Ethyl Acrylate Methyl Chloride Quaternary Salt with Acrylic Acid and 2-Methylene Butane-1,4-Dioic Acid Monomers in Aqueous Solutions. Materials Sciences and Applications, v. 01, n. 03, p. 162–167, 2010.

KODELA, S. P. et al. Novel agar–stearyl alcohol oleogel-based bigels as structured delivery vehicles. International Journal of Polymeric Materials and Polymeric Biomaterials, v. 66, n. 13, p. 669–678, 2017.

KUHN, K. R.; CAVALLIERI, Â. L. F.; CUNHA, R. L. DA. Cold-set whey protein-flaxseed gum gels induced by mono or divalent salt addition. Food hydrocolloids, v. 25, n. 5, p. 1302–1310, 2011.

KUMARI, P.; RAZA, W.; MEENA, A. Lemongrass derived cellulose nanofibers for controlled release of curcumin and its mechanism of action. Industrial Crops and Products, v. 173, n. October, p. 114099, 2021.

LEI, H. et al. The behavior of whey protein isolate-curcumin complex at the oil-water interface. Food Hydrocolloids, v. 145, n. July, p. 109046, 2023.

LU, Y. et al. Structural Modification of O/W Bigels by Glycerol Monostearate for Improved Co-Delivery of Curcumin and Epigallocatechin Gallate. Food Science & Technology, v. 2, p. 975–983, 2022.

LUPI, F. R. et al. A rheological and microstructural characterization of bigels for cosmetic and pharmaceutical uses. Materials Science & Engineering C, v. 69, p. 358–365, 2016.

MACHADO, A. R. et al. Liposomes loaded with phenolic extracts of Spirulina LEB-18: Physicochemical characterization and behavior under simulated gastrointestinal conditions. Food Research International, v. 120, n. June 2018, p. 656–667, 2019.

MADALENA, D. A. et al. In vitro digestion and stability assessment of β-lactoglobulin/riboflavin nanostructures. Food Hydrocolloids, v. 58, p. 89–97, 2016.

MARTINS, A. J. et al. Hybrid gels: Influence of oleogel/hydrogel ratio on rheological and textural properties. Food Research International, v. 116, n. July, p. 1298–1305, 2019.

MINEKUS, M. et al. A standardized static in vitro digestion method suitable for food-an international consensus. Food and Function, v. 5, n. 6, p. 1113–1124, 2014.

NICOLAI, T.; BRITTEN, M.; SCHMITT, C. β-Lactoglobulin and WPI aggregates: Formation, structure and applications. Food Hydrocolloids, v. 25, n. 8, p. 1945–1962, 2011.

NUTTER, J. et al. Designing and characterizing multicomponent, plant-based bigels of rice bran wax, gums, and monoglycerides. Food Hydrocolloids, v. 138, n. December 2022, p. 108425, 2023.

RODRIGUES, R. M. et al. Effects of moderate electric fields on cold-set gelation of whey proteins – From molecular interactions to functional properties. Food Hydrocolloids, v. 101, n. November 2019, 2020.

SABET, S. et al. Clustering of oleogel production methods reveals pitfalls and advantages for sustainable, up scalable, and oxidative stable oleogels. Journal of Food Engineering, v. 357, n. March, p. 111659, 2023.

SAGIRI, S. S. et al. Stearate organogel-gelatin Hydrogel based bigels: Physicochemical, thermal, mechanical characterizations and in vitro drug delivery applications. Journal of the Mechanical Behavior of Biomedical Materials, 2014.

SAMUI, T. et al. The development and characterization of novel in-situ bigel formulation. Food Hydrocolloids, v. 113, n. September 2020, p. 106416, 2021.

SARKAR, A.; GOH, K. K. T.; SINGH, H. Colloidal stability and interactions of milk-protein-stabilized emulsions in an artificial saliva. Food Hydrocolloids, v. 23, n. 5, p. 1270–1278, 2009.

SHAKEEL, A. et al. Key characteristics and modelling of bigels systems: A review. Materials Science & Engineering C, v. 97, n. February 2018, p. 932–953, 2019.

SHAKEEL, A. et al. Bigels and multi-component organogels: An overview from rheological perspective. Food Hydrocolloids, v. 111, n. July 2020, p. 106190, 2021.

SHISHIR, M. R. I. et al. Advances in micro and nano-encapsulation of bioactive compounds using biopolymer and lipid-based transporters. Trends in Food Science & Technology, 2018.

SILVA, P. M. et al. Oleogels and bigels as alternatives to saturated fats: A review on their application by the food industry. JAOCS, Journal of the American Oil Chemists' Society, v. 99, n. 11, p. 911–923, 2022.

SIMÕES, L. S. et al. Suitability of β-lactoglobulin micro- and nanostructures for loading and release of bioactive compounds. Food Hydrocolloids, v. 101, n. November 2019, 2020a.

SIMÕES, L. S. et al. β-lactoglobulin micro- and nanostructures as bioactive compounds vehicle: In vitro studies. Food Research International, v. 131, n. January, p. 108979, 2020b.

SINGH, V. K. et al. Guar gum and sesame oil based novel bigels for controlled drug delivery. Colloids and Surfaces B: Biointerfaces, 2014.

TRUJILLO-RAMÍREZ, D. et al. Cooling rate, sorbitan and glyceryl monostearate gelators elicit different microstructural, viscoelastic and textural properties in chia seed oleogels. Food Research International, n. October, p. 0–1, 2018.

VERGARA, D. et al. Povidone-iodine loaded bigels: Characterization and effect as a hand antiseptic agent. Journal of Drug Delivery Science and Technology, v. 72, n. November 2021, 2022.

WANG, F. C.; MARANGONI, A. G. Internal and external factors affecting the stability of glycerol monostearate structured emulsions. Royal Society of Chemistry, v. 5, n. 001, p. 93108–93116, 2015.

WU, S. et al. Fabrication of high strength cold-set sodium alginate/whey protein nanofiber double network hydrogels and their interaction with curcumin. Food Research International, v. 165, n. October 2022, p. 112490, 2023.

XIE, D. et al. Influence of oleogel/hydrogel ratios and emulsifiers on structural and digestion properties of food-grade 3D printed bigels as carriers for quercetin and catechin. Food Hydrocolloids, v. 144, n. March, p. 108948, 2023.

YALLAPU, M. M.; JAGGI, M.; CHAUHAN, S. C. β-Cyclodextrin-curcumin self-assembly enhances curcumin delivery in prostate cancer cells. Colloids and Surfaces B: Biointerfaces, v. 79, n. 1, p. 113–125, 2010.

YAN, S. et al. Controlled release of curcumin from gelatin hydrogels by the molecular-weight modulation of an oxidized dextran cross-linker. Food Chemistry, v. 418, n. November 2022, p. 135966, 2023.

YANG, C. et al. Cold-set oat protein isolate-gellan gum binary gels with various microstructures: Fabrication, characterization, formation mechanism, and controlled release properties. Food Hydrocolloids, v. 131, n. May, p. 107818, 2022.

ZHENG, H. et al. Development of food-grade bigels based on κ-carrageenan hydrogel and monoglyceride oleogels as carriers for β-carotene: Roles of oleogel fraction. Food Hydrocolloids, v. 105, n. February, p. 105855, 2020.

ZHONG, W. et al. Formation, stability and in vitro digestion of curcumin loaded whey protein/ hyaluronic acid nanoparticles: Ethanol desolvation vs. pH-shifting method. Food Chemistry, v. 414, n. February, p. 135684, 2023.

ZHU, Q. et al. Development and characterization of novel bigels based on monoglyceride-beeswax oleogel and high acyl gellan gum hydrogel for lycopene delivery. Food Chemistry, v. 365, n. December 2020, p. 130419, 2021.

ZHU, Q. et al. Rational design cold-set interpenetrating network hydrogel based on wheat bran arabinoxylans and pea protein isolates for regulating the release of riboflavin in simulated digestion. International Journal of Biological Macromolecules, v. 223, n. PA, p. 961–970, 2022.

SUPLEMENTARY MATERIAL

Figure 5.1S. Representative behavior of cold-set bigels with different hydrogel:oleogel ratios.

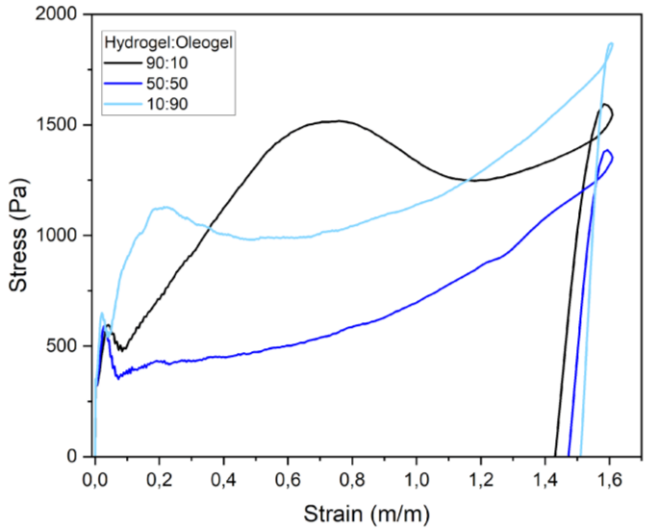

Table 5.1S. Fitting parameters of curcumin and riboflavin release data from cold-set bigels. The parameters RMSE and R^2 were used to evaluate the quality of the regression.

Sample	Food Simulant	RMSE	R^2	Kf (min^{-1})	n
C – 90:10	50 %	0.1323	0.76	0.083 ± 0.016	0.29 ± 0.03
C – 50:50	50 %	0.1449	0.76	0.077 ± 0.016	0.31 ± 0.03
C – 10:90	50 %	0.0984	0.70	0.222 ± 0.023	0.16 ± 0.01
R – 90:10	10 %	0.0803	0.91	0.138 ± 0.018	0.24 ±0.02
R – 50:50	10 %	0.0802	0.92	0.081 ± 0.012	0.33 ± 0.02
R – 10:90	10 %	0.0238	0.99	0.065 ± 0.003	0.32 ± 0.01
CR – 90:10	50 %	0.1295	0.83	0.030 ± 0.008	0.43 ± 0.04
CR – 50:50	50 %	0.0557	0.96	0.050 ± 0.005	0.36 ± 0.01
CR – 10:90	50 %	0.0563	0.89	0.228 ± 0.013	0.16 ± 0.01
CR – 90:10	10 %	0.0533	0.96	0.083 ± 0.006	0.31 ± 0.01
CR – 50:50	10 %	0.0502	0.93	0.174 ± 0.010	0.20 ± 0.01
CR – 10:90	10 %	0.0853	0.56	0.502 ± 0.100	0.15 ± 0.06

C: Curcumin; R: Riboflavin; CR: Curcumin + Riboflavin

CAPÍTULO 6.

Effect of incorporating *Hibiscus Sabdariffa* L. leaves extract into WPI bigels with soy lecithin

6. EFFECT OF INCORPORATING *HIBISCUS SABDARIFFA* L. LEAVES EXTRACT INTO WPI BIGELS WITH SOY LECITHIN

Gabrielli Nunes Clímaco[a]; Raquel F.S Gonçalves[b]; Jean-Michel Fernandes[b]; Ana C. Pinheiro[b]; António A Vicente[b]; Luiz Henrique Fasolin[a]

[a] Department of Food Engineering and Technology, School of Food Engineering, University of Campinas, CEP 13083-862, Campinas, SP, Brazil
[b] CEB- Centre of Biological Engineering, University of Minho, 4710-057 Braga, Portugal

ABSTRACT

The effect of soy lecithin and the incorporation of *Hibiscus Sabdariffa* L. leaves extract into bigels with whey protein isolated (WPI) and glycerol monostearate was assessed. Hydrogel phase was produced with WPI (11% w/v) and for oleogel sunflower oil and glycerol monostearate (GM) (10% w/v) were used. Soy lecithin (SL) (5% w/v) and extract from hibiscus (0.01 g of GAE/ml of extract and 0.001 g of GAE/ml of extract, for SFE and PLE extracts) were added to the oil phase. Bigels were produced by hot emulsification (18.000 min^{-1}, 2 min, at 55 °C) with different hydrogel:oleogel ratios (90:10, 50:50 and 10:90). NaCl (200 mM) was added to the aqueous phase prior the emulsification. Bigels were evaluated through structural, thermal, texture, release kinetics and *in vitro* digestion analyzes. XRD showed that the addition of lecithin and the extracts led to some possible structural differences in the gel structure. FTIR spectra presented some influence of the extracts on the bigels, by modifying some peaks observed only in pure extracts, showing physical and chemical interaction. Confocal images showed an increase of oil droplets proportionally to the amount of oil present, some coalescing drops in bigel 50:50, and a predominantly oily network in bigel 10:90, probably due a conversion of the structure from oil in water (O/W) to water in oil (W/O). The addition of lecithin strengthens the network, and along with the GM, could promote a better arrangement of the network. However, the addition of extracts weakened the structure. In relation to release kinetics, both extracts show better recovery for 90:10 system, with no release for bigel 10:90, probably due to the way the oil droplets were dispersed in the matrix, and the ease of the protein network to erode. For bioaccessibility, the same behavior was observed, with better recovery for 90:10 system, and higher values for bigels with PLE extract.

Key-words: Hydrogel, oleogel, hibiscus, phenolic compounds, vehicle

6.1 INTRODUCTION

The protection and vehiculation of bioactive compounds in food systems have been increasing over the years, aiming to enhance their bioavailability, nutritional and pharmacological effects (BEHERA et al., 2015; LUPI et al., 2016; PINHEIRO et al., 2017; SAGIRI et al., 2014; SINGH et al., 2014a). Among the different innovative forms, there are the mixed gels or bigels defined as a mixture of hydrogel and oleogel, organized into different

systems, such as oil-in-water, water-in-oil, or bicontinuous structure with strong characteristics of each phase (SHAKEEL et al., 2019; SINGH et al., 2014a).

These systems are formulated without surfactant addition. Despite this, they have been shown high stability when compared with emulsions (water-in-oil and oil-in-water), creams, emulgels, hydrogels, and oleogels, probably due to the complex three-dimensional gelled network, that prevent phase separation when stored at room temperature (SINGH et al., 2014b, 2018). These bigels with different structures can act as texturizing agents in different food products, being also potential substitutes for saturated and/or trans-fat. (SAGIRI et al., 2014; SILVA et al., 2022; NUTTER et al., 2023). In addition, they allow the simultaneous incorporation and protection of bioactive compounds with different polarities due to the presence of an oil and water gelled phases in addition to allowing the simultaneous incorporation of bioactive compounds of different polarities (BOLLOM; CLARK; ACEVEDO, 2020; FASOLIN et al., 2021).

One of the most widely used hydro-gelling agent is the whey protein isolated (WPI), which is a product with a high nutritional value from the residue of cheese production (JIANG et al., 2021). WPI protein fractions can be divided into 2 major groups, β-lactoglobulin and α-lactalbumin, which represent approximately 9% and 4% of the total milk protein, respectively. These proteins have been extensively studied and presented several interesting technofuncional as well as emulsifying, foaming and gelling ability with high water retention (KUMAR et al., 2022; BOLLOM; CLARK; ACEVEDO, 2020; HAZRATI; MADADLOU, 2021; KUHN; CAVALLIERI; CUNHA, 2011; RODRIGUES et al., 2020; SHISHIR et al., 2018). WPI can be gelled in two ways, by heat-set or cold-set method. The cold-set method consists of two steps, the first being heating the WPI solution to partially denature the proteins, followed by adding salt or changing the pH towards the protein isoelectric point (pI) to form the gel (HAZRATI & MADADLOU, 2021; BRYANT & MCCLEMENTS, 2000).

Concerning the oil phase, the gel network can be produced by direct and indirect method. The direct method consists of solubilizing, at high temperatures, the gelling agent in the oil. They can be classified as high molecular weight (HMOGs) or low molecular weight oleogelators (LMOGs) (CERQUEIRA et al., 2017). HMOGs, or polymeric, form a 3D network through covalent bonds, whereas LMOGs through non-covalent bonds, such as H-bonding, π-π stacking and solvophobic forces (FASOLIN et al., 2018). The glyceryl monostearate (GM) is one of the most LMOGs used as a gelling agent for food application, since it is considered GRAS by the US Food and Drug Administration (CFR 21 - Section 182.1324) and approved

by the European Union for food use (EUROPEAN, 2018). In addition, GM presents low cost and highly efficient in structuring edible oils at low concentrations (TRUJILLO-RAMÍREZ et al., 2018).

The study and development of bigels began focusing on cosmetic and pharmaceutical applications. Only in the last years bigels formulated with GRAS ingredients for food application started to be studied (BOLLOM; CLARK; ACEVEDO, 2020; FASOLIN et al., 2021; VERGARA et al., 2022; XIE et al., 2023; ZHAI et al., 2022; ZHENG et al., 2020; ZHU et al., 2021). However, food processing is a complex combination of unit operation that generally use heat and shear. The process conditions can destabilize bigels since the arrangement between oleogel and hydrogel phases are purely physical in most of cases and the absence of surfactants. Therefore, the use of surfactant could improve the stability of bigels during food process, storage and consumption.

Soy lecithin is a natural mixed surfactant, composed of various phospholipid derivatives, which have physiological functions such as regulating blood lipids, strengthening the brain and delaying aging (ZHANG et al., 2022). Ikeda and Foegeding (1999) evaluated the effect of lecithin on WPI gels and found that even at low concentrations, lecithin brought about considerable improvements in gel properties. Samui et al (2021) developed a bigel of gelatin + glycerol monostearate + lecithin and also verified a great effect of lecithin in stabilizing the water-oil interface, thus contributing to the strength and stability of the bigel. Moreover, due to its gelling properties, lecithin can positively aggregate the 3D network, facilitating the incorporation and protection of encapsulated compounds (ZHANG et al., 2022).

Some of the recent works discuss the modification in the physicochemical properties of bigels due to the incorporation of bioactive compounds, such as curcumin and epigallocatechin gallate into a bigel with gelatin and GM (LU et al., 2022), lycopene into a bigel with gellan gum, monoglyceride and beeswax (ZHU et al., 2021), β-carotene into bigels with κ-carrageenan and monoglyceride (ZHENG et al., 2020). Moreover, different structures were also evaluated as well as β-lactoglobulin micro- and nanostructures for delivery of quercetin and caffein (SIMÕES et al., 2020) and pea protein microparticles for delivery of riboflavin (DJOULLAH; SAUREL, 2021).

In addition to model compounds, plant extracts have been studied since they have a high nutritional content and high antioxidant activity. However, there are still no studies of bigels as vehicles for plant extracts, but some authors have already studied the application in other systems such as olive leaf extract into pectin-sodium caseinate hydrogel (AHMADZADEH et

al., 2021), phenolics from grape seed into alginate and chitosan hydrogel microbeds (PEDRALI; BARBARITO; LAVELLI, 2020), purple sweet potato extract into agar-beeswax bigels (ZHAI et al., 2022).

Plants in general are recognized for having a great diversity of compounds that are used in the development of new drugs, functional foods or as food additives. These compounds can perform several functions, acting as preservatives and dyes, or even performing pharmacological and/or nutraceutical effects in the human body (CHEMAT et al., 2019; CVJETKO BUBALO et al., 2018). Besides, the recovery of agro-industrial by-products or residues to obtain macronutrients and bioactive compounds is very advantageous for the environment, as it promotes a reduction in the amounts of waste generated. So, the complete use of the raw material for the recovery of bioactive compounds is already widespread among researchers, opening the way for other nutrients.

Hibiscus sabdariffa L. is an herbaceous plant available during the whole year, widely cultivated in many areas and known for having beneficial biological properties. Among the parts of the plant, the calyx and the flowers are the most studied parts, due to the greater knowledge related to their nutritional value (ZHEN et al., 2016). However, the hibiscus leaves are a potential source of bioactive compounds, presenting yields comparable or superior to those observed for hibiscus calyx and flowers (CLIMACO; VARDANEGA; FASOLIN, 2023). Several authors have already studied the nutraceutical effects of hibiscus leaves extracts obtained through different methods (ALVES et al., 2022; CAVALCANTI et al., 2011; KARAASLAN, 2019; SOUZA et al., 2019; SUBHASWARAJ et al., 2017; VARDANEGA et al., 2019; VEGGI; CAVALCANTI; MEIRELES, 2014; WANG et al., 2014), showing that this matrix can act as a source of bioactive compounds that can improve the nutritional content of a product.

Thus, the aim of this work was evaluating the effect of the incorporation of hibiscus leaf extract in cold-set bigels formulates with WPI, sunflower oil, glyceryl monostearate and soy lecithin, on the physicochemical properties. Moreover, the release kinetics of the extracts in food simulants and *in vitro* digestion were assessed.

6.2 MATERIALS AND METHODS

Materials

Whey Protein Isolate (WPI) powder (Lacprodan DI-9224, Arla Foods Ingredients, Viby, Denmark), glyceryl monostearate (GM) (Alfa Aesar, Kandel, Germany), NaCl (AppliChen,

Darmstadt, Germany), commercial sunflower oil, soy lecithin (SL) (Lipoid GmbH, Ludwigshafen, Germany), ethanol 96% (Valente e Ribeiro LTDA, Belas, Portugal) and distillate water were used for bigel's production. Pepsin from porcine gastric mucosa (1735,8 $U.mg^{-1}$), bile extract porcine, pancreatin from porcine pancreas (39 $U.mg^{-1}$), Pefabloc® SC, salts used to prepare oral, gastric and intestinal electrolyte solutions were used for in vitro digestibility assays.

Methods

Hibiscus leaves extract

The extracts were obtained through supercritical fluid extraction (SFE) and pressurized liquid extract (PLE) according to the methodology describe in Clímaco et al. (2023). SFE extract was obtained at 100 bar, 60 ºC and 15% (w/v) of co-solvent, with S/F ratio set at 25 (g/g), CO_2 flow rate of 1.7 g/min and the ethanol flow rate of 0.3 g/min. PLE extract was obtained at 80ºC and 99.5% (v/v) of ethanol, with a volumetric flowrate of 3.47 ml/min.

Bigel production

Bigels were produced without (CSB) and with soy lecithin (CBL) as a structuring agent together with the GM. Hydrogel (H) was produced with WPI 11% (w/v) through cold-set gelation, according the methodology describe by Rodrigues et al. (2020). For that, WPI were dispersed in distillate water under magnetic stirring for 2 hours at room temperature (25 °C) and kept overnight, for complete hydration and protein solubilization. The solutions were subject to heat treatment at 90 °C during 10 min under magnetic stirring (500 min^{-1}). Then, the thermal denatured partially WPI was cooled to 55 ºC using an ice bath, and the ionic strength was adjusted to 0.2 M with NaCl 5 M solution (25 °C).

Oleogel (OG) was prepared by heating the mixture of GM 10% (w/w) with or without SL 5% (w/w) and sunflower oil at 80 °C during 30 min under magnetic stirring (Heidolph, Magnetic stirrer Hei-Tec) (500 min^{-1}) in order to solubilize the gelling agent (CERQUEIRA et al., 2017). Then, the solution was cooled to 55 °C.

For bigels' production the OG and CH solutions were emulsified (18.000 min^{-1}, 2 min, at 55 °C) using Ultra Turrax (T18, IKA, Germany) at different CH:OG ratios (90:10, 50:50 and 10:90). The emulsions were put in cylindrical molds (diameter = 22 mm) and stored at room temperature (25 °C) to gel formation.

Bigels with hibiscus leaves extract

Bigels containing the extract were produced with lecithin, as describe before. Hibiscus leaves extract was added to the oil phase after the homogenization of the gelling agents, in the concentration of 0.01 g of GAE/ml of extract and 0.001 g of GAE/ml of extract, for SFE and PLE extracts, respectively.

Confocal microscopy

A Leica TCS SP5 confocal laser scanning microscope (CLSM), was operated in fluorescence mode with a 63× oil-immersion objective. The protein phase was stained with Fit C, and the oil phase with Nile red. The samples were stained with Nile Red (0.1 g/L) and Fit C (0.2 g/L) at 1:10 ratio (dye:sample, v/v), which enabled the oil droplets to become visible. The samples were then placed onto a microscope slide with a cavity and covered by a coverslip. The CLSM images were recorded using a He–Ne laser with an excitation wavelength of 517 nm for Fit C and 636 nm for Nile Red. All measurements were performed at 25 ºC and the experiments were carried out at least in duplicate.

Infra-red spectrophotometry (FTIR)

FTIR spectra was performed to evaluated the possible interactions among the gel's compounds, following the methodology describe by Sagiri et al. (2014). The spectrums of FTIR were measured using one spectrophotometer (FTIR – MID/FAR Agilent 660), operated in attenuated total reflectance mod (ATR). The measures were between 4000 and 400 cm^{-1} in resolution of 1 cm^{-1}.

Mechanical Proprieties

The mechanical proprieties were determined by uniaxial compression measurements in a TA XTplus Texture Analyzer (Stable Micro Systems, United Kingdom) equipped with a 7 cm of diameter plate. The gels (diameter = 14 mm) were compressed to 80% of the initial height with crosshead speed of 1 mm s^{-1}. The force x height data were transformed into Hencky stress (σ_H) and Hencky deformation (ε_H) (Equation 1 and 2) (FASOLIN et al., 2013; RODRIGUES et al., 2020).

$$\sigma_H = F(t)\left[\frac{H(t)}{H_0 A_0}\right] \quad (1)$$

$$\varepsilon_H = -ln\ ln\left[\frac{H(t)}{H_0}\right] \quad (2)$$

were *F(t)* being the force (N) in time *t*, A_0 (m^2) and H_0 (m) are the sample area and initial high, respectively and *H(t)* is the high (m) in time *t*. Stress x deformation curves were used to evaluate the rupture point (first maximum point of the curve), while elasticity or Young's modulus (*E*) was calculated as the slope of the linear region.

Rheological analyses

Viscoelastic properties of the bigels were evaluated with a Discovery HR1 rheometer (TA Instruments, Crawley, UK) equipped with a cone plate (60 mm, 2º angle, truncation 64 μm). Approximately 2 g of the sample was placed on the surface of rheometer plate for the test. Linear viscoelastic region (LVR) of the samples was firstly determined by dynamic strain sweep test at the strain range of 0.01%–100%. Temperature (90 to 25 ºC at a heating rate of 5 ºC/min) sweeps were performed within the LVR (0.5% strain). Both storage modulus (G') and loss modulus (G'') were recorded.

X-ray Diffraction (XRD)

XRD patterns of bigels were taken using an X-ray diffractometer (Bruker D8 Discover, USA), equipped with an X-ray tube Cu source (λ = 1.54056 Å) operated at 45 kV and 40 mA, with calibration offset to 2θ = -0.0372°, and with sweeps ranging from 5.0 to 50° (2θ) (step 0.050 °C/s), at room temperature, for 174s (FASOLIN et al., 2021).

In vitro digestion

The process was made using the harmonized static *in vitro* digestion model described by Minekus *et al*. (2014), that simulates the mouth, stomach and intestinal phases, using 3 standard fluids, being Simulated Salivary Fluid (SSF) (KCl 15.1 mM, KH_2PO_4 3.7 mM, $NaHCO_3$ 13.6 mM, $MgCl_2(H2O)_6$ 0.15 mM, $(NH_4)_2CO_3$ 0.06 mM and HCl 1.1 mM), Simulated Gastric Fluid (SGF) (KCl 6.9 mM, KH_2PO_4 0.9 mM, $NaHCO_3$ 25 mM, NaCl 47.2 mM, $MgCl_2(H_2O)_6$ 0.12 mM, $(NH_4)_2CO_3$ 0.5 mM and HCl 15.6 mM, and Simulated Intestinal Fluid (SIF) (KCl 6.8 mM, KH2PO4 0.8 mM, NaHCO3 85 mM, NaCl 38.4 mM, MgCl2(H2O)6 0.33 mM and HCl 8.4 mM).

The oral phase was composed for the simulated salivary fluid (SSF), $CaCl_2(H_2O)_2$ 0.3 M (in order to achieve 0.75 mM at the final mixture) and Milli-Q water (in order to make up the final volume), added to 5 g of sample. The mixture was incubated at 37 ºC for 2 min under orbital agitation at 120 min^{-1}. α-amylase was not used as samples did not contain starch

(SARKAR; GOH; SINGH, 2009). For the gastric phase, simulated gastric fluid (SGF), $CaCl_2(H_2O)_2$ 0.3 M (in order to achieve 0.075 mM at the final mixture) and pepsin solution (with final activity of 40000 U/mL in the final mixture) were added to the previous mixture. The pH was adjusted to 3.0 with HCl 1 M and Milli-Q water was added to make up the final volume. The samples were incubated for 2 h at 37 ºC under orbital agitation at 120 min^{-1}. Finally, the intestinal phase consisted of simulated intestinal fluid (SIF), $CaCl_2(H_2O)_2$ 0.3 M (in order to achieve 0.3 mM at the final mixture), bile salts (in order to achieve 10 mM at the final mixture) and pancreatin solution (with final activity of 800 U/mL in the final mixture). The pH was adjusted to 7.0 with NaOH 1 M or HCl 1 M and then Milli-Q water was added to achieve the final volume. The samples were incubated during 2 h at 37 ºC under orbital agitation at 120 min^{-1}. At the end of digestion, the reaction was stopped adding enzyme inhibitor Pefabloc® (1 mM) (10 µL for each 1 mL of sample), and after that, samples were collected. All the samples were tested in triplicate.

Phenolic compounds bioaccessibility

The content of phenolic compounds was determined at the end of the digestion based on the methodology described by Singleton et al. (1999) using gallic acid as standard. The digesta (10 mL) was centrifuged (Allegra 64R, Beckman Coulter Inc., USA) at 18.700 g at room temperature for 30 min, and the supernatant (which was assumed as the micelle phase) was collected. In each test tube 1 ml of supernatant, 6 ml of distilled water and 0.5 ml of Folin-Ciocalteu reagent were mixed and incubated at room temperature for 3 min. Then, 1.5 ml of 20% Na_2CO_3 solution and 1.9 ml of distilled water were added, and the mixture was incubated in the dark for 2 h at room temperature. The absorbance was read at 760 nm using a UV-Vis spectrophotometer (V-560, Jasco, USA). The assays were performed in triplicate and were expressed as mg of gallic acid equivalent (GAE) per g of dry extract (mg GAE/g of dry extract).

Release kinetics

The release kinetics of phenolic compounds in food simulant was evaluated by the dissolution test following the methodology described in Simões et al. (2020) with some modifications. The food simulant solution composed of 50% ethanol, were used to simulate hydrophobic food matrices, in accordance with Commission Regulation (EU) No. 10/2011 of January 14, 2011 (2011), and were conducted at 25°C (simulating room temperature).

The gels containing the extract were prepared inside a syringe (5ml) with the cap removed and left to rest for 24 hours before analysis, for complete gelation. Afterwards, the syringes were placed vertically immersed in a reactor with 30 ml of solution, under continuous magnetic stirring at 200 min^{-1}. At appropriate time intervals, 0.25 mL of supernatant was removed and replaced by the same amount of original solution, in order to keep the volume constant. Each sample collected was frozen until the end of the day, in order to quantify the phenolics.

Total phenolic content was determined according to the Singleton et al. (1999) with modifications. 4ml of water, 250 µL of sample and 250 µL of Folin-Ciocalteu reagent (Dinâmica, São Paulo, Brazil) were mixed and agitated in vortex. After 3 min, 500 µL of sodium carbonate solution (20%) were added. The solutions were agitated in vortex and kept for 2 h in the dark. The absorbance was determined at 760 nm in a microplate reader (BMG LABTECH, Ortenberg, Germany). Gallic acid was used as standard. All analyses were carried out in triplicate and the results were expressed in mg GAE (gallic acid equivalent)/ml of extract.

The compounds release profile was evaluated using an equation that considers the effects of Fickian and Case II transport in hydrophilic matrices (KATIME; MENDIZÁBAL, 2010).

$$\frac{M_t}{M_\infty} = K_F * t^n \quad (1)$$

were M_t is the mass released at time t, M_∞ is the mass release at equilibrium, K_f is the Fickian diffusion rate constant and n is a characteristic exponent of the transport mode. Depending on the polymer diffusion and relaxation rates, three different classes of mechanisms can be observed: 1) Case I or Fickian diffusion, in which the diffusion rate is much lower than the relaxation rate (n = 0.50), 2) Diffusion case II, in which diffusion is superior to the relaxation process (n = 1), and 3) non-Fickian or anomalous diffusion that occurs when diffusion and relaxation rates are comparable ($0.50 < n < 1$).

6.3 RESULTS AND DISCUSSION

All the cold-set bigels (CSB and CBL) and CLB with hibiscus extract were self-supported and the hydrogel:oleogel ratio led to some visual differences in bigels with the extract. Besides, bigels with high hydrogel content had a more rigid structure and those with more oil, a softer structure, like cream or ointment. This behavior was observed both for pure bigels and for those encapsulated with extract. However, the presence of bioactive compounds

can interact physically and/or chemically, changing its microstructure and consequently their physicochemical properties. Regarding the crystallinity of the samples, Figure 6.1A showed a broad and non-defined peak, which is typical of amorphous materials (MACHADO et al., 2019). However, differences regarding the hydrogel:oleogel ratio and amount of extract were observed.

Figure 6.1. X-Ray scattering profile of Cold-set bigels (CSB) (A) and Cold-set bigels with soy lecithin (CBL) with SFE extract (B) and PLE extract (C).

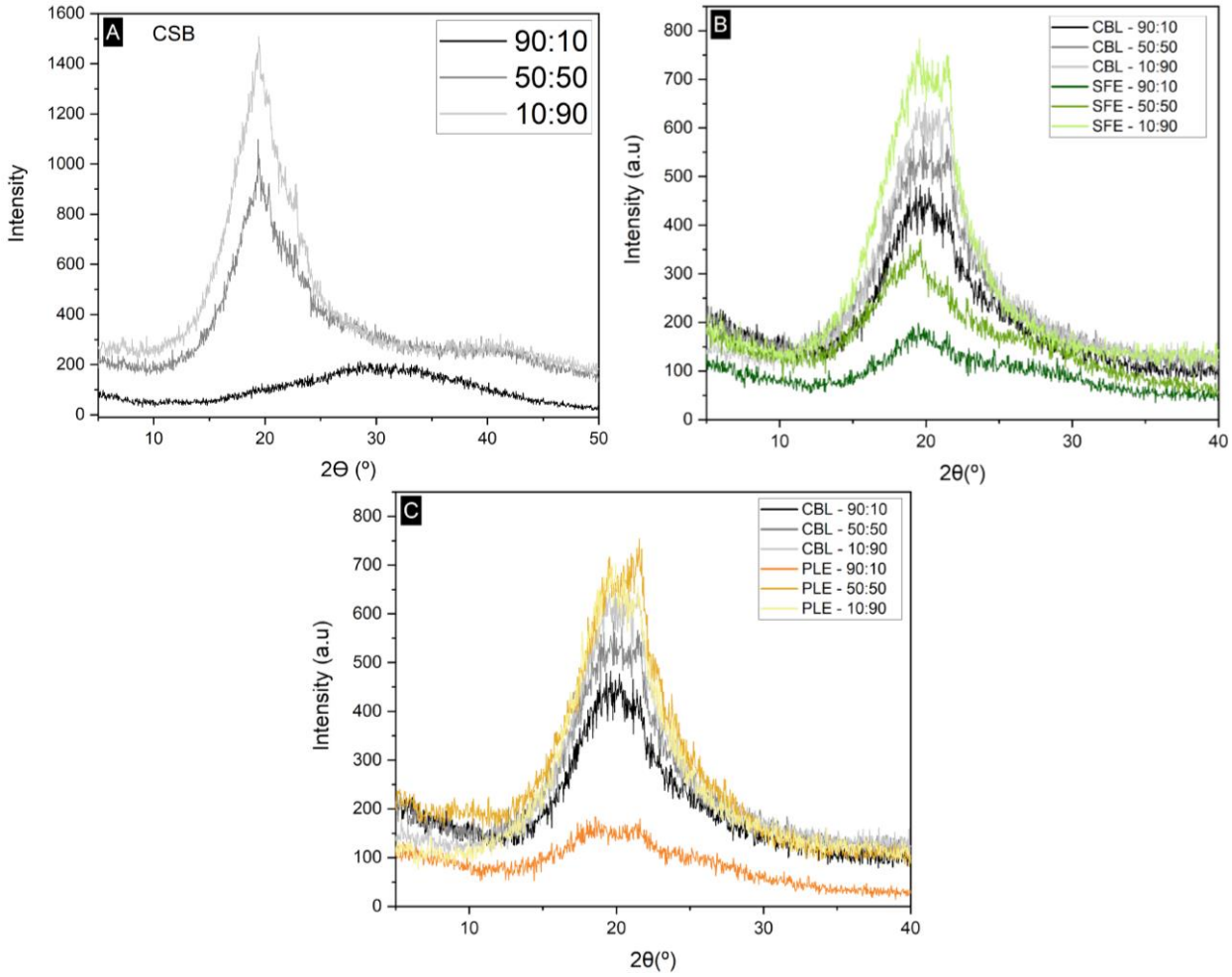

In relation to pure bigels (Figure 6.1A), a broad band around 20º 2θ was observed, with an increase in intensity proportional to the increase in oleogel in the system, probably due to the GM spectrum, which has sharp peaks at 19.6◦ and 23.7º 2θ (FASOLIN et al., 2021) which may have resulted in a different arrangement of the molecules. The presence of lecithin (Figures 6.1B and C) led a reduction in the intensity of the peaks, probably due to the interaction with GM, which conferred the crystalline characteristic of the oleogel. Regarding encapsulation, it was noticed that the extracts did not change the observed peaks, they only caused changes in intensity.

PLE extracts increased the intensity for 50:50 and 10:90 bigels, while SFE showed the same effect only for 10:90, i.e., for these systems, the extracts assisted the formation of crystals. This increase in intensity may be related to the compound-protein interaction (AHMADZADEH et al., 2021), since the more hydrogel in the sample, the greater this intensity. In addition to not having data confirming the interaction of polyphenols with GM (CHEN et al., 2023). In addition, the greater presence of phenolic acids in PLE extracts caused a greater modification when compared to bigels with SFE extracts.

However, for the 90:10 system, both led to the reduction in the intensity of the peaks, probably due to the low amount of extract when compared to the hydrogel, which prevailed. Similar behavior was observed in a study of olive leaf extract-nano lipid carrier into pectin-sodium caseinate hydrogel (AHMADZADEH et al., 2021). The authors demonstrated that despite the NCL having a crystalline structure, the amorphous characteristic of the hydrogel and the extract stood out. The extracts did not influence the construction of the peaks, only in the intensity of the amorphous characteristic (AHMADZADEH et al., 2021).

FTIR analysis was performed to verify interactions among the hydro/oleogelators and the extract trough changes in the functional groups. Similar to X-Ray diffractograms, the FTIR spectra showed some differences between the pure gels and the gels with hibiscus extract. The addition of the extract interacted with the components of the bigel, promoting physical and chemical changes.

For all formulations (Figure 6.2), a broad band around 3250 and 600 cm^{-1}, being related to O-H stretching vibrations participating in the hydrogen bond within the hydrogel and N–H bending vibrations of amide I, respectively, and a peak at 1650 cm^{-1} characteristic of the C=O bond, was observed (VERGARA et al., 2022). Moreover, as expected, this bands were reduced as the percentage of oil in the sample increases.

Comparing the bigels with and without lecithin, it was observed that the peaks 2920 cm^{-1} and 2850 cm^{-1}, referring to the asymmetric and symmetric stretching vibrations of methylene present in oil and GM (FASOLIN et al., 2021), were also present in lecithin (DAS et al., 2022). Thus, these peaks were presented in all formulations even when in a low amount of oil. However, GM increase and the presence of lecithin led to higher intensity of these peaks. On the other hand, theses peaks disappear in the formulations 90:10 and 50:50 with the incorporation of hibiscus' extract, showing that there was probably some chemical interaction between the phenolic compounds present in the extract, such as quercetin and chlorogenic acid, and whey protein (BABA; MCCLEMENTS; MAQSOOD, 2021; ZHAO; LI; XUE, 2023), as

observed in the XRD spectrums. A similar result was observed by Wang et al. (2022) between WPI and rose anthocyanin extracts at different pH. The authors observed that the extract concentration increase changed the FTIR spectrum intensity due the interaction between the components. In addition, the study of the encapsulation of *Triphasia trifolia* extracts in WPI-chitosan hydrogels demonstrated that some functional groups of the extract interacted effectively with chitosan, resulting in the adhesion of the extract to the porous network of the hydrogel (DO et al., 2023). However, these interactions were not as strong, since the highest peaks observed in the extracts related to chlorogenic acid, 1620 cm^{-1} and 1118 cm^{-1}, referring to the C=C stretching of aromatics and the C-OH stretching, respectively (TAIB et al., 2019) did not influence the bigel spectra.

Figure 6.2. FTIR spectra of CBL loaded with hibiscus leaves extract. Pure bigels CSB and CBL (A) and CBL with SFE and PLE extracts (B).

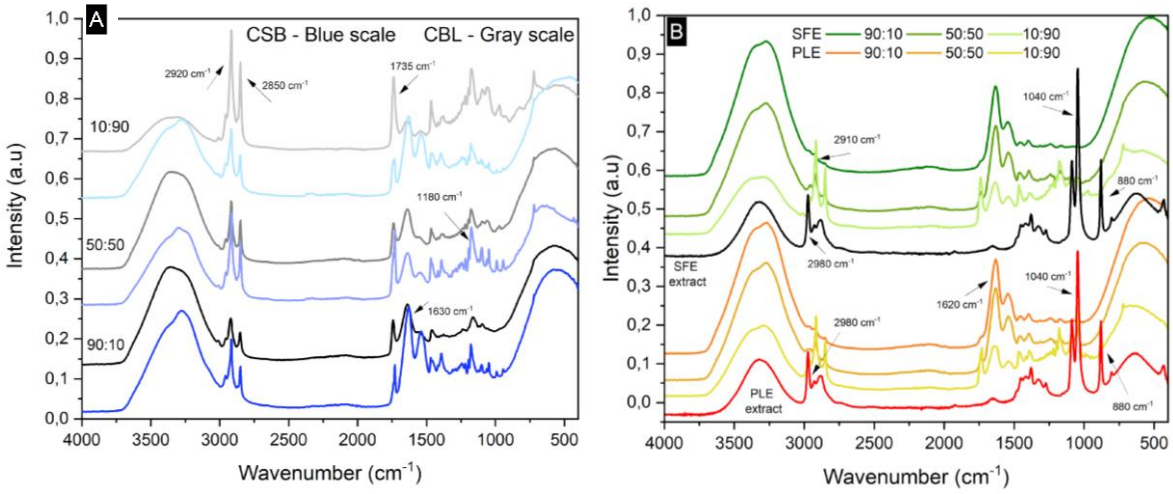

Microscopy and confocal images showed differences between the formulations (Figure 6.3), in which the oil droplets increase proportionally to the amount of oil present. In the 90:10 system, the particles were well dispersed, uniformly distributed in an O/W structure. For pure bigels, 50:50 system shows an increase in the number of the particles, and in 10:90 it is possible to visualize a different formation, where the oil is the continuous phase (W/O structure), and the aqueous network presents coalescence between water molecules. This phase conversion probably occurred due the inability of the system to stabilize the W/O emulsion during the cooling process, causing the oil droplets to coalesce until their total crystallization. Besides, the addition of lecithin promoted better structuring, especially in the 50:50 bigel, with smaller and more defined particles.

Figure 6.3. Microscopic images of cold-set bigel (CBS), bigel with lecithin (CBL) and confocal imagens (magnification of 63x) of bigels loaded with hibiscus leaves extract through SFE and PLE method.

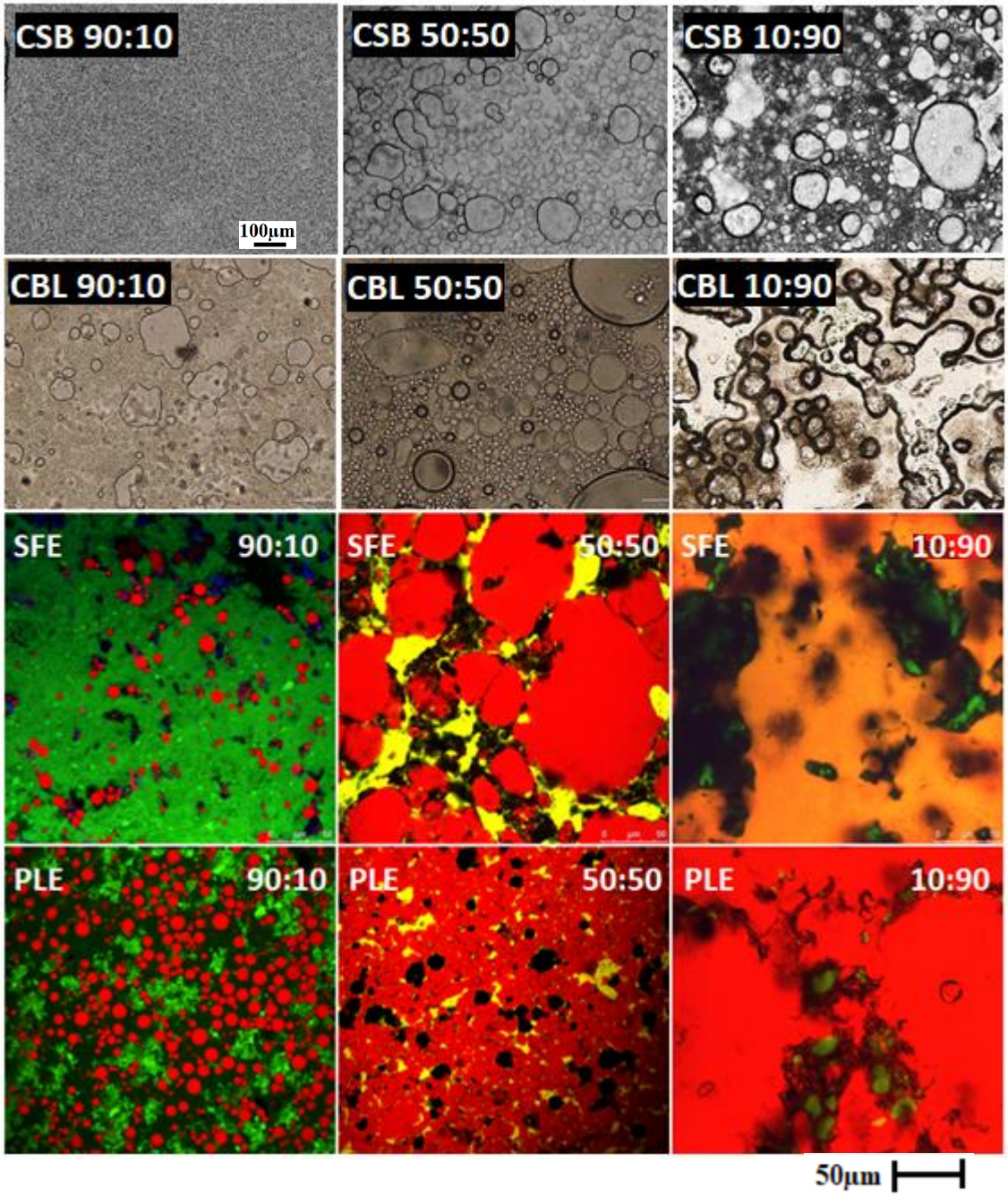

Regarding the confocal images, a similar behavior was observed, with an increase in the number of oil droplets directly proportional to the increase in oleogel. In addition, the presence of the extracts from hibiscus did not change the expected O/W structure, as also observed by Kulawik-Pióro et al. (2023) in the study of bigels with *Centella asiática* extract.

However, in the 50:50 formulation, the SFE bigel showed large particles, probably due to coalescence, differing from the PLE bigel, which had small particles and uniform distributed.

This difference may have occurred due to the composition of the extracts in relation to the type and amount of compounds present. The phenolic compounds, such as quercetin and chlorogenic acid, present in greater amounts in PLE extracts, can act in the oil-water surface, improving its structure during gelation (BABA; MCCLEMENTS; MAQSOOD, 2021; ZHAO; LI; XUE, 2023). This fact was also observed in the study of the interaction of epigallocatechin-gallate (EGCG) and caseins, in which the authors described the interaction of polyphenols with the protein, and also the changes in physical-chemical properties of the emulsions (SABOURI; GENG; CORREDIG, 2015).

The effects observed in microscopy directly reflects on the mechanical properties of the gels, in which the size and arrangement of the particles can weaken or strengthen the network. Observing Figure 6.4, it was noticed that for all pure bigels, the addition of lecithin strengthens the network, and along with the GM, could promote a better arrangement of the network. Besides, the W/O CBL 10:90, the system that have the greater percentage of oleogel, and consequently more lecithin, presented a more structured network, and consequently more resistant to deformation. Both GM and lecithin have excellent gelling capacity and the possibility of self-aggregating to form a three-dimensional network, but they have a different hydrophile-lipophile balance (HLB), being 3.8 and 7 respectively. This characteristic means that lecithin has more hydrophilic sites, thus allowing greater binding with water, while GM tends to be more soluble in oil, thus a balance between solubility and insolubility of the gelling agents can be a crucial factor for the formation of the gel and modification of mechanical properties (GHAN et al., 2022). On the other hand, CBL 90:10, O/W system didn't turn out to be much different than 50:50.

For CSB bigels 90:10 and 10:90, a rubber-like behavior was observed, with higher Young’s modulus, when compared with 50:50, that showed a squeezing gel behavior, probably due to a more disorganized structure. However, the addition of lecithin in the system 90:10 was not able to structure in way to enhance the resistance and present a rubber-like behavior, so this system and 50:50 present itself as a squeezing gel. In contrast, in system 90:10 there was a great increase in resistance to deformation, showing a better arrangement of the network, due to the properties of lecithin to act as a stabilizer at the water-oil interface (SAMUI et al., 2021), but no differences were observed in Young's modulus. Despite the observed differences in the gel formatted, the same behavior was repeated, where the increase of oleogel up to 50% caused a reduction in the gel rigidity, showing that the oil particles disrupted the continuity of the WPI network, but for proportions greater than 50%, with the changing the structure to W/O, the gel

recovers its resistance. This shows that despite the visible performance of lecithin, the hydrogel:oleogel ratio still exerts a great effect.

Figure 6.4. Effect of lecithin into cold-set bigels (CSB) and the incorporation of hibiscus leaf extract (SFE and PLE) in lecithin bigels (CBL) with different hidrogel:oleogel ratios. Maximum stress (A), strain at "breaking point" (B), Young Modulus (C) and Representative stress-strain behavior of bigels loaded with hibiscus leaves extract (D).

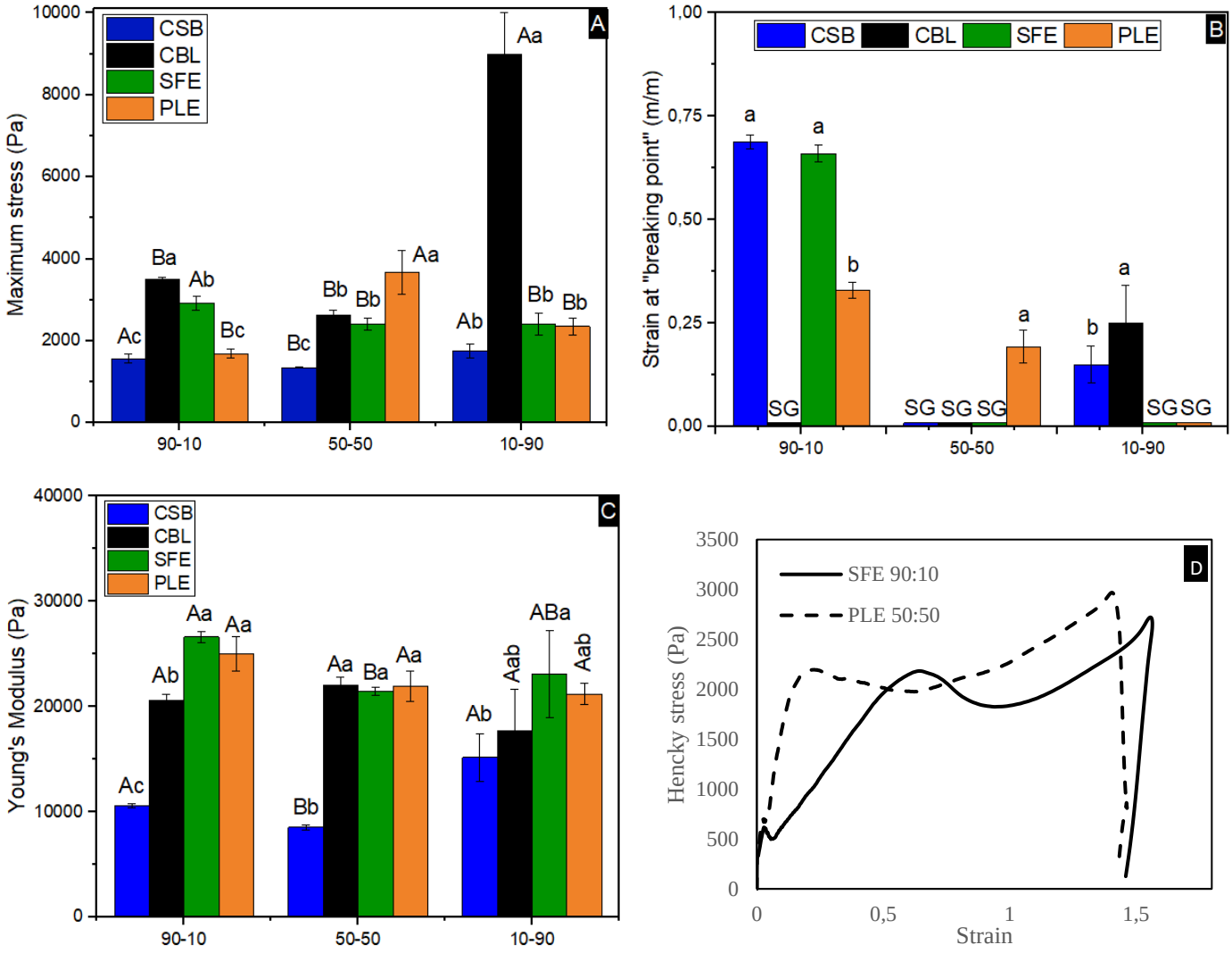

Values in the same set of bars (CSB, CBL, SFE or PLE) followed by different capital letters are significantly different by Tukey's test ($p < 0.05$); Values in the same ratio (90-10, 50-50, 10-90) followed by different lowercase letters are significantly different by Tukey's test ($p < 0.05$); SG: Squeezing gel.

Regarding the incorporation of hibiscus leaves extract in the bigel with lecithin, it was noticed that the amount encapsulated directly affects the structure. Starting from the point where the extract obtained by SFE is more concentrated, in relation to the content of phenolic compounds, a smaller amount was needed to reach the desired final concentration of bioactive, so the amount of extract available was too little to interact with the protein in a way that would

cause many changes in the maximum stress, what differs from bigels with PLE extract. However, the data show that the formulations 50:50 and 10:90 with SFE extracts behavior like a squeezing gel, differing from the pure bigels, that is, the increase in the amount of extract was not enough to maintain or strengthen the structure. For the bigels with PLE extracts, the opposite happened, the 90:10 and 50:50 systems had a rubber-like behavior, differing from the CBL, however, when the encapsulated amount was very high (10:90 system), the gel behaved like squeezing gel. In this case, the large amount of extract, and consequently the large amount of ethanol, may have impaired the bonds between oil molecules, thus making structuring difficult. Furthermore, the amount of protein available in this system for cross-linking with phenolic compounds was very low, so a lower structure than that observed for systems with more protein was expected.

Besides texture, hydrogel:oleogel ratio and the amount of hibiscus leaves extract also affect the rheological properties (Figure 6.5). Analyzing the role of lecithin during the temperature scanning, it was noticed, similarly to the texture analysis, that there was a strengthening of the network for the 50:50 and 10:90 systems and no effect on 90:10 formulation. Furthermore, the crystallization temperature, which was previously around 59°C, increased to 65°C with the addition of lecithin, which further demonstrates a better organized structure. So, at higher temperatures (>70 °C) the CBL 50:50 and 10:90 present almost fully structured network, with G' higher that G", with magnitude around 10 Pa. In addition, as the temperature is reduced, it was observed a more structured gel network, with G' higher. This behavior did not occur for bigel 90:10, which showed to be structured even at high temperatures, showing that the non-hydrophobic interactions are the main forces present in the stabilization of the protein. In addition, this increase in strength may be due to the stiffness imposed by hydrogen bonds and van der Waals forces due to temperature reduction, consequently promoting gel hardening during cooling (MCCLEMENTS; KEOGH, 1995).

Figure 6.5. Rheological properties of CBL with different hydrogel:oleogel ratios fractions during temperature sweep (cooling) tests. Pure bigels G' and G" Moduli (A), CBL Complex Modulus G* (B), CBL Tan delta (-) (C), G' and G" Moduli for SFE and PLE bigels (D), SFE and PLE bigels Complex Modulus G* (E), SFE and PLE bigels Tan delta (-) (F).

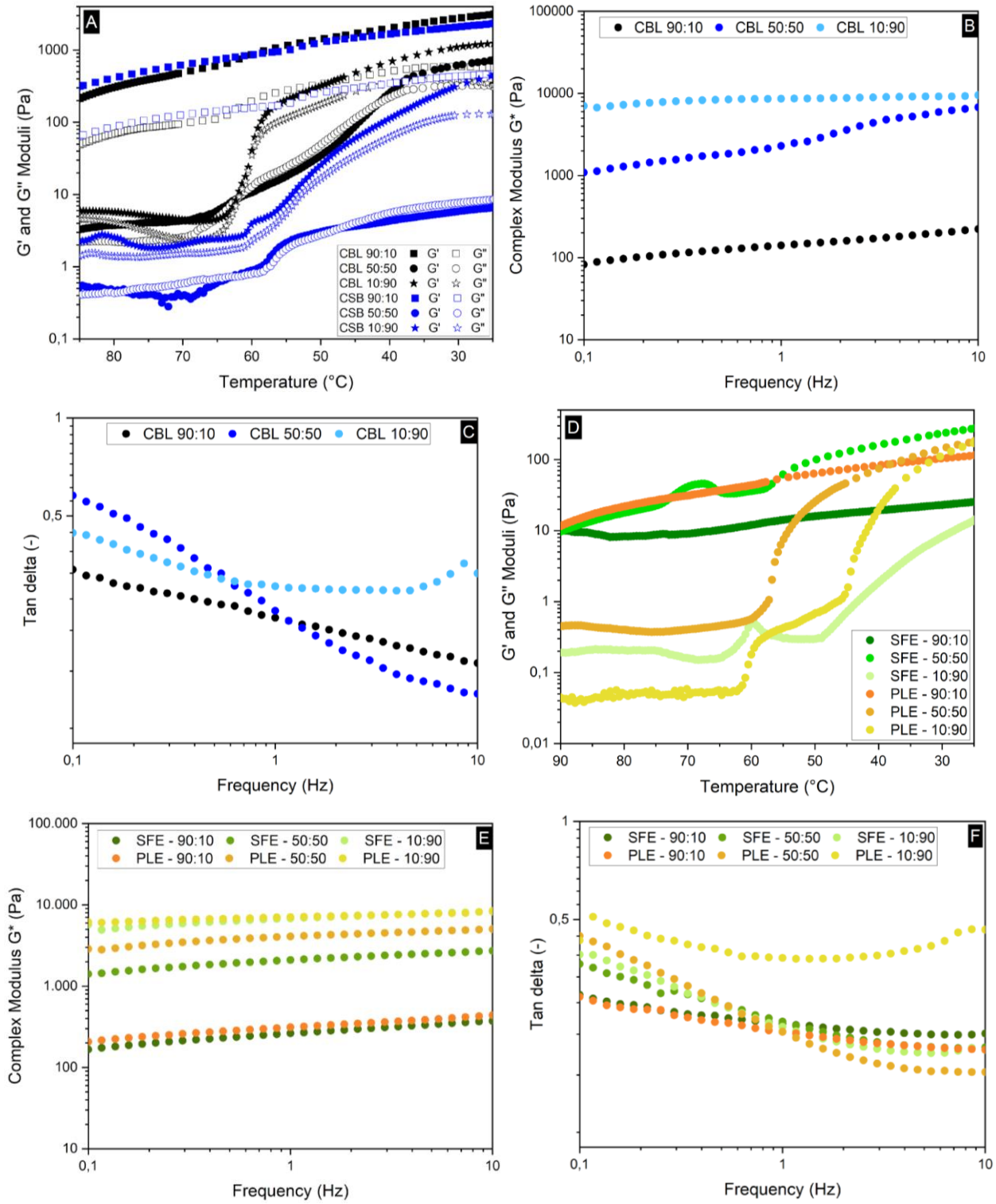

Moreover, the crystallization temperature is the same for all CBL, around 65 ºC, which goes according to Bollom; Clark & Acevedo (2020) in the lecithin-stearic acid and whey protein concentrate bigel, that state its crystallization temperature for 63ºC.

Regarding the incorporation of the extract, a texture-like behavior was observed, with a weakening of the gel network with the addition of hibiscus leaves extract, leading to a decrease in Modulus G*, and significant differences were observed in relation to each extract. For SFE extracts, formulations 90:10 and 50:50 behave like a solid, with a better arrangement of the gel network, as observed in the microscopy (Figure 6.3) and texture analyses (Figure 6.4), where there were no statistical differences between these systems for the maximum stress. For PLE extracts, as expected, the formulation 90:10 had a better arrangement than 50:50, as also observed in microscopy.

In relation to release kinetics, the bigel 10:90 for both extracts were unable to release the compounds. In addition, the best release of phenolic compounds was observed in formulation 90:10 (Figure 6.6). The small particles dispersed in the matrix showed a large surface area available for the release of curcumin. In addition, the protein network has the ability to erode easily, thus facilitating the access of the solvent to the oil droplets.

Figure 6.6. Release profile of phenolic compounds loaded in CBL through ethanol solution 50 % (v/v).

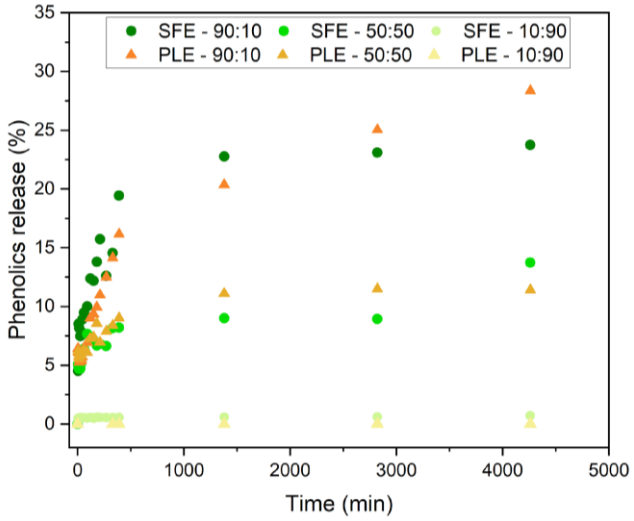

Observing Table 6.1, it was noticed that all tests showed $n<0.5$, in which the release rate by relaxation is greater than by diffusion. Besides, the model fitted well to data, with a $R^2 > 0.75$, indicating that this model was suitable to describe the release mechanisms of hibiscus leaves extract from bigels. Moreover, it is important to observe the constant that indicates the type of network formed (K). Higher values mean a more compact structure in the presence of

hydrophilic compounds, which lead to a greater physical restriction in the network, thus impairing the release (KATIME; MENDIZÁBAL, 2010). This factor was clearly observed in formulations with 50% or more of oleogel, which showed the lowest release rates of extracts.

Table 6.1. Experimental values of kinetics rate constant (K) and diffusion exponent (n) for CBL bigels load with hibiscus leaves extract.

Sample	RMSE	R^2	K	n
SFE – 90:10	0.096	0.92	0.224 ± 0.01	0.181 ± 0.008
SFE – 50:50	0.060	0.77	0.344 ± 0.03	0.103 ± 0.013
PLE – 90:10	0.066	0.91	0.181 ± 0.01	0.208 ± 0.011
PLE – 50:50	0.056	0.82	0.500 ± 0.02	0.084 ± 0.006

Figure 6.7 shows the bioaccessibility of phenolic compounds at the end of the *in vitro* digestion process, for the bigels with PLE and SFE extracts. For bigel with SFE extract, it was possible to observe a bioaccessibility of 46% for formulation 90:10, 14% for 50:50 and 1.5% for 10:90. On the other hand, for bigel with PLE extract the values were 82%, 6.5% and 2%, respectively. A similar result was observed in the study of bigels with elderflower (*Sambucus Nigra* L.) extract, in which the highest content of flavonoids was released from hydrophilic gels, and that the release rate decreases with increasing oleogel content in the system (RAMANAUSKIENE; INKENIENE; PUIDOKAITE, 2019).

Figure 6.7. Bioaccessibility of phenolic compounds loaded in CBL, after in vitro digestion process. Error bars represent the standard deviation of n = 3 replications.

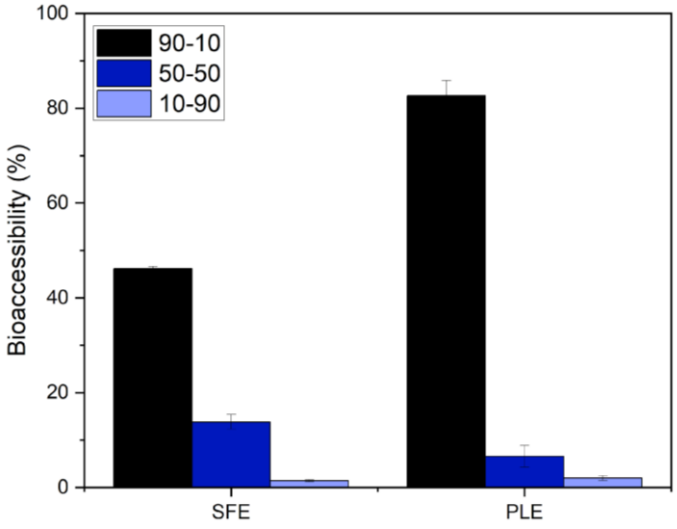

The highest percentage observed for formulation 90:10, in both extracts, may be related to arrangement of the network. In this case, the oil droplets are smaller, so they have a greater surface area, allowing greater lipase adhesion and interactions with bile salts, which consequently causes an increase in the production of micelles responsible for encapsulating the extract (GONÇALVES et al., 2021). In addition, in those systems where there is a greater amount of protein, the solvent was able to access the oil droplets better, as the protein matrix has this characteristic of being more easily eroded.

Another interesting detail observed in this system was the amount released from each extract, which was almost twice as high for the bigel with PLE extract. As previously mentioned, since the SFE extract is more concentrated a lower amount was sufficient to obtain the desired concentration of phenolic compounds. However, because the PLE extract was more diluted, it was better distributed within the matrix, as observed in the microscopy (Figure 6.3), that is, the greater number of drops, and consequently a greater surface area, favored the release.

For 50:50 system, a lower bioaccessibility was observed for both extracts, probably due to the bicontinuous structure, that was previously discussed, that impairs the release of the compounds (KODELA et al., 2017). Furthermore, in agreement with the simulant release results, the rigid structure of the 10:90 system prevented the release of bioactives.

6.4 CONCLUSION

The presence of lecithin and the incorporation of hibiscus leaf extracts showed considerable changes in the structure of bigels produced by cold gelation. The presence of lecithin caused changes in intensity of the peaks of XRD, probably due to the interaction with GM, which has a more crystalline characteristic. FTIR spectra showed some characteristic peaks of the extracts, evidencing the presence of physical and chemical interactions. Microscopy and confocal images show that the addition of lecithin promoted better structuring, especially in the 50:50 bigel, with smaller and more defined drops. The mechanical proprieties show that lecithin strengthened the network in all formulations, but the presence of extracts caused a weakening, perhaps due to the amount of ethanol present, which may have impaired the bonds during network formation. Regarding the release in food simulant and the gastro intestinal tract, a decreasing behavior was observed, with higher values for bigel 90:10, and PLE allowed a greater release when compared to SFE. Besides, no release was observed for 10:90 bigel, for both extracts. However, there are still few works that address the incorporation of plant extracts

in bigels, making it difficult to perceive the real influence that can be exerted on the 3D network, thus leaving a wide field for research.

REFERENCES

AHMADZADEH, F. et al. Pectin-sodium caseinate hydrogel containing olive leaf extract-nano lipid carrier: Preparation, characterization and rheological properties. LWT, v. 148, n. May, p. 111757, 2021.

ALVES, T. P. et al. Improved extraction of bioactive compounds from Monteverdia aquifolia leaves by pressurized-liquid and ultrasound-assisted extraction: Yield and chemical composition. The Journal of Supercritical Fluids, v. 181, n. March 2021, 2022.

BABA, W. N.; MCCLEMENTS, D. J.; MAQSOOD, S. Whey protein–polyphenol conjugates and complexes: Production, characterization, and applications. Food Chemistry, v. 365, p. 130455, dez. 2021.

BEHERA, B. et al. Physical and mechanical properties of sunflower oil and synthetic polymers based bigels for the delivery of nitroimidazole antibiotic – A therapeutic approach for controlled drug delivery. European Polymer Journal, v. 64, p. 253–264, 2015.

BOLLOM, M. A.; CLARK, S.; ACEVEDO, N. C. Development and characterization of a novel soy lecithin-stearic acid and whey protein concentrate bigel system for potential edible applications. Food Hydrocolloids, p. 105570, 2020.

BRYANT, C. M.; MCCLEMENTS, D. J. Influence of NaCl and CaCl2 on cold-set gelation of heat-denatured whey protein. Journal of Food Science, v. 65, n. 5, p. 801–804, 2000.

CAVALCANTI, R. N. et al. Supercritical fluid extraction with a modifier of antioxidant compounds from jabuticaba (*Myrciaria cauliflora*) by- products: economic viability. Procedia Food Science, v. 1, p. 1672–1678, 2011.

CERQUEIRA, M. A. et al. Structural and mechanical properties of organogels: Role of oil and gelator molecular structure. Food Research International, v. 96, p. 161–170, 2017.

CHEMAT, F. et al. Green extraction of natural products. Origins, current status, and future challenges. TrAC - Trends in Analytical Chemistry, v. 118, p. 248–263, 2019.

CHEN, Z.; SHI, Z.; MENG, Z. Development and characterization of antioxidant-fortified oleogels by encapsulating hydrophilic tea polyphenols. Food Chemistry, v. 414, p. 135664, 15 jul. 2023.

CLIMACO, G. N.; VARDANEGA, R.; FASOLIN, L. H. *Hibiscus sabdariffa* L. leaves as an alternative source of bioactive compounds obtained through high pressure technologies. The Journal of Supercritical Fluids, v. 200, n. May, p. 105968, 2023.

CVJETKO BUBALO, M. et al. New perspective in extraction of plant biologically active compounds by green solvents. Food and Bioproducts Processing, v. 109, p. 52–73, 2018.

DJOULLAH, A.; SAUREL, R. Controlled release of riboflavin encapsulated in pea protein microparticles prepared by emulsion-enzymatic gelation process. Journal of Food Engineering, v. 292, n. July 2020, 2021.

DO, N. H. N. et al. Encapsulation of *Triphasia trifolia* extracts by pH and thermal dual-sensitive chitosan hydrogels for controlled release. Carbohydrate Polymers, v. 320, n. May, p. 121264, 2023.

EUROPEAN, C. Commission Regulation of the European Parliament and of the Council as regards food category 17 and the use of food additives in food supplements. No 1333/2008 of 8 October 2018. Official Journal of the European Union, n. October, p. 20–30, 2018.

EUROPÉIA, C. Regulamento (UE) No 10/2011 da Comissão de 14 de Janeiro de 2011. Jornal Oficial das Comunidades Europeias, p. 1–89, 2011.

FASOLIN, L. H., PICONE, C. S. F., SANTANA, R. C., AND CUNHA, R. L. Production of hybrid gels from polysorbate and gellan gum. Food Research International, v. 54, n.1, p. 501–507. 2013.

FASOLIN, L. H. et al. Thermodynamic, rheological and structural properties of edible oils structured with lmogs: influence of gelator and oil phase. Food Structure, 2018.

FASOLIN, L. H. et al. Modulating process parameters to change physical properties of bigels for food applications. Food Structure, v. 28, n. June 2019, p. 100173, 2021.

GHAN, S. Y. et al. Palm Olein Organogelation Using Mixtures of Soy Lecithin and Glyceryl Monostearate. Gels, v. 8, n. 1, p. 30, 4 jan. 2022.

GONÇALVES, R. F. S. et al. Lipid-based nanostructures as a strategy to enhance curcumin bioaccessibility: Behavior under digestion and cytotoxicity assessment. Food Research International, v. 143, n. March, 2021.

HAZRATI, Z.; MADADLOU, A. Gelation by bioactives: Characteristics of the cold-set whey protein gels made using gallic acid. International Dairy Journal, v. 117, p. 104952, 2021.

IKEDA, S.; FOEGEDING, E. A. Effects of lecithin on thermally induced whey protein isolate gels. Food Hydrocolloids, v. 13, n. 3, p. 239–244, 1999.

JIANG, L. et al. Acid / alkali shifting of *Mesona chinensis* polysaccharide-whey protein isolate gels: Characterization and formation mechanism. Food Chemistry, v. 355, n. March, p. 129650, 2021.

KARAASLAN, N. M. A comprehensive study about Hibiscus sabdariffa leaves: antioxidant activity, polyphenol profile and macro- and micro-element content. Chemical Papers, v. 73, n. 4, p. 791–799, 2019.

KATIME, I.; MENDIZÁBAL, E. Swelling Properties of New Hydrogels Based on the Dimethyl Amino Ethyl Acrylate Methyl Chloride Quaternary Salt with Acrylic Acid and 2-Methylene Butane-1,4-Dioic Acid Monomers in Aqueous Solutions. Materials Sciences and Applications, v. 01, n. 03, p. 162–167, 2010.

KUHN, K. R.; CAVALLIERI, Â. L. F.; CUNHA, R. L. DA. Cold-set whey protein-flaxseed gum gels induced by mono or divalent salt addition. Food hydrocolloids, v. 25, n. 5, p. 1302–1310, 2011.

KULAWIK-PIÓRO, A.; OSAK, E.; MENDRYCKA, M. Bigels as novel systems for the delivery active compounds from *Centella asiatica*. Soft Materials, v. 00, n. 00, p. 1–23, 2023.

KUMAR, L. et al. Influence of whey protein isolate on pasting, thermal, and structural characteristics of oat starch. Journal of Dairy Science, v. 105, n. 1, p. 56–71, 2022.

LU, Y. et al. Structural Modification of O/W Bigels by Glycerol Monostearate for Improved Co-Delivery of Curcumin and Epigallocatechin Gallate. Food Science & Technology, v. 2, p. 975–983, 2022.

LUPI, F. R. et al. A rheological and microstructural characterization of bigels for cosmetic and pharmaceutical uses. Materials Science & Engineering C, v. 69, p. 358–365, 2016.

MACHADO, A. R. et al. Liposomes loaded with phenolic extracts of Spirulina LEB-18: Physicochemical characterization and behavior under simulated gastrointestinal conditions. Food Research International, v. 120, n. June 2018, p. 656–667, 2019.

MCCLEMENTS, D. J.; KEOGH, M. K. Physical properties of cold-setting gels formed from heat-denatured whey protein isolate. Journal of the Science of Food and Agriculture, v. 69, n. 1, p. 7–14, 1995.

MINEKUS, M. et al. A standardized static in vitro digestion method suitable for food-an international consensus. Food and Function, v. 5, n. 6, p. 1113–1124, 2014.

NUTTER, J. et al. Designing and characterizing multicomponent, plant-based bigels of rice bran wax, gums, and monoglycerides. Food Hydrocolloids, v. 138, n. December 2022, p. 108425, 2023.

PEDRALI, D.; BARBARITO, S.; LAVELLI, V. Encapsulation of grape seed phenolics from winemaking byproducts in hydrogel microbeads – Impact of food matrix and processing on the inhibitory activity towards α -glucosidase. LWT, v. 133, n. April, 2020.

PINHEIRO, A. C. et al. Towards the understanding of the behavior of bio-based nanostructures during in vitro digestion. Current Opinion in Food Science, v. 15, p. 79–86, 2017.

RAMANAUSKIENE, K.; INKENIENE, A. M.; PUIDOKAITE, E. Quality analysis of semisolid formulations with the liquid extract of elderflower (Sambucus Nigra L.). PHARMACEUTICAL TECHNOLOGY, v. 76, n. 6, p. 1061–1071, 2019.

RODRIGUES, R. M. et al. Effects of moderate electric fields on cold-set gelation of whey proteins – From molecular interactions to functional properties. Food Hydrocolloids, v. 101, n. November 2019, 2020.

SABOURI, S.; GENG, J.; CORREDIG, M. Tea polyphenols association to caseinate-stabilized oil–water interfaces. Food Hydrocolloids, v. 51, p. 95–100, 1 out. 2015.

SAGIRI, S. S. et al. Stearate organogel-gelatin Hydrogel based bigels: Physicochemical, thermal, mechanical characterizations and in vitro drug delivery applications. Journal of the Mechanical Behavior of Biomedical Materials, 2014.

SAMUI, T. et al. The development and characterization of novel in-situ bigel formulation. Food Hydrocolloids, v. 113, n. June 2020, p. 106416, 2021.

SARKAR, A.; GOH, K. K. T.; SINGH, H. Colloidal stability and interactions of milk-protein-stabilized emulsions in an artificial saliva. Food Hydrocolloids, v. 23, n. 5, p. 1270–1278, 2009.

SHAKEEL, A. et al. Key characteristics and modelling of bigels systems: A review. Materials Science & Engineering C, v. 97, n. February 2018, p. 932–953, 2019.

SHISHIR, M. R. I. et al. Advances in micro and nano-encapsulation of bioactive compounds using biopolymer and lipid-based transporters. Trends in Food Science & Technology, 2018.

SILVA, P. M. et al. Oleogels and bigels as alternatives to saturated fats: A review on their application by the food industry. JAOCS, Journal of the American Oil Chemists' Society, v. 99, n. 11, p. 911–923, 2022.

SIMÕES, L. S. et al. Suitability of β-lactoglobulin micro- and nanostructures for loading and release of bioactive compounds. Food Hydrocolloids, v. 101, n. November 2019, 2020.

SINGH, V. K. et al. Guar gum and sesame oil based novel bigels for controlled drug delivery. Colloids and Surfaces B: Biointerfaces, 2014a.

SINGH, V. K. et al. Preparation and characterization of novel carbopol based bigels for topical delivery of metronidazole for the treatment of bacterial vaginosis. Materials Science and Engineering C, v. 44, p. 151–158, 2014b.

SINGH, V. K. et al. Bigels. Polymeric Gels, p. 265–282, 2018.

SINGLETON, V. L.; ORTHOFER, R.; LAMUELA-RAVENTÓS, R. M. Analysis of Total Phenols and Other Oxidation Substrates and Antioxidants by Means of Folin-Ciocalteu reagent. Polyphenols and Flavonoids, v. 299, n. 1974, p. 152–178, 1999.

SOUZA, A. R. C. DE et al. Assessment of composition and biological activity of *Arctium lappa* leaves extracts obtained with pressurized liquid and supercritical CO2 extraction. The Journal of Supercritical Fluids, v. 152, p. 104573, 2019.

SUBHASWARAJ, P. et al. Determination of antioxidant activity of *Hibiscus sabdariffa* and *Croton caudatus* in *Saccharomyces cerevisiae* model system. Journal of Food Science and Technology, v. 54, n. 9, p. 2728–2736, 2017.

TAIB, S. H. M. et al. Electrooxidation of nitrite based on green synthesis of gold nanoparticles using *Hibiscus sabdariffa* leaves. Journal of the Taiwan Institute of Chemical Engineers, v. 95, p. 616–626, 2019.

TRUJILLO-RAMÍREZ, D. et al. Cooling rate, sorbitan and glyceryl monostearate gelators elicit different microstructural, viscoelastic and textural properties in chia seed oleogels. Food Research International, n. October, p. 0–1, 2018.

VARDANEGA, R. et al. Selective extraction of bioactive compounds from annatto seeds by sequential supercritical CO_2 process. The Journal of Supercritical Fluids, v. 150, p. 122–127, 2019.

VEGGI, P. C.; CAVALCANTI, R. N.; MEIRELES, M. A. A. Production of phenolic-rich extracts from Brazilian plants using supercritical and subcritical fluid extraction: Experimental data and economic evaluation. Journal of Food Engineering, v. 131, p. 96–109, 2014.

VERGARA, D. et al. Povidone-iodine loaded bigels: Characterization and effect as a hand antiseptic agent. Journal of Drug Delivery Science and Technology, v. 72, n. November 2021, 2022.

WANG, J. et al. Antioxidant activity of leaf extracts from different Hibiscus Sabdariffa accessions and simultaneous determination five major antioxidant compounds by LC-Q-TOF-MS. Molecules, v. 19, n. 12, p. 12226–12238, 2014.

WANG, Y. et al. Interaction between whey protein isolate and rose anthocyanin extracts at different pHs: Structure, emulsification and digestibility of complexes. Food Bioscience, v. 49, n. July, p. 101888, 2022.

XIE, D. et al. Development and characterization of food-grade bigel system for 3D printing applications: Role of oleogel / hydrogel ratios and emulsifiers. Food Hydrocolloids, v. 139, n. September 2022, p. 108565, 2023.

ZHAI, X. et al. Anthocyanins-encapsulated 3D-printable bigels: A colorimetric and leaching-resistant volatile amines sensor for intelligent food packaging. Food Hydrocolloids, v. 133, n. March, p. 107989, 2022.

ZHAO, X.; LI, C.; XUE, F. Effects of whey protein-polyphenol conjugates incorporation on physicochemical and intelligent pH-sensing properties of carboxymethyl cellulose based films. Future Foods, v. 7, p. 100211, jun. 2023.

ZHANG, T. et al. Effect of soy lecithin concentration on physiochemical properties and rehydration behavior of egg white protein powder: Role of dry and wet mixing. Journal of Food Engineering, v. 328, n. December 2021, p. 111062, 2022.

ZHEN, J. et al. Phytochemistry, antioxidant capacity, total phenolic content and anti-inflammatory activity of Hibiscus sabdariffa leaves. Food Chemistry, v. 190, p. 673–680, 2016.

ZHENG, H. et al. Development of food-grade bigels based on κ-carrageenan hydrogel and monoglyceride oleogels as carriers for β-carotene: Roles of oleogel fraction. Food Hydrocolloids, v. 105, n. February, p. 105855, 2020.

ZHU, Q. et al. Development and characterization of novel bigels based on monoglyceride-beeswax oleogel and high acyl gellan gum hydrogel for lycopene delivery. Food Chemistry, v. 365, n. December 2020, p. 130419, 2021.

SUPLEMENTARY MATERIAL

Figure 6.1S. Macroscopic images of lecithin cold-set bigels (CBL) with different hydrogel:oleogel ratios, CBL1 - 90:10 (A), CBL2 - 50:50 (B), CBL3 - 90:10 (C)

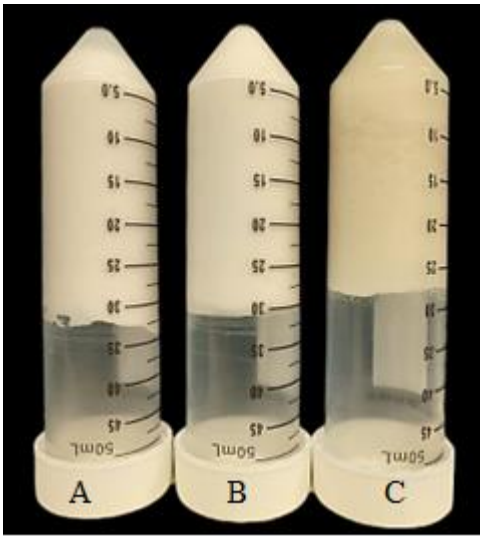

CAPÍTULO 7.
DISCUSSÃO E CONCLUSÕES GERAIS

7. DISCUSSÃO E CONCLUSÕES GERAIS

7.1 DISCUSSÃO

Os resultados discorridos mostram que as folhas de hibisco são uma fonte potencial de compostos bioativos, apresentando rendimentos comparáveis ou superiores aos observados para cálices e flores de hibisco ou mesmo para outras matrizes vegetais reconhecidas por serem fontes de fitoquímicos. Além disso, ambas tecnologias, SFE e PLE, foram eficientes na obtenção de extratos ricos em compostos que podem ser utilizados pelas indústrias alimentícia, farmacêutica e cosmética. Essas tecnologias podem ser empregadas como uma alternativa às tecnologias convencionais, pois além de possibilitarem a utilização de outros solventes não nocivos ao ser humano e meio ambiente, economizarem tempo e consequentemente energia, ainda apresentaram maior recuperação para todos os compostos avaliados (fenólicos totais, taninos e flavonoides) em comparação à maceração.

Além da presença de diferentes classes de compostos, foi possível identificar ácido clorogênico e quercetina, por HPLC. Entretanto, comparando os dois métodos de extração, o SFE permitiu um melhor resultado em termos de teor de compostos, pois resultou em extratos mais concentrados. Porém, em termos de rendimento de compostos o PLE foi superior, permitindo a recuperação de uma maior quantidade de compostos da matéria-prima, demandando menos tempo e solvente.

Em relação aos bigéis, tanto os métodos de gelificação cold-set e heat-set, quanto a relação hidrogel:olegel levaram a diferentes organizações estruturais e exerceram efeito sobre as propriedades mecânicas. A formulação 90:10, para ambos os métodos, mostrou uma fase dispersa de oleogel muito bem definida e uma estrutura de “favo de mel” de proteína semelhante a hidrogéis puros. No entanto, o oleogel não formou partículas isoladas, em vez disso, elas se interconectam e se entrelaçam na rede de proteínas como parte da estrutura. Com isso, provocaram um efeito negativo nas propriedades mecânicas, que causou uma redução mais pronunciada na resistência do gel, até concentração de oleogel até 50:50, mas o CSB conseguiu manter a estrutura O/W, enquanto o HSB apresentou uma rede mais desorganizada, com gotículas de diferentes tamanhos e expressiva coalescência. Esse fator pode ter sido causado pela alta temperatura, que atua na redução da tensão interfacial e viscosidade da fase contínua, permitindo a coalescência das gotas e a desestabilização da emulsão.

Para concentração de oleogel acima de 50:50, o bigel mudou para estruturas A/O. No entanto, apenas o CSB ainda apresentava uma estrutura organizada. Portanto, pode-se dizer que as diferenças estruturais foram estritamente relacionadas ao mecanismo de gelificação da proteína, uma vez que o processo de resfriamento desencadeia o processo de cristalização, evitando um alto grau de coalescência, que permitiu serem observadas estruturas O/A ou A/O bem definidas.

Assim, constatou-se que os diferentes métodos de gelificação permitem modular a estrutura e consequentemente as propriedades mecânicas dos bigéis formulados com WPI. Dito isso, optou-se por seguir o estudo apenas com o método de gelificação a frio das proteínas, para avaliar o efeito da incorporação de diferentes compostos nas propriedades dos bigéis.

A incorporação de compostos modelos (curcumina e riboflavina) apresentara mudanças consideráveis na estrutura dos bigéis produzidos por gelificação à frio. Os espectros de DRX mostraram um pico muito amplo, indicando que os bigéis possuem uma estrutura não cristalina quando comparados aos oleogéis, o que é típico de materiais amorfos. A presença da riboflavina aumentou levemente a intensidade, enquanto a curcumina diminuiu, mas o efeito dos dois compostos juntos promoveu uma grande redução na intensidade, mostrando que existe efeito sinergético entre os compostos. O FTIR mostrou que o arranjo entre as fases hidrogel e oleogel foi puramente físico. No entanto, a adição dos compostos resultou no aparecimento de alguns picos, característicos dos compostos, evidenciando interações químicas entre os compostos.

As imagens de microscopia mostraram um aumento das gotas de óleo proporcionalmente à quantidade de oleogel, com gotas coalescentes no bigel 50:50 e uma rede predominantemente oleosa no bigel 10:90, devido a uma conversão da estrutura de óleo em água (O/A) para água em óleo (A/O), que afetou diretamente as propriedades mecânicas. Os bigéis com os compostos isolados, tiveram uma melhora na rede do gel, tornando-a mais estruturada, de acordo com a fase que está sendo adicionada, provavelmente devido a interação dos compostos com a proteína, que favoreceram uma melhor estruturação. A riboflavina, quando exposta à luz, reagem com as moléculas de proteínas, formando ligações covalentes que provocam aumento de resistência e rigidez. Já a curcumina, apesar de mostrar menor efeito, também pode ter interagido com a proteína, melhorando as ligações intramoleculares, aumentando a rigidez do sistema.

Durante os testes de liberação não foi observada liberação de curcumina em simulador com etanol a 10%, pois, devido à sua natureza lipofílica, é difícil particioná-la em soluções aquosas. O mesmo comportamento foi observado para a riboflavina no simulador de etanol

50%. A curcumina teve uma recuperação de quase 80% em etanol 50% e esta quantidade diminuiu com o aumento do oleogel no sistema, provavelmente devido a formação da estrutura O/A no bigel 90:10. Nessa formulação as partículas de óleo estão dispersas na matriz e apresentam grande área superficial disponível para liberação. Porém, quando a estrutura é bicontínua ou o óleo se torna a fase contínua, a área superficial é drasticamente reduzida. A riboflavina teve melhor recuperação para bigel 90:10 (20%). Neste sistema foi observada migração da riboflavina para o oleogel, facilitando a liberação quando comparado ao sistema 50:50. De modo geral, conforme observado na análise de microestrutura e textura, a riboflavina liga-se fortemente à rede proteica, fortalecendo a estrutura e consequentemente não ficando disponível para ser liberada. No entanto, quando a curcumina e a riboflavina foram veiculadas simultaneamente, algumas diferenças foram observadas.

Em relação à bioacessibilidade, a curcumina apresentou valores iguais para bigels 90:10 e 10:90. Esse comportamento pode estar correlacionado com a estrutura na qual foi encapsulada, pois para um sistema O/A, as partículas de óleo eram menores e com maior área superficial, mas para o sistema A/O, a maior área de contato permitiu a adesão da lipase na fase oleosa além de interagir com sais biliares. e a riboflavina, apresentou bioacessibilidade decrescente, com valores menores para bigel 90:10, provavelmente devido a interação com a proteína, como comentado anteriormente.

A partir destes resultados, de forma a melhorar a rede de gel para incorporação dos extratos da folha do hibisco, decidiu-se incorporar também lecitina de soja, pois devido sua ação direta da interface água-óleo, poderia provocar melhorias na rede de gel. Assim, de posse dos resultados, percebeu-se que tanto a utilização de lecitina como a incorporação de extratos de folhas de hibisco apresentaram alterações consideráveis na estrutura dos bigels produzidos por gelificação a frio.

A lecitina provocou mudanças na intensidade dos picos, provavelmente devido a interação com o GM, que tem característica cristalina. Em relação à adição dos extratos, não houve deslocamento ou aparecimento de novos picos, mas o SFE provocou redução na intensidade, principalmente para o sistema 90:10, enquanto que o PLE provocou aumento na intensidade para os sistemas 50:50 e 90:10. O FTIR mostrou que o papel dos *fillers* (hidrogel e oleogel) foi puramente físico. No entanto, a adição dos extratos resultou no aparecimento de alguns picos diferentes, evidenciando interações químicas.

As imagens de microscopia mostraram um aumento das gotas de óleo proporcionalmente à quantidade de oleogel, porém, a lecitina promoveu uma melhor

estruturação no bigel 50:50, com gotas de diferentes tamanhos, mas bem definidas. Já o bigel 90:10 se mostrou uma rede predominantemente oleosa, devido a uma conversão da estrutura de óleo em água (O/A) para água em óleo (A/O). Essas diferenças nos sistemas afetaram diretamente as propriedades mecânicas. A lecitina provocou uma grande estruturação da rede, quando comparado aos bigéis sem lecitina, principalmente para o bigel 10:90, pois agiu juntamente com GM na estabilização da interface água-óleo. Entretanto, a adição dos extratos afetou negativamente a resistência à deformação, provavelmente devido a interações entre os compostos presentes. Comportamento similar foi observado nos ensaios de reologia, onde a lecitina proporcionou uma melhor estruturação da rede, porém a adição dos extratos provocou enfraquecimento da rede.

Em relação à liberação de compostos fenólicos, a melhor estrutura continua sendo o sistema 90:10, como também foi observado para os compostos modelos, com maior liberação para os bigéis com extratos de PLE, provavelmente devido a forma menos concentrada na qual foram encapsulados. Para bioacessibilidade, o comportamento se repete, com melhor recuperação para o sistema 90:10 dos bigéis com extrato de PLE.

7.2 CONCLUSÕES GERAIS

Os resultados do presente estudo demonstram que as folhas de hibisco são uma fonte potencial de compostos bioativos, apresentando rendimentos comparáveis ou superiores aos observados para cálices e flores de hibisco ou mesmo para outras matrizes vegetais. Ambas as tecnologias SFE e PLE foram eficientes na obtenção de extratos ricos em compostos, com máximos nas condições de 60 ºC, 100 bar e 15% de etanol para SFE e 80 ºC e 99,5% de etanol para PLE. Além disso, o SFE permitiu um melhor resultado em termos de teor de compostos, pois resulta em extratos mais concentrados, mas em termos de rendimento de compostos o PLE foi superior, permitindo a recuperação de uma maior quantidade dos compostos, exigindo menos tempo e solvente. Em relação a produção dos bigéis, tanto os métodos de gelificação cold-set e heat-set, quanto a relação hidrogel:olegel levaram a diferentes organizações estruturais e exerceram efeito sobre as propriedades mecânicas. Os bigéis produzidos à quente resultaram em géis de ruptura com maior módulo de elasticidade, enquanto os produzidos à frio foram mais elásticos e não apresentaram ruptura. Dito isso, optou-se por seguir o estudo apenas com o método de gelificação a frio das proteínas, para avaliar o efeito da incorporação de diferentes compostos nas propriedades dos bigéis. A incorporação de compostos modelos (curcumina e riboflavina)

apresentara mudanças consideráveis na estrutura dos bigéis produzidos por gelificação à frio. Foi observado conversão da estrutura de óleo em água (O/A) para água em óleo (A/O), e uma melhor estruturação da rede do gel, quando incorporado os compostos insolados. Estes fatores afetaram diretamente a liberação em simultante alimentar e no trato gastrointestinal, que apresentaram resultados semelhantes, com melhor liberação para o sistema 90:10. A partir destes resultados, decidiu-se incorporar também lecitina de soja, justamente com os extratos da folha do hibisco, e percebeu-se que ambos provocaram alterações consideráveis na estrutura dos bigels produzidos por gelificação a frio. A lecitina provocou grande estruturação da rede, enquanto que os extratos a enfraqueceram. Além disso, similar a incorporação dos compostos modelos, a liberação dos compostos fenólicos em simulante alimentar e no trato gastrointestinal foi melhor observada no sistema 90:10, com maior liberação para os bigéis com extratos de PLE.

7.3 SUGESTÃO PARA TRABALHOS FUTUROS

- Avaliar o efeito do micro-ondas na extração de compostos bioativos da *Hibiscus Sabdariffa* L.
- Avaliar a atividade antioxidante dos extratos através de diferentes métodos, objetivando delinear o perfil antioxidante mais completo da matriz;
- Realizar uma avaliação econômica dos processos de extração com alta pressão, bem como o micro-ondas, para estimar os custos de manufatura dos extratos obtidos;
- Avaliar a encapsulação de diferentes concentrações de compostos modelos, de forma a avaliar os efeitos na rede de gel formada;
- Avaliar a encapsulação dos extratos do hibisco na forma de pó, ou solubilizados em outro solvente que não seja o etanol, para facilitar uma futura aplicação;
- Avaliar a toxicidade dos bigéis produzidos os extratos do hibisco;
- Produção de um molho tipo maionese com incorporação do bigel com extrato do hibisco e avaliação das propriedades reológicas e vida de prateleira.

7.4 MEMÓRIA DO DOUTORADO

Apesar dos percalços enfrentados durante a pandemia, foi possível a realização de várias atividades que só engrandeceram minha experiência como aluna de doutorado. A primeira, no

ano de 2020, foi a participação no 14º SLACA – Simpósio Latino Americano de Ciência de Alimentos, com apresentação do trabalho "Quantificação de compostos bioativos da *Hibiscus sabdariffa* L. extraídos por tecnologia supercrítica", na qual pude explicar um pouco sobre a extração com fluido supercrítico, bem como os primeiros resultados obtidos. Ainda no mesmo ano tive a oportunidade de participar como PED (Programa de Estágio Docente) da matéria Mecânica dos Materiais, no semestre 2S/2020, sob orientação dos Professores Dr. Carolina Picone e Dr. Luiz Henrique Fasolin. Além disso, este período foi dedicado à finalização das disciplinas obrigatórias e escrita da revisão bibliográfica, pois devido a pandemia, os laboratórios ficaram fechados para utilização até dezembro deste ano.

No ano de 2021 pude dar início aos experimentos, começando pela extração dos compostos bioativos da folha do *Hibiscus Sabdariffa* L. que deu origem ao meu primeiro artigo, em parceria com a Dr. Renata Vardanega, intitulado "*Hibiscus sabdariffa* L. leaves as an alternative source of bioactive compounds obtained through high pressure technologies" publicado na revista *Journal of Supercritical Fluids*.

No ano seguinte, os trabalhos foram concentrados no desenvolvimento do bigel, bem como na avaliação de suas propriedades. Este trabalho deu origem ao meu segundo artigo, intitulado "Effect of the gelling mechanism on the physical properties of bigels formulated with glycerol monostearate + sunflower oil and whey protein isolated", que foi submetido da revista *Food Research International*. Além disso, tive a oportunidade de atuar como coorientadora da aluna Tathiane Marx Sequinho, estudante do curso de graduação em Engenharia de Alimentos (FEA-UNICAMP) durante a realização do trabalho de Iniciação Científica "Avaliação de géis mistos para veiculação de bioativos em sistemas alimentares". Colaborei novamente como PED da matéria Mecânica dos Materiais, no semestre 1S/2022, sob orientação dos mesmos professores. Por fim, participei da seleção do Print/CAPES, que me permitiu realizar um intercâmbio de seis meses em Braga - Portugal, no laboratório do Professor Dr. Antônio Vicente, para concretização da última parte do meu doutorado, que foi a avaliação da digestibilidade dos bigéis veiculados com os compostos modelos (curcumina e riboflavina) e com os extratos da folha do hibisco.

Em 2023, tive a incrível oportunidade de participar do "SAKURA SCIENCE Exchange Program", em Kumamoto – Japão, organizado pelo *Japan Science and Technology Agency*, em nome do Professor Dr. Armando Quitain. Nessa experiência pude apresentar um pouco o Brasil e a FEA, bem como meu trabalho desenvolvido na primeira parte do doutorado, que ia de

encontro com o tema do evento “3rd International Symposium on Green Chemistry and Engineering”.

Nesse intermédio, participei do desenvolvimento do capítulo “Rheology and Texture Analysis” no livro "Fat Mimetics for Food Applications", em parceria com Dr. Miguel Cerqueira e Lorenzo Pastrana. Dando seguimento, parte do meu trabalho sobre os bigéis, foi apresentado no CIPCA - IX Conferência Internacional de Proteínas e Coloides Alimentares, realizado nos dias 9 a 11 de maio, no Rio de Janeiro, e outra parte envolvendo a encapsulação da curcumina, foi apresentado no ICEF 14 – International Congress on Engineering and Food, realizado nos dias 20 a 23 de junho, em Nantes – França.

Por fim, meus últimos 2 trabalhos, que discorrem sobre o efeito dos compostos modelos e dos extratos do hibisco na estrutura dos bigéis e na digestibilidade, que finalizam esses 4 anos de estudo estão em fase de finalização, e serão publicados em 2024.

CAPÍTULO 8.
REFERÊNCIAS GERAIS

8. REFERÊNCIAS

A.S. of A.E. ASAE, ASAE Standards: Standards, Engineering Practices and Data Adopted by the American Society of Agricultural Engineers, American Society of Agricultural Engineers, 1993. https://books.google.com.br/books?id=GrYdAQAAMAAJ.

AGREGÁN, R. et al. Recent advances in the extraction of polyphenols from eggplant and their application in foods. LWT, v. 146, n. March, p. 111381, 2021.

AHANGARI, H. et al. Supercritical fluid extraction of seed oils – A short review of current trends. Trends in Food Science and Technology, v. 111, n. February, p. 249–260, 2021.

AHEARNE, M.; COYLE, A. Application of UVA-riboflavin crosslinking to enhance the mechanical properties of extracellular matrix derived hydrogels. Journal of the Mechanical Behavior of Biomedical Materials, v. 54, p. 259–267, 2016.

AHMADZADEH, F. et al. Pectin-sodium caseinate hydrogel containing olive leaf extract-nano lipid carrier: Preparation, characterization and rheological properties. LWT, v. 148, n. May, p. 111757, 2021.

ALAÑÓN, M. et al. A novel sustainable approach for the extraction of value-added compounds from Hibiscus sabdariffa L. calyces by natural deep eutectic solvents. Food Research International, v. 137, September, 2020.

ALARA, O. R.; ABDURAHMAN, N. H.; UKAEGBU, C. I. Extraction of phenolic compounds: A review. Current Research in Food Science, v. 4, n. March, p. 200–214, 2021.

ALEXANDRE, E. M. C. et al. Emerging technologies to extract high added value compounds from fruit residues: Sub/supercritical, ultrasound-, and enzyme-assisted extractions. Food Reviews International, v. 34, n. 6, p. 581–612, 2018.

ALVES, T. P. et al. Improved extraction of bioactive compounds from Monteverdia aquifolia leaves by pressurized-liquid and ultrasound-assisted extraction: Yield and chemical composition. The Journal of Supercritical Fluids, v. 181, n. March 2021, 2022.

AMORIM, E.L.C. et al. A simple and accurate procedure for the determination of tannin and flavonoid levels and some applications in ethnobotany and ethnopharmacology. Functional Ecosystems and Communities, v. 2, n. 1, p. 88–94, 2008.

ANDRADE, T. A. et al. Ultrasound-assisted pressurized liquid extraction of anthocyanins from Aronia melanocarpa pomace. Separation and Purification Technology, v. 276, n. April, 2021.

ANDREU, V.; PICÓ, Y. Pressurized liquid extraction of organic contaminants in environmental and food samples. TrAC - Trends in Analytical Chemistry, v. 118, p. 709–721, 2019.

ANWAR, Z. et al. Photochemical preparation, characterization and formation kinetics of riboflavin conjugated silver nanoparticles. Journal of Molecular Structure, v. 1289, p. 135863, 2023.

BABA, W. N.; MCCLEMENTS, D. J.; MAQSOOD, S. Whey protein–polyphenol conjugates and complexes: Production, characterization, and applications. Food Chemistry, v. 365, p. 130455, 2021.

BABAEI, J., KHODAIYAN, F., MOHAMMADIAN, M., AND SHEIKHI, M. (2022). In vitro digestibility and functional attributes of the whey protein heat-induced hydrogels reinforced by various polysaccharides and CaCl2. Journal of Food Measurement and Characterization, v. 16, n.1, p. 19–28, 2022.

BALOGUN, M. E. et al. Ameliorative effect of aqueous extract of hibiscus sabdariffa (roselle) on salt-induced hypertension in wistar rats. Pharmacology OnLine, v. 2, n. August, p. 247–258, 2019.

BARBA, F.J. et al. Green alternative methods for the extraction of antioxidant bioactive compounds from winery wastes and by-products: A review. Trends Food Sci. Technol. 2016.

BARBOSA, A. M. et al. Separation and Purification Technology Separation of antibacterial biocompounds from Hancornia speciosa leaves by a sequential process of pressurized liquid extraction. Separation and Purification Technology, v. 222, p. 390–395, 2019.

BARRECA, D. et al. Food flavonols: Nutraceuticals with complex health benefits and functionalities. Trends in Food Science and Technology. 2021.

BASTANTE, C. C. et al. Characterization of olive leaf extract polyphenols loaded by supercritical solvent impregnation into PET / PP food packaging films. The Journal of Supercritical Fluids, v. 140, p. 196–206, 2018.

BEHERA, B. et al. Physical and mechanical properties of sunflower oil and synthetic polymers based bigels for the delivery of nitroimidazole antibiotic – A therapeutic approach for controlled drug delivery. European Polymer Journal, v. 64, p. 253–264, 2015.

BENDIF, H., et al. Essential oils (EOs), pressurized liquid extracts (PLE) and carbon dioxide supercritical fluid extracts (SFE-CO2) from Algerian Thymus munbyanus as valuable sources of antioxidants to be used on an industrial level. Food Chem. v. 260, p. 289–298, 2018.

BERMEJO, D. V. et al. High catechins/low caffeine powder from green tea leaves by pressurized liquid extraction and supercritical antisolvent precipitation. Separation and Purification Technology, v. 148, p. 49–56, 2015.

BOLLOM, M. A.; CLARK, S.; ACEVEDO, N. C. Development and characterization of a novel soy lecithin-stearic acid and whey protein concentrate bigel system for potential edible applications. Food Hydrocolloids, p. 105570, 2020.

BOTELHO, J. R. S. et al. Copaíba (Copaifera sp.) leaf extracts obtained by CO2 supercritical fluid extraction: Isotherms of global yield, kinetics data, antioxidant activity and neuroprotective effects. The Journal of Supercritical Fluids, 2014.

BOU, R.; COFRADES, S.; JIM, F. Physicochemical properties and riboflavin encapsulation in double emulsions with different lipid sources. LWT - Food Science and Technology, v. 59, p. 621–628, 2014.

BOURBON, A. I.; CERQUEIRA, M. A.; VICENTE, A. A. Encapsulation and controlled release of bioactive compounds in lactoferrin- glycomacropeptide nanohydrogels: curcumin and caffeine as model compounds. Journal of Food Engineering, 2016.

BRYANT, C. M., AND MCCLEMENTS, D. J. Molecular basis of protein functionality with special consideration of cold-set gels derived from heat-denatured whey. Trends in Food Science & Technology, v. 9, n. 4, p. 143-151, 1998.

BRYANT, C. M., AND MCCLEMENTS, D. J. Influence of NaCl and CaCl2 on cold-set gelation of heat-denatured whey protein. Journal of Food Science. v. 65, n. 5, p. 801–804, 2000.

CADENA-CARRERA, S. et al. Biological activity of extracts from guayusa leaves (Ilex guayusa Loes.) obtained by supercritical CO2 and ethanol as cosolvent. The Journal of Supercritical Fluids, v. 152, 2019.

CARRILLO-NAVAS, H. et al. Inertial effects of adsorbed glycerol monostearate crystals on the shear rheology of water / canola oil interfaces. Journal of Food Engineering, v. 125, p. 112–118, 2014.

CAVALCANTI, R. N. et al. Supercritical fluid extraction with a modifier of antioxidant compounds from jabuticaba (Myrciaria cauliflora) by- products: economic viability. Procedia Food Science, v. 1, p. 1672–1678, 2011.

CAVALCANTI, R. N.; MEIRELES, M. A. A. Fundamentals of Supercritical Fluid Extraction. [s.l.] Elsevier, 2012. v. 2

CERQUEIRA, M. A., FASOLIN, L. H., PICONE, C. S. F., PASTRANA, L. M., CUNHA, R. L., AND VICENTE, A. A. Structural and mechanical properties of organogels: Role of oil and gelator molecular structure. Food Research International. v. 96, p. 161–170, 2017.

CHAI, Y. H. et al. Supercritical fluid extraction and solubilization of Carica papaya linn. leaves in ternary system with CO2 + ethanol solvents. Chemical Engineering Research and Design, v. 156, p. 31–42, 2020.

CHEDEA, V. S.; POP, R. M. Total Polyphenols Content and Antioxidant DPPH Assays on Biological Samples. In: Polyphenols in Plants. 2. ed. [s.l.] Elsevier Inc., 2019. p. 169–183.

CHEMAT, F. et al. Green extraction of natural products. Origins, current status, and future challenges. TrAC - Trends in Analytical Chemistry, v. 118, p. 248–263, 2019.

CHEMAT, F. et al. Review of Green Food Processing techniques - Preservation, transformation, and extraction. Innovative Food Science and Emerging Technologies, v. 41, p. 357–377, 2017.

CHEN, H., MAO, L., HOU, Z., YUAN, F., AND GAO, Y. (2020). Roles of additional emulsifiers in the structures of emulsion gels and stability of vitamin E. Food Hydrocolloids, v. 99, 2020.

CHEN, J., C. WANG, C. WANG, J. SHEU, C. LIN, H. LIN. Hibiscus sabdariffa leaf polyphenolic extract inhibits LDL oxidation and foam cell formation involving up-regulation of LXRa / ABCA1 pathway. Food Chem. v. 141, p. 97–406, 2013

CHEN, Z. et al. Novel bigels constructed from oleogels and hydrogels with contrary thermal characteristics: Phase inversion and 3D printing applications. Food Hydrocolloids, v. 134, n. June 2022, p. 108063, 2023.

CHEN, Z.; SHI, Z.; MENG, Z. Development and characterization of antioxidant-fortified oleogels by encapsulating hydrophilic tea polyphenols. Food Chemistry, v. 414, p. 135664, 2023.

CHENG, F., CAO, Q., GUAN, Y., CHENG, H., WANG, X., AND MILLER, J. D. FTIR analysis of water structure and its influence on the flotation of arcanite (K2SO4) and epsomite (MgSO4·7H2O). International Journal of Mineral Processing. 2013

CHEW, S. Y. et al. Optimization of ultrasonic extraction condition for maximal antioxidant, antimicrobial, and antityrosinase activity from Hibiscus cannabinus L. leaves by using the single factor experiment. Journal of Applied Research on Medicinal and Aromatic Plants, v. 25, n. 1, p. 100321, 2021.

CHUESIANG, P. et al. Observation of curcumin-loaded hydroxypropyl methylcellulose (HPMC) oleogels under in vitro lipid digestion and in situ intestinal absorption in rats. International Journal of Biological Macromolecules, v. 208, n. January, p. 520–529, 2022.

CLIMACO, G. N; VARDANEGA, R.; FASOLIN, L. H. Hibiscus sabdariffa L. leaves as an alternative source of bioactive compounds obtained through high pressure technologies. The Journal of Supercritical Fluids, v. 200, 2023.

CRUZ, P. N. et al. Antioxidant activity and fatty acid profile of yacon leaves extracts obtained by supercritical CO2 + ethanol solvent. The Journal of Supercritical Fluids, v. 146, p. 55–64, 2019.

CVJETKO BUBALO, M. et al. New perspective in extraction of plant biologically active compounds by green solvents. Food and Bioproducts Processing, v. 109, p. 52–73, 2018.

CYGNAROWICZT, M.L., SEIDER, W.D. Effect of Retrograde Solubility on the Design Optimization of Supercritical Extraction Processes. Ind. Eng. Chem. Res. v. 28, p. 1497–1503, 1989.

DA-COSTA-ROCHA, I. et al. Hibiscus sabdariffa L. – A phytochemical and pharmacological review. Food Chemistry, v. 165, p. 424–443, 2014.

DE HOYOS-MARTÍNEZ, P. L. et al. Tannins extraction: A key point for their valorization and cleaner production. Journal of Cleaner Production, v. 206, p. 1138–1155, 2019.

DIAMANTIDES, N. et al. Correlating rheological properties and printability of collagen bioinks: The effects of riboflavin photocrosslinking and pH. Biofabrication, v. 9, n. 3, 2017.

DJOULLAH, A.; SAUREL, R. Controlled release of riboflavin encapsulated in pea protein microparticles prepared by emulsion-enzymatic gelation process. Journal of Food Engineering, v. 292, 2020.

DO, N. H. N. et al. Encapsulation of Triphasia trifolia extracts by pH and thermal dual-sensitive chitosan hydrogels for controlled release. Carbohydrate Polymers, v. 320, p. 121264, 2023.

DUAN, Y. et al. Genotypic variation of flavonols and antioxidant capacity in broccoli. Food Chemistry, v. 338, 2021.

ĐUROVIC, S. et al. Recovery of biologically active compounds from stinging nettle leaves part I: Supercritical carbon dioxide extraction. Food Chemistry, v. 373, 2022.

EL-BELTAGI, H. S. et al. Evaluation of some chemical constituents, antioxidant, antibacterial and anticancer activities of beta Vulgaris L. Root. Fresenius Environmental Bulletin, v. 27, n. 9, p. 6369–6378, 2018.

ESSIEN, S. O.; YOUNG, B.; BAROUTIAN, S. Recent advances in subcritical water and supercritical carbon dioxide extraction of bioactive compounds from plant materials. Trends in Food Science and Technology, v. 97, n. January, p. 156–169, 2020.

EUROPEAN, C. Commission Regulation of the European Parliament and of the Council as regards food category 17 and the use of food additives in food supplements. No 1333/2008 of 8 October 2018. Official Journal of the European Union, n. October, p. 20–30, 2018.

EUROPÉIA, C. Regulamento (UE) No 10/2011 da Comissão de 14 de janeiro de 2011. Jornal Oficial das Comunidades Europeias, p. 1–89, 2011.

FALSAFI, S. R. et al. Insights into whey protein-based carriers for targeted delivery and controlled release of bioactive components. Food Hydrocolloids, v. 133, 2022.

FASOLIN, L. H. et al. Modulating process parameters to change physical properties of bigels for food applications. Food Structure, v. 28, n. June 2019, p. 100173, 2021.

FASOLIN, L. H., CERQUEIRA, M. A., PASTRANA, L. M., VICENTE, A. A., AND CUNHA, R. L. Thermodynamic, rheological and structural properties of edible oils structured with LMOGS: influence of gelator and oil phase. Food Structure. 2018.

FASOLIN, L. H., PICONE, C. S. F., SANTANA, R. C., AND CUNHA, R. L. Production of hybrid gels from polysorbate and gellan gum. Food Research International, v. 54, n.1, p. 501–507. 2013.

FENG, G. et al. Temperature and pH dual-responsive supramolecular hydrogels based on riboflavin sodium phosphate and 2, 6-Diaminopurine with thixotropic and fluorescent properties. Colloids and Surfaces A: Physicochemical and Engineering Aspects, v. 630, p. 127548, 2021.

FERNÁNDEZ-PONCE, M. T. et al. Use of high-pressure techniques to produce Mangifera indica L. leaf extracts enriched in potent antioxidant phenolic compounds. Innovative Food Science and Emerging Technologies, v. 29, p. 94–106, 2015.

FERRO, D. M. et al. Integrated extraction approach to increase the recovery of antioxidant compounds from Sida rhombifolia leaves. The Journal of Supercritical Fluids, v. 149, p. 10–19, 2019.

FORMAGIO, A. S. N. et al. Phenolic compounds of Hibiscus sabdariffa and influence of organic residues on its antioxidant and antitumoral properties. Brazilian Journal of Biology, v. 75, n. 1, p. 69–76, 2015.

FOSTER, N.R. et al. Significance of the Crossover Pressure in Solid-Supercritical Fluid Phase Equilibria, Ind. Eng. Chem. Res. v. 30, p. 1955–1964, 1991.

FROHLICHA, P. C. et al. Evaluation of the effects of temperature and pressure on the extraction of eugenol from clove (Syzygium aromaticum) leaves using supercritical CO2. The Journal of Supercritical Fluids, v. 143, n. September 2018, p. 313–320, 2019.

GALLEGO, R.; BUENO, M.; HERRERO, M. Sub- and supercritical fluid extraction of bioactive compounds from plants, food-by-products, seaweeds and microalgae – An update. TrAC - Trends in Analytical Chemistry, v. 116, p. 198–213, 2019.

GAONKAR, A. G. Effects of salt, temperature, and surfactants on the interfacial tension behavior of a vegetable oil/water system. Journal of Colloid and Interface Science. v. 149, n. 1, p. 256–260, 1992.

GARAVAND, F. et al. Encapsulation of phenolic compounds within nano/microemulsion systems: A review. Food Chemistry, v. 364, n. April, p. 130376, 2021.

GARCIA, C.; BLESSO, C. N. Antioxidant properties of anthocyanins and their mechanism of action in atherosclerosis. Free Radical Biology and Medicine, v. 172, n. March, p. 152–166, 2021.

GBASSI, G.; YOLOU, F.; SARR, S.; ATHEBA, P.; AMIN, C. AND AKE, M. Whey proteins analysis in aqueous medium and in artificial gastric and intestinal fluids. International Journal of Biological and Chemical Sciences. v. 6, p. 1828-1837, 2012.

GE, X. et al. The thermal resistance and targeting release of zein-sodium alginate binary complexes as a vehicle for the oral delivery of riboflavin. Journal of Food Science and Technology. v. 60, n. 1, p. 92–102, 2023.

GHAN, S. Y. et al. Palm Olein Organogelation Using Mixtures of Soy Lecithin and Glyceryl Monostearate. Gels, v. 8, n. 1, p. 30, 2022.

GHIASI, F., AND GOLMAKANI, M. T. Fabrication and characterization of a novel biphasic system based on starch and ethylcellulose as an alternative fat replacer in a model food system. Innovative Food Science and Emerging Technologies. v. 78, p. 103028, 2022.

GONÇALVES, R. F. S. et al. Lipid-based nanostructures as a strategy to enhance curcumin bioaccessibility: Behavior under digestion and cytotoxicity assessment. Food Research International, v. 143, 2021.

GONÇALVES, R. F. S.; VICENTE, A. A.; PINHEIRO, A. C. Incorporation of curcumin-loaded lipid-based nano delivery systems into food: Release behavior in food simulants and a case study of application in a beverage. Food Chemistry, v. 405, 2023.

GONZÁLEZ, M. et al. Ultrasound assisted extraction of bioactive compounds in fresh and freeze-dried Vitis vinifera cv Tannat grape pomace. Food and Bioproducts Processing, v. 124, p. 378–386, 2020.

GOSAIN, S. et al. Hypolipidemic effect of ethanolic extract from the leaves of Hibiscus sabdariffa L. in hyperlipidemic rats. Acta Poloniae Pharmaceutica, v. 67, n. 2, p. 179–184, 2010.

GOULA, A. M. et al. Green ultrasound-assisted extraction of carotenoids from pomegranate wastes using vegetable oils. Ultrasonics Sonochemistry, v. 34, p. 821–830, 2017.

GOYENECHE, R. et al. Supercritical CO2 extraction of bioactive compounds from radish leaves: Yield, antioxidant capacity and cytotoxicity. The Journal of Supercritical Fluids, v. 135, n. January, p. 78–83, 2018.

GUO, L. et al. Optimization of tannin extraction from Coriaria nepalensis bark as a renewable resource for use in tanning. Industrial Crops and Products, v. 149, n. January, p. 112360, 2020.

HABIBI, A., KASAPIS, S., AND TRUONG, T. Effect of hydrogel particle size embedded into oleogels on the physico-functional properties of hydrogel-in-oleogel (bigels). LWT, v. 163, 2022.

HASHEMI, B., ASSADPOUR, E., JAFARI, S. M. Bigels as novel carriers of bioactive compounds: Applications and research trends. Food Hydrocolloids, v. 147, Part B, 2024.

HASHIM, A. F., EL-SAYED, S. M., & EL-SAYED, H. S. Bigel formulations based on sesame oleogel with probiotics alginate hydrogel: A novel structure for nutritious spreadable butter. International Journal of Biological Macromolecules. v. 242, 124782, 2023.

HAZRATI, Z.; MADADLOU, A. Gelation by bioactives: Characteristics of the cold-set whey protein gels made using gallic acid. International Dairy Journal, v. 117, p. 104952, 2021.

HE, M. et al. Fabrication of soy protein isolate-succinic anhydride-dextran nanogels: Properties, performance, and controlled release of curcumin. LWT, v. 160, p. 113259, 2022.

HE, Z. et al. Heat-induced gel formation by whey protein isolate - Lycium barbarum polysaccharides at varying pHs. Food Hydrocolloids, v. 115, 2021.

HEO, J. et al. Riboflavin-induced photo-crosslinking of collagen hydrogel and its application in meniscus tissue engineering. Drug Delivery and Translational Research, v. 6, n. 2, p. 148–158, 2016.

HERBST, G. et al. Pressurized liquid extraction of brewer's spent grain: Kinetics and crude extracts characterization. Journal of Industrial and Engineering Chemistry, v. 102, p. 370–383, 2021.

HOFFMANN, M., & VAN MIL, P.J. Heat-Induced Aggregation of β-Lactoglobulin: Role of the Free Thiol Group and Disulfide Bonds. Journal of Agricultural and Food Chemistry. v. 45, p. 2942-2948, 1997.

HOFMANN, T. Structure and Antioxidant Efficiency of Beech (Fagus sylvatica L.) Bark Polyphenols Unraveled by High-Performance Liquid Chromatography/Photodiode Array Detection/Multistage Electrospray Mass Spectrometry and Chemometrics. In: Polyphenols in Plants. [s.l: s.n.]. p. 83–109.

HONGSPRABHAS P., BARBUT S. Ca2+-Induced cold gelation of whey protein isolate: effect of two-stage gelation. Food Research International. v.30, 1997.

HWANG, H.-S. A critical review on structures, health effects, oxidative stability, and sensory properties of oleogels. Biocatalysts and Agricultural Biotechnology, v. 26, n. March, p. 101657, 2020.

IKEDA, S.; FOEGEDING, E. A. Effects of lecithin on thermally induced whey protein isolate gels. Food Hydrocolloids, v. 13, n. 3, p. 239–244, 1999.

JABEUR, I. et al. Hibiscus sabdariffa L. as a source of nutrients, bioactive compounds and coloring agents. Food Research International, v. 100, n. August, p. 717–723, 2017.

JACOBS, M.B. Determination of moisture, in: Chem. Anal. Foods Food Prod., 3th ed., Van Nostrand Reinhold, New York, p. 22–23, 1973.

JIANG, L. et al. Acid / alkali shifting of Mesona chinensis polysaccharide-whey protein isolate gels: Characterization and formation mechanism. Food Chemistry, v. 355, n. March, p. 129650, 2021.

JOSHI, M., ALDRED, P., PANOZZO, J. F., KASAPIS, S., AND ADHIKARI, B. Rheological and microstructural characteristics of lentil starch-lentil protein composite pastes and gels. Food Hydrocolloids, v. 35, p. 226–237, 2014.

KAPEPULA, P.M. et al. Comparison of metabolic profiles and bioactivities of the leaves of three edible Congolese Hibiscus species. Nat. Prod. Res. v. 31, p. 2885–2892, 2017.

KARAASLAN, N. M. A comprehensive study about Hibiscus sabdariffa leaves: antioxidant activity, polyphenol profile and macro- and micro-element content. Chemical Papers, v. 73, n. 4, p. 791–799, 2019.

KATIME, I.; MENDIZÁBAL, E. Swelling Properties of New Hydrogels Based on the Dimethyl Amino Ethyl Acrylate Methyl Chloride Quaternary Salt with Acrylic Acid and 2-Methylene Butane-1,4-Dioic Acid Monomers in Aqueous Solutions. Materials Sciences and Applications, v. 01, n. 03, p. 162–167, 2010.

KAZEMI-TASKOOH, Z., AND VARIDI, M. Designation and characterization of cold-set whey protein-gellan gum hydrogel for iron entrapment. Food Hydrocolloids, v. 111, p. 106205, 2021.

KODELA, S. P. et al. Novel agar–stearyl alcohol oleogel-based bigels as structured delivery vehicles. International Journal of Polymeric Materials and Polymeric Biomaterials, v. 66, n. 13, p. 669–678, 2017.

KOVAČEVIĆ, D. B. et al. Innovative technologies for the recovery of phytochemicals from Stevia rebaudiana Bertoni leaves: A review. Food Chemistry, v. 268, n. March, p. 513–521, 2018.

KRAUJALIENE, V.; PUKALSKAS, A.; VENSKUTONIS, P. R. Biorefining of goldenrod (Solidago virgaurea L.) leaves by supercritical fluid and pressurized liquid extraction and evaluation of antioxidant properties and main phytochemicals in the fractions and plant material. Journal of Functional Foods, v. 37, p. 200–208, 2017.

KUHN, K. R.; CAVALLIERI, Â. L. F.; CUNHA, R. L. DA. Cold-set whey protein-flaxseed gum gels induced by mono or divalent salt addition. Food hydrocolloids, v. 25, n. 5, p. 1302–1310, 2011.

KULAWIK-PIÓRO, A.; OSAK, E.; MENDRYCKA, M. Bigels as novel systems for the delivery active compounds from Centella asiatica. Soft Materials, v. 00, n. 00, p. 1–23, 2023.

KUMAR, L. et al. Influence of whey protein isolate on pasting, thermal, and structural characteristics of oat starch. Journal of Dairy Science, v. 105, n. 1, p. 56–71, 2022.

KUMAR, S. S. et al. Effect of different drying methods on chlorophyll, ascorbic acid and antioxidant compounds retention of leaves of Hibiscus sabdariffa L. Journal of the Science of Food and Agriculture, v. 95, n. 9, p. 1812–1820, 2015.

KUMARI, B. et al. Recent Advances on Application of Ultrasound and Pulsed Electric Field Technologies in the Extraction of Bioactives from Agro-Industrial By-products. Food Bioprocess Technol. v.11, p. 223–241, 2018.

KUMARI, P.; RAZA, W.; MEENA, A. Lemongrass derived cellulose nanofibers for controlled release of curcumin and its mechanism of action. Industrial Crops and Products, v. 173, p. 114099, 2021.

KUSHWAHA, R. et al. Optimization of Different Variable for Eco-friendly Extraction of Betalains and Phytochemicals from Beetroot Pomace. Waste and Biomass Valorization, 2017.

LAMA-MUÑOZ, A. et al. Content of phenolic compounds and mannitol in olive leaves extracts from six Spanish cultivars: Extraction with the Soxhlet method and pressurized liquids. Food Chemistry, v. 320, n. September 2019, p. 126626, 2020.

LAVADO, G.; LADERO, L.; CAVA, R. Cork oak (Quercus suber L.) leaf extracts potential use as natural antioxidants in cooked meat. Industrial Crops and Products, v. 160, n. July 2020, p. 1–9, 2021.

LEI, H. et al. The behavior of whey protein isolate-curcumin complex at the oil-water interface. Food Hydrocolloids, v. 145, n. July, p. 109046, 2023.

LENUCCI, M.S. et al. Enzyme-aided extraction of lycopene from high-pigment tomato cultivars by supercritical carbon dioxide, Food Chem. v. 170, p. 193–202, 2015.

LEYVA-JIMÉNEZ, F. J. et al. Comparative study of conventional and pressurized liquid extraction for recovering bioactive compounds from Lippia citriodora leaves. Food Research International, v. 109, n. March, p. 213–222, 2018.

LIN, H. H. et al. Hibiscus sabdariffa leaf induces apoptosis of human prostate cancer cells in vitro and in vivo. Food Chemistry, v. 132, n. 2, p. 880–891, 2012.

LU, Y. et al. Structural Modification of O/W Bigels by Glycerol Monostearate for Improved Co-Delivery of Curcumin and Epigallocatechin Gallate. Food Science & Technology, v. 2, p. 975–983, 2022.

LUPI, F. R. et al. A rheological and microstructural characterization of bigels for cosmetic and pharmaceutical uses. Materials Science & Engineering, v. 69, p. 358–365, 2016.

MACHADO, A. P. DA F. et al. Pressurized liquid extraction of bioactive compounds from blackberry (Rubus fruticosus L.) residues: a comparison with conventional methods. FRIN, p. 9, 2014.

MACHADO, A. R. et al. Liposomes loaded with phenolic extracts of Spirulina LEB-18: Physicochemical characterization and behavior under simulated gastrointestinal conditions. Food Research International, v. 120, p. 656–667, 2019.

MACHADO, A.P.D.F., PEREIRA, A.L.D., BARBERO, G.F., MARTÍNEZ, J. Recovery of anthocyanins from residues of Rubus fruticosus, Vaccinium myrtillus and Eugenia brasiliensis by ultrasound assisted extraction, pressurized liquid extraction and their combination. Food Chem. v. 231, p. 1–10, 2017.

MACHADO, M., SOUSA, S. C., RODRÍGUEZ-ALCALÁ, L. M., PINTADO, M., GOMES, A. M. Functional lipid enriched probiotic cheese: Gastrointestinal stability and potential health benefits. International Dairy Journal, v. 144, p. 105700, 2023.

MADALENA, D. A. et al. In vitro digestion and stability assessment of β-lactoglobulin/riboflavin nanostructures. Food Hydrocolloids, v. 58, p. 89–97, 2016.

MARTÍNEZ-MALDONADO, M. A. et al. Effect of high pressure processing on heat-induced gelling capacity of blue crab (Callinectes sapidus) meat. Innovative Food Science and Emerging Technologies, v. 59, n. May 2019, p. 102253, 2020.

MARTÍN-GARCÍA, B. et al. Box-Behnken experimental design for a green extraction method of phenolic compounds from olive leaves. Industrial Crops & Products, v. 154, n. June, p. 112741, 2020.

MARTINS, A. J. et al. Hybrid gels: Influence of oleogel/hydrogel ratio on rheological and textural properties. Food Research International, v. 116, n. July, p. 1298–1305, 2019.

MARTINS, A. J. et al. Food-grade bigels: Evaluation of hydrogel:oleogel ratio and gelator concentration on their physicochemical properties. Food Hydrocolloids. v. 143, 2023.

Martins, J. T. et al. Protein-Based Structures for Food Applications: From Macro to Nanoscale. Frontiers in Sustainable Food Systems, v. 2, p. 1–18, 2018

MCCLEMENTS, D. J.; KEOGH, M. K. Physical properties of cold-setting gels formed from heat-denatured whey protein isolate. Journal of the Science of Food and Agriculture, v. 69, n. 1, p. 7–14, 1995.

MEIRELES, M.A.A. Extraction of bioactive compounds from latin american plants, CRC Press - Taylor & Francis Group, Boca Raton, 2008.

MEIRELES, M.A.A., Supercritical extraction from solid: process design data (2001 – 2003), Curr. Opin. Solide State Mater. Sci. 7 (2003) 321–330.

MENA-GARCÍA, A. et al. Green techniques for extraction of bioactive carbohydrates. TrAC Trends in Analytical Chemistry, v. 119, p. 115612, 2019.

MILELLA, R. A. et al. Optimized ultrasonic-assisted extraction of phenolic antioxidants from grape (Vitis vinifera L.) skin using response surface methodology. Journal of Food Science and Technology, v. 56, n. 10, p. 4417–4428, 2019.

MINEKUS, M. et al. A standardized static in vitro digestion method suitable for food-an international consensus. Food and Function, v. 5, n. 6, p. 1113–1124, 2014.

MIRANDA, R. C. DE; SCHIEFERDECKER, M. E. M.; SCHMIDT, S. T. Uso de inquéritos alimentares na avaliação da ingestão de antioxidantes. Nutrire, v. 39, n. 1, p. 154–165, 2014.

MOURA, S. C. S. R. DE et al. Release of anthocyanins from the hibiscus extract encapsulated by ionic gelation and application of microparticles in jelly candy. Food Research International, v. 121, p. 542–552, 2019.

MUHAMMAD, U. et al. Effects of Extraction Variables on Pharmacological Activities of Vine Tea Extract (Ampelopsis grossedentata). International Journal of Pharmacology, v. 14, p. 495–505, 2018.

NÁTHIA-NEVES, G., VARDANEGA, R., MEIRELES, M.A.A. Extraction of natural blue colorant from Genipa americana L. using green technologies: Techno-economic evaluation, Food Bioprod. Process. v. 114, p. 132–143, 2019.

NICOLAI, T.; BRITTEN, M.; SCHMITT, C. β-Lactoglobulin and WPI aggregates: Formation, structure and applications. Food Hydrocolloids, v. 25, n. 8, p. 1945–1962, 2011.

NIPORNRAM, S., W. TOCHAMPA, P. RATTANATRAIWONG, R. SINGANUSONG. Optimization of low power ultrasound-assisted extraction of phenolic compounds from mandarin (Citrus reticulata Blanco cv. Sainampueng) peel. Food Chem. v. 241, p. 338–345, 2018.

NUTTER, J. et al. Designing and characterizing multicomponent, plant-based bigels of rice bran wax, gums, and monoglycerides. Food Hydrocolloids, v. 138, p. 108425, 2023.

OKASHA, T. M. Investigation of the effect of temperature and pressure on interfacial tension and wettability. International Symposium of the Society of Core Analysts. Trondheim, Norway, 27-30, 2018.

OKOLIE, C. L. et al. Influence of conventional and recent extraction technologies on physicochemical properties of bioactive macromolecules from natural sources: A review. Food Research International, v. 116, p. 827–839, 2019.

OLEJAR, K. J. et al. Thermo-chemical conversion of cannabis biomass and extraction by pressurized liquid extraction for the isolation of cannabidiol. Industrial Crops and Products, v. 170, n. April, p. 113771, 2021.

OLIVEIRA, D. M. DE; BASTOS, D. H. M. Biodisponibilidade de ácidos fenólicos. Química Nova, v. 34, n. 6, p. 1051–1056, 2011.

OLIVEIRA, P. H. R. DE; REIS, R. R. Ácido Benzóico (CAS 65-85-0). Revista Virtual de Quimica, v. 9, n. 6, p. 2673–2687, 2017.

OREOPOULOU, A.; TSIMOGIANNIS, D.; OREOPOULOU, V. Extraction of Polyphenols From Aromatic and Medicinal Plants: An Overview of the Methods and the Effect of Extraction Parameters. In: Polyphenols in Plants. 2. ed. [s.l.] Elsevier Inc., 2019. p. 243–259.

OU, B. et al. Analysis of antioxidant activities of common vegetables employing oxygen radical absorbance capacity (ORAC) and ferric reducing antioxidant power (FRAP) assays: A comparative study. J. Agric. Food Chem. v. 50, 2002.

PANJA, P. Green extraction methods of food polyphenols from vegetable materials. Current Opinion in Food Science, v. 23, p. 173–182, 2018.

PEDRALI, D.; BARBARITO, S.; LAVELLI, V. Encapsulation of grape seed phenolics from winemaking byproducts in hydrogel microbeads – Impact of food matrix and processing on the inhibitory activity towards α -glucosidase. LWT, v. 133, 2020.

PENG, W.L. et al. Optimization of process variables using response surface methodology for tocopherol extraction from Roselle seed oil by supercritical carbon dioxide. Ind. Crops Prod. v. 143, p. 111886, 2020.

PERALTA, J. et al. Aqueous hibiscus extract as a potential natural pH indicator incorporated in natural polymeric films. Food Packaging and Shelf Life, v. 19, n. December 2018, p. 47–55, 2019.

PIMENTEL-MORAL, S. et al. Supercritical CO2 extraction of bioactive compounds from Hibiscus sabdariffa. Journal of Supercritical Fluids. v. 147, p. 213–221, 2019.

PINHEIRO, A. C. et al. Towards the understanding of the behavior of bio-based nanostructures during in vitro digestion. Current Opinion in Food Science, v. 15, p. 79–86, 2017.

POPESCU V. et al. The Influence of Enzymatic Hydrolysis of Whey Proteins on the Properties of Gelatin-Whey Composite Hydrogels. Materials. v. 14, n. 13, p. 3507, 2021.

RAGHU, K.; NAIDOO, Y.; DEWIR, Y. H. Secretory structures in the leaves of Hibiscus sabdariffa L. South African Journal of Botany, v. 121, p. 16–25, 2019.

RAMANAUSKIENE, K.; INKENIENE, A. M.; PUIDOKAITE, E. Quality analysis of semisolid formulations with the liquid extract of elderflower (Sambucus Nigra L.). Pharmaceutical Technology, v. 76, n. 6, p. 1061–1071, 2019.

RASHEED, D. M. et al. Comparative analysis of Hibiscus sabdariffa (roselle) hot and cold extracts in respect to their potential for α -glucosidase inhibition. Food Chemistry, v. 250, n. January, p. 236–244, 2018.

RASHMI, H. B.; NEGI, P. S. Phenolic acids from vegetables: A review on processing stability and health benefits. Food Research International, v. 136, n. April, p. 109298, 2020.

RATHOD, S. et al. Advances on nanoformulation approaches for delivering plant-derived antioxidants: A case of quercetin. Int. J. Pharm. v. 625, p. 122093, 2022.

RE, R. et al. Antioxidant activity applying an improved ABTS radical cation decolorization assay. Free Radic. Biol. Med. v. 26, p. 1231–1237, 1999.

RICE-EVANS, C.A., N.J. MILLER, G. PAGANGA, Structure-antioxidant activity relationships of flavonoids and phenolic acids, Free Radic. Biol. Med. v. 20, p. 933–956, 1996.

RODRIGUES, R. M. et al. Effects of moderate electric fields on cold-set gelation of whey proteins – From molecular interactions to functional properties. Food Hydrocolloids, v. 101, 2020.

RODRIGUES, V. H.; MELO, M. M. R. DE; SILVA, C. M. Extraction of Eucalyptus leaves using solvents of distinct polarity. Cluster analysis and extracts characterization. The Journal of Supercritical Fluids, v. 135, n. January, p. 263–274, 2018.

SABET, S. et al. Clustering of oleogel production methods reveals pitfalls and advantages for sustainable, up scalable, and oxidative stable oleogels. Journal of Food Engineering, v. 357, n. March, p. 111659, 2023.

SABOURI, S.; GENG, J.; CORREDIG, M. Tea polyphenols association to caseinate-stabilized oil–water interfaces. Food Hydrocolloids, v. 51, p. 95–100, 2015.

SAGIRI, S. S. et al. Stearate organogel-gelatin Hydrogel based bigels: Physicochemical, thermal, mechanical characterizations and in vitro drug delivery applications. Journal of the Mechanical Behavior of Biomedical Materials, 2014.

SALAZAR, M.A.R. et al. Chemical composition, antioxidant activity, neuroprotective and anti-inflammatory effects of cipó-pucá (Cissus sicyoides L.) extracts obtained from supercritical extraction, J. Supercrit. Fluids. v. 138, p. 36–45, 2018.

SAMADI, S., RAOUF FARD, F. Phytochemical properties, antioxidant activity and mineral content (Fe, Zn and Cu) in Iranian produced black tea, green tea and roselle calyces, Biocatal. Agric. Biotechnol. v. 23 p. 101472, 2020.

SAMMANI, M.S., CLAVIJO, S., CERDÀ, V. Recent, advanced sample pretreatments and analytical methods for flavonoids determination in different samples, TrAC - Trends Anal. Chem. v. 138, 2021.

SAMUI, T. et al. The development and characterization of novel in-situ bigel formulation. Food Hydrocolloids, v. 113, n. June 2020, p. 106416, 2021.

Sanches, V.L. et al. Comprehensive analysis of phenolics compounds in citrus fruits peels by UPLC-PDA and UPLC-Q/TOF MS using a fused-core column, Food Chem. v. 14, 2022.

SANTANA, Á. L. et al. Pressurized liquid- and supercritical fluid extraction of crude and waste seeds of guarana (Paullinia cupana): Obtaining of bioactive compounds and mathematical modeling. Food and Bioproducts Processing, v. 117, p. 194–202, 2019.

SANTOS, K. A.; DA SILVA, E. A.; DA SILVA, C. Supercritical CO2 extraction of favela (Cnidoscolus quercifolius) seed oil: Yield, composition, antioxidant activity, and mathematical modeling. Journal of Supercritical Fluids, v. 165, 2020.

SANTOS, M. DOS et al. Emulsion gels based on pork skin and dietary fibers as animal fat replacers in meat emulsions: An adding value strategy to byproducts. LWT, v. 120, n. August 2019, p. 108895, 2020a.

SANTOS, K. A. et al. Extraction of Morus alba leaves using supercritical CO2 and ultrasound-assisted solvent: Evaluation of β-sitosterol content. Journal of Supercritical Fluids, v. 159, 2020b.

SANTOS, P. et al. Supercritical carbon dioxide extraction of capsaicinoids from malagueta pepper (Capsicum frutescens L.) assisted by ultrasound. Ultrasonics Sonochemistry, v. 22, p. 78–88, 2015.

SANTOS, P. H. et al. Antioxidant and antibacterial compounds from feijoa leaf extracts obtained by pressurized liquid extraction and supercritical fluid extraction. Food Chemistry, v. 344, p. 128620, 2021.

SARGIN, S.A. Potential anti-influenza effective plants used in Turkish folk medicine: A review. J. Ethnopharmacol. v. 265, p. 113319, 2021.

SARKAR, A.; GOH, K. K. T.; SINGH, H. Colloidal stability and interactions of milk-protein-stabilized emulsions in an artificial saliva. Food Hydrocolloids, v. 23, n. 5, p. 1270–1278, 2009.

SCALZINI, G. et al. Effect of withering process on the evolution of phenolic acids in winegrapes: A systematic review. Trends in Food Science & Technology, v. 116, n. August, p. 545–558, 2021.

SCHIASSI, M. C. E. V. et al. Fruits from the Brazilian Cerrado region: Physico-chemical characterization, bioactive compounds, antioxidant activities, and sensory evaluation. Food Chemistry, v. 245, p. 305–311, 2018.

SEIWERT, K. et al. Development and characterization of whey protein isolate and xylan composite films with and without enzymatic crosslinking. Food Hydrocolloids, v. 120, n. May, 2021.

SHAKEEL, A. et al. Bigels and multi-component organogels: An overview from rheological perspective. Food Hydrocolloids, v. 111, n. July 2020, p. 106190, 2021.

SHAKEEL, A. et al. Key characteristics and modelling of bigels systems: A review. Materials Science & Engineering, v. 97, n. February 2018, p. 932–953, 2019.

SHISHIR, M. R. I. et al. Advances in micro and nano-encapsulation of bioactive compounds using biopolymer and lipid-based transporters. Trends in Food Science & Technology, 2018.

SIACHOU C, ZAMPOUNI K, KATSANIDIS E. Bigels as Fat Replacers in Fermented Sausages: Physicochemical, Microbiological, Sensory, and Nutritional Characteristics. Gels. v. 9, n. 4, p. 340, 2023.

SILVA, P. M. et al. Oleogels and bigels as alternatives to saturated fats: A review on their application by the food industry. JAOCS, Journal of the American Oil Chemists' Society. v. 99, n. 11, p. 911–923, 2022.

SILVA, R. P. F. F.; ROCHA-SANTOS, T. A. P.; DUARTE, A. C. Supercritical fluid extraction of bioactive compounds. Trends in Analytical Chemistry, 2015.

SIMÕES, L. S. et al. Suitability of β-lactoglobulin micro- and nanostructures for loading and release of bioactive compounds. Food Hydrocolloids, v. 101, n. November 2019, 2020a.

SIMÕES, L. S. et al. β-lactoglobulin micro- and nanostructures as bioactive compounds vehicle: In vitro studies. Food Research International, v. 131, n. January, p. 108979, 2020b.

SINDI, H. A.; MARSHALL, L. J.; MORGAN, M. R. A. Comparative chemical and biochemical analysis of extracts of Hibiscus sabdariffa. Food Chemistry, v. 164, p. 23–29, 2014.

SINGH, M., T. THRIMAWITHANA, R. SHUKLA, B. ADHIKARI, Extraction and characterization of polyphenolic compounds and potassium hydroxycitrate from Hibiscus sabdariffa. Futur. Foods. v. 4, 2021.

SINGH, S. et al. Changes in phytochemicals, anti-nutrients and antioxidant activity in leafy vegetables by microwave boiling with normal and 5% NaCl solution. Food Chemistry, v. 176, p. 244–253, 2015.

SINGH, S. et al. Estimation of proximate composition, micronutrients and phytochemical compounds in traditional vegetables from Andaman and Nicobar Islands. International Journal of Food Science and Nutrition, v. 62, p. 765–773, 2011.

SINGH, V. K. et al. Bigels. Polymeric Gels, p. 265–282, 2018.

SINGH, V. K. et al. Guar gum and sesame oil based novel bigels for controlled drug delivery. Colloids and Surfaces B: Biointerfaces, 2014.

SINGH, V. K. et al. Preparation and characterization of novel carbopol based bigels for topical delivery of metronidazole for the treatment of bacterial vaginosis. Materials Science and Engineering, v. 44, p. 151–158, 2014.

SINGLETON, V. L.; ORTHOFER, R.; LAMUELA-RAVENTÓS, R. M. Analysis of Total Phenols and Other Oxidation Substrates and Antioxidants by Means of Folin-Ciocalteu reagent. Polyphenols and Flavonoids, v. 299, n. 1974, p. 152–178, 1999.

SONG, L. et al. Supercritical CO2 fluid extraction of flavonoid compounds from Xinjiang jujube (Ziziphus jujuba Mill.) leaves and associated biological activities and flavonoid compositions. Industrial Crops & Products, v. 139, n. June, p. 111508, 2019.

SOQUETTA, M. B.; TERRA, L. DE M.; BASTOS, C. P. Green technologies for the extraction of bioactive compounds in fruits and vegetables. CYTA - Journal of Food, v. 16, n. 1, p. 400–412, 2018.

SOUZA, A. R. C. DE et al. Assessment of composition and biological activity of Arctium lappa leaves extracts obtained with pressurized liquid and supercritical CO2 extraction. The Journal of Supercritical Fluids, v. 152, p. 104573, 2019.

SUBHASWARAJ, P. et al. Determination of antioxidant activity of Hibiscus sabdariffa and Croton caudatus in Saccharomyces cerevisiae model system. Journal of Food Science and Technology, v. 54, n. 9, p. 2728–2736, 2017.

SUCUPIRA, N.R. et al. Métodos Para Determinação da Atividade Antioxidante de Frutos, UNOPAR Científica. Ciências Biológicas e Da Saúde. v. 14, p. 263–270, 2012.

SUN, L. et al. Integrated assessment of the sustainable water-energy-food nexus in China: Case studies on multi-regional sustainability and multi-sectoral synergy. J. Clean. Prod. v. 334, p. 130235, 2022.

TAIB, S. H. M. et al. Electrooxidation of nitrite based on green synthesis of gold nanoparticles using Hibiscus sabdariffa leaves. Journal of the Taiwan Institute of Chemical Engineers, v. 95, p. 616–626, 2019.

TIAN, W. et al. Flexible Control of Bigel Microstructure for Enhanced Stability and Flavor Release during Oral Consumption. Food Research International. v. 174, 2023.

TONG, C. et al. Shining natural flavonols in sensing and bioimaging. TrAC - Trends in Analytical Chemistry, v. 137, p. 116222, 2021.

TORRES, T. M. S. et al. Neuroprotective potential of extracts from leaves of ora-pro-nobis (Pereskia aculeata) recovered by clean compressed fluids. The Journal of Supercritical Fluids, v. 179, n. May 2021, 2022.

TRUJILLO-RAMÍREZ, D. et al. Cooling rate, sorbitan and glyceryl monostearate gelators elicit different microstructural, viscoelastic and textural properties in chia seed oleogels. Food Research International, n. October, p. 0–1, 2018.

TSIMOGIANNIS, D.; OREOPOULOU, V. Classification of Phenolic Compounds in Plants. In: Polyphenols in Plants. [s.l.] Elsevier Inc., 2019. p. 263–284.

U. NATIONS, Trasnforming our world: 2030 agenda for sustainable development, 2017.

VARDANEGA, R. et al. Selective extraction of bioactive compounds from annatto seeds by sequential supercritical CO2 process. The Journal of Supercritical Fluids, v. 150, p. 122–127, 2019.

VARDANEGA, R.; PRADO, J. M.; MEIRELES, M. A. A. Adding value to agri-food residues by means of supercritical technology. The Journal of Supercritical Fluids, 2014.

VARGAS-RAMELLA, M. et al. Impact of pulsed light processing technology on phenolic compounds of fruits and vegetables. Trends in Food Science & Technology, v. 115, n. April, p. 1–11, 2021.

VAZQUEZ-ROIG, P.; PICÓ, Y. Pressurized liquid extraction of organic contaminants in environmental and food samples. Trends in Analytical Chemistry, v. 71, p. 55–64, 2015.

VEGGI, P. C.; CAVALCANTI, R. N.; MEIRELES, M. A. A. Production of phenolic-rich extracts from Brazilian plants using supercritical and subcritical fluid extraction: Experimental data and economic evaluation. Journal of Food Engineering, v. 131, p. 96–109, 2014.

VERGARA, D. et al. Povidone-iodine loaded bigels: Characterization and effect as a hand antiseptic agent. Journal of Drug Delivery Science and Technology. v. 72, 2022.

VIGANÓ, J. et al. Pressurized liquids extraction as an alternative process to readily obtain bioactive compounds from passion fruit rinds, Food Bioprod. Process. v. 100, p. 382–390, 2016.

WAGNER, J. et al. Effect of ethanol on the microstructure and rheological properties of whey proteins: Acid-induced cold gelation. LWT, v. 139, n. November 2020, p. 110518, 2021.

WANG, F. C.; MARANGONI, A. G. Internal and external factors affecting the stability of glycerol monostearate structured emulsions. Royal Society of Chemistry, v. 5, n. 001, p. 93108–93116, 2015.

WANG, F. et al. Research on structure and antioxidant activity of polysaccharides from Ginkgo biloba leaves. Journal of Molecular Structure, v. 1252, p. 132185, 2022.

WANG, J. et al. Antioxidant activity of leaf extracts from different Hibiscus Sabdariffa accessions and simultaneous determination five major antioxidant compounds by LC-Q-TOF-MS. Molecules, v. 19, n. 12, p. 12226–12238, 2014.

WANG, Y. et al. Interaction between whey protein isolate and rose anthocyanin extracts at different pHs: Structure, emulsification and digestibility of complexes. Food Bioscience, v. 49, p. 101888, 2022.

WU, S. et al. Fabrication of high strength cold-set sodium alginate/whey protein nanofiber double network hydrogels and their interaction with curcumin. Food Research International, v. 165, p. 112490, 2023.

XIE, D. et al. Development and characterization of food-grade bigel system for 3D printing applications: Role of oleogel / hydrogel ratios and emulsifiers. Food Hydrocolloids, v. 139, p. 108565, 2023.

XIE, D. et al. Influence of oleogel/hydrogel ratios and emulsifiers on structural and digestion properties of food-grade 3D printed bigels as carriers for quercetin and catechin. Food Hydrocolloids, v. 144, p. 108948, 2023.

YALLAPU, M. M.; JAGGI, M.; CHAUHAN, S. C. β-Cyclodextrin-curcumin self-assembly enhances curcumin delivery in prostate cancer cells. Colloids and Surfaces B: Biointerfaces, v. 79, n. 1, p. 113–125, 2010.

YAN, S. et al. Controlled release of curcumin from gelatin hydrogels by the molecular-weight modulation of an oxidized dextran cross-linker. Food Chemistry, v. 418, n. November 2022, p. 135966, 2023.

YANG, B.; CHEN, X. D.; MERCADÉ-PRIETO, R. Stress relaxation of particulate whey protein hydrogels. Food Hydrocolloids, v. 118, n. March, 2021.

YANG, C. et al. Cold-set oat protein isolate-gellan gum binary gels with various microstructures: Fabrication, characterization, formation mechanism, and controlled release properties. Food Hydrocolloids, v. 131, p. 107818, 2022.

Yang, Y.C., Wei, M.C. A combined procedure of ultrasound-assisted and supercritical carbon dioxide for extraction and quantitation oleanolic and ursolic acids from Hedyotis corymbosa, Ind. Crops Prod. v. 79, p. 7–17, 2016.

ZENG, L. et al. Recent advances of organogels: from fabrications and functions to applications. Progress in Organic Coatings, v. 159, n. March, p. 106417, 2021.

ZHAI, X. et al. Anthocyanins-encapsulated 3D-printable bigels: A colorimetric and leaching-resistant volatile amines sensor for intelligent food packaging. Food Hydrocolloids, v. 133, p. 107989, 2022.

ZHANG, J. et al. Recent advances in the extraction of bioactive compounds with subcritical water: A review. Trends in Food Science & Technology, 2019.

ZHANG, N. et al. Structure and functional properties of active packaging films prepared by incorporating different flavonols into chitosan-based matrix. International Journal of Biological Macromolecules, v. 165, p. 625–634, 2020.

ZHANG, T. et al. Effect of soy lecithin concentration on physiochemical properties and rehydration behavior of egg white protein powder: Role of dry and wet mixing. Journal of Food Engineering, v. 328, n. December 2021, p. 111062, 2022.

ZHAO, X.; LI, C.; XUE, F. Effects of whey protein-polyphenol conjugates incorporation on physicochemical and intelligent pH-sensing properties of carboxymethyl cellulose based films. Future Foods, v. 7, p. 100211, 2023.

ZHEN, J. et al. Phytochemistry, antioxidant capacity, total phenolic content and anti-inflammatory activity of Hibiscus sabdariffa leaves. Food Chemistry, v. 190, p. 673–680, 2016.

ZHENG, H. et al. Development of food-grade bigels based on κ-carrageenan hydrogel and monoglyceride oleogels as carriers for β-carotene: Roles of oleogel fraction. Food Hydrocolloids, v. 105, n. February, p. 105855, 2020.

ZHENG, R. et al. Microstructure and physical properties of novel bigel-based foamed emulsions. Food Hydrocolloids, p. 108097, 2022.

ZHONG, W. et al. Formation, stability and in vitro digestion of curcumin loaded whey protein/ hyaluronic acid nanoparticles: Ethanol desolvation vs. pH-shifting method. Food Chemistry, v. 414, p. 135684, 2023.

ZHU, Q. et al. Development and characterization of novel bigels based on monoglyceride-beeswax oleogel and high acyl gellan gum hydrogel for lycopene delivery. Food Chemistry, v. 365, p. 130419, 2021.

ZHU, Q. et al. Rational design cold-set interpenetrating network hydrogel based on wheat bran arabinoxylans and pea protein isolates for regulating the release of riboflavin in simulated digestion. International Journal of Biological Macromolecules, v. 223, n. PA, p. 961–970, 2022.

ZHUANG X, CLARK S, ACEVEDO N. Bigels-oleocolloid matrices-as probiotic protective systems in yogurt. J Food Sci. v. 86. n. 11, p. 4892-4900, 2021.